HYDROGEN EXCHANGE PATHWAYS BETWEEN ARENES AND DIHYDROARENES: AN EXPERIMENTAL AND MECHANISTIC MODELING STUDY OF HIGH TEMPERATURE HYDROGEN TRANSFER PATHWAYS.

Tom Autrey, Emily Alborn-Cleveland, Don M. Camaioni and James A Franz.
Pacific Northwest Laboratory Richland WA 99352

Introduction

One of the major areas of interest in thermal hydroliquefaction involves the mechanisms of hydrogen shuttling by aromatic/hydroaromatic donor solvents to coal structure, engendering the scission of thermally-stable alkylaromatic linkages. Derbyshire et al.[1] and McMillen and Malhotra[2] were among the first to recognize that hydrogen donor solvents can play an active role in the scission of thermally stable C-C bonds in coal structures. At least two "conventional" hydrogen-transfer pathways, hydrogen atoms (HA) and reverse radical disproportionation (RRD), and two "unconventional" hydrogen transfer pathways, radical hydrogen-transfer (RHT)[3] and addition-transfer-elimination,[4] could play a role in the shuttling of hydrogen from donor solvent to the ipso positions of substituted aromatic linkages in coal structures. It is unreasonable to assume that any one of these pathways is responsible for all solvent-engendered bond scission. Depending on the reaction conditions, one pathway may be more dominate than the others, or several of them could contribute simultaneously. A quantitative understanding of competing hydrogen-transfer pathways between aromatic structures can yield valuable information regarding the efficient cleavage of bonds in coal structures during hydroliquefaction. It is the goal of this work to quantify the importance of the conventional hydrogen-transfer pathways and make qualitative predictions regarding the unconventional pathways.

(1) $ArH\cdot \rightarrow Ar + H\cdot$
$H\cdot + ArR \rightarrow ArHR\cdot$ HA

(2) $ArH_2 + ArR \rightarrow ArH\cdot + ArHR\cdot$ RRD

(3) $ArH\cdot + ArR \rightarrow ArH\text{-}ArR\cdot$ Addition
$ArH\text{-}ArR\cdot \rightarrow \cdot Ar\text{-}ArRH$ Transfer
$Ar\text{-}ArRH \rightarrow Ar + ArHR\cdot$ Elimination

(4) $ArH. + ArR \rightarrow Ar + ArHR.$ RHT

We have undertaken mechanistic kinetic modeling (MKM) studies and experimental thermolysis studies of model compounds to quantify the importance of individual hydrogen-transfer pathways involved in the scission of alkyl-arene C-C bonds in diarylmethanes as a function of donor solvent composition.[5] In this paper, we report the role of hydrogen-transfer pathways in the aromatic/hydroaromatic solvent mixtures naphthalene/dihydronaphthalene (Nap/NapH$_2$), phenanthrene/dihydrophenanthrene (Phen/PhenH$_2$), anthracene/diydroanthracene (An/AnH$_2$), and cyclohexadiene/benzene (Ph/PhH$_2$) for promoting bond scission in a family of diarylmethanes (Ar-R)-diphenylmethane (PhCH$_2$-Ph), 1-benzylnaphthalene (PhCH$_2$-Nap), 9-benzylphenanthrene (PhCH$_2$-Phen) and 9-benzylanthracene (PhCH$_2$-An).

The results of this work will 1) show the significance of the role of free hydrogen atoms and 2) question the necessity of invoking the radical hydrogen-transfer pathway in promoting c-c bond scission in alkylarenes.

Results and Discussion

One of the advantages of MKM is the ability to quantify individual reaction pathways that compete from the same intermediate or yield the same products. It is a challenging experimental task to separate the amount of alkylarene bond scission by competing RRD and HA pathways This difficulty has led to ambiguous results regarding the role of solvent-induced bond scission. MKM permits "computer labeling" studies to quantify each competing pathway.

The activation barriers for the two conventional hydrogen-transfer pathways, HA and RRD, can be estimated to within a few kcal/mol because of the "product" like or "reactant" like nature of the transition state. On the other hand, there is no a priori means to estimate the intrinsic activation barriers for the two unconventional hydrogen-transfer pathways, ATE and RHT. Theoretical approaches and rigorously-designed experiments must be undertaken to quantitatively evaluate the feasibility of competing unconventional hydrogen transfer pathways.[6]

The Model. A mechanistic model composed of the free radical hydrogen-transfer pathways, initiation, termination, hydrogen scission, abstraction, addition, and reverse radical disproportionation, was developed for each mixed-solvent system and diarylmethane substrate (Scheme I). Arrhenius rate parameters were derived from the literature values of the thermochemical estimates of the heat of formation (ΔHf) of the products, reactants, and intermediate radicals.[7] We utilized the regimen of Malhotra and McMillen[3a] and Manka and Stein[8] to calculate the temperature-dependant rate for each individual reaction step. For concise introduction, we separate our model in three sections, 1) initiation and termination events, 2) efficient utilization of solvent and bond scission by HA and RRD pathways, and 3) inefficient utilization of solvent.

The initiation pathway utilized in this modeling study is the RRD between the dihydroarene and arene solvent molecules. Only radical disproportionation was considered as a termination event in our model since solvent derived radical coupling products have been shown to be unstable at temperatures above 350°C.[9]

Efficient solvent utilization pathways are defined as pathways leading to the scission of C-C bonds by RRD and H atom pathways. The rate determining step of the two-step HA pathway is scission from the hydroaryl radical. Addition of the hydrogen atom to an arene ring is not expected to be very selective relative to hydrogen transfer by the RRD pathway. Hydrogen atom addition to the solvent will also occur in competition with hydrogen transfer to diarylmethanes. Thus hydrogen from the solvent can be consumed without the scission of C-C bonds, and in some solvent mixtures is predicted to dominate the hydrogen-transfer chemistry.

To compare the rate of product formation from the H atom pathway to the RRD pathway, we utilized a computer "label" of the products arising from each competing pathway. In this way, competitive pathways involving the same intermediates can be quantitatively predicted. For example, we "label" the alkyl-arene bond-scission precursor, ipso addition of a hydrogen atom by to the alkyl position of Ar-x, arising from the RRD pathway as ArXH (equation 14), whereas ipso addition of a hydrogen atom by to the alkyl position of Ar-x arising from the HA pathway, gives ArxH (equation 4). Both "ipso adducts", Ar*X*H and ArxH, are "chemically" the same intermediate; they cleave at the same rate to yield the scission product, labelled RRD(H) (equation 18) and HA(H) (equation 17) respectively. In this manner, we can account for the yield of scission by each competing pathway even when the same intermediate is involved. To calculate the relative rates of solvent-induced scission of Ar-x by each pathway, we compared the predicted yield of the scission product as a function of thermolysis time. Thus, the percent C-C bond scission by H atom pathway = [HAH] /{[HAH] + [RRDH]}.

Scheme I. Example of kinetic hydrogen-transfer pathways in An/AnH_2

intiation/termination								
1	AnH_2	+	An	->	AnH	+	AnH,	
2,	AnH	+	AnH	->	AnH_2	+	An,	
H atom pathways								
4,	Anx	+	H	->	AnxH			ipso
5,	Anx	+	H	->	AnHx			nonipso
6,	AnHx			->	Anx	+	H	solvent
7,	AnH			->	An	+	H	
8,	An	+	H	->	AnH			
9,	AnH_2	+	H	->	AnH	+	H_2	
10,	AnH_2	+	An	->	HAn	+	AnH	1-4,5-8 position
11,	HAn	+	AnH_2	->	H_2An	+	AnH	
12,	H_2An	+	AnH_2	->	H_3An	+	AnH	
13,	H_3An	+	AnH_2	->	H_4An	+	AnH	
RRD								
14,	AnH_2	+	Anx	->	AnH	+	An*X*H	
15,	AnH_2	+	Anx	->	AnH	+	AnHx	abstraction
16,	AnH_2	+	AnHx	->	AnH_2x	+	AnH	
scission								
17,	AnxH			->	AnH	+	HA(H)	HA
18,	An*X*H			->	AnH	+	RRD(H)	RRD
19,	AnH_2x			->	AnH	+	RED'C(H)	nonipso

Examination of Table I clearly shows the importance of free hydrogen atoms in the scission of diarylmethane coal linkages. The only clear case of C-C bond scission by the RRD pathway is in An/AnH_2 solvent mixtures. This can be explained by the stability of the 9-hydroaryl radical. Table II lists the predicted relative total rate of diarylmethane bond scission (the sum total of both RRD and H atom contributions) in the series of solvent mixtures for each substrate, giving an indication of the "best" solvent for a given diarylmethane structure. A comparison of bond-induced scission of Nap-CH_2Ph in An/AnH_2 verses Phen/$PhenH_2$ illustrates the selectivity differences between the HA and RRD pathways. The model predicts nearly equal rates of solvent-induced scission; however, the selectivity of bond scission is expected to be greater in An/AnH_2 because of the contribution bond scission by the more selective RRD pathway. McMillen and Malhotra[3a] have observed that although there is very little difference in the rate of bond scission of 1,2-dinaphthylmethane in Phen/$PhenH_2$ and An/AnH_2 solvents, there is a substantial difference in the observed selectivity. They suggest that the difference in selectivity is due to the operation of the RHT pathway in An/AnH_2 solvents; however, our current analysis suggests that the increase in selectivity is due to the operation of the RRD pathway in An/AnH_2 solvents.

EXPERIMENTAL STUDIES.

To test both the rate and selectivity predictions of our mechanistic model of hydrogen transfer pathways from dihydroarenes to diarylmethanes, we have utilized experimental thermolysis studies of 1,2-dinaphthylmethane (DNM) in AnH_6 and An/AnH_2 solvent mixtures. Our model suggests that cyclic olefins, e.g. AnH_6, will be faster and less selective than An/AnH_2 solvent mixtures with less selectivity in the solvent-induced scission of DNM.

Cyclic Olefins. 1,4,5,8,9,10-Hexahydroanthracene **AnH_6**.

The predicted rate of bond scission in Ph/PhH_2 solvent mixtures as shown in Table II suggests that cyclic olefins are a special class of dihydroarenes donor solvents. Bedell and Curtis[10] have demonstrated that cyclic olefins provide enhanced liquefaction yields relative to their dihydroarene isomers. However, we note a chain-decomposition pathway of the cyclic olefins can limit the efficiency of C-C bond scission by this family of donors as shown in Scheme II.

Scheme II Chain Decomposition Pathways of Cyclic Olefin Donor Solvents.

Abstraction

$AnH_6 + H \rightarrow AnH_5 + H_2$
$AnH_5 \rightarrow AnH_4 + H$
$AnH_4 + H \rightarrow AnH_3 + H_2$
$AnH_3 \rightarrow AnH_2 + H$
$AnH_2 + H \rightarrow AnH + H_2$

Addition

$AnH_6 + H \rightarrow H_7An$
$H_7An + AnH_6 \rightarrow H_8An + AnH_5$
$H_8An + H \rightarrow H_9An$
$H_9An + AnH_6 \rightarrow H_{10}An + AnH_5$

Thermolysis of neat AnH_6 at 380°C results in a variety of hydroanthracene isomers with total consumption of the cyclic olefin in less than 20 minutes. The conversion of 1,2'-dinaphthylmethane (DNM) in hexahydroanthracene at 380°C is dependant on the starting concentration of DNM; at lower DNM concentrations, hydrogen atoms add competitively to the solvent AnH_6. Thermolysis of DNM in AnH_6 results in a 20-30% consumption of DNM in the first 20 minutes followed by a much slower conversion.[11] The observed selectivity of bond scission as measured by the yield of 2-Methylnaphthalene/1-Methylnaphthalene (1.6) is what is expected for a free-hydrogen-atom scission pathway.[3a]

Dihydroarene. Anthracene/9,10-Dihydroanthracene **An/AnH_2**

Thermolysis of mixtures of An/AnH_2 at temperatures above 380°C result in a dynamic exchange of hydrogen atoms between the anthracene structures with very little hydrogen formation of hydrogen gas. The process results in a shift of hydrogen from 9,10-dihydroanthracene (AnH_2) to anthracene to yield 1,2,3,4-tetrahydroanthracene (AnH_4). Formation of the AnH_4 has been suggested to occur by a series of RHT steps from AnH∘ to the outer ring of anthracene.[12] However, we have found that the time-dependant formation of AnH_4 can be fit to a series of RRD steps without the need to invoke the RHT pathway.

Thermolysis of DNM in mixtures of An/AnH_2 yields <1% consumption in the first 20 minutes (as compared to >30% in AnH_6). The selectivity of bond scission as measured by 2-Methylnaphthalene/1-Methylnaphthalene is higher, between 4-6. As predicted by our MKM results, the selectivity does not change substantially as the ratio of An/AnH_2 is increased as has been previously suggested[3a]. However, the selectivity is predicted to be very sensitive to the addition of a diluent, such as biphenyl (BP). Adding BP lowers the rate of bond scission by the RRD pathway, but has little effect on the rate of scission by the HA pathway. The net result of the dilution studies is thus a predicted decrease in rate as well as selectivity. The results of the thermolysis study and the predictions of our mechanistic model are shown in Figure I. A set of control experiments was performed to investigate the occurrence of secondary thermolysis events. When a small amount of tetralin, 10% by weight, was added to the starting reaction mixtures of DNM in An/AnH_2, we found that the tetralin was consumed under the reaction conditions at high An/AnH_2 solvent ratios. This is most likely due to the low concentration of AnH_2 donor available for capping the radicals formed by the solvent induced scission. Formation of tetralin products can arise from adding of hydrogen to nonipso positions of DNM.[3c] If these reduced products are consumed in secondary events under the reaction conditions, e.g. low donor concentration and long reaction times, one could be led into believing that a change in hydrogen-transfer pathways was leading to a more efficient utilization of hydrogen from the donor solvent when in fact, the same hydrogen-transfer process could be in operation but the hydrogen is recycled.

Conclusions. MKM and thermochemical kinetic estimates predict that hydrogen atoms dominate the chemistry of strong bond scission. Cyclic olefins are predicted by MKM and have been found experimentally to be extremely rapid with little selectivity and only limited by competition with self reactions consumpting the solvent.

All model compound studies that we have examined[13] can be explained by conventional hydrogen transfer pathways when consideration is given for the uncertainty in estimating the arrhenius-rate parameters. We are gratified that the results from our simple mechanistic model, utilizing only free hydrogen atoms and reverse radical disproportionation pathways, reproduced our own experimental observations regarding relative rates and selectivities of diarylmethane alkyl-arene bond scission in hydroarene donor solvents as well as other published observations.

While the uncertainty in the thermochemical data of free radical pathways does not rule out the possibility of some contributing RHT type pathway, it does require faith to propose a novel hydrogen pathway such as RHT based solely on MKM results. Until either rigorous theoretical approaches or direct, unambiguous experimental evidence is obtained, we suggest caution in invoking the RHT pathway between arenes. On a note of RHT optimism, we suggest that further studies of the RHT pathway should be investigated when polarized transition states are possible.[14]

Experimental. All solvents and reagents were purchased from Aldrich. Anthracene was sublimed, and dihydroanthracene was recrystallized three times from 95% ethanol. Thermolysis experiments of mixtures containing anthracene and dihydroanthracene were prepared in sealed pyrex tubes. Stock mixtures 1/1, 1/5, 5/1 wt/wt were prepared in bulk by grinding the pure compounds together with a roller-ball mixer. Mechanistic Modeling. Acuchem[15] utilizes a variable step integrator to solve stiff integration problems. Temperature dependent molar density of anthracene was obtain from the API reference guide available through Chemical Abstracts online service in file DIPPR.

ACKNOWLEDGEMENT

This work was supported by the U.S. Department of Energy, Office of Basic Energy Research. The Pacific Northwest Laboratory is operated for the U.S. Department of Energy by Battelle Memorial Institute under Contract DE-AC06-76RLO 1830.

REFERENCES AND NOTES

1. Derbyshire, F. J., Varghese, P., and Whitehurst, D. D. *Fuel*, **1982**, *61*, 859.
2. McMillen, D. F., and Malhotra, R. *Fuel Preprints*, **1984**, *30*(4), 297.
3. (a) Malhotra, R., and McMillen, *Energy Fuels* **1990**, *4*, 184. (b) Malhotra, R. and McMillen, D. F., *Energy Fuels* **1993**, *7*, 227. (c) McMillen, D. F., and Malhotra, R *Energy Fuels* **1991**, *5*, 179.
4. Stein, S. E., *Acc. Chem. Res.* 1991, *24*, 350.
5. Diarylmethanes $Ar\text{-}CH_2Ar$, are one of the most thermally stable carbon-carbon bonds in coal related structures. Homolytic bond scission of diarlmethane is BDE >90 kcal/mol.
6. Franz, J. A., Ferris, K. F., Camaioni, D. M., and Autrey, S. T., submitted to *Energy Fuels*
7. a) Stein, S. E., and Brown, R. L, *J. Am. Chem. Soc.* **1991**, *113*, 787. (b) Freund, H., Matturro, W. N., Olmstead, W. N., Reynolds, R. P. Upton, T. H. *Energy Fuels* **1991**, *5*, 840. (c) Tsang, W. *J., Phys. Chem.*, **1986**, *90*, 1152. (d) Nicovich, J. M., and Ravishankara, A. R. *J. Phys. Chem.*, **1984**, *88*, 2534. (e) Burkey, T. J., Majewski, M., and Griller, D., *J. Am. Chem. Soc.*, **1986**, *108*, 2218. (f). Lias, S. G., Bartmass, J. E., Liebman, J. F., Holmes, J. L., Levin, R. D., and Mallard, W. G. *J. Phys. Chem. Ref. Data*, **1988**, *17*, 1. (g) reference 3a.
8. Manka, M. J., and Stein, S. E., *J. Phys. Chem.* **1984**, *88*, 5914.
9. Billmers, R., Griffith, L. L., Stein, S. E., *J. Phys. Chem.* **1986**, *90*, 517.
10. Bedell, M. W., and Curtis, C. W. *Energy Fuels* **1991**, *5*, 469.
11. The slower reaction is from RRD from the AnH_2 formed under the reaction conditions.

12. Arends, I. W. C. E., in *Thermolysis of Arene Derivatives with Coal-Type Hydrogen Donors*, Ph.D. Thesis, 1993, Leiden University, The Netherlands.
13. (a) Camaioni, D. M., Autrey, S. T., and Franz, J. A., *J. Phys. Chem.*, **1993**, *97*, 5791 (b) Autrey, S. T., Camaioni, D. M., Ferris, K. F., and Franz. J. A., *Coal Science Proceedings, International Conference on Coal Science*, **1993**, 336.
14. (a) Metzger, J. O., and *Angew. Chem.* **1986**, *25*, 80. (b) Wagner, P. J., Zhang, Y. and Puchalski, A. E., *J. Phys. Chem.* **1993**, *97*, 13368. (c) Naguib, Y. M. A., Steel, C, and Cohen, S. G. *J., Phys. Chem.* **1988**, *92*, 6574. (d) reference 12.
15. Braun, W., Herron, J. T., and Kahaner, D. K. *Int. J. Chem. Kinet.*, **1988**, *20*, 51.

Table I. Predicted contribution of scission by H-atom pathway, balance RRD. 400°C (Ar/ArH$_2$ 3/1) 10% by weight substrate Ar-R.

	Ph/Ph$_2$	Nap/NapH$_2$	Phen/PhenH$_2$	An/AnH$_2$
Ph-R	100	100	100	98
Nap-R	100	99	99	29
Phen-R	100	69	82	13
An-R	76	58	56	0

Table II. Relative Rate of scission by RRD and H atom pathways. 400°C (Ar/ArH$_2$ 3/1) 10% by weight substrate Ar-R.

	Ph/Ph$_2$	Nap/NapH$_2$	Phen/PhenH$_2$	An/AnH$_2$
Ph-R	3100	40	6	1
Nap-R	1900	80	10	6
Phen-R	1560	100	13	17
An-R	100000	2300	650	12600

Figure I. Mechanistic kinetic model predicted and experimental observed selectivity of Bond Scission. Thermolysis of DNM in Anthracene/Dihydroanthracene (An/AnH$_2$) with (w) and without (w/o) biphenyl and a cyclic olefin 1,4,5,8,9,10-Hexahydroanthracene (AnH$_6$).

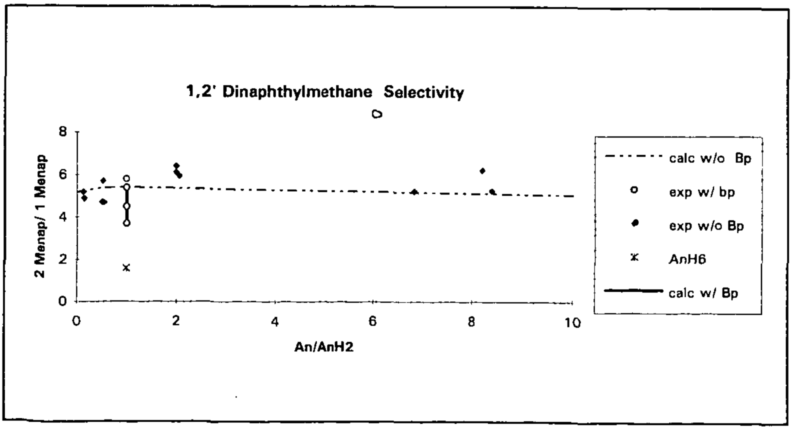

IS RHT ALIVE AND LIVING IN VENEZUELA?

Donald F. McMillen and Ripudaman Malhotra
SRI International, Menlo Park, California 94025

Key Words: Hydrogen transfer, bond cleavage, coal liquefaction.

INTRODUCTION

Under coal liquefaction conditions, hydrogen transfer reactions of various types are so facile, and coal structures so varied and unknown, that were it not for model compounds, the concept of "hydrogen transfer" in coal liquefaction would be little more than a mantra which we recite. Several years ago, studies of hydrogen-transfer reactions in model compounds led to the suggestion, if not the rigorous proof, that a "missing link" in the system of known H-atom transfer reactions was not only kinetically accessible under liquefaction conditions, but also played a key role in bond cleavage during liquefaction.(1-4) More recently, however, specific model-compound and computational studies (5-7) have led researchers to question the general accessibility of "radical hydrogen-transfer" (RHT) compared to other H-transfer pathways. In light of this recent work, it is important to articulate more clearly the limited "window of opportunity" originally posited (2) for RHT, and to reconsider some other model compound systems in each of which one or more of the various alternative transfer pathways are themselves insufficient to account for the observed reaction. The particular difficulty embodied in the following discussion is that no single system has yet been identified in which RHT can be claimed to be free of competition with *all* other H-transfer routes. The ultimate goal of this reconsideration of model compound studies is to obtain an improved view of the probable importance of RHT in coal liquefaction and in catalytic hydrotreatment of heavy oils.

There are two aspects of hydrogen transfer as related to fossil fuel conversion: what hydrogen transfer accomplishes, and how the transfer takes place. In recent years there has been an evolution of thinking related to both aspects. H-transfer was once considered to come only after weak-bond homolysis, serving merely to prevent retrogressive reactions of fragment radicals. In recent years, however, many model compound studies (1,2,4,8-10) have shown beyond a doubt that H-atom transfer, both abstractive and additive, and not involving free H-atoms, induces the cleavage of strong bonds in coal-related structures under the conditions of coal liquefaction. However, the precise modes by which the additive H-transfer occur under any specific conditions have been very difficult to determine with any certainty. It is this latter aspect that we primarily address in this paper.

EXPERIMENTAL SECTION

This paper relys primarily on thermochemical data from the literature and on published model compound kinetic studies, including those of the authors. In most cases, the experimental techniques have involved batch reaction at 350-400°C in borosilicate or fused-silica ampoules housed in a pressure vessel, or in small stainless steel micro-reactors.(2-4) Analyses were generally performed by GC-FID and GC-MS.

RESULTS AND DISCUSSION

Trends in RHT competitiveness with Shifts in Thermochemistry. As reiterated recently (7), it has been asked repeatedly over the last 50 years (2,3,6,11,12) whether direct bimolecular transfer of a hydrogen atom from a hydrocarbon radical to an unsaturated system (RHT) might occur directly. That is, might a direct bimolecular reaction, occurring without the intervention of a free H-atom, be competitive under some conditions with the well-established sequence of H-atom elimination, followed by a separate step in which the H-atom adds to the unsaturated reactant? The answer to that limited question is probably yes. However, because RHT has to compete not only with sequential elimination and addition of H-atoms, but also with H-transfer from closed-shell H-atom sources (e.g., reverse radical-disproportionation, or RRD from hydroaromatic donor molecules themselves), there is likely a substantial range of structures and conditions for which RHT cannot easily be competitive. Notwithstanding difficulty of experimentally determining the precise contribution of RHT when the competitive reactions produce an identical set of products, the thermochemical requirements for a competitive RHT process can be easily delineated.

We will discuss these criteria starting with the anthracene-dihydroanthracene system, since it was the principal solvent used by us in the presentation of the case for RHT, and because Stein and coworkers (13) have used it as both the solvent system and the reaction substrate in studying the kinetics of the net process shown in Reaction 1 (An* in Reaction 1 below is simply anthracene, labeled with an ethyl group at the relatively unreactive 2-position).

$$AnH_2 + An^* \rightleftharpoons An + An^*H_2 \qquad 1)$$

In this case, the reverse radical-disproportionation we have posited as a common initiation step for RHT (often rapid enough to be a pre-equilibrium) simply becomes the stoichiometric transfer step.

$$AnH_2 + An^* \rightleftharpoons 2\,An^*H\bullet \qquad 2)$$

The overall process is completed by H-abstraction (Reaction 3).

$$An^*H\bullet + AnH_2 \rightleftharpoons An^*H_2 + H + AnH\bullet \qquad 3)$$

First, it should be stressed that the system in Reaction 1 is not really a good case for RHT, as becomes clear when the component steps are examined. As we have already noted, in the system studied by Stein (13), RRD is the stoichiometric transfer step; by the time that RHT potentially appears on the scene, the net H-transfer has already been accomplished. Obviously, the only possibility for RHT to play a substantial role in the production of An^*H_2 would be in the limit where the labeled acceptor was in a substantial minority, with respect to an unlabeled acceptor or solvent.

Even in the case where the dominant acceptor is not the substrate to be cleaved, one may ask the intuitively appropriate question, "Why would it be favorable , if the original source of hydrogen in any case is to be AnH_2, to shuttle the hydrogen through the carrier radical AnH•, when this does not in any way change the overall ΔH°?" This question is posed schematically in Figure 1. The answer to the question is (a) in coal liquefaction, an entire assembly of acceptor species, polycyclic Ar, are likely to be present in the solvent at high concentration, and may be statistically (and perhaps thermochemically) favored as the first acceptor of hydroaromatic donor hydrogen, and (b) the stoichiometry of AnH• production by RRD means that two molecules of the carrier radical AnH• are produced in each RRD step, so that the steady state concentration of ArH• varies exponentially with $1/2\ \Delta H°_{RRD}$ (i.e., the thermodynamic "cost" of producing ArH• is only one-half that of producing two ArH•). This is illustrated in Figure 1 by the hypothetical potential energy diagram where anthracene, dihydroanthracene, and dinaphthylmethane are representatives of the generalized system of aromatic /hydroaromatic solvent system (Ar/ArH_2) and cleavable acceptor Ar'-X.

$$ArH_2 + Ar\ \ 2ArH\bullet \qquad 4)$$

$$ArH_2 + Ar'\text{-}X \rightarrow ArH\bullet\ Ar'\text{-}XH\bullet \qquad 5)$$

$$ArH\bullet\ Ar'\text{-}X \rightarrow Ar + Ar'\text{-}XH\bullet \qquad 6)$$

$$Ar'\text{-}XH\bullet \xrightarrow{fast} Ar' + X \qquad 7)$$

$$\frac{Rate_{RRD}}{Rate_{RHT}} = \frac{k_{RRD}\,[ArH_2]\,[Ar'\text{-}X]}{k_{RHT}\,[ArH\bullet]\,[Ar'\text{-}X]} = \frac{k_{RRD}\,[ArH_2]}{k_{RHT}\,(K_4\,[ArH_2]\,[Ar])^{1/2}}$$

$$\frac{A_{RRD}\,(e^{-E°_{RRD}/RT})\,[ArH_2]}{A_{RHT}\,e^{-E_{RHT}/RT}\,([e^{\Delta S°/R}\,e^{-\Delta H°_{RRD}/RT}]\,[ArH_2]\,[Ar])^{1/2}}$$

For $[Ar] = [ArH_2]$, $\Delta S°_{RRD} = 0$, $E_{RRD} = \Delta H°_{RRD}$, $A_{RRD} = A_{RHT}$, and where Ar and Ar'-X are equally good H-acceptors, at equal concentrations, this becomes:

$$\frac{Rate_{RRD}}{Rate_{RHT}} = \frac{e^{-\Delta H°_{RRD}/RT}}{e^{-(E_{RHT} + \frac{1}{2}\Delta H°_{RRD})/RT}}$$

Thus, when Ar and Ar'-X are equally good acceptors, reaction via RHT ArH• (Reaction 6) will tend to be preferred to the extent that the activation energy for the thermoneutral RHT is $< 1/2\ \Delta H°_{RRD}$. One-half of $\Delta H°_{RRD}$ is 17 kcal/mol in the anthracene system; all other kinetic factors being equivalent, an activation energy for RHT of less than 17 kcal/mol or a concentration of Ar greater than that of ArH_2 will favor transfer via RHT, rather than directly from ArH_2 to Ar'-X.

As it happens, our original fitting of data for dinaphthylmethane cleavage in anthracene/dihydroanthracene (14) resulted in an activation energy for thermoneutral RHT of

16.5 kcal/mol, that is, putting RHT in the $An/AnH_2/An'$-X system only at the threshold of RHT feasibility. However, as the H-accepting thermochemistry of the substrate Ar'-X moves away from being thermoneutral, the RHT process can become more accessible, depending on whether its major competition is from RRD or free H-atom addition.

If, as will commonly be the case with an anthracene/dihydroanthracene solvent system, RRD is the major competitor to an (actual or potential) RHT, then a shift in the substrate (or solvent) thermochemistry so as to make the substrate to be a relatively *poorer* acceptor, raising the ΔH° for both RRD and RHT, will make RHT relatively more favorable. While this may seem counter-intuitive, it results because on the one hand, the increase in ΔH°_{RRD} leads to an exactly equal increase in E_{RRD} (as a reaction with zero intrinsic activation energy, i.e., essentially no activation energy in the reverse direction, there can be no further lowering of the intrinsic activation energy). On the other hand, the activation energy for RHT will increase, in the terms of the Evans-Polanyi formalism, by only a fraction of the increase in ΔH°_{RHT} (the fraction being given by $1-\alpha$, where α is the Evans-Polyani factor describing the fraction of a change in the thermodynamics ($\Delta\Delta G^\circ$) of an exothermic reaction that is applied to the kinetics (E_a) of the reaction). Thus an increase in ΔH°_{RHT} from 0 to roughly +13 kcal/mol as the substrate Ar'-X in an anthracene/dihydroanthracene solvent system goes from an H• acceptor that is equally as good as anthracene to one that is 13 kcal/mol poorer (e.g., naphthalene) (14), will result in an increase of 13 kcal/mol in E_{RRD}, but in an expected increase of only roughly 50 to 70% of this value, or 6 to 9 kcal/mol, in E_{RHT}. At 400°C, this will result in a shift toward RHT, relative to RRD, by a factor of 20 to 200. Thus the thermochemistry predicts that RHT will be relatively more favored, in anthracene, by an Ar'-X that is a *poorer* acceptor than anthracene.

In contrast to the case for competition with RRD, if the major competition for an RHT process is sequential elimination and addition of a free H atom, then change in the substrate (or solvent) so as to make RHT more *exothermic* will be a relative benefit to RHT. This is a more easily intuited result than that discussed above: if the solvent system is one in which the carrier radical ArH• eliminates an H atom fairly readily (e.g., phenanthrene/dihydrophenanthrene), then making the substrate Ar'-X a better acceptor, so that the RHT is exothermic, will obviously not influence the unimolecular H-elimination, but will facilitate the RHT step by $\alpha(\Delta\Delta H^\circ_{RHT})$, or 30 to 50% of the $\Delta\Delta H^\circ_{RHT}$. In the case of moving from a phenanthrene-like to an anthracene-like acceptor, this will result, At 400°C, in a shift toward RHT *relative* to free H-atom transfer, by a factor of 10 to 40.

The above considerations reiterate that we expect the contribution of RHT to be sandwiched in a limited region between dominance by RRD on the one hand, and dominance by free H-atoms on the other. More specifically, they indicate that the thermoneutral-RHT system, anthracene/dihydroanthracene/anthracene-X, investigated by Stein (13) is, as he indicated, not the best system for observing RHT, whereas the anthracene/dihydroanthracene/naphthalene-X in which we claimed to have observed RHT (2,14), is relatively much better for this purpose. The exothermic-RHT system, phenanthrene/dihydrophenanthrene/anthracene-X, where Stein did claim (3) to observe substantial RHT, is a relatively good system for that purpose, much better than the near-thermomeutral-RHT system, phenanthrene/dihydrophenanthrene/naphthalene-X, where our data fitting (14) suggested transfer by free H-atoms was twice as important as RHT, even at an aromatic/hydroaromatic ratio of 2/1.

H-Transfer Efficiency and Selectivity. In those of the above cases where the cleavage of dinaphthylmethane was involved, the task of determining the dominant pathway was often made more difficult by competition from indirect cleavage pathways involving initial H-transfer to a non-ipso position on Ar'-X, followed by additional H-transfers to generate reduced, uncleaved products. These uncleaved products can then undergo cleavage either by homolysis of bonds that have been made doubly benzylic by the partial reduction, or by H-abstraction to produce the initially desired, easily fragmentable ipso-radical. In the case of our studies on the anthracene/dihydroanthracene/dinaphthylmethane system, we attempted to limit this additional difficulty by focusing on reaction conditions that minimized multiple H-transfers , i.e., high ratios of anthracene/dihydroanthracene. The high aromatic/hydroaromatic ratio increases H-transfer efficiency by limiting the chances that an initial hydrogen transfer to a non-ipso position (by whatever transfer mechanism) would be followed by additional transfers so as to result in a reduced-uncleaved product. This observed increase in efficiency under conditions of high PAH content, which has been previously discussed 10,14), is strikingly parallel to observed shifts in efficiency in both liquefaction (16) and gasification. (17)

The additional route to cleavage through multiple-H-atom reduction that is discussed in the previous paragraph has made it somewhat difficult to unambiguously apply the otherwise very definitive selectivity diagnostic for the active H-transfer agent. Nevertheless, we believe that positional selectivity in H-atom transfer is a least arguably a useful indicator. Free H-atoms are highly reactive and are expected, and found (14), to show relatively little positional preference for attack at the electronically favored 1-position of naphthalene, as compared to the slightly less favored 2-position. Thus, dominant free H-atom-induced cleavage of 1,2-dinaphthylmethane approaches a 2-methylnaphthalene/1-methylnaphthalene ratio of about 1.6. (14) Any increase from this this ratio necessarily represents a contribution from some other, more selective, H-transfer agent. Cleavage in the anthracene/dihydroanthracene system is found (14) to be highly selective, with the above ratio reaching a value of about 6. However, both RHT and RRD are expected to be very selective, and so this high value, by itself, does not constitute evidence for RHT. In dihydrophenanthrene, however, where RRD is ruled out as a stoichiometric H-transfer step (and where free H-atoms are the main RHT competitor), the observed ratios are 3.0 to 3.5, still substantially higher than 1.6. The higher selectivity ratio would be unequivocal evidence for RHT contribution, were it not for the fact that, even at fairly high phenanthrene/dihydrophenanthrene ratios, there is still a substantial amount of product derived from reduction followed by cleavage.

In the pyrene/dihydropyrene system, the observed selectivity appears still more suggestive, even if not fully unambiguous. Since cleavage rates are about two times higher than in the anthracene solvent system under comparable conditions, and the C-H bond strength in dihydropyrene is 5 kcal/mol *higher* than in dihydroanthracene (14), transfer by RRD is completely ruled out as the cleavage-inducing step. On the other hand, the 2-methylnaphthalene/1-methylnaphthalene selectivity ratio is about 4, well above the 1.6 expected for free H-atoms.(2) The obvious conclusion is that H transfer by RHT is substantial in the case of pyrene; however, here too, the result remains somewhat tainted by the contribution of pathways that involve reduction followed by cleavage.

1,2-Dihydronaphthalene Disproportionation. As is well appreciated by those who have attempted to use either simple product identification or kinetic modeling of total rates, determination by these means of the precise portion of reaction that is accounted for by RHT tends to be very difficult. The best chance for distinction usually lies with an internal comparison and its shift as concentrations change, such as in simple dilution. One of the earliest cases of this approach was that of 1,2-dihydronaphthalene (DHN) disproportionation.(1) The radical-chain disproportionation of 1,2-dihydronaphthalene gives equal amounts of tetralin and naphthalene. The propagation steps, as shown in Scheme 1, are abstraction of a hydrogen from the 3-position of DHN by tetralyl radical (T•), followed by either an RHT to transfer a hydrogen from the 1-hydronaphthyl (NH•) radical to DHN, or sequential H-atom elimination from NH• and addition to DHN, to accomplish the same net change.

The sole difference between these disproportionation pathways involving either free H-atoms or RHT stems from the fact that free H atoms can not only add to DHN, but also abstract from DHN to form H_2. RHT cannot produce H_2. In the case of H-abstraction by H•, the net products of DHN self-reaction become naphthalene and H_2, rather than naphthalene and tetralin. Since the H-transfer by RHT with which the elimination-addition sequence may be competing is a bimolecular reaction, its rate will be decreased by dilution, whereas that for the unimolecular elimination will be unaffected. The subsequent addition of, and abstraction by, H atoms are bimolecular reactions that will be slowed by dilution, but since they both involve reactions with the same molecule, namely DHN (Reactions 7a and 7b in Scheme X), their ratio will not shift with dilution. Thus, the only change with dilution will be the competition between RHT (Reaction 4) and H-atom elimination (Reaction 6). Increasing dilution will increase the relative chance of H-atom elimination, and, to the extent that abstraction by H• competes with addition of H•, the parasitic production of H_2 and naphthalene production without tetralin production will increase.

The quantitative expectations from a steady-state analysis of this system are shown in Figure 2 (reprinted from reference 1), as a series of calculated lines, each of which is based on a particular values of the fraction of free H• that add to (rather than abstract from) DHN. If the reactions in Scheme 1 correctly describe the disproportionation, then the data should be fittable to one of the curves in Figure 2 simply by adjustment of the k_4/k_6 ratio.

Although the naphthalene-tetralin ratios did not vary widely for a substantial range of dilutions, the data are not scattered, and they fit the function form very well, so as to leave little room for adjustment. The very existence of a curved data plot in Figure 2 is significant: if there is no H-transfer by RHT, there will be no competition for the chain propagation by free H-atoms, and there can be no shift in the naphthalene/tetralin ratios with dilution. In fact, these measurements were prompted by related data of Allen and Gavalas (18), and of Franz and coworkers (19), which indicated shifting H_2 yields with changes in dilution. Thus, the observation of *any* shift in the naphthalene/tetralin ratio is evidence for a competing RHT reaction. This conclusion is uniquivocal, *if* (a) the chain length is long and the reverse of the intiation step (a bimolecular reaction) is not a significant product generator, and (b) other side reactions do not distort the product ratio. Both of these qualifications were considered in our original publication and judged to be unimportant.(1) Nevertheless, given the apparently unequivocal nature of the evidence for RHT from this earlier dilution study, and current questions about the accessibility and generality of RHT, we believe the case of 1,2-dihydronaphthalene disproportionation should be re-examined.

SUMMARY

Re-examination of the trends in competition between RHT, RRD, and free H-atom elimination/addition that one expects from thermochemical consideration, reiterates that the supposed case of RHT that has been most called into question by recent studies (7), is in fact expected to be among the poorest of all specific examples of RHT yet claimed. Specific cases of either exothermic or endothermic RHT (e.g., phenanthrene/dihydrophenanthrene, anthracene, or anthracene/dihydroanthracene/dinaphthylmethane, or pyrene/dihydropyrene/dinaphthylmethane are all more expected and more credible. Reexamination of the original 1,2-dihydronaphthalene disproportionation data continues to make this case appear a very credible example of RHT. Nevertheless, the framework of thermochemical considerations discussed here again makes it clear that there is a limited window of opportunity for RHT, in between RRD on the one hand and free H-atom elimination/addition on the other. Current attention would be most usefully directed to this window.

In any event, the case of shifting hydrogen-utilization efficiencies illustrates the important point that competing and shifting competition between various transfer pathways does not render consideration of them irrelevant. On the contrary, the shifting competition makes for situations in which liquefaction effectiveness can vary substantially with shifts in solvent composition or temperature. The situation is indeed complex, and model compounds, judiciously chosen and interpreted in light of data with actual coals or heavy oils, represent the only feasible route for us mortals into the labyrinth of fossil fuel chemistry.

ACKNOWLEDGMENT

The results reviewed in this paper were made possible, in substantial part, by support through several different DOE research contracts.

REFERENCES

1. McMillen, D. F.; Chang, S.-J., Nigenda, S. E.; Malhotra, R. *Am. Chem. Soc. Div. Fuel Chem. Preprints* **1985**, *30*(4), 297.
2. McMillen, D. F.; Malhotra, R.; Chang, S.-J., Ogier, W. C.; Nigenda, S. E.; Fleming R. H. *Fuel* **1987**, *66*, 1611.
3. Bilmers, R.; Brown, R. L.; Stein, S. E. *Int. J. Chem. Kinetics*, **1989**, *21*, 375.
4. Smith, C. M.; Savage, P. E., *Chem. Eng. Sci.* **1993**, *49*, 259.
5. Camaioni, D. M.; Autrey, S. T.; Franz, J. A. *J. Phys. Chem.* **1993**, *97*, 5791.
6. Ruchardt, C.; Gerst, M.; Nolke, M. *Angew. Chem. Int. Ed. Engl.* **1992**, *31*, 1523.
7. Franz., J. A.; Ferris, K. F.; Camaioni, D. M.; Autrey, S. T. *Energy Fuels* **1994**, *8*, XXX.
8. McMillen, D. F.; Malhotra, Hum, G. P.; R. Chang, S.-J. *Energy Fuels* **1987**, *1*, 193.
9. Malhotra, R.; McMillen, D. F., Tse, D. S.; St.John, G. A. *Energy Fuels* **1989**, *3*, 465.
10. McMillen, D. F.; Malhotra, R.; Nigenda, S. E.; *Fuel* **1968**, *68*, 380.
11. Jackson, R. A.; Waters, W. A. *J. Chem. Soc.* **1958**, 4632.
12. Metzger, J. O. *Angew. Chem.* **1986**, *25*, 80.
13. Billmers, R.; Griffith, L. L; Stein, S. E.*J. Phys. Chem.* **1986**, *90*, 517.
14. Malhotra, R.; McMillen, D. F.*Energy Fuels* **1990**, *4*, 184.
15. McMillen, D. F. ; Malhotra, R.; Tse, D. S. *Energy Fuels* **1991**, *5*, 179.
16. Mochida, I.; Yufu, A.; Sakanishi, K. Korai, Y. *Fuel* **1988**, *67*, 114.
17. Gorbaty, M. L.; Maa, P. S. *Am. Chem. Soc. Div. Fuel Chem. Preprints* **1986**, *31*(4), 5.
18. Allen, D. T.; Gavalas, G. R. *Int. J. Chem. Kinetics*, **1983**, *15*, 219.
19. Franz, J. A.; Barrows, B. O.; Camaioni, D. M. *J. Am. Chem. Soc.* **1984**, *106*, 3964.
20. Franz, J. A.; Camaioni, D. M.; Beishline, R. R.; Dalling, D. K. *J. Org. Chem.* **1984**, *49*, 3563.

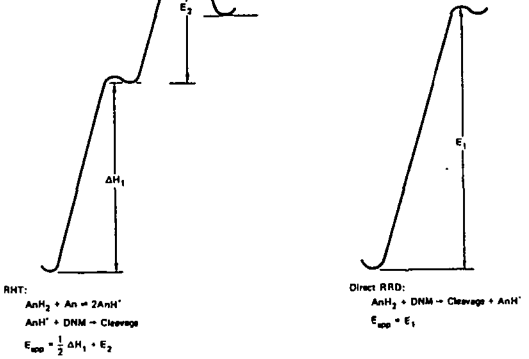

E_2
ΔH_1
E_1
RHT:
$AnH_2 + An \rightleftharpoons 2AnH^{\cdot}$
$AnH^{\cdot} + DNM \rightarrow Cleavage$
$E_{app} = \frac{1}{2}\Delta H_1 + E_2$
Direct RRD:
$AnH_2 + DNM \rightarrow Cleavage + AnH^{\cdot}$
$E_{app} = E_1$

Figure 1. Illustrative potential energy diagram for direct- (RRD) and carrier-radical-mediated hydrogen-transfer (RHT) in the anthracene/9,10-dihydroanthracene/1,2-dinaphthylmethane system.

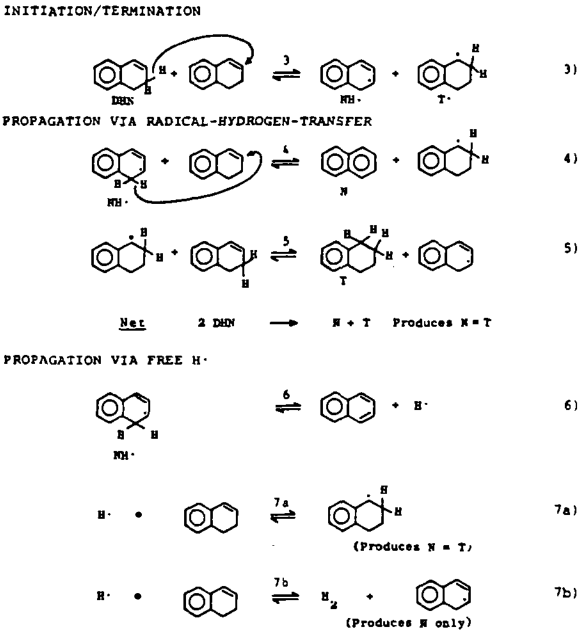
INITIATION/TERMINATION
DHN
NH·
T·
3)
PROPAGATION VIA RADICAL-HYDROGEN-TRANSFER
NH·
N
4)
T
5)
Net 2 DHN → N + T Produces N = T
PROPAGATION VIA FREE H·
NH·
H·
6)
7a)
(Produces N = T)
H_2
7b)
(Produces N only)

Scheme 1. Radical-chain reaction sequence for 1,2-dihydronaphthalene disproportionation.

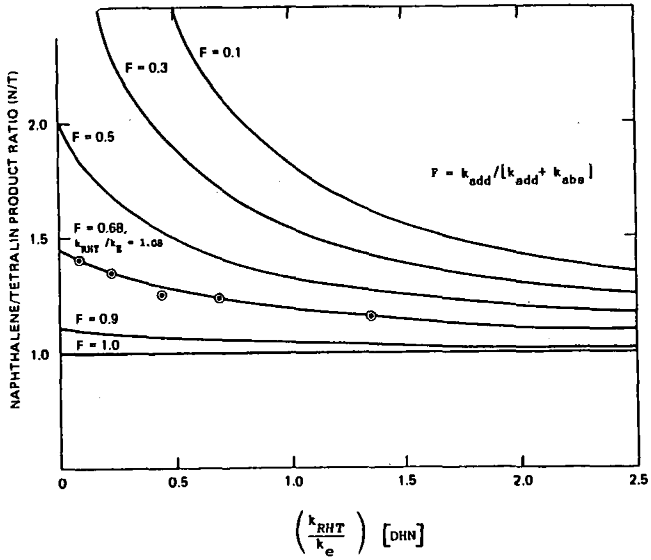

Figure 2. Observed and calculated effect of dilution with biphenyl on the naphthalene/tetralin product ratio in the disproportionation of 1,2-dihydronaphthalene at 385°C.

INTRINSIC BARRIERS FOR H-ATOM TRANSFER REACTIONS

Donald M. Camaioni, S. Tom Autrey, and James A. Franz
Pacific Northwest Laboratory, PO Box 999, Richland, WA 99352

Keywords. H-abstraction, Radical hydrogen transfer, intrinsic barrier

Hydrogen transfer reactions play a well recognized role in coal liquefaction. While H–abstraction reactions between radicals and H–donors have been well studied, understanding of structure-reactivity relationships remains surprisingly incomplete. The Bell-Evans-Polanyi relationship[1] expressed by Equation 1 is used routinely to correlate and predict rates of H–abstraction from a homologous series of donors.

$$E_a = \alpha\Delta H_r + C \qquad 1)$$

The constant, C, is interpreted as the activation barrier if the reactions were to occur with zero enthalpy change. For hydrocarbon radicals, the value of C is usually assigned the barrier for the identity reaction of methyl plus methane with justification being that the few identity reactions that have been measured are all within a few kcal/mol of this value. However, uncertainties of this amount when combined with uncertainties in the reaction enthalpy can lead to orders of magnitude errors in rate estimates.

Another form of hydrogen transfer known as radical hydrogen transfer (RHT)[2,3,4,5,6] is currently the subject of much speculation with respect to its role in coal liquefaction. RHT is unusual in that the radical donates a β–hydrogen to an acceptor molecule rather than abstracting hydrogen from a donor molecule. RHT is known to take place readily between ketones and ketyl radicals.[6] But in hydrocarbon systems, it remains controversial due to a lack of information about its activation barrier. The reaction is thought to be important in high temperature liquid-phase reactions of hydrocarbons[3,4c] and in coal liquefaction[4c,5] where it provides a simple route for migration of hydrogen from hydroaryl to aryl structures and for cleavage of aryl-alkyl bonds. However, multi-step reaction pathways to the same products are usually possible. For RHT to be important, its activation barrier must be sufficiently low to compete with these alternative pathways. In particular, RHT must compete with unimolecular scission of H–atom from the radical and subsequent rapid reactions of free H atoms. Thus, RHT remains controversial due to the lack of information about activation barriers for RHT reactions.

Marcus Theory[7] has been shown to be applicable to atom transfer reactions in the form of Equation 2 but it has received little attention until recently.[8,9,10]

$$E_a = \Delta E^{\ddagger}_i\left(1 + \frac{\Delta E_r}{4\Delta E^{\ddagger}_i}\right)^2 \qquad 2)$$

Marcus theory[7] defines the intrinsic barriers as above and equates it with one-fourth of the bond reorganization energy for forming the transition state (TS) structure. Marcus theory also recognizes that the intrinsic barrier may depend on both the attacking radical and the H donor, and defines the intrinsic barriers for unsymmetrical reactions as the average of the barriers for contributing symmetrical identity reactions. Finally, the Marcus equation simplifies to the Bell-Evans-Polanyi equation when Equation 2 is expanded and the quadratic term is negligible (*i.e.*, reactions that exhibit small exothermicities and large intrinsic barriers). Nonetheless, the possibility that intrinsic barriers are unique for each set of radical and donor should not be neglected.

Recent theoretical[8,11,12] studies of H–abstraction reactions of simple hydrocarbons and functionalized methanes have shown significant variation in intrinsic barrier heights and essentially have validated the assumption of Marcus theory that the intrinsic barrier for cross reactions are approximately the average of that for the two contributing identity reactions. However, a complete understanding of structural effects is still incomplete: for although these studies have shown how the effects of alkyl and heteroatom functional groups attached to the reaction site effect the intrinsic barrier, the effects of delocalizing groups such as vinyl and aryl groups on intrinsic barriers for H–abstraction remain to be examined. Since no kinetic data are available for hydrocarbon RHT reactions, theory-based insights to rate-controlling factors are needed to aid experimental verification and elucidation of this pathway.

COMPUTATIONAL METHODOLOGY. MNDO-PM3[13] calculations of TS geometries and energies (ΔH°_f) were performed using MOPAC (Quantum Chemistry Program Exchange, Department of Chemistry, Indiana University, Bloomington, IN; QCPE No. 455 ver. 6.0). Geometries of transition states for H-atom transfer reactions were optimized using the Hartree-Fock (RHF) half–electron Hamiltonian. TSs for identity reactions were located using the default optimizer by forcing the breaking/forming C-H bonds to have equal lengths. TS geometries for nonidentity reactions were optimized using one or more of the following methods available in MOPAC ver. 6: Bartel's nonlinear least squares minimization routine, McIver-Komornicki gradient minimization routine, and the eigenvector follower optimizers. Force calculations were performed to establish that optimized geometries actually were saddle points for H transfer (only one negative vibrational frequency). The TS energies for twenty H-abstraction reactions were correlated with experimental energies (obtained by summing experimental ΔH°_{f} of the abstracting radicals and hydrogen donors, and experimental activation enthalpies). The least squares fit yielded the following equation and statistical parameters: $\Delta H^{\circ\ddagger}_{f}(\text{expt})=1.14\Delta H^{\circ\ddagger}_{f}(\text{calc})-8.1$ kcal/mol; $r^2=0.9984$; standard error $\Delta H^{\circ}_{f}(\text{calc.})=1.9$ kcal/mol. ΔH°_{f} for radicals and donors were obtained from the literature[14] or derived from standard estimation methods[14] when experimental data were unavailable. Rate data for H–abstraction reactions are from the literature.[15,16] For reactions in which temperature-dependent rate data are lacking, Arrhenius activation energies ($E_{a,x}$) were estimated using Equation 3, which equates the difference in activation energies between the reaction of interest and a basis reaction of known activation energy with the log of the relative rate constant at a known temperature and statistically corrected for the number of donatable-hydrogens.

$$E_{a,2} - E_{a,1} = n_1/n_2 \bullet \ln(k_2/k_1) \qquad 3)$$

RESULTS. Analysis of Errors in the MNDO-PM3 Method. PM3 yields ΔH°_{f} that differ systematically from experimental values with different errors for different structural classes.[17] For example, experimental ΔH°_{f} for polycyclic aromatic hydrocarbons show a linear correlation with PM3 heats. The fit to benzene, naphthalene, phenanthrene and anthracene is excellent ($r^2=0.99993$). Inclusion of higher aromatic hydrocarbons gives a very good fit as well, except for benz[a]phenanthrene, triphenylene, pyrene and tetracene data which are sufficiently far from the line to warrant skepticism about their accuracy. An important feature of the fit is that its has non-unit slope and non-zero intercept. Thus, agreement between theory and experiment differs according to the magnitude of a compound's ΔH°_{f}. In the case of radicals, the errors are systematic for families of structurally-related radicals. For example, primary, secondary and tertiary radicals each exhibit an excellent correlation, deviating -12, -16, and -18 kcal/mol from experiment. We find that experimentally-determined H-abstraction TS energies correlate with PM3 calculated energies, too. The linear correlation between experimental[18] and calculated TS enthalpies is surprisingly good, especially considering that the data base includes reactions of methyl, ethyl, benzyl, and diphenylmethyl radicals with alkane, alkene and aromatic donors and reaction enthalpies range from thermoneutral to -20 kcal/mol. Unlike the correlation for alkyl radicals, a simple offset correction will not suffice to reproduce experimental data. The least squares fit (see Methodology section) to the data yields a non-unit slope of 1.15 and a negative intercept. Therefore, calculated TS energies may be lower than experiment, approximately equal to experiment, or higher than experiment depending on the magnitude of the TS energy.

Barriers for H-Transfer Identity Reactions. The above findings indicate that energy minima and maxima on PM3 potential energy surfaces for H-transfer correlate with experiment. With this insight, reliable structure-barrier trends can be obtained for H-transfer identity reactions provided that the necessary corrections are applied to the reactant energies when the barrier is obtained by taking the difference between TS and reactant energies. We have opted to use experimental data for reactants in our calculations because it reduces the number of structures to be calculated and eliminates the need to determine reactant errors. Barriers so obtained reproduce experimental trends qualitatively.

Barriers for H-Abstraction Identity Reactions. Figure 1 shows results for alkyl radical systems. Intrinsic barriers for H–abstractions decrease in the order: methyl > ethyl ≈ *t*–butyl > *i*–propyl.[19] The barriers for methyl, ethyl and *i*–propyl correlate well with the decrease in bond dissociation energies (BDE) of the R–H bond as expected from ab initio calculations and valence-bond curve-crossing models.[11] We think that the *t*–butyl system is anomalous because PM3 over compensates for methyl group repulsions that develop in the pyramidal TS. Support for this explanation is found in comparisons of the calculated and experimental energies for the isomeric alicyclic butanes and pentanes.[14] PM3 ΔH°_{f} errors parallel the degree of branching. The calculated ΔH°_{f} for *n*-butane is 1.3 kcal/mol larger than the experimental value whereas isobutane is larger by 2.9 kcal/mol. For the pentanes, the calculated ΔH°_{f} are larger by 0.6 kcal/mol for *n*-pentane, 2.4 kcal/mol for isopentane, and 4.5 kcal/mol for neopentane. Allowing for this error, the overall trend in alkyl radical H-abstraction identity barriers is in keeping with experiment[20] and higher level theory.[11] *The downward trend in intrinsic barriers with methyl group substitution shows that the effect of branching at the reaction site stabilizes the TS more than the reactants.*

The effect of conjugation with the reaction site operates in the opposite direction. Results for systems involving π–delocalizing aryl and vinyl groups also appear in Figure 1. Intrinsic barriers for phenyl substitutions increase in the order: ethyl < benzyl < diphenylmethyl. This effect was first noted by Stein[21] who compared the reactivity of methyl, benzyl and diphenylmethyl radicals. A similar effect is calculated for alicyclic polyenyl and arylmethyl systems with intrinsic barriers for increase the order: allyl < pentadienyl < heptatrienyl and benzyl < 1–naphthylmethyl < 9–anthrylmethyl. Good linear correlation with R–H BDEs are obtained for these homologous series, especially when uncertainties associated with radical ΔH°_{f} and BDEs are taken into consideration. *These consistent trends indicate that the TS is stabilized less than the reactants by π–delocalization.*

Interestingly, cyclic donors have lower intrinsic barriers than acyclic polyenyl and arylmethyl systems. Barriers for cyclohexadienyl-plus-cyclohexadiene and hydroanthryl-plus-dihydroanthracene systems are substantially lower than barriers for 1,4-pentadien-3-yl plus 1,4-pentadiene and diphenylmethyl plus diphenylmethane. This trend is attributed to the release of strain in the TS that is present in the cyclic donors but not in the acyclic donors. Cyclic hydroaromatic donors are better than arylalkyl donors for coal liquefaction. Having lower intrinsic barriers for donating H is probably an important but unrecognized contributing factor.

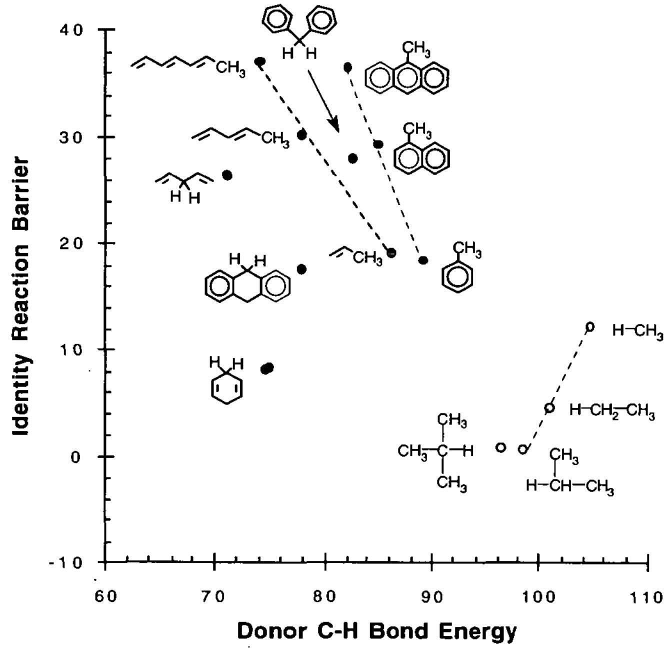

Figure 1. The effects of radical-site branching and conjugation on calculated barriers for H-abstraction identity reactions of hydrocarbon systems: barriers for alkyl systems (o) decrease with donor C-H bond dissociation energy; barriers for conjugated systems (•) show the opposite trend.

Barriers for RHT Identity Reactions. Due to the complete lack of rate data for RHT reactions, a correlation for TS energies cannot be demostrated. However, a rigorous ab initio calculation has been carried out on the prototypical reaction, ethyl plus ethylene. The barrier (26.9 kcal/mol) we calculate using PM3 agrees well with the ab initio barrier (27.2 kcal/mol),[22] provided that the PM3 barrier is obtained from the calculated TS energy and the experimentally-derived ΔH°_f for ethyl and ethylene. PM3 also reproduces the salient features of the ab initio transition structure (linear C–"inflight H"–C bond angle, planar carbons β to inflight H, pyramidal carbons α to "inflight H").[23]

Calculations of TS energies for higher homologs were performed to elucidate structure-reactivity trends for the RHT reaction. In all cases, RHT barriers were obtained from the difference between PM3 TS energies and experimental reactant energies. Barriers for RHT identity reactions were calculated for a series of hydroaryl-plus-arene systems as well as 1-methylallyl plus butadiene. Figure 2 shows trends for conjugated systems plotted against donor radical (HA•) C–H bond energies (estimated from thermochemical data[14] as follows: cyclohexadienyl, 25; 1–hydronaphthyl, 31; ethyl, 36; 9–hydroanthryl, 43; 1–methylallyl, 46). The barriers for hydroaryl radicals *increase* in the series: cyclohexadienyl < 2–hydronaphthyl < 1-hydronaphthyl < 9-hydrophenanthryl < 9-hydroanthryl. The barriers correlate well with the C–H bond strengths for the AH• donor radicals indicating that the BDE is an indicator of the relative RHT barrier heights for aromatic systems. A similar trend is apparent for ethyl and methylallyl radical donors. BDEs for AH• increase because the radicals derive more resonance energy than the olefins or arenes from π–delocalizing benzo and vinyl groups. Similarly, RHT barriers increase because the reactants (mainly the radicals) are being stabilized more than the TS by conjugation effects.

DISCUSSION. It is most noteworthy and surprising that RHT barriers are a substantial fraction (~80% for ethyl-plus-ethylene) of the β-C-H bond energy. In contrast, H-abstraction reactions occur with barriers that are a small fraction (~15% for ethyl-plus-ethane) of the donor C-H bond energy. Our calculations indicate clearly that RHT is intrinsically more difficult than H abstraction. Furthermore, they show that barriers vary significantly with structure such that a single or average intrinsic barrier cannot be used to estimate H-transfer reaction rates accurately. Inspection of the TS geometries calculated for H–abstraction and RHT reactions provides fundamental insight to both the noted effects of π-delocalizing groups and the substantial difference between H-abstraction and RHT barriers. TS structures for H abstraction resemble an H atom in transit between two alkyl groups, not alkyl radicals. A radical sp^2 carbon exhibits a relatively low barrier to pyramidal distortion compared to that for planar distortion of alkyl sp^3 carbon.[24] Consequently, most of the structural reorganization occurs at the radical carbon. Overlap with adjacent π–delocalizing groups is diminished in the TS with the net result being that the reactants are most effected by π-stabilization. For the RHT reaction, the radical site remains planar because it is remote to the carbons that are transferring the H atom. Carbons with greater reorganization energies, sp^3 alkyl and sp^2 alkene/arene, are at the reaction site and must deform to achieve the TS geometry. The sp^3 carbon that is donating the H–atom deforms substantially towards sp^2 character to achieve the TS. Thus, the RHT TS resembles an H atom interacting with the termini of two olefinic or aromatic moieties. With these insights, the greater barriers for RHT compared to H-abstraction are not surprising. The increase in barrier with benzannelation of the cyclohexadienyl–plus–benzene and vinylogous homologation of the ethyl–plus–ethylene systems is also consistent with these insights. Radicals derive relatively more stabilization from conjugation than olefins and arenes. Otherwise, the HA• BDEs would not increase with conjugation. The loss of radical character and development of olefin/arene character on forming the RHT TS causes the reactants to be stabilized more by conjugation; which explains why RHT barriers correlate so well with the AH• BDEs.

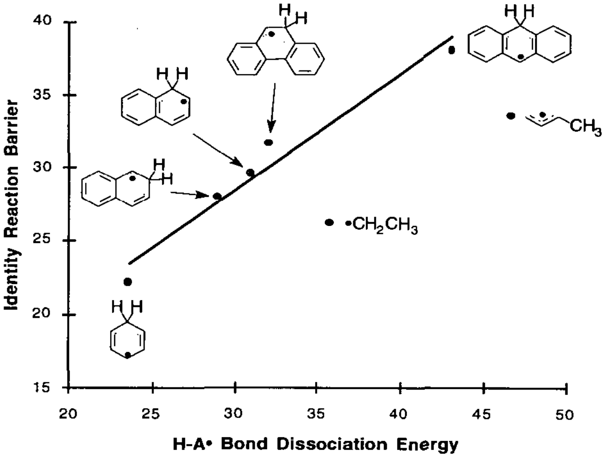

Figure 2. Barriers for radical hydrogen transfer identity reactions of conjugated systems increase with degree of conjugation. The effect correlates well with the bond dissociation energies of homologous radicals.

ACKNOWLEDGEMENT. This work was supported by the U.S. Department of Energy, Office of Basic Energy Research, Division of Chemical Sciences, Processes and Techniques Branch. The authors thank Dr. Kim F. Ferris (PNL) for discussions and Terrance E. Salinas (undergraduate summer research fellow, Northwest Association of Colleges and Universities for Science) for assistance.

REFERENCES

1. Bell, R. P.; Proc. R. Soc. (*London*)**1936**, *A154*, 414. Evans, M. G.; Polanyi, M. *Trans. Faraday Soc.* **1936**, *32*, 1333.

2. Jackson, R. A.; Waters, W. A. *J. Chem. Soc.* **1958**, 4632.

3. Metzger, J. O.; *Angew. Chem. Int. Ed. Engl.*. **1986**, *25*, 80.

4. a) Billmers, R.; Griffith, L. L.; Stein, S. E. *J. Phys. Chem.* **1986**, *90*, 517. b) Billmers, R.;

Brown, R. L.; Stein, S. E. *Int. J. Chem. Soc.* **1989**, 21, 375. c) Stein, S. E. *Acc.. Chem. Res.* **1991**, *24*, 350.

5. (a) Malhotra, R.; McMillen, D. F. *Energy and Fuels* **1993**, *7*, (b) McMillen, D. F., Malhotra, R., Tse, D. S. *Energy and Fuels* **1991**, *5*, 179. (c) Malhotra, R. and McMillen, D. F. *Energy and Fuels* **1990**, *4*, 184. (d) McMillen, D. F.; Malhotra, R.; Hum, G. H.; Chang, S. -J. *Energy and Fuels* **1987**, *1*, 193. (e) McMillen, D. F.; Malhotra, R.; Chang, S. -J.; Ogier, W. C.; Nigenda, S. E. *Fuel* **1987**, *66*, 1611.

6. (a) Wagner, P. J.; Zhang, Y.; Puchalski, A. E. *J. Phys. Chem.* **1993**, *97*, 13368. (b) Neckers, D. C.; Schaap, A. P.; Harry, J. *J. Am. Chem. Soc.* **1966**, *88*, 1265.

7. Marcus, R. A. *J. Phys. Chem.* **1968**, *72*, 891.

8. Lluch, J. M.; Bertran, J.; Dannenberg, J. J. *Tetrahedron* **1988**, *44*, 7621-7625. Dannenberg, J. J. *Adv. Molec. Modelling* **1990**, 2, 1.

9. Fox, G. L.; Schlegel, H. B. *J. Phys. Chem. Soc.* **1992**, *96*, 298-302

10. Denisov, E. T.*Mendeleev Commun.* **1992**, 1-2; *Kinet. Katal.*, **1991**,*32*, 461-5.

11. Yamataka, H.; Nagase, S. *J. Org. Chem.* **1988**, *53*, 3232.

12. Pross, A.; Yamataka, H.; Nagase, S. *J. Phys. Org. Chem.* **1991**, *4*, 135.

13. Steward, J. J. P. *J. Comput. Chem.* **1989**, *10*, 209, 221.

14. Lias, S. G.; Bartmess, J. E.; Liebman, J. F.; Holmes, J. L.; Levin, R. D.; Mallard, W. G. *J. Phys. Chem. Ref. Data* **1988**, *17*, Sup. 1. Cox, J. D.; Pilcher, G. *Thermochemistry of Organic and Organometallic Compounds*; Academic Press: New York, 1970, pp 516. Griller, D.; Martinho Simoes, J. A.; Sim, B. A.; Wayner, D. D. M. *J. Am. Chem. Soc.* **1989**, *111*, 7872. Nagaoka, T.; Berinstain, A. B.; Griller, D.; Wayner, D. D. M. *J .Org. Chem.* **1990**, *55*, 3707. Seakins, P. W.; Pilling, M. J.; Niiranen, J. T.; Gutman, D.; Krasnoperov, L. N. *J. Phys. Chem.* **1992**, *96*, 9847.

15. Kerr, J. A. *Free Radicals;* Kochi, J. K., Ed.; Wiley, New York: 1973; Vol. 1; p. 15; Ingold, K. U. *ibid.*, pp. 74, 75.

16. Bockrath, B.; Bittner, E.; McGrew, J. *J. Am. Chem. Soc.* **1984**, *106*, 135; Franz, J. A.; Alnajjar, M. S.; Barrows, R. D.; Kaisaki, D. L.; Camaioni, D. M.; Suleman, N. K. *J. Org. Chem.* **1986**, *51*, 1446; Manka, M. J.; Brown, R. L.; Stein, S. E. *Int. J. Chem. Kinet.* **1987**,*19*, 943.

17. The AM1 Hamiltonian yields similar results. Camaioni, D. M. *J. Am. Chem. Soc.* **1991**, *112*, 9475.

18. TS energies are obtained by summing values for the experimental activation enthalpy, and ΔH_f of reactants, $\Delta H_f(\mathrm{TS}) = E_a - \mathrm{RT} + \Delta H_f(\mathrm{R\text{-}H}) + \Delta H_f(\mathrm{R}\bullet)$

19. If the barriers are obtained using PM3 energies for the reactants, then an opposite and erroneous trend is obtained: methyl, 11.7; ethyl, 13.5; isopropyl, 14.7; *t*–butyl, 18.6.

20. Identity barriers for *t*-butyl and isopropyl radicals are estimated to be 9 and 11 kcal/mol respectively from experimental data[15] for the cross reactions of isobutane and propane with methyl and ethyl radicals.

21. Manka, M. J.; Brown, R. L.; Stein, S. E. *Int. J. Chem. Kinet.* **1987**, *19*, 943-957

22. The cited value is for a PMP2/6-31G** calculation that includes corrections for spin annihilation, thermal and zero point energy differences, and basis set superposition errors. Franz, J. A.; Autrey, T. A.; Camaioni, D. M.; Ferris, K. F., To be published.

23. Reaction site parameter, ab initio value, PM3 value: C_α-"inflight H", 1.36 Å, 1.42 Å; C_β–C_α–"inflight H", 113°, 106°; C_β-C_α-H-H reaction site torsional angle, 143°, 152°.

24. Yamada, C. Hirota, E.; Kawaguchi, K. *J. Chem. Phys.* **1981**, *75*, 5256.

MECHANISTIC MODELLING OF 9,10-DIMETHYLANTHRACENE THERMOLYSIS

P.S. Virk and V.J. Vlastnik
Department of Chemical Engineering
M. I. T., Cambridge, MA 02139

KEYWORDS: Thermolysis, Mechanism, Kinetics, Numerical Simulation, Modelling.

INTRODUCTION

Motivation. The present work on modelling thermolysis of a methylated aromatic acene continues our studies [1,2] of simple substrates that mimic the chemical moieties found in complex fossil materials of engineering interest. The 9,10-dimethylanthracene, abbr. 910DMA, substrate was chosen because its acene ring is prototypical of the aromatic ring systems found in fossil materials, while its methyl groups typify the electron-donating substituents commonly pendant thereon.

Previous Work. Thermolysis of 910DMA has not previously been studied by other authors.

Outline. Our modelling of 910DMA thermolysis is based upon a 10-step mechanism, valid at low conversions, that was recently formulated to describe experimental observations [1,2]. Thermochemical parameters for all stable and radical species occurring in the mechanism were estimated from first principles. Next, enthalpies of reaction were calculated for each elementary step and used to infer Arrhenius parameters in both forward and reverse directions. Rate constants were then calculated for each reaction at a selected temperature, and these were used in conjunction with the differential conservation relations for each species to effect a full numerical solution of the model system, starting from an initial condition of pure substrate. The numerical simulation of 910DMA thermolysis kinetics and product selectivities was directly compared with experimental observations at the same conditions. A sensitivity analysis was performed to discern how errors in the estimated Arrhenius parameters affected the model results. Finally, the Arrhenius parameters of certain elementary steps were adjusted, within their error limits, to provide an optimized model that best-fit the experimental observations.

REACTION PATHWAYS & MECHANISM

Pathways. Earlier experiments have identified three primary parallel pathways for thermolysis of 910DMA, namely: (P1) hydrogenation to *cis-* and *trans*-9,10-dihydro-9,10-dimethylanthracene, abbr. DHDMA, (P2) demethylation to 9-methylanthracene, abbr. 9MA, and (P3) methylation to 1,9,10- and other trimethylanthracene isomers, abbr. TMA. The primary demethylation product 9MA is associated with methane gas formation, and considerable amounts of heavy products are formed, including both pure- and cross-termination types of dimeric species related to 910DMA and DHDMA.

Mechanism. A possible mechanism for 910DMA thermolysis is presented in Fig. 1. This elementary step "graph" is constructed with substrate and all stable molecular products arrayed in the bottom row and unstable radical intermediates arrayed in the top row. Reaction "nodes", arrayed in the middle row, connect the individual species in the bottom and top rows with arrows indicating the initial direction of reaction (all reactions are, of course, reversible). Initiation reactions are denoted by solid interconnecting lines, propagation reactions by various kinds of dashed lines and termination reactions by dotted lines. Arrow weights depict the relative elementary reaction traffic, to be discussed in the next section.

The free-radical cycle is initiated by the bimolecular disproportionation of substrate (R1), an intermolecular hydrogen transfer reaction, to form the respectively dehydrogenated and hydrogenated radical species 910DMA* and HDMA*. Of these, the latter can either abstract hydrogen from 910DMA by (R2), to form DHDMA products, or undergo a β-scission type of radical decomposition by (R3), forming 9MA product and a methyl radical CH_3*. The CH_3* can either abstract H from 910DMA by (R4), to form methane product, or add to 910DMA by (R5), to form the trimethyl radical HTMA1*. The latter can then abstract H from 910DMA via (R6) to form the observed TMA product. The radical cycle is terminated by the species 910DMA* and HDMA* engaging in both pure- and cross-combinations, (R7-R9), to form various dimeric products. HDMA* radical can also terminate by disproportionation, (R10), to form 910DMA and DHDMA.

The proposed mechanism accounts for the major products, 9MA, TMA, DHDMA, CH_4 and heavies, observed during the initial stages of 910DMA thermolysis. Each of the observed triad of primary pathways arise naturally as limiting cases of the graph, with P1, hydrogenation, comprising the set [R1, R2, R7]; P2, demethylation, the set [R1, R3, R4, R7]; and P3, methylation, the set [R1, R3, R5, R6, R8]. The stoichiometry of these sets restricts the maximum selectivity of each major product to 1/3, which is of the magnitude of the highest selectivities observed. The mechanism also suggests that the relative kinetics of the observed hydrogenation and demethylation pathways, (P1)/(P2), are controlled by the HDMA* radical, through the ratio of its H-abstraction to β-scission reactions (R2)/(R3). Further, the observed methylation to demethylation pathway ratio, (P3)/(P2), is governed by competition between methyl radical reactions (R4) and (R5), in which CH_3* either abstracts H from or adds to the 910DMA substrate.

MODELLING

Thermochemistry. Enthalpies of formation, ΔH^0_f, for all chemical species participating in our 910DMA thermolysis model were estimated by a "macro" group-additivity technique, using a basis set of bond strengths, D^0 kcal/mol, steric corrections, C^0 kcal/mol, and stable species enthalpies of formation, ΔH^0_f, assembled from a variety of literature sources [3-10]. Fig. 2 illustrates the estimation procedures. For the stable species 9MA in (a), we started with the largest, most structurally similar basis species available, namely ANT; other basis species and steric corrections, in this case 1MN, NAP and an alkene gauche interaction, were then either added or subtracted to bridge the structural differences between the starting and the desired species. The method provided both ΔH^0_f, kcal/mol, and its rms error, kcal/mol. Calculations for a radical species, HDMA*, are shown in Fig. 2(b).

Arrhenius Parameters. Arrhenius expressions of the form $\log_{10} k = \log_{10} A - E^*/\Theta$, with rate constant k (l, mol, s units), pre-exponential factor A (same units as k), activation energy E^* (kcal/mol), and scaled temperature $\Theta = 0.004573*(T\ C + 273.2)$, were generated for each elementary step of the 910DMA thermolysis mechanism, as summarized in Table 1. An elementary reaction was first classified (column 2), using standard free-radical reaction notation. Next, kinetic data [5, 11-14] for that type of reaction was analyzed to ascertain its activation parameters. Of these, $\log_{10}A = \log_{10}A_{int} + \log_{10}(rpd)$ was decomposed into an intrinsic portion, $\log_{10} A_{int}$ (column 3) and a reaction path degeneracy, rpd (column 4). Activation energy E^* was determined by an Evans-Polanyi expression (column 5), of form $E^* = E_0 + \alpha.\Delta H^0_r$ with α = 0 (combinations), 0.5 (H-abstraction and transfer) or 1 (homolysis, beta-scission). Values of the enthalpy of reaction ΔH^0_r (column 6), derived from thermochemical estimates of the previous section, then led to E^* (column 7) and the final Arrhenius expression (column 8).

Numerical Solution. The model 910DMA thermolysis reaction system was solved by a computer code called ACUCHEM [15]. This program numerically solves a system of differential equations that describe the temporal behavior of a spatially homogeneous, isothermal, multicomponent chemical reaction system. Integrations are performed by the method of Gear [16], appropriate for the stiff differential equations encountered in the present case. Two types of tests were performed to ensure reliable results. First, in regard to stability, it was verified that the program generated the same concentration profiles, regardless of the time step size. Second, in regard to fidelity, the concentrations of all species, both radical and stable, calculated by the numerical solution at low conversions $X < 0.1$ were found to agree with the corresponding concentrations obtained from pseudo-steady-state algebraic solutions at similar conditions.

RESULTS & DISCUSSION

Original Model. Numerical solutions of the 910DMA thermolysis model were obtained at selected conditions covering the entire experimental grid, $315 < T\ C < 409$ and $0.082 < [910DMA]_0$ mol/l < 2.47. The complete concentration histories of all radical and stable species obtained from each simulation were then used to prepare the illustrations in Figs. 1, 3 and 4.

Reaction Traffic. The arrows in Fig. 1 graphically depict the elementary reaction traffic as calculated at T = 355 C, $[910DMA]_0$ = 0.82 mol/l, and conversion X = 0.31, the thicker arrows denoting reactions with the greater net (forward - reverse) rates. The 910DMA substrate decomposes mainly, but not exclusively, by (R1). The rates of hydrogenation (R2) and of demethylation (R3) are of comparable magnitudes, with (R3) > (R2). Methyl radical quenching by H-abstraction from substrate (R4) greatly exceeds its addition to the substrate (R5). Among termination reactions, (R7 - R10), 910DMA* combination (R7) is dominant.

Kinetics. Fig. 3 compares substrate decay half-lives t* calculated from the model (hollow points and dashed lines) with those observed experimentally, (solid points and lines). Fig. 3(a), a semi-logarithmic Arrhenius-type plot of t^* vs. $1/\Theta$, shows that, at constant $[910DMA]_0$ = 0.82 mol/l, the calculated t* are about 3-fold higher than experimental at all temperatures. Decomposition kinetics predicted by the model are thus slower than experimental, but exhibit roughly the same apparent activation energy. Fig. 3(b), a log-log plot of t^* vs. $[910DMA]_0$ at constant T = 355 C, shows that the calculated t* are 2- to 10-fold higher than experimental, the more so at the lowest $[910DMA]_0$, with the model predicting an apparent decomposition reaction order ~2, somewhat greater than the experimentally observed order ~1.5.

Product Selectivities. Fig. 4 compares (a) the selectivity to 9MA product and (b) the ratio of TMA/9MA products, as calculated from the model, with those observed experimentally, using semi-logarithmic Arrhenius-type coordinates of either S(9MA) or R(TMA/9MA) vs. $1/\Theta$ at constant $[910DMA]_0$ = 0.82 mol/l. In Fig. 4(a) the model is seen to predict a 9MA selectivity S(9MA) from 0.1 to 0.7 orders of magnitude below experimental, while in Fig. 4(b) model predictions of the major product ratio R[TMA/9MA] lie within ±0.2 orders of magnitude of the experimental observations.

Sensitivity Analyses. The significance of the differences between model predictions and experimental observations was sought from sensitivity analyses at T = 355 C and $[910DMA]_0$ = 0.82 mol/l, the central point of the experimental grid, by separately perturbing the kinetics of selected elementary steps. The effects of these perturbations on the predicted decay half-life t^*, 9MA selectivity S(9MA), and the primary product ratio R[TMA/9MA], are shown by the vertical dashed lines in Figs. 3 and 4. In Figs. 3(a) and (b), for example, the uncertainty in t* was estimated by perturbing the activation energy E^*_1 by ± 4.4 kcal/mol (the inherent error in ΔH^0_{r1}), since the elementary reaction R1 contributes most heavily to the destruction of 910DMA substrate in our model. The upper and lower ends of the vertical dashed lines in each portion of Fig. 3 represent values of t^* obtained by negative and positive perturbations, respectively, of E^*_1. This sensitivity analysis shows that the inherent uncertainties of ± 1.5 orders of magnitude in values of t^* calculated by the model considerably exceed the 0.5 to 1.0 order of magnitude differences between the model results and experimental observations. That is, within its (large) error limits, the model yields half-lives in agreement with experiments. Similar sensitivity analyses provided the vertical dashed lines in each of Figs. 4(a) and (b), showing that, within its error limits, the model also yielded 9MA selectivities and TMA/9MA ratios in accord with experiment.

Optimized Model. The preceding comparisons between model and experimental results are mildly noteworthy because all the kinetic parameters employed in the original model were derived from first principles and used without adjustments. However, these comparisons also revealed the empirical alterations that might permit a best-fit of experimental results for engineering purposes, termed the "optimized" model. Specifically, the best-fit of all experimental data for 910DMA thermolysis at T = 355 C with $[910DMA]_0$ = 0.82 mol/l arose by altering the original activation energies E^*_1, E^*_2, E^*_{-2} and E^*_3 by respective amounts of -1.2, +1.2, -1.2 and -1.2 kcal/mol, all of these changes being well within the inherent uncertainties of these parameters, respectively, ±4.4, ±2.4, ±2.4 and ±3.7 kcal/mol. Figs. 5 (a) and (b) compare substrate and product histories obtained from the optimized model (lines) to the experimental data (points) for 910DMA, 9MA, TMA, CH4, and DHDMA. Fig. 5(a) shows the optimized model to well predict the observed 910DMA decay, with decay half-lives t^* = 25000 s from the model versus 22000 s experimental. The absolute amounts of 9MA and of TMA formed by the model are both about 1.5-fold lower than experimental in Fig. 5(a), but the model well predicts the relatively small amounts of DHDMA, and its delicate variation with time, in Fig. 5(b). Finally, Figs. 6(a) and (b) show that the optimized model provides the correct magnitudes of the major product ratios R[DHDMA/9MA] and R[TMA/9MA], as well as a qualitative indication of their respective variations with conversion. For example, at all conversions $0.0 < X < 0.54$ the ratio R[TMA/9MA] ~ 0.25 from the model lies astride the experimental data.

Modelling Perspective. In regard to both thermolysis kinetics and the selectivities of major products, the predictions of the optimized model are appreciably closer to the experimental observations than those of the original model. However, the differences between the activation parameters of the optimized and original models, of order 1.2 kcal/mol, are small relative to the inherent uncertainties in these parameters, of order 3.5 kcal/mol. Thus, although the optimized model effects an appealing cosmetic improvement over the original model, of possible value in engineering applications, the two models remain statistically similar. Substantive scientific improvements in modelling thermolyses such as the present must await better methods, and more reliable data, for deriving the kinetics of the underlying elementary reactions.

ACKNOWLEDGEMENT: This work was supported in part by Cabot Corporation, Boston, MA.

REFERENCES

[1] Virk, P.S.; Vlastnik, V.J.: PREPRINTS, Div. of Petrol. Chem., ACS, 38(2), 422 (1993).

[2] Virk, P.S.; Vlastnik, V.J.: PREPRINTS, Div. of Fuel Chem., ACS, 39(2), 546 (1994).

[3] Stull, D.R.; Westrum, Jr., E.F.; Sinke, G.C.: The Chemical Thermodynamics of Organic Compounds, Wiley, New York (1969).

[4] Benson, S.W.; Cruickshank, F.R.; Golden, D.M.; Haugen, G.R.; O'Neal, H.E.; Rodgers, A.S; Shaw, R.; Walsh, R.: Chem. Rev., 69, 279 (1969).

[5] Benson, S.W.: Thermochemical Kinetics, 2nd Ed., Wiley, New York (1976).

[6] Stein, S.E.; Golden D.M.; Benson, S.W.: J. Phys. Chem., 81, 314 (1977).

[7] Shaw, R.; Golden, D.M.; Benson, S.W.: J. Phys. Chem., 81, 1716 (1977).

[8] Pedley, J.B.; Naylor, R.D.; Kirby, S.P.: Thermochemical Data of Organic Compounds, Chapman & Hall, London (1986).

[9] Bordwell, F.G.; Cheng, J.P.; Harrelson, Jr., J.A.: J. Am. Chem. Soc., 110, 1229 (1988).

[10] Stein, S.E.; Rukkers, J.M.; Brown, R.L.: Structures and Properties Database and Estimation Program, Ver. 1.1, NIST, (1991).

[11] Ingold, K.U.; pp 37-66 in Kochi, J.K.: Free Radicals Vol. I, Wiley, New York, (1969).

[12] Kerr, J.A.; pp 1-36 in Kochi, J.K.: Free Radicals Vol. I, Wiley, New York, (1969).

[13] Holt, P.M.; Kerr, J.A.: Int. J. Chem. Kinet., 9, 185 (1977).

[14] Billmers, R.; Griffith, L.L.; Stein, S.E.: J. Phys. Chem., 90, 517 (1986).

[15] Braun, W.; Herron, J.T. and Kahaner, D.K.: Int. J. Chem. Kinet., 20, 51 (1988).

[16] Gear, C.W.: Numerical Initial Value Problems in Ordinary Differential Equations, Prentice-Hall, N.J., 1971.

Table 1. Evans-Polanyi Relations and Arrhenius Parameters for Model Elementary Reactions.

	Type of Reaction	$\log_{10} A_{int}$ $l\ mol^{-1}\ s^{-1}$	rpd	Evans-Polanyi Relation: $E^* =$	ΔH_r° kcal/mol	E^* kcal/mol	Arrhenius Expression: $\log_{10} k =$
R1	molecular disproportionation	8.5	24	ΔH_r°	43.4	43.4	$9.9 - 43.4/\theta$
R-1	radical disproportionation	8.5	1	0	-43.4	0	8.5
R2	H-abstraction	8.1	6	$17.5 + \Delta H_r^\circ/2$	1.2	18.1	$8.9 - 18.1/\theta$
R-2	H-abstraction	8.1	2	$17.5 + \Delta H_r^\circ/2$	-1.2	16.9	$8.4 - 16.9/\theta$
R3	methyl scission	13.5	1	$2.1 + \Delta H_r^\circ$	29.5	31.6	$13.5 - 31.6/\theta$
R-3	$CH3^\bullet$ addition	8.3	1	2.1	-29.5	2.1	$8.3 - 2.1/\theta$
R4	H-abstraction	8.1	6	$17.5 + \Delta H_r^\circ/2$	-22.7	6.2	$8.9 - 6.2/\theta$
R-4	H-abstraction	8.1	4	$17.5 + \Delta H_r^\circ/2$	22.7	28.9	$8.7 - 28.9/\theta$
R5	$CH3^\bullet$ addition	8.3	4	5.1	-18.6	5.1	$8.9 - 5.1/\theta$
R-5	methyl scission	13.5	1	$5.1 + \Delta H_r^\circ$	18.6	23.7	$13.5 - 23.7/\theta$
R6	radical H transfer	8.1	2	$17.5 + \Delta H_r^\circ/2$	-13.2	10.9	$8.4 - 10.9/\theta$
R-6	radical H transfer	8.1	1	$17.5 + \Delta H_r^\circ/2$	13.2	24.1	$8.1 - 24.1/\theta$
R7	radical combination	9.3	1	0	-54.2	0	9.3
R-7	homolytic dissociation	15.5	1	ΔH_r°	54.2	54.2	$15.5 - 54.2/\theta$
R8	radical combination	9.3	1	0	-52.4	0	9.3
R-8	homolytic dissociation	15.5	1	ΔH_r°	52.4	52.4	$15.5 - 52.4/\theta$
R9	radical combination	9.3	1	0	-50.7	0	9.3
R-9	homolytic dissociation	15.5	1	ΔH_r°	50.7	50.7	$15.5 - 50.7/\theta$
R10	radical disproportionation	8.5	1	0	-42.2	0	8.5
R-10	molecular disproportionation	8.5	4	ΔH_r°	42.2	42.2	$9.1 - 42.2/\theta$

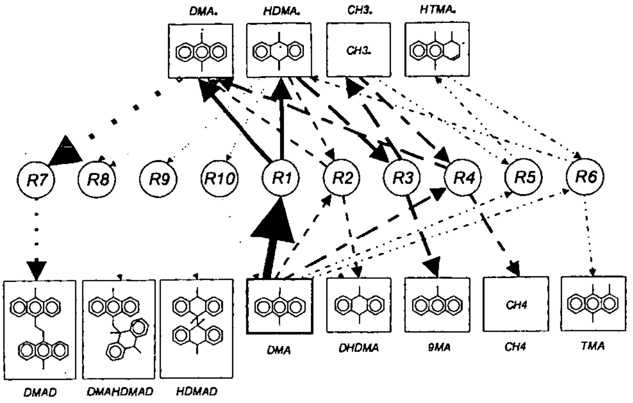
DMA.
HDMA.
CH3.
HTMA.
CH3.
R7
R8
R9
R10
R1
R2
R3
R4
R5
R6
DMAD
DMAHDMAD
HDMAD
DMA
DHDMA
9MA
CH4
CH4
TMA

Figure 1. Elementary Step Graph of 910DMA Thermolysis Mechanism. Arrow weights depict relative reaction traffic at T = 355 C, [910DMA]o = 0.82 mol/l, and conversion X = 0.31, as calculated from the original model (see text).

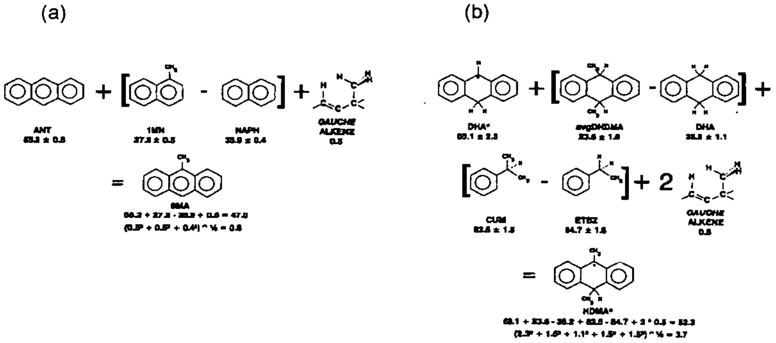
(a)
(b)
ANT
1MN
NAPH
GAUCHE ALKENE
9MA
DHA*
avgDHDMA
DHA
CUM
ETBZ
GAUCHE ALKENE
HDMA*

Figure 2. Illustration of Macro-Group Additivity Scheme for Estimation of Thermochemical Properties of (a) Stable and (b) Radical Species.

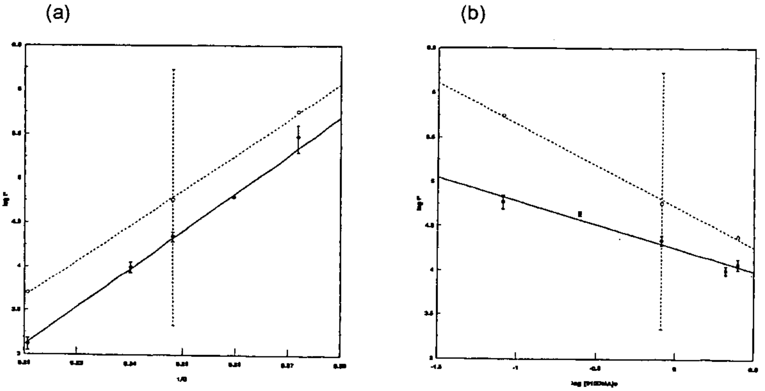

Figure 3. Decay Half-Lives t* Experimental (solid circles and lines) Versus Calculated From Original Model (hollow circles, dashed lines) at (a) constant [910DMA]o = 0.82 mol/l and (b) constant T= 355 C.

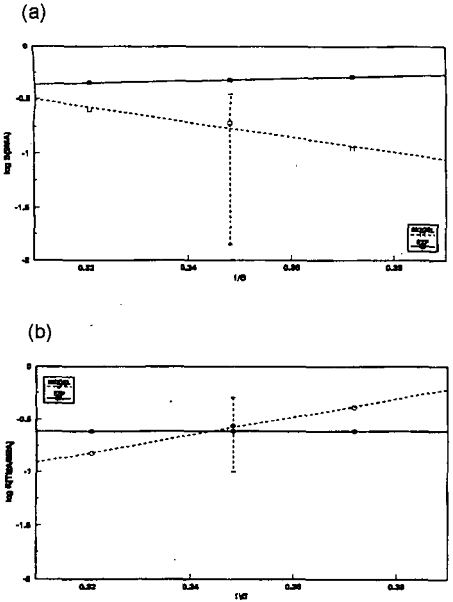

Figure 4. Original Model Results
(hollow points, dashed lines) vs.
Experiments (solid points, solid lines).
(a) *Selectivity to 9MA*, (b) Ratio [TMA/9MA].

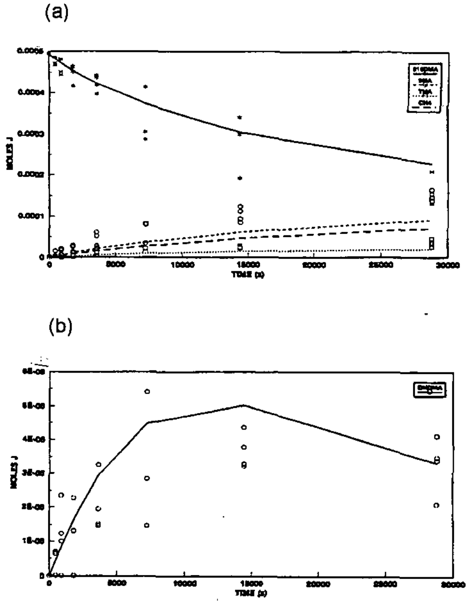

Figure 5. Optimized Model Results
(lines) vs. Experiments (points) at
T = 355 C with [910DMA]o = 1.82 mol/l.
(a) 910DMA, 9MA, CH4, TMA, (b) DHDMA.

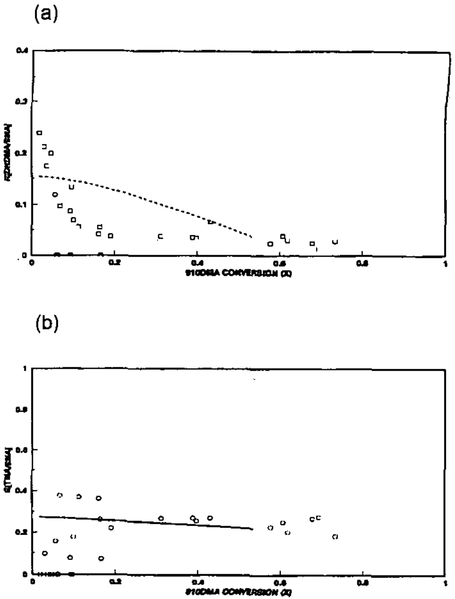

Figure 6. Optimized Model Results
(lines) vs. Experiments (points) at
T = 355 C with [910DMA]o = 1.82 mol/l.
(a) *Ratio DHDMA/9MA*, (b) *Ratio TMA/9MA*.

HEAT TREATMENT OF COALS IN HYDROGEN-DONATING SOLVENTS AT TEMPERATURES AS LOW AS 175-300℃

Masashi Iino and Jianli Shen
Institute for Chemical Reaction Science, Tohoku University,
Katahira 2-1-1, Aoba-ku, Sendai 980, Japan

Keywords;Heat treatment,Bituminous coal,Hydrogen-donating solvent

INTRODUCTION

CS_2-N-methyl-2-pyrrolidinone(NMP) mixed solvent(1:1 by volume) gave high extraction yields(40-65%, daf) at room temperature for many bituminous coals(1). We also found that the extracts obtained include a considerable amount of the very heavy extract component which is not soluble in THF or pyridine, but soluble in the mixed solvent(2). This mixed solvent was used as an extraction solvent for the heat treatment products of the bituminous coals at 300-450℃ in tetralin(TET) or naphthalene (NAP)(3). The results showed that retrogressive reactions occur more readily for the heaviest fraction, i.e., THF-insoluble, CS_2-NMP mixed solvent soluble fraction(TIMS) than other lighter fractions such as benzene-insoluble , THF-soluble(preasphaltene). The heat treatment of TIMS itself, which was obtained from the extraction of Zao Zhuang coal with the CS_2-NMP mixed solvent at room temperature, in several solvents at 100-350℃ showed that retrogressive reaction, i.e., the conversion of TIMS to the mixed solvent insoluble fraction (MI), was suppressed by adding a strong hydrogen-donating solvent such as 9,10-dihydroanthracene(DHA) or 1,4,5,8,9,10-hexahydroanthracene(HHA)(4). It was also found that as more hydrogen was transferred from the solvent to TIMS, the extent of the retrogressive reaction decreased.

In this study, heat treatments of raw Zao Zhuang and Upper Freeport coals were carried out at 175-300℃ in various solvents. The coal was found to undergo either retrogressive or dissolution reaction even at temperatures as low as 175℃, depending on the hydrogen donatability of the solvnet used. The mechanisms for these reactions are discussed.

EXPERIMENTAL

Zao Zhuang(China) and Upper Freeport(Argonne Premium Coal, USA) coals were used. The ultimate and proximate analyses are given in Table 1. Heat treatment solvents used are TET, NAP, 1-methylnaphthalene(MNA), DHA, HHA and liquefaction recycle solvent(LRS). LRS(88.5%C, 9.7%H) was obtained from the 1t/day liquefaction plant of Wyoming coal operated by NEDO(New Energy Development Organization, Japan).

Heat treatment of the coal was performed in 50mL magnetically stirred autoclave at 175, 250, and 300℃, respectively. 1g of the coal and 5g of the solvent were charged to the autoclave, which was pressurized with nitrogen to 5.0 MPa at room temperature. After the heat treatment, the coal components were fractionated into the CS_2-NMP mixed solvent-insoluble fraction (MI) and -soluble fraction(MS), and then MS further into TIMS and TS(and the solvent), with the mixed solvent and THF at room temperature under ultrasonic irradiation, as shown in Figure 1. The quantity of MI and TIMS was determined after drying overnight in cacuum oven at 80℃ and that of TS was calculated by difference, i.e., 100-MI-TIMS. The dissolution yield was defined here as the sum of TIMS and TS.

The quantity of hydrogen transferred from DHA and HHA to the coal was determined from GC analysis. GC showed that the main solvent-derived products are anthracene for the heat treatment in DHA, and tetrahydroanthracene and octahydroanthracene for that in HHA, respectively. Hydrogen transferred in both treatments was determined from the quantity of anthracene, and from the difference of tetrahydroanthracene and octahydroanthracene, respectively.

RESULTS

Figure 2 shows the fraction distribution after the heat treatment of Zao Zhuang coal in 5 solvents at 175℃, 250℃ and 300℃, together with that for the raw coal, which was obtained from the fractionation of the extract of the raw coal with the CS_2-NMP mixed solvent at room temperature. At 175℃ and 250℃ in NAP and TET, MI increased and TIMS decreased, compared with those for the raw coal. While, in a strong hydrogen-donating solvent such as DHA and HHA, MI decreased and TS increased by the treatment. Contrary to the results at 175℃ and 250℃, MI decreased and TS increased in TET at 300℃. The same tendency was observed, to a lesser extent in NAP, than TET. In DHA, HHA and LRS the decrease of MI and the increase of TS was further enhanced at 300℃. Especially, in HHA, TS increased to 42.1% from 13.8% of the raw coal and the dissolution yield, i.e., TIMS + TS increased to 83.4% from 63.0% of the raw coal. The dissolution yield and TS are the order of HHA > DHA > LRS. Figure 3 shows that Upper Freeport coal gave similar results as those for Zao Zhuang coal, except that MI did not decrease at 300℃ with MNA or TET, and the dissolution yields are 86.8% and 90.6% at 300℃ in DHA and HHA, respectively, which are higher than that for Zao Zhuang coal.

Figure 4 shows the dependence of the fraction distribution on the heat treatment time for Zao Zhuang coal in HHA at 250℃. The Figure shows that for the reaction times up to 1 h MI decreases and TS increases with increasing reaction time, but little change occurs over 1 h. Figure 5 and 6 show the dependence of hydrogen transferred from the solvent to the coal and the dissolution yield on the heat treatment temperature. The Figures indicate that the increase of the dissolution yield is closely related to the hydrogen transferred, and hydrogen transferred are always higher for HHA than those for DHA, indicating that HHA is a stronger hydrogen donating solvent than DHA. Figure 7 also shows that hydrogen transferred is well correlated with the dissolution yield when the heat treatment time was varied. Table 2 shows that spin concentration of acetone-insoluble fraction(AI) after the heat treatment of ZZ coal in HHA is much smaller than that of the raw ZZ coal. The yields(raw coal base) were more than 90% and acetone-soluble fraction has much smaller spin density than AI.

DISCUSSION

The result that MI increased and TIMS decrease at 175℃ and 250℃ in TET indicates the occurrence of retrogressive reactions. Although TET is often used as a hydrogen-donating solvent in the study of coal liquefaction above 350℃, this result indicates that TET was little hydrogen-donating like NAP or MNA at the low temperatures. While, in a much stronger hydrogen-donating solvent than TET, i.e., DHA or HHA, the hydrogen donation from the solvent to the coal occurs even at 175℃ and 250℃, resulting in the dissolution reactions, i.e., the decrease of MI and the increase of TS. These dissolution reactions occur more easily at 300℃.

When temperature rises to 300℃, the hydrogen donatability of TET and the reactivity of the coal radicals may increase. So, the retrogressive reaction in TET was suppressed. NAP, which has no donatable hydrogens, gave no suppression of the retrogressive reaction even at 300℃. MNA also gave a similar result as NAP. It should be noticed that LRS is a better solvent than TET in this treatment. It is probably due to the fact that LRS contains a lot of hydrogenated condensed aromatic compounds which can easily donate hydrogens.

The close relationship between the dissolution yield and the quantity of hydrogen transferred from the solvent to the coal and the decrease of radical concentration after the heat treatment indicated that coal radicals may be responsible for the results observed here. When the radicals are stabilized by the hydrogen donation, the dissolution occurs. While, in a poor hydrogen donating solvent which hardly donate hydrogen to the radicals, retrogressive reactions such as the addition to aromatic rings of coal network and coupling reactions between them may occur. It is not clear that the radicals, which are responsible for the dissolution and retrogressive reaction, are formed by the scission of weak covalent bonds and/or indigenous radicals activated by heat at 175-300℃. The fact that the extent of the dissolution reaction increased with the heat treatment time up to 1 h suggests that the dissolution reactions are rather slow. So, the radicals may be formed by slow bond scissions, not indigenous ones, since the thermal activation of the latter radicals seems to be a rapid process. There are several kinds of weak covalent bonds which break at these low temperatures. For example, it is well known that as the number of phenyl groups replacing hydrogen atoms in ethane increases, its central C-C bond strength markedly decreases, and pentaphenylethane readily dissociates into the triphenylmethyl and diphenylmethyl radicals below 100℃. Stronger bonds than described above are possibly broken by solvent-mediated hydrogenolysis proposed by Malhotra and McMillen(5).

Finally, it should be noted that the results above described were obtained by the use of the CS_2-NMP mixed solvent as an extraction solvent for the reaction mixture. If THF is used as an extraction solvent instead of the mixed solvent, we can only see small change of TS by the heat treatments carried out here.

CONCLUSIONS

Heat treatments of Zao Zhuang and Upper Freeport coals were carried out in several hydrogen-donating solvents at 175-300℃ under N_2 atmosphere. Retrogressive reaction of the coal was observed in TET at temperatures as low as 175-250℃. While, in DHA or HHA, which are much stronger hydrogen donors than TET, the coal underwent dissolution reactions at 175-300℃. The quantity of hydrogen transferred from the solvents to coals was found to be well correlated with the degree of the dissolution reactions, and spin concentration in coal components decreased after the dissolution reactions, suggesting hydrogen donation to coal radicals in this heat treatment.

ACKNOWLEDGEMENT

The authors thank NEDO(New Energy and Development Organization, Japan) for providing LRS sample used in this research. This work was supported by a Grant-in Aid for Energy Research from Ministry of Education, Science and Culture, Japan.

REFERENCES

(1) Iino,M.; Takanohashi,T.; Ohsuga,H.; Toda, K. *Fuel* 1988, *67*, 1639-1647.
(2) Iino,M.; Takanohashi,T.; Obara,S.; Tsueta,H.; Sanokawa,Y. *Fuel* 1989, *68*, 1588-1593.
(3) Wei,X.; Shen,J.; Takanohashi,T.; Iino,M. *Energy Fuels* 1989, *3*, 575-579.
(4) Shen, J.; Takanohashi,T.; Iino, M. *Energy Fuels* 1992, *6*, 854-858.
(5) Malhotra, R.; McMillen, D.F. *Energy Fuels* 1993, *7*, 227-233.

Table 1 Ultimate and Proximate analyses of the coals

	Ultimate analysis (wt%, daf)					Proximate analysis (wt%, db)		
	C	H	N	S	O[a]	VM	Ash	FC
Zao Zhuang	86.9	5.1	1.5	1.6	4.9	28.6	7.4	64.0
Upper Freeport	86.2	5.1	1.9	2.2	4.6	28.2	13.1	58.7

[a] By difference

Table 2 Spin Concentration of Zao Zhuang coal and acetone-insoluble fraction(AI) of coal components after the heat treatment in HHA

	heat treatment (HHA, 1 h)	yield[a] (wt %, db)	spin concentration (10^{19} spin / g, daf)
raw coal	-	-	2.34
AI	175 °C	96.3	2.04
AI	250 °C	94.4	1.68
AI	300 °C	89.8	0.91

[a] Based on the raw coal

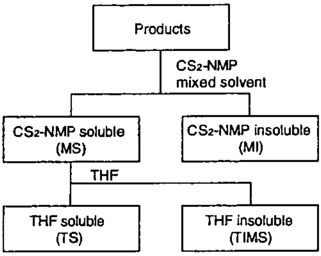
Products
CS_2-NMP mixed solvent
CS_2-NMP soluble (MS)
CS_2-NMP insoluble (MI)
THF
THF soluble (TS)
THF insoluble (TIMS)

Figure 1 Extraction and fractionation procedures for the heat treatment mixture.

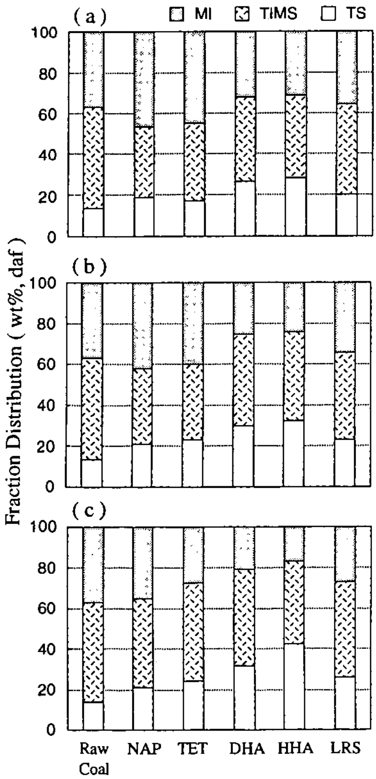

Figure 2 Fraction distribution after the heat treatment of Zao Zhuang coal in NAP, TET, DHA, HHA and LRS at 175°C(a), 250°C(b) and 300°C(c) for 1h, together with that for the raw coal.

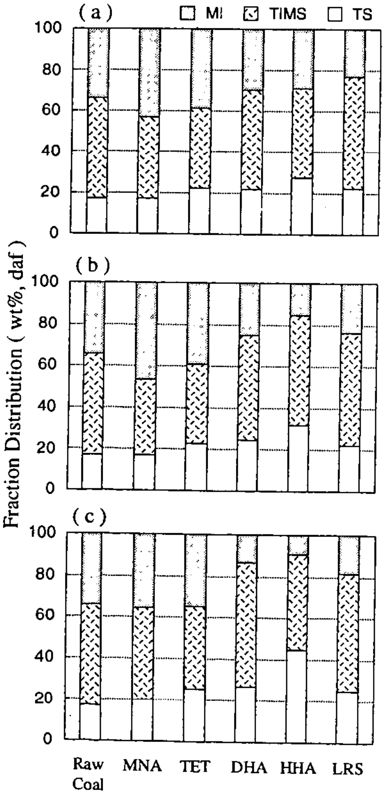

Figure 3 Fraction distribution after the heat treatment of Upper Freeport coal in MNA, TET, DHA, HHA and LRS at 175°C(a), 250°C(b) and 300°C(c) for 1h, together with that for raw coal.

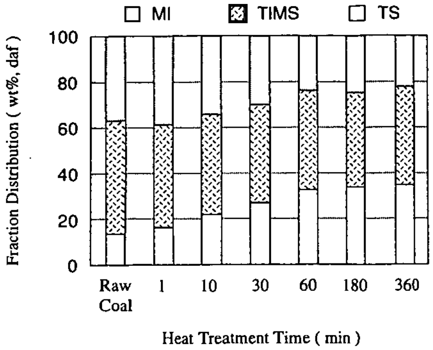

Figure 4 Fraction distribution after the heat treatment of Zao Zhuang coal in HHA at 250℃ for 1-360 min, together with that for the raw coal.

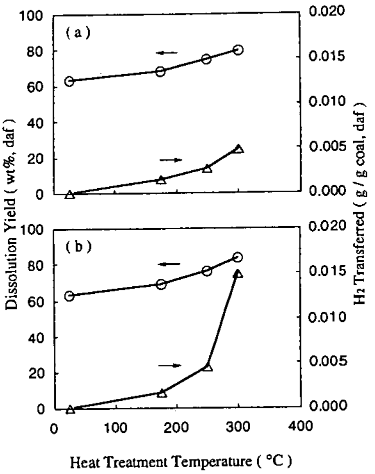

Figure 5 Plots of dissolution yield(○) and H_2 transferred(△) with heat treatment temperature for Zao Zhuang coal in DHA(a) and HHA(b) for 1h.

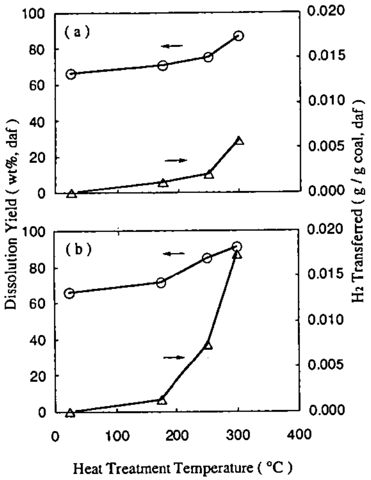

Figure 6 Plots of dissolution yield(○) and H_2 transferred(△) with heat treatment temperature for Upper Freeport coal in DHA(a) and HHA(b) for 1h.

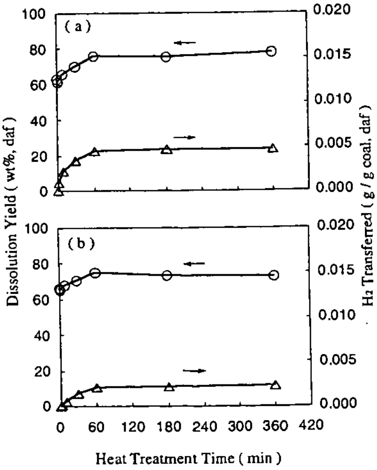

Figure 7 Plots of dissolution yield(○) and H_2 transferred(△) with heat treatment time for Zao Zhuang coal in HHA(a) and Upper Freeport coal in DHA(b) at 250℃.

SUBSTITUENT EFFECTS ON C-H BOND STRENGTHS OF THE BENZYLIC POSITIONS IN COAL-MODEL COMPOUNDS: EFFECTS OF SULFUR, OXYGEN, NITROGEN AND AROMATIC MOIETIES ON THE STABILITIES OF RADICALS.

Mikhail Alnajjar,*[1] Gerald Gleicher,[2] James Franz,[1] Scott Truksa,[2] Xian-Man Zhang,[3] and Frederick Bordwell,[3]. [1]Pacific Northwest Laboratory, P. O. Box 999, Richland, Wa USA 99352-0999 [2]Department of Chemistry, Oregon State University, Corvallis, OR USA 97331-4003 and the [3]Department of Chemistry, Northwestern University, Evanston, IL USA 60201

Key Words: Coal-Model Compounds, BDEs, Thermochemical Cycle

Abstract: Incorporation of equilibrium acidities of week acids (A-H) and the oxidation potentials of their conjugate bases (A^-) in a thermochemical cycle enable accurate determination of the effects of substituents on bond dissociation energies (BDEs) of the adjacent C-H bonds. Substraction of these (BDEs) from the BDE of methane provided a measure of the radical stabilization energies (RSEs) for the corresponding radicals relative to that of methyl radical. In this study, we have examined the effects of sulfur, oxygen, nitrogen, aromatic and coal-model structures on RSEs in RX(CH·)**A**, where the acceptor function (**A**) is phenyl, fluorenyl and PhC(O). For the heteroatom substituents with **A** equal to PhC(O), RSEs follow the trend: N > S = O). Substitution of phenyl group stabilizes the adjacent carbon radical by 10.5 kcal/mole (referred to hereafter as kcal). Naphthyl, phenanthrenyl, and 9-anthracenyl substituents provided less stabilization to the radical center than a phenyl group. Explanations are given for the difference in stabilities of these radicals and of other types of radicals studied.

Introduction: The effects of electron donors and electron acceptors on the stability of an attached carbon radical center have been well recognized. The electron donor and acceptor groups often stabilize the radical to an extent greater than would be expected on the basis of the individual contributions of both substituents.[4-8] The terms push-pull resonance,[5] merostabilization,[6] and captodative[7] have been used to describe the extra stabilization that results from the presence of both donor and acceptor groups. Kinetic data and theoretical calculations have been used to support as well as deny the existence of substituent effects on radical stabilities.[9,10] Viehe and his co-workers[7] have concluded on the basis of electron spin resonance data and qualitative theoretical interpretation that the effects are always synergistic. However, the recent results of theoretical calculations by Pasto[10] cast doubt on the existence of the captodative phenomenon and suggest that the effects will vary depending on the nature of the donors and acceptors.

The discrepancies outlined above demonstrate the difficulties in obtaining BDEs and in establishing the existence of synergistic stabilization that results from the interactions between the unpaired electron of the radical and the adjacent substituents. The measurement of homolytic bond dissociation energies have been proven to be difficult[11,12] even in the simplest of molecules.[13-15] The values of the C-H bond strengths of labile systems are even more scarce. For example, the homolytic bond dissociation energies and the thermochemistry associated with labile high molecular weight hydrocarbons and sulfur-containing organic structures important to coal are lacking because these systems are inappropriate for the most common gas-phase techniques.

Recently, we have used an electrochemical method[16-20] to estimate BDEs of the acidic H-A bonds in weak acids (eq. 1).

$$\mathrm{BDE} = 1.37\mathrm{p}K_{\mathrm{HA}} + 23.1E_{\mathrm{OX}}(\mathrm{A}^-) + 73.3 \qquad (1)$$

The method requires that the acids be strong enough to allow acidity measurements to be made in DMSO solution.
Equation (1) is based on a thermochemical cycle[17,18] in which the factors **1.37** and **23.1** are used to convert $\mathrm{p}K_{\mathrm{H\text{-}A}}$ units and oxidation potential (eV) units to kcal/mol. The constant

73.3, relates the free energies in solution to gas-phase ΔH° values, and is made up of the free energies of formation (ΔG°_f) and solvation (ΔG°_s) of the hydrogen atom, the free energy of proton transfer (ΔG°_t) from water to DMSO, and TΔS° for the reaction of RH ---> R· + H·. The oxidation potential values of the conjugate bases (A^-) are obtained from cyclic voltammetric measurements in dilute DMSO relative to ferrocene/ferrocenium ion. This electrochemical method is very powerful as it provides BDEs for large numbers of compounds that otherwise would be difficult or impossible to obtain. Also, the effects of electron donor (**D**) and acceptor (**A**) groups attached to a radical center can now be accurately determined. The experimental conditions used are very mild[16], so that the BDEs of acidic C-H bonds of thermally labile molecules can be easily estimated.

In this paper we have obtained quantitative experimental estimates of the size of radical stabilization energies (RSEs) of radicals of the type **D-(CH·)-A** and $\mathbf{D_2}$**-(C·)-A** from the homolytic bond dissociation energies of the C-H bonds in α-substituted acetophenones by using eq. 1. These BDEs provide good estimates of the RSEs, relative to the stability of the methyl radical (BDE of C-H in CH_4 is 105 kcal).[11] For example, the BDEs of the acidic C-H bond in $PhCOCH_2Me$ and $PhCOCH_2OMe$ are 88 and 81 kcal respectively, and that of the acidic C-H bond in acetophenone is 93 kcal. Therefore, the RSE of the $PhCOCH_2(\cdot)$ radical is estimated to be 12 kcal, and the RSEs estimated for PhCOCH(·)Me and PhCOCH(·)OMe radicals are 17 and 24 kcal respectively. This means that the presence of the methyl and methoxy groups has increased the stability of the $PhCOCH_2(\cdot)$ radical by 5 and 12 kcal respectively. We have also examined the effects of aromatics, sulfur and other heteroatoms on the donor-CH-acceptor type radicals and have found that, for sulfur functions, the RSEs increased progressively as the acceptors changed along the series: Ph, fluorene and PhCO. Most of the polyaromatic substituents were studied with the acceptor being PhCO. The RSE reached the minimum when the α-substituent was 9-anthracenyl system, presumably due to the large steric inhibition.

Results and Discussion: The radical stabilization energies (RSEs)[21] of carbon-centered radicals attached to sulfur, oxygen and nitrogen groups are presented in Table I. Our study of the effects of heteroatom substitution on homolytic bond dissociation energies provides new bond strengths and new insights into structural features controlling stabilization energies.

RSEs for PhCH(·)-SPh. Examination of the data in Table I (entry 2) shows that the BDE of the acidic C-H in $PhCH_2$-SPh is 84 kcal. This value was estimated by the combination of the pK_{HA} of $PhCH_2$-SPh and the E_{OX} of the conjugate base using eq. 1. Comparison with the known BDE value for toluene (88), leads to 4 kcal extra stabilization relative to the $PhCH_2(\cdot)$, or 21 kcal compared to the $CH_3(\cdot)$ radical.[22] The sum of the RSEs for the $PhSCH_2(\cdot)$ radical (12 kcal, 105 -93) and $PhCH_2(\cdot)$ radical (17 kcal, 105 - 88) is 8 kcal larger than the RSE of PhCH(·)-SPh (29 vs. 21 respectively).

RSE for 9-PhS-Fl(·). Entry 5 of table I shows that the PhS group has a larger radical-stabilizing effect (2 extra kcal) on the fluorenyl radical (Fl·) than on the benzyl radical (compare entries 2 and 5). It is surprising to observe such behavior since Fl· is supposed to be stabilized more than benzyl radical by delocalization. Because of this inherent stabilization of Fl· radical, one would expect that the stabilizing power of the sulfur atom be less in the fluorenyl system than in the benzyl system.[23] The extra stabilization of the PhS-substituted Fl· may be explained by virtue of contributor **I**.

$$\text{9-PhS-Fl}(\cdot) \quad \longleftrightarrow \quad \underset{(\mathrm{I})}{\text{9-PhS}^{+\cdot}\text{-Fl}(^-)}$$

RSEs for PhS-CH(·)COPh: The BDE of the C-H bond in $PhS-CH_2COPh$ is 81.5 kcal. The RSE for the corresponding radical is 23.5 kcal relative to $CH_3(\cdot)$ radical. The value of 23.5 kcal is 0.5 kcal lower than the combined RSEs for $PhSCH_2(\cdot)$ and $(\cdot)CH_2COPh$ radicals (24 kcal, 12 + 12). Table I shows clearly that RSEs for sulfur containing radicals increase progressively as the acceptors change along the series: Ph, fluorene (Fl), and COPh with the latter being the most stabilizing acceptor (12 kcal relative to acetophenone). The special electronic effects of the carbonyl in combination with the sulfur substituents is probably due to the conjugative and electrostatic interactions between the negatively charged oxygen and the positively charged sulfur (**II**). However, the RSEs of PhSCH(·)-**A** radicals are always smaller than the sum of the RSEs estimated from the individual radicals $\{PhSCH_2(\cdot)$ and $(\cdot)CH_2\text{-}\mathbf{A}\}$.

$$\mathrm{PhSCH(-)\text{-}COPh} \xrightarrow{-e_-} \mathrm{PhSCH(\cdot)COPh} \longleftrightarrow \underset{\textbf{(II)}}{\mathrm{PhS^{+\cdot}CH = CO(^-)Ph}}$$

The effect of a second PhS substitution into already doubly substituted methane (entries 3, and 9) is negligible. The small decrease in BDE compares well with the third phenyl substitution into methane (ΔBDE = 1 kcal) and is probably due to a large steric effect.[11,16]

Also from Table I, it is evident that the alkyl or aryl groups attached to the sulfur are not exerting any appreciable effects on the radical center connected to the sulfur atom (compare entries 5 & 6, and 8 & 10). The sulfur atom appears to act as an insulator thereby preventing the conjugation between the radical center and the group attached to the sulfur donor.

RSEs for MeO-CH(·)COPh and c-C_5H_{10}NCH(·)COPh: The acidic C-H bonds in $MeOCH_2COPh$ and c-$C_5H_{10}NCH_2COPh$ are 81 and 72 kcal respectively, giving RSEs of 24 and 33 kcal (Table I, entry 11 and 12). The RSEs for the corresponding radicals are equal to the sum of the RSEs of the individual radicals, indicating the apparent absence of synergism in the systems studied.

α-Substituent effects on BDEs of the α-C-H bond in acetophenone: In table I we saw that the introduction of phenylthio group into the α-position of acetophenone causes a 11.5 kcal increase in RSE of $PhCOCH_2(\cdot)$ radical. However, in table II (entries 2-6) we see that the introduction of a phenyl, naphthyl, phenanthrenyl, or anthracenyl substituent causes a smaller increase in RSE. The 9-anthracenyl substituent (entry 7) gave the smallest increase probably because of the greater steric and stereoelectronic demands of the 9-anthracenyl than the PhS and the other aryl groups. Furthermore, the role of a polar contributor must be larger for the PhS to show greater ability than the aryl groups in stabilizing the phenylacetyl radical. For example, contributor (**III**) dominates over contributor (**IV**) due to the electrostatic interaction between the sulfur and the oxygen atoms. The Ph group is less effective in this delocalization because contributor (**IV**) is higher in energy due to the loss of aromaticity of the phenyl ring. Substitution of an α-hydrogen in acetophenone by a pyrenyl group lowers the BDE of the α-C-H bond by 12.5 kcal (entry 8). This increase in RSE, compared to the other aromatic systems, is attributed to the delocalization of the unpaired electron into the larger pyrenyl moiety, an effect comparable in magnitude to that of aryl methyl radicals.[24]

$$\mathbf{PhS}\mathrm{\text{-}CH(\cdot)\text{-}COPh} \longleftrightarrow \underset{\textbf{(III)}}{\mathbf{PhS^{+\cdot}}\mathrm{\text{-}CH = CO(^-)Ph}}$$

$$\mathbf{Ph}\mathrm{\text{-}CH(\cdot)\text{-}COPh} \longleftrightarrow \underset{\textbf{(IV)}}{\mathbf{Ph^{+\cdot}}\mathrm{\text{-}CH = CO(^-)Ph}}$$

Remote substituent effects on BDEs of the α-C-H bond in ketones: The BDEs of acetone, acetophenone, p-methyl-, p-methoxy-, p-cyano-acetophenone are also presented in table II. Examination of entries 9-13 show that remote electron donating and electron accepting groups make the ketone less or more acidic, but have no effect on BDE's of the α-C-H bonds. The changes in acidities of the ketones are offset in eq.1 by shifts of $E_{ox}(A^-)$ to less or more positive potentials. The result is no change in BDE. This observation indicates that the remote substituent is not interacting directly with the incipient radical to provide additional stabilization.

Chromium tricarbonyl effect on BDE of the α-C-H bond in phenylacetophenone: We have shown so far the effectiveness of eq.1 in estimating the BDEs of the acidic α-C-H bonds in substituted acetophenones. We now extend our studies to chromium tricarbonyl complex of α-phenylacetophenone. The π-coordination of $Cr(CO)_3$ to benzene ring attached to the α-position is conclusive based on the NMR data. Our objective here is to obtain the first quantitative information concerning the effect of transition metal complexes on the PK_{AH} values and BDEs of the acidic C-H bonds. Entry 14 of table II shows that $Cr(CO)_3$ group increases the acidity of the α-C-H bond by 4.7 pK units (6.3 kcal; compare entries 2 & 14). This large increase is probably due to the field and inductive effects of the three carbonyl groups attached to the chromium atom. Similar acidity effects were observed when $Cr(CO)_3$ was π-coordinated to benzoic and phenylacetic acids.[25] The oxidation potential of the complex anion is less negative than that of the parent compound giving once again no net change in BDE.

Conclusion: Homolytic bond dissociation energies in DMSO for α-C-H bonds in aryl, sulfur-, oxygen-, and nitrogen-containing compounds have been measured using pK_{HA} and $E_{OX}(A^-)$ data in eq 1. In every case, the radical stabilization energies (RSEs) of RXCH(·)-**A** are always equal or smaller than the sum of RSEs of the two radicals. The increase in RSEs for sulfur group along the series: Ph, Fl, and COPh, is in correspondence with the ability of the acceptor to stabilize the negative charge on carbon for contributor of the type **PhS**$^{+\cdot}$-CH = CO($^-$)Ph. Remote electron withdrawing, electron accepting and $Cr(CO)_3$ groups have little or no effects on BDEs of the acidic α-C-H bonds indicating that these groups do not interact directly with the unpaired electron situated on the carbon radical center.

References and Notes:

1. Supported by the Office of Basic Energy Sciences, U. S. Department of energy, under contract DE-AC06-76RLO 1830.
2. Same as in 1.
3. Supported by the Donors of Petroleum Research Fund administered by the American Chemical Society, and by National Science Foundation.
4. (a) Bausch, M. J.; Guadalupe-Fasano, C.; Peterson, B. M. J. Am. Chem. Soc. **1991**, 113, 6384. (b) Crans, D.; Clark, T.; Schleyer, P. V. R. Tetrahedron Lett. **1980**, 3681.
5. Negoita, N.; baican, R.; Balaban, A. T. Tetrahedron Lett. **1973**, 1877.
6. (a) Baldock, R. W.; Hudson, P.; Katritzky, A. R.; Soti, F. J. Chem. Soc., Perkin Trans. 1, **1974**, 1422. (b) Katritzky, A. R.; Soti, F. Ibid, **1974**, 1427.
7. (a) Viehe, N. C.; Mer'enyi, R.; Stella, L.; Janousek, Z. Angew. Chem., Int. ed. Engl. **1979**, 18, 917. (b) Viehe, H. G.; Janousek, Z.; Mer'enyi, R.; Stella, L. Acc. Chem. Res. **1985**, 18, 148.
8. Dewar, M. J. S. J. Am. Chem. Soc. **1952**, 74, 3353.
9. Korth, H. G.; Sustmann, R.; Merenyi, R.; Viehe, H. G. J. Chem. Soc., Perkin Trans. 2, **1983**, 67.
10. Pasto, D. J. J. Am. Chem. Soc. **1988**, 110, 8164.
11. McMillen, D. F.; Golden, D. M. Annu. Rev. Phys. Chem. **1982**,33, 493.
12. Castelhano, A. L.; Griller, D. J. Am. Chem. Soc. **1982**, 104, 3655.
13. Coa, J.-R.; Back, M. H. Int. J. Chem. Kinet. **1984**, 16, 961.
14. Islam, T. S. A.; Benson, S. W. Int. J. Chem. Kinet. **1984**, 16, 995.
15. Tsang, W. J. Am. Chem. Soc. **1985**, 107, 2872.

16. Bordwell, F. G.; Cheng, J. P.; Harrelson, J. A. J. Am. Chem. Soc. **1988**, 110, 1229.
17. Friedrich, L. E. J. O. Chem. **1983**, 48, 3851.
18. Nicholas, A. M. P; Arnold, D. R. Can. J. Chem. **1982**, 60, 2165.
19. Bordwell, F. G.; Zhang, Xian-Man.; Alnajjar, M. J Am. Chem. Soc. **1992**, 114, 7623.
20. Bordwell, F. G.; Bausch, M. J. J. Am. Chem. Soc. **1986**, 108 , 2473.
21. The radical stabilization energies are defined as RSE = ΔBDE = BDE(A-CH_2-H) - BDE(A-CH_2-D), where A and D are the acceptors and the donors respectively.
22. The BDE of CH_3-H = 105 kcal[3]. The RSE of PhCH(·)-SPh relative to methyl radical is 21 kcal (105 - 84).
23. Katritzky, A. R.; Zerner, M. C.; Karelso, M. M. J. Am. Chem. Soc. 1986, 108, 7213.
24. Herndon, W. C. J. Org. Chem. **1981**, 46, 2119.
25. Nicholls, B.; Whiting, M. C. J Chem. Soc. **1959**, 551.

Table I. Acidities and Bond Dissociation Energies (BDEs) for the α-C-H Bonds in Heteroatom-Containing Systems.

Entry	Substrates	pK_{HA}[a]	$E_{ox}(A^-)$[b]	BDE[c]	RSE[g]
1.	$PhCH_2$-H			88[d]	0.0
2.	$PhCH_2$-SPh	30.8	-1.353	84	4
3.	$PhCH(SPH)_2$	23.0	-1.000	82	6
4.	H-FL-H	22.6	-1.064	80	0.0
5.	9-PhS-FL-H	15.1	-0.860	74[e]	6
6.	9-MeS-FL-H	18.0	-1.015	74.5	5.5
7.	H-CH_2COPh	24.7	-0.607	93	0.0
8.	PhS-CH_2COPh	17.1	-0.660	81.5[f]	11.5
9.	$(PhS)_2$-CHCOPh	12.0	-0.370	81	12
10.	PrS-CH_2COPh	19.9	-0.850	81	12
11.	MeO-CH_2COPh	22.9	-1.030	81	12
12.	c-$C_5H_{10}NCH_2COPh$	23.5	-1.439	72	21

[a] Measured in DMSO against two indicators. [b] In volts; irreversible oxidation potentials (E_p) measured in DMSO by cyclic voltammetry and referenced to the ferrocene/ferrocenium couple. [c] Calculated(in kcal/mol)using eq 1. [d] Radical stabilization energy(RSE = 17 kcal/mol)relative to CH_3-H(BDE = 105 kcal/mol). [e] Relative to H-FL-H(BDE = 80 kcal). [f] Relative to $PhCOCH_2$-H(BDE = 93 kcal). [g] RSE = ΔBDE.

Table II. Acidities and Bond Dissociation Energies (BDEs) for the α-C-H Bonds in Ketones.

Entry	Substrates	pK_{HA}[a]	$E_{ox}(A^-)$[b]	BDE[c]	RSE[f]
1.	$PhCOCH_3$	24.7	-0.607	93	0.0
2.	$PhCOCH_2Ph$	17.7	-0.650	82.5	10.5
3.	$PhCOCH_2$Naph-1	17.6	-0.626	83	10.0
4.	$PhCOCH_2$Phen-3	17.2	-0.576	83.5	9.5
5.	$PhCOCH_2$Phen-9	17.5	-0.597	83.5	9.5
6.	$PhCOCH_2$Anth-1	17.2	-0.625	82.5	10.5
7.	$PhCOCH_2$Anth-9	18.9	-0.635	84.5	8.5
8.	$PhCOCH_2$Py-1	15.7	-0.618	80.5	12.5
9.	CH_3COCH_3	26.5	-0.674	94	0.0
10.	$PhCOCH_3$	24.7	-0.607	93[d]	1.0
11.	p-$MePhCOCH_3$	25.0	-0.597	94	0.0
12.	p-$MeOPhCOCH_3$	25.7	-0.657	93	1.0
13.	p-$CNPhCOCH_3$	22.0	-0.436	93	1.0
14.	$PhCOCH_2Ph$ $\pi Cr(CO)_3$	13.1	-0.377	82.5	10.5

For [a], [b], and [c] See footnotes in table I. [d] Relative to acetone (BDE = 94 kcal). [e] Relative to $PhCOCH_2$-H(BDE = 93 kcal). [f] Radical stabilization energy (RSE).[21]

SOLUTION PHASE REACTIONS OF ATOMIC HYDROGEN[1]

Dennis D. Tanner
Department of Chemistry, University of Alberta
Edmonton, Alberta, Canada T6G 2G2

Key words: Hydrogen atoms, olefins, arenes, organosulfur compounds.

INTRODUCTION

We have recently developed a method for studying the reactions of hydrogen atoms in solution. The hydrogen atoms are generated in a flow system at 3 torr by a microwave discharge (2540-MHz) to produce a plasma of H_2 and He or H_2 alone (see Fig. 1).

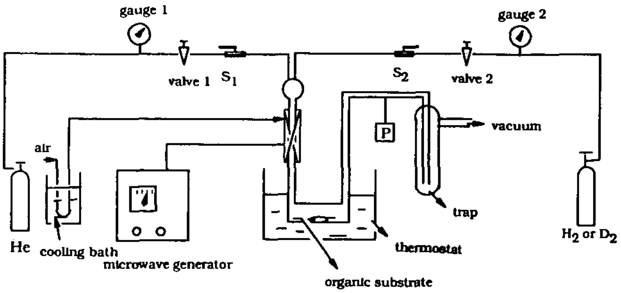

Fig. 1. Diagram of the Apparatus Used for the Generation of Atomic Hydrogen

The discharge gases are passed over a stirred solution of the substrate. Reactions take place and produce thermolyzed intermediates. The correlation of the products produced from these intermediates with the structure of the reactants yields fundamental and potentially useful information.

The reactions are efficient and surprisingly selective. Qualitatively the reaction rates follow the order:

disulfides > sulfides > olefins > aromatics > alkanes

Reactions with Olefins - Hydrogen or deuterium atoms produced from hydrogen or molecular deuterium in the cavity of a microwave generator were allowed to react with two olefins: 1-octene and 1-methylcyclohexene. A detailed mechanism for the formation of the products, both monomers and dimers, was determined. The addition reactions were regioselective, >99% addition to the terminal carbon of 1-octene and >99% to the secondary carbon of 1-methylcyclohexene. No products from allylic abstraction were detected. The product ratios for the addition of deuterium and protium were the same, see Tables 1 and 2.

[Table 1 and 2]

The disproportionation to combination ratios (k_d/k_c) of the 1-methylheptyl and 1-methylcyclohexyl radicals were determined at several temperatures. The extrapolated ratios were found to be in good agreement with the literature values reported for reactions studied at room temperature.

The 1-methyl-5-hexenyl radical formed by the addition of a hydrogen atom to the terminal position of 1,6-heptadiene led to a complex mixture of products resulting from open chain and cyclized radicals, see Table 3.

[Table 3]

The cyclized radicals were formed reversibly and the final product mixture contained only minor amounts of *cis*-1,2-dimethylcyclopentane (the product of kinetic control) while the major cyclized product was methylcyclohexane. Although an equilibrium mixture could not be obtained the dimethylcyclopentyl and 3-methylcyclohexyl radicals were shown to be formed reversibly, see Scheme 1.

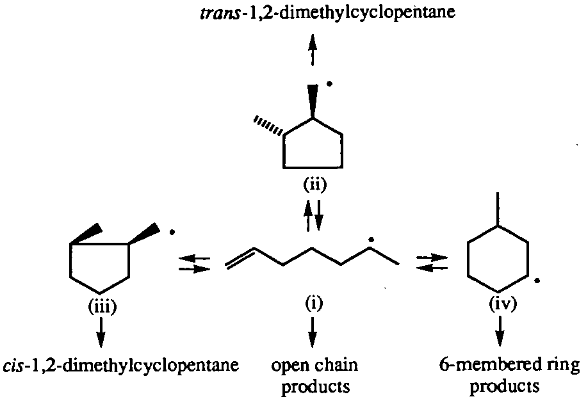
trans-1,2-dimethylcyclopentane
(ii)
(iii)
(i)
(iv)
cis-1,2-dimethylcyclopentane
open chain products
6-membered ring products

Scheme 1

Reactions with Sulfides and Disulfides - The reactions of hydrogen atoms with a series of unsymmetric disulfides were carried out. The regioselectivities and mechanisms of the reactions were investigated. The primary products of the reactions are thiol and thiyl radicals. The symmetric disulfides in the product mixtures were formed at -78°C by radical combination reactions, and not by radical displacements on the unsymmetric disulfides. The displacement, which favors attack of hydrogen on the least hindered sulfur is proposed to involve a metastable trivalent sulfur intermediate. The reactions of hydrogen atoms with a series of unsymmetric sulfides were carried out. A mechanism was proposed in which atomic hydrogen adds to the sulfur and forms an intermediate. The cleavage of the intermediate favors the most stable radical.

Reactions with Arenes[2] - When hydrogenation atom promoted sidechain fragmentation of arenes was investigated it was concluded that addition to the aromatic ring was reversible but that when ipso-attack occurs alkyl radical fragmentation may take place. Saturation of the ring is competitive with reversal or sidechain fragmentation. Polymerization of the arenes occurs even at 135°C. The model compounds studied were: toluene, bibenzyl, 9-dodecylanthracene and dodecylbenzene.

ACKNOWLEDGMENT: We wish to thank the Natural Sciences and Engineering Research Council of Canada, the University of Alberta and the Department of Energy, Mines and Resources - CANMET for their generous support of the work.

LITERATURE CITED

1. Taken in part from the Ph.D. dissertation of Liying Zhang, University of Alberta, 1994.
2. Taken in part from the CANMET Final Report on "Low Temperature Hydrogenation of Bitumen Vacuum Reside and Syncrude Products Using Microwave Generated Hydrogen Free Radicals", 1993.

Table 1. The products, yields and mechanisms for the reaction of H• with 1-octene (-78°C)[a]

Products	Yield (%)	Mechanism[c]
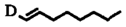	17.1	addition-disproportionation
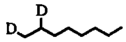	26.9	addition-addition
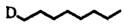	30.8	addition-disproportionation
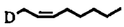	2.8	addition-disproportionation
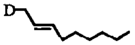	9.1	addition-disproportionation
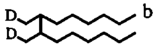	11.8	addition-dimerization
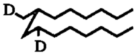	1.4	addition-radical addition

[a] Neat 1-octene.
[b] A (1:1) mixture of *meso*- and *d,l*-dimers.
[c] Monodeuterated alkane/monodeuterated alkene = 1.
[d] k_d/k_c = 2.4 at -78°C.

Table 2. The products, yields and mechanisms for the reaction of H• with 1-methylcyclohexene (-78°C)[a,b]

Products	Yield (%)	Mechanism[d]
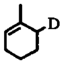	15.3	addition-disproportionation
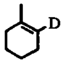	7.9	addition-disproportionation
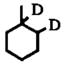	20.2	addition-addition
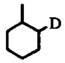	39.4	addition-disproportionation
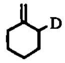	15.3	addition-disproportionation
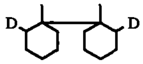	1.5	addition-dimerization
other[c]	0.5	addition-dimerization

[a] Neat 1-methylcyclohexene.
[b] Monodeuterated alkane/monodeuterated alkene = 1.
[c] Five dimeric products.
[d] k_d/k_c = 26.2.

Table 3. Reaction of D• with 1,6-Heptadiene[a,b]

	Product %	Proposed Mechanism[c]
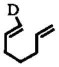	12.5	D atom addition - disproportionation
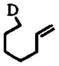	26.3	D atom addition - disproportionation
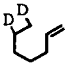	8.7	D atom addition - D atom addition
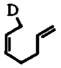 (*trans*- + *cis*-)	11.4	D atom addition - disproportionation
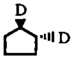	6.0	D atom addition - cyclization - D atom addition
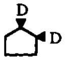	5.3	D atom addition - cyclization - disproportionation
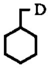	3.9	D atom addition - cyclization - disproportionation
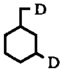	7.0	D atom addition - cyclization - D atom addition
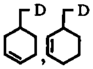	5.8	D atom addition - cyclization - disproportionation
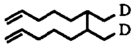 (*d,l*- and *meso*-, 1:1)	13.1	D atom addition - combination

[a] Concentration in acetone (0.16 M).

[b] Conversion = 3.1%.

[c] P_6/P_5 = 1.46 (six membered ring/five membered ring products); monodeuterated alkane/monodeuterated alkene; k_d/k_c = 2.3 (-78°C).

THERMODYNAMIC AND KINETIC EVALUATIONS OF RADICAL STABILITIES

M.J. Bausch, David Autry, Carlos Garcia, Yong Gong, Rudy Gostowski, and Weixing Li
Department of Chemistry and Biochemistry
Southern Illinois University at Carbondale, Carbondale IL 62901

Key words: free radicals, substituent effects, dimerization kinetics

Abstract When inserted into appropriate thermochemical cycles, redox data have proven invaluable in the studies of heterolytic and homolytic bond strengths. Judicious use of microelectrode-based cyclic voltammetry also enables determinations of the rates of degradation for several classes of solution phase reactive intermediates. Described in this paper are (a) new bond strength results from our group that shed light on the effects of ß-substituents on the thermodynamic stabilities of various carbon- and nitrogen- centered radicals; and (b) recent evaluations of second-order rate constants for dimerization reactions of electrochemically-generated carbon-centered radicals.

Introduction

It has been shown that insertion of selected acid-base[1] and redox data into thermochemical cycles[2] (as in eq 1[3]) results in accurate (±1-2 kcal/mol) determinations of relative and absolute

$$\Delta G^{\circ}_{hom}(R\text{–}H) = 1.36pK_a(R\text{–}H) + 23.1[E_{NHE}(R^{-}/R\bullet)] + 57.2 \text{ kcal/mol} \qquad (1)$$

free energies of homolysis[3] [$\Delta G^{\circ}_{hom}(R\text{–}H)$] for several classes of reactions.[4] For example, we have shown that the C–H homolytic bond dissocation energies for phenalene (1) and its isomeric

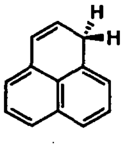

1

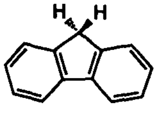

2

analogue fluorene (2) are 65 and 80 kcal/mol, respectively.[5] These data are of interest due to the persistence of the planar phenalenyl radical, as well as the continuing interest in polycyclic aromatic chemistry.

In other published work, evidence for the importance of charge separation as it pertains to radical stabilization was provided from studies of the effects of electron-withdrawing and electron-donating moieties on #9C–H anthrylmethyl homolytic bond strengths, for the substituted anthracenes (3) depicted below. Specifically, while the singular presence of G=CN, or G'=PhO,

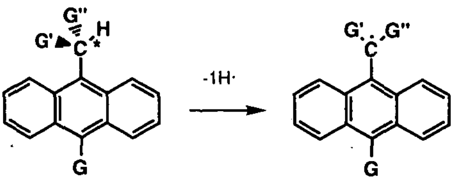

3

weakens the indicated (*) bond by ca. 1.5 and 3 kcal/mol, respectively, the simultaneous presence of these substituents weakens the same bond by ca. 9 kcal/mol.[6] These results provided support for the idea that appropriately substituted solution-phase radicals can be stabilized *via* delocalization of the unpaired electron even when that delocalization results in some charge separation.[6]

Results and Discussion

N-H Bond Strengths

In light of the importance of nitrogen in the chemistry of coal, we have therefore endeavored to collect the pK_a (R–H) and E_{NHE}(R$^-$/R•) data that enable determination of the $\Delta G°_{hom}$(R–H) values for several variously substituted perimidines (4), a nitrogen analogue of

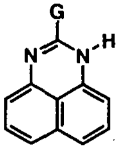

4

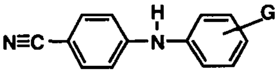

5

phenalene, as well as several diphenylamine analogues (5). The bond strengths for **4** shed important light on the effects of ß-substituents on N–H bond strengths, while the analogous data for **5** provide new insights into the effects of aryl substituents on N–H bond strengths. The acidity and bond strength data are listed in Tables I and II.

ß-Effects on N–H Bond Strengths Inspection of the acidity data in Table I reveals that ß-substituents have relatively large effects on N–H equilibrium acidities. For example, 2-methylperimidine (pK_a=17.2) is ca. 8 kcal/mol less acidic than 2-chloroperimidine (pK_a=11.4). The magnitude of the acidifying effects of the ß-substituents is surprising since there we are not aware of the existence of resonance contributing structures in which formal negative charge is present on the sp^2-hybridized #2-carbon atom. It is also of interest to compare the C–H pK_a for phenalene (18.2^5) with the N–H pK_a for perimidine (16.2). The 2 pK unit greater acidity of the nitrogen analogue is not surprising in light of the pK_a's for fluorene (22.6) and carbazole (19.9),[1] and is readily explained by the greater electronegativity of nitrogen, compared to carbon.

Examination of the $\Delta G°_{hom}$(R–H) data for the substituted perimidines reveals that the substituent effects on homolytic bond strengths are substantially smaller (by a factor of three) than the substituent-induced variation in the pK_a's for the same species. These results are consistent with a hypotheses which states that inductive (de)stabilizing effects of substituents on radical stabilities are small, compared to the resonance effects of those same substituents. The $\Delta G°_{hom}$(R–H) value for carbazole (88 kcal/mol)[7], when compared to the $\Delta G°_{hom}$(R–H) value for perimidine (75 kcal/mol), is reasonable in light of the $\Delta G°_{hom}$(R–H) values for fluorene and phenalene (76 and 61 kcal/mol, respectively). Both sets of data are consistent with the notion that N–H bonds are generally stronger, in a homolytic sense, than C–H bonds found in structurally similar species.

Remote Substituent Effects on N–H Bond Strengths Inspection of the pK_a and $\Delta G°_{hom}$(R–H) data in Table II reveals that substituents that weaken N–H bonds in **5** in an acid-base sense (i.e. electron-withdrawing substituents such as 4-nitro, 4-cyano, and 3-chloro) strengthen the same N–H bonds in a free radical (i.e. homolytic) sense. Although the pK_a results are readily understood and indicative of planarity in the diphenylamine nitranion (Hammett treatment of the data yields a linear plot with a ρ value of 2.6, r=0.99),[8] the $\Delta G°_{hom}$(R–H) values are perhaps best rationalized by noting the electron-deficient nature of the nitrogen-centered radicals.

In an effort to comprehend the $\Delta G°_{hom}$(R–H) values for **5**, it is instructive to compare the $\Delta G°_{hom}$(R–H) data in Table II with $\Delta G°_{hom}$(R–H) data for (4-nitrophenyl)phenylamine; (4-cyanophenyl)phenylamine; (3-chlorophenyl)phenylamine; diphenylamine; (4-methylphenyl)-phenylamine; and (4-methoxyphenyl)phenylamine (87,[7] 85, 84,[7] 83,[7] 83,[7] and 82[7] kcal/mol, respectively). Here too the acidifying electron-withdrawing substituents appear to strengthen the diphenylamine N–H bond in a homolytic sense. The results therefore suggest that nitranion-stabilizing substituents act to *de*stabilize nitrogen-centered radicals. For both sets of $\Delta G°_{hom}$(R–H) data, a complex interplay of resonance and inductive effects must be considered. Therefore, we are currently investigating the N–H bond strengths for several additional diphenylamines, including ten different nitrodiphenylamines, in an attempt to gain additional understanding of these phenomena.

C-H Bond Strengths

The previous section described results which indicate that more data are needed regarding resonance and inductive effects as they pertain to homolytic bond strengths and radical stabilities. In an effort to separate resonance and inductive effects, we have synthesized and evaluated the bond cleavage chemistry for 9-(trimethylsilylmethyl)fluorene (6) and 9-(cyanomethyl)fluorene (7).

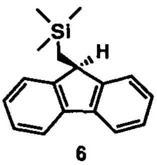

6

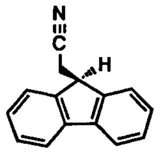

7

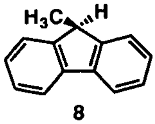

8

The relevant pK_a and ΔG°_{hom}(R–H) data for **6** and **7**, along with similar data for 9-methylfluorene (**8**), are listed in Table III.

Inspection of the data in Table III reveals that the ß-trimethylsilyl and ß-cyano substituents both acidify 9-methylfluorene. These results are consistent with the notion of an enhanced electron accepting ability for silicon atoms[9] and cyano moieties (relative to hydrogen). On the other hand, comparison of the ΔG°_{hom}(R–H) data for **6**, **7**, and **8** reveals that the electron-withdrawing ß-cyano substituent strengthens the #9C–H bond in fluorene by ca. 2 kcal/mol, while the ß-trimethylsilyl substituent appears to weaken the same bond by about 3 kcal/mol. In other work, we have shown that the ß-trimethylsilylmethyl and ß-cyano substituents have somewhat similar effects on fluorenium *cation* stabilities.[10a] Specifically, ß-trimethylsilylmethyl weakens the #9C–H bond, in a heterolytic cation-hydride forming sense, by 8 kcal/mol (relative to hydrogen), while ß-cyano strengthens the same bond by 3 kcal/mol.[10a] It appears, then, that the inductive and/or hyperconjugative effects of these two ß-substituents on radical stabilities is similar to their effects on carbocation stabilities, in suggesting that (1) electron-withdrawing inductive effects destabilize carbon-centered radicals; and (2) electron-donating hyperconjugative effects stabilize carbon-centered radicals. These results provide additional evidence for rationalizing much of the chemistry of carbon-centered radicals as if they were electron-deficient species. We are currently examining several other ß-substituted organic molecules in an effort to better understand these results.

Kinetics of Radical Dimerizations

A limitation of bond strength data obtained from thermochemical cycles that utilize irreversible redox potentials is that the peak potentials are not truly thermodynamic. This fact introduces some degree of uncertainty in bond strengths obtained using irreversible data. That the irreversible peak potentials (obtained at scan rates of 0.1 V/s) for various nitranion oxidations were nearly equal to the reversible $E_{1/2}$ values (obtained at scan rates of 1,000 V/s) for the same oxidations provided some evidence for the viability of irreversible potentials when used judiciously.[10b] In addition, data obtained using the FSCV technique can be used to derive rate constants for the chemical reactions that follow the initial electrochemical reaction.

For example, shown in Fig 1 are two CV traces for the oxidation of the 9-(2-methylphenyl)fluorenide anion. Examination of Fig 1 reveals that the carbanion oxidation is fully reversible at 1,000 V/s scan rates, but essentially ireversible at 0.1 V/s scan rates. Use of the equations developed by Nicholson and Shain[11] enables evaluation of the velocity of the reaction that removes the electrochemically generated radical from solution (*via* a second-order reaction) prior to its reduction on the reverse scan. With a microelectrode-equipped apparatus, second-order rates as high as 10^8 $M^{-1}s^{-1}$ are accessibile. Listed in Table IV are rates determined in this way for the second order reactions of variously substituted fluorenyl radicals that have been generated anodically at a platinum working electrode.

Steric Effects on Radical Dimerizations Examination of the rate data listed in Table IV reveals that the tertiary 9-methylfluorenyl radical dimerizes[12] at the same rate as the 9-cyanofluorenyl and 9-phenylfluorenyl radicals, since the uncertainty in the rates listed in Table IV is estimated to be ca. ±10%. Significantly, none of these species dimerizes at the diffusion-limited rate in DMSO (estimated at 2 x 10^9 $M^{-1}s^{-1}$). It is likely that solvation effects and solvent reorganization plays some role in the slight rate retardation.

Comparison of the k_2 values for 9-*tert*-butylfluorenyl and 9-methylfluorenyl radicals (5 x 10^5 and 3 x 10^7, respectively) provides direct evidence for the importance of steric effects on radical persistence. Evidently, the sterically demanding 9-*tert*-butyl group slows the dimerization rate by about two powers of ten (compared to 9-methyl), despite the fact that the homolytic bond strength data for these two species indicates that the 9-*tert*-butylfluorenyl radical is about 4 kcal/mol *less stable* than the 9-methylfluorenyl radical.

Furthermore, molecular models as well as bond strength data for 9-phenylfluorene, 9-(2-

methylphenyl)fluorene, and 9-mesitylfluorene [ΔG°_{hom}(R–H)=70, 71, and 72 kcal/mol, respectively] suggest that the presence of *ortho* methyl groups on the #9-phenyl moiety causes the phenyl ring in 9-phenylfluorenyl radicals to twist out of the plane of the fluorene. Kinetic evidence for this assertion is provided in Table IV, since the k_2 values for 9-phenylfluorenyl, 9-(2-methylphenyl)fluorenyl, and 9-mesitylfluorenyl radicals are 1×10^7, 8×10^3, and 1 $M^{-1}s^{-1}$, respectively). These results (i.e. solution-phase dimerization rates for delocalized fluorenyl radicals) are the first of their kind, and provide additional evidence for the notion that radical persistence is largely a kinetic phenomenon that is usually associated with steric hindrance in the immediate vicinity of the unpaired electron. We are continuing studies of the kinetics of dimerization reactions of delocalized carbon-centered radicals, and have also embarked on similar evaluations of the dimerization reactions of delocalized nitrogen-centered radicals.

Experimental Section

DMSO was purified, potassium dimsylate was synthesized, and the pK_a and redox experiments were carried out as described previously.[5,6,10] ΔG°_{hom}(R–H) values calculated as described in Reference 10a. Substrates synthesized as described in references 6, 8, and 10. The PMV device was using specifications described by Griller et al.[14] Reference 12 (submitted to *J. Org. Chem.*) contains experimental details of the FSCV device.

Acknowledgment We are grateful to the United States Department of Energy Office of Basic Energy Science for their financial support of this research. We also are grateful to Dr. Chang-ling Miaw for collecting some of the diphenylamine nitranion redox data. We also are grateful to Dr. D.D.M. Wayner (Steacie Institute for Molecular Sciences) for his advice as it pertained to the set-up and operation of the photo-modulated voltammetry apparatus

References

(1) Bordwell, F.G. *Acc. Chem. Res.* **1988**, *21*, 445-463.
(2) Wayner, D.D.M.; Parker, V.D. *Acc. Chem. Res.* **1993**, *26*, 287-294.
(3) Parker, V.D. *J. Am. Chem. Soc.* **1992**, *114*, 7458-7462.
(4) (a) Bordwell, F.G.; Bausch, M.J.; Wilson, C. *J. Am. Chem. Soc.* **1987**, *109*, 5465-5470. (b) Bordwell, F.G.; Cheng, J.-P.; Harrelson, J. *J. Am. Chem. Soc.* **1988**, *110*, 1229-1231.
(5) Bausch, M.J.; Gostowski, R.; Jirka, G.; Selmarten, D.; Winter, G. *J. Org. Chem.* **1990**, *55*, 5805-5806.
(6) Bausch, M.J.; Guadalupe-Fasano, C.; Peterson, B.M. *J. Am. Chem. Soc.* **1991**, *113*, 8384-8388.
(7) Bordwell, F.G.; Zhang, X.; Cheng, J.-P. *J. Org. Chem.* **1991**, *56*, 3216-3219.
(8) Bausch, M.J.; Li, W. *J. Org. Chem.* submitted.
(9) On theoretical grounds: Stang, P.J.; Ladika, M.; Apeloig, Y.; Stanger, A.; Schiavelli, M.D.; Hughey, M.R. *J. Am. Chem. Soc.* **1982**, *104*, 6852-6854. From gas phase experiments: Wetzel, D.M.; Brauman, J.I. *J. Am. Chem. Soc.* **1988**, *110*, 8333-8336.
(10) (a) Bausch, M.J.; Gong, Y. *J. Am. Chem. Soc.* in press. (b) Bausch, M.J.; Gostowski, R. *J. Org. Chem.* **1991**, *56*, 6260-6262.
(11) Nicholson, R. S.; Shain, I. *Anal. Chem.* **1964**, *35*, 706-723.
(12) Product analyses: chemical oxidation of the 9-methylfluorenide carbanion resulted in the production and isolation of substantial quantities of the head-to-head 9-methylfluorene dimer. NMR and mass spectral evidence was used to confirm the existence of the 9-methylfluorene dimer. Reference 11 contains detailed discussions of the protocol used to verify that the electrochemically-generated product degrades *via* a second-order process. While product analyses were *not* carried out for the balance of the reactions in Table IV, the data are clear in their indication that the electrochemically-generated fluorenyl radicals are degrading in a reaction that is second-order in fluorenyl radical.[13]
(13) Bausch, M.J.; Gostowski, R. *J. Org. Chem.* submitted.
(14) Wayner, D.D.M.; McPhee, D.J.; Griller, D. *J. Am. Chem. Soc.* **1988**, *110*, 132-137.

Table I. Dimethyl Sulfoxide (DMSO) Acidity (pK_a and ΔpK_a) and Homolytic Bond Strength [(ΔG°_{hom}(R–H) and $\Delta\Delta G^{\circ}_{hom}$(R–H)] Values for 2-Substituted Perimidines (**4**).

Substrate	pK_a	ΔpK_a (kcal/mol)	ΔG°_{hom}(R–H) (kcal/mol)	$\Delta\Delta G^{\circ}_{hom}$(R–H) (kcal/mol)
2-methylperimidine	17.2	+1.4	75	0
perimidine	16.2	(0)	75	(0)
2-phenylperimidine	14.7	-2.0	73	-2
2-thiomethylperimidine	13.3	-4.0	72	-3
2-chloroperimidine	11.4	-6.6	73	-2

Table II. Dimethyl Sulfoxide (DMSO) Acidity (pK_a and ΔpK_a) and Homolytic Bond Strength [(ΔG°_{hom}(R–H) and $\Delta\Delta G^{\circ}_{hom}$(R–H)] Values for Remotely Substituted Diphenylamines (**5**).

Substrate	pK_a	ΔpK_a (kcal/mol)	ΔG°_{hom}(R–H) (kcal/mol)	$\Delta\Delta G^{\circ}_{hom}$(R–H) (kcal/mol)
4-methoxyphenyl-4-cyanophenylamine	21.2	+1.1	84	-1
4-methylphenyl-4-cyanophenylamine	20.8	+0.5	85	0
phenyl-4-cyanophenylamine	20.4	(0)	85	(0)
3-chlorophenyl-4-cyanophenylamine	18.9	-2.1	87	+2
bis(4-cyanophenyl)amine	17.4	-4.1	88	+3
4-nitrophenyl-4-cyanophenylamine	15.5	-6.7	89	+4

Table III. Dimethyl Sulfoxide (DMSO) Acidity (pK_a and ΔpK_a) and Homolytic Bond Strength [(ΔG°_{hom}(R–H) and $\Delta\Delta G^{\circ}_{hom}$(R–H)] Values for Variously Substituted Fluorenes **6**, **7**, and **8**.

Substrate	pK_a	ΔpK_a (kcal/mol)	ΔG°_{hom}(R–H) (kcal/mol)	$\Delta\Delta G^{\circ}_{hom}$(R–H) (kcal/mol)
9-(trimethylsilylmethyl)fluorene	21.4	-1.6	69	-3
9-(cyanomethyl)fluorene	19.9	-3.7	74	+2
9-methylfluorene	22.6	(0)	72	(0)

Table IV. Dimethyl Sulfoxide (DMSO) Acidity (pK_a and ΔpK_a) and Homolytic Bond Strength [(ΔG°_{hom}(R–H) and ΔG°_{hom}(R–H)] Values for Variously Substituted Fluorenes **6**, **7**, and **8**.

Radical (R•)	ΔG°_{hom}(R–H) (kcal/mol)	$\Delta\Delta G^{\circ}_{hom}$(R–H) (kcal/mol)	k_2 ($M^{-1}s^{-1}$)
9-methylfluorenyl	72	(0)	3×10^7
9-cyanofluorenyl	71	-1	2×10^7
9-phenylfluorenyl	70	-2	1×10^7
9-*tert*-butylfluorenyl	76	+4	5×10^5
9-(2-methylphenyl)fluorenyl	71	-1	8×10^3
9-mesitylfluorenyl	72	0	<1

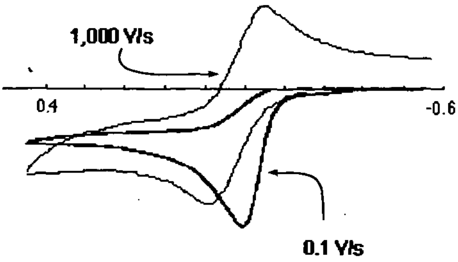

Fig 1. CV traces (at 1000 and 0.1 V/s scan rates) for the anodic oxidation of the 9-(2-methylphenyl)fluorenide anion.

THERMOLYSIS OF SILICA-IMMOBILIZED 1-(4'-HYDROXYPHENYL)-2-PHENYLETHANE UNDER D_2. A HYDROLIQUEFACTION MODEL.

Robert D. Guthrie
Sreekumar Ramakrishnan
Department of Chemistry
University of Kentucky
Lexington, KY 40506

Phillip F. Britt
A. C. Buchanan, III
Oak Ridge National Laboratory
P. O. Box 2008
Oak Ridge, TN, 37381

Burtron H. Davis
Kentucky Center for Applied Energy Research
3572 Iron Works Pike, Lexington, KY 40511

Keywords: hydroliquefaction, surface-attached, phenol H/D exchange

INTRODUCTION

In previous work, reactions of coal model compounds with D_2 at temperatures to 450 °C and pressures of 2000 psi in isolation from metal surfaces were studied. The distribution of deuterium in recovered starting materials and products, determined by GC/MS and by ^1H and ^2H NMR allowed identification of viable pathways for hydroliquefaction with increased certainty. Studies carried out with 1,2-diphenylethane (bibenzyl), **DPE**,[1] various deuterium-labeled diphenylethanes,[2] 1,2,3,4-tetraphenylbutane,[3] 2,2,5,5-tetramethyl-3,4-diphenylhexane,[4] and 1-[4-(2-phenylethyl)benzyl]naphthalene[5] model a mechanistic scheme for hydroliquefaction in which radicals formed by the homolysis of weak bonds, react with D_2 in competition with hydrogen-atom abstraction from benzylic sites. The reaction with D_2 produces deuterium atoms which react reversibly at unsubstituted positions in monocyclic aromatic compounds by the sequence of eqs 1 and 2.

$$R\bullet + D_2 \longrightarrow R\text{-}D + D\bullet \qquad (1)$$

$$D\bullet + H\text{-}Ar \longrightarrow D\text{-}Ar + H\bullet \qquad (2)$$

where H-Ar represents any aromatic compound. Eq 2 is probably a two-step process. Reaction of D or H atoms at alkyl-substituted positions produces alkyl radicals as proposed by Vernon.[6] These react relatively unselectively with available H- and D-atom donors. Kinetic chains involving D (H) atoms are short because of addition of these species to alkenes and polycyclic arenes as well as abstraction of benzylic C-H. The radicals produced in these processes undergo termination through disproportionation, reducing overall hydrocracking efficiency.

In 1986, Buchanan, Poutsma and coworkers demonstrated that the attachment of 1-(4'-hydroxyphenyl)-2-phenylethane, **DPE-OH**, to a silica surface via a carbon-oxygen-silicon linkage dramatically changes the distribution of thermolysis products when compared with unattached DPE in the absence of H_2.[7] Large increases in the amounts of rearrangement and cyclization products, removed from the surface subsequent to thermolysis, signaled the involvement of radicals which were not free to undergo the chain transfer and termination processes typical of solution and gas-phase chemistry. Subsequently, Buchanan, Britt and Biggs, for several different substrates, showed that H-atom transfer reactions on silica surfaces can be moderated by the presence of labile H-atoms in interspersed spacer molecules.[8]

We felt it would be interesting and instructive, concerning possible effects produced by the restricted mobility of the coal matrix, to examine the reaction of surface-immobilized substrates under hydroliquefaction conditions with D_2. Clearly, in order for the results to be easily interpretable, the substrates must not be removed from the surface through the action of D_2. Earlier temperature-programmed hydropyrolysis experiments suggested that this would not be a problem.[9]

EXPERIMENTAL

DPE-OH was attached to fumed silica (Cabosil M-5, Cabot Corp.) in the manner prescribed by

Buchanan, et. al.[7] The sample used for the experiments reported in Tables I and II had a surface loading of 0.32 or 0.51 mmoles/g. Samples of surface-attached material (500 mg) were placed in glass reactors described earlier.[1] The substrate was heated under N_2 or D_2 pressure in a fluidized sand bath. Temperatures reported are corrected by using a thermocouple-containing reactor and are measured under H_2. Times reported are actual time-in-bath measurements and should be shortened by approximately 5 min to allow for a measured 8 min heat-up period. Reaction mixtures were analyzed by vacuum transfer of volatile materials at 2 X 10^{-5} Torr and 80 - 100 °C into a liquid nitrogen-cooled trap for 2 h. The contents of the trap were treated with a measured amount of biphenyl in CH_2Cl_2 and the solution analyzed by gas chromatography on a 30 m, 0.25 mm capillary column coated with DB-1 at 0.25 μm. Samples were also subjected to GC/MS analysis. After removal of volatile materials, the residual coated silica (150 - 200 mg samples) was hydrolyzed with 30 to 35 mL of 1 N NaOH for 12 to 16 h at 25 °C then treated with a measured amount of a standard solution of 4-hydroxybiphenyl in 0.1 N NaOH. The hydrolysis mixture was acidified and extracted with CH_2Cl_2. After removal of the solvent, the residue was treated with a solution of N,O-bis(trimethylsilyl)trifluoroacetamide containing pyridine and trimethylsilyl chloride. The trimethylsilylated material was analyzed by GC and GC/MS as described above. Control experiments to document silica-promoted aromatic hydrogen exchange were carried out by sealing phenol-$\underline{d}_6$ (Aldrich Chemical Co.) with Cabosil and any other desired reactants into a ca. 7" X 10 mm Pyrex tube under argon and heating for the desired time. Work up was carried out as described above for N_2 and D_2 reactions.

RESULTS AND DISCUSSION

Hydropyrolysis of **DPE-OH** attached to fumed silica at a coverage of 0.51 mmoles/g (close to maximum level) at 410 °C was carried out under both N_2 and D_2 at 2000 psi in a glass reactor as previously described for the hydropyrolysis of **DPE**.[1] The reactor design is necessarily different from that employed by Buchanan, Britt, and coworkers[7,8,9] in their studies of silica-bound **DPE-OH** which was configured so that volatile products, including small amounts of phenol driven from the surface in the early stages of the reaction were continuously removed from the reaction zone. In the present study, volatile materials remain in the hot reactor throughout the heating period. The product distribution under N_2 pressure (Table I) is, nevertheless, consistent with that previously reported in vacuum with a relatively high yield of rearrangement product, HOPhCHMePh (isolated after hydrolysis of silica as its trimethylsilylated derivative).[7] For comparison purposes, we have carried out the gas-phase thermolysis of **DPE-OH** itself in D_2 under comparable conditions and found the amount of HOPhCHMePh to be less than 0.5 mole%. Thus, D_2 does not diminish the rearrangement reaction under conditions of restricted mass transport.

The most significant effect of D_2 is the increased yields of hydrocracking products: benzene, ethylbenzene (PhEt), phenol (PhOH) and 4-ethylphenol (EtPhOH) shown in Table I. Also, the amount of 4'-hydroxystilbene (HOPhCH=CHPh), is reduced under D_2. These effects were also observed in the hydropyrolysis of free **DPE**.[1,6]

An unanticipated outcome of the surface attachment experiments was the change in deuterium distribution pattern. Table II summarizes the free **DPE-OH** data (column 3) and compares them to those for silica-attached **DPE-OH**, **DPE-OSi**, (columns 1 and 2). In comparing 10 min runs for attached and free material it is apparent that the preference for deuterium incorporation in oxygen-substituted rings has increased substantially for **DPE-OSi**. This is particularly evident in the material with lower surface coverage, column 1, where the D content of oxygen-substituted rings is two to three times greater than that of unsubstituted rings. This effect is particularly dramatic (a factor of 3 to 6) where the different rings of **DPE-OH** are compared, but is also evident when comparing PhMe with HOPhMe, etc. This selectivity is somewhat reduced for high coverage **DPE-OSi** at 410 °C but is observed for this material as well at lower temperature.[10]

In previous experiments with **DPE**, it was clear that in the presence of thermolysis-produced radicals, aromatic exchange takes place by eqs 1 and 2. It is reasonable to assume that the same sequence occurs for **DPE-OH**. Because radical reactions might be expected to be insensitive to ring substituents, particularly at the temperatures involved, it was expected, and indeed found, that when **DPE-OH** is heated with D_2 the unsubstituted and HO-substituted rings contain equal numbers of D atoms after reaction.

We suspected that the most reasonable explanation for selective deuteration of oxygen-substituted rings is that the exchange process becomes electrophilic. If, for example, the underivatized SiOH groups remaining on the surface were somehow to be converted to SiOD groups it seemed possible that, at temperatures of the order of 400 °C, these might catalyze exchange at suitably reactive ring positions. To test this, we subjected phenol-$\underline{d}_6$ to treatment with silica (Cabosil) at 400 °C and indeed observed exchange. With excess silica, up to three of the ring D atoms in phenol-$\underline{d}_6$ could be replaced by H. Moreover, a mixture of phenol-$\underline{d}_6$ and MePhOH heated with silica produced MePhOH deuterated at ring positions. The temperature threshold for the exchange of phenol-$\underline{d}_6$ with silica could be shown to be about 140 °C and thus at 400 °C, the exchange goes rapidly to an equilibrium distribution. Thus it seemed clear that, were a mechanism available to exchange D atoms from D_2 with SiOH groups on the silica, our results could be explained. In support of this scheme, we were able to determine the presence of SiOD groups on recovered silica by infrared spectroscopy after removal of volatile products. It is important to note that the silica-catalyzed exchange reaction (using phenol-$\underline{d}_6$), in the absence of D_2, works only for phenolic compounds and not for benzene or even for anisole (methyl phenyl ether).

It seems almost certain, despite the apparently heterolytic nature of the reaction of SiOD with PhOH, the exchange of SiOH with D_2, moderated by phenolic compounds, must have radical components. D_2 thermolysis of surface-attached PhOH, **Ph-OSi**, which offers no obvious route for radical production, led to some exchange in the recovered PhOH. However, the amount of D is small relative to comparable **DPE-OSi** experiments and, moreover, radical processes must contribute even here as evidenced by the formation of trace amounts of benzene with relatively high D content.

We have noted above that small amounts of phenolic compounds driven from the surface and removed from the reaction zone in vacuum experiments[7,8,9] remain in the reaction vessel under the conditions of the present studies. The phenolic species are presumably generated by a process analogous to that for dehydroxylation of silica at elevated temperatures ($\equiv$Si-OAr + $\equiv$Si-OH → $\equiv$Si-O-Si$\equiv$ + HOAr). Moreover, molecules of water absorbed on the surface prior to reaction are available to hydrolyze Si-OAr bonds under D_2. Under present conditions, this typically leads to 5 to 10% of free phenolic material (based on materials obtained following vacuum transfer).

Stein,[11] Bockrath,[12] and others have noted that even though the ArO-H and $ArCH_2$-H bond energies are about the same, H abstraction by ArO• radicals is inherently faster. At 170 °C, Bockrath[12] has found that benzyl radicals abstract H atoms from ArO-H roughly 15 times faster than from benzylic structures in $PhCH_2CH_2Ph$, etc. Given that radicals produced in these thermolyses seem likely to be reacting with small amounts of phenolic compounds shown to be free of the surface (eq 3), the phenoxyl radicals produced seem certain to react with D_2 to produce D atoms by eq 4.

$$ArOH + R\bullet \longrightarrow ArO\bullet \qquad (3)$$

$$ArO\bullet + D_2 \longrightarrow ArOD + D\bullet \qquad (4)$$

D atoms produced in this way could be involved in the usual exchange at aromatic sites (eq 2), but could also react with phenols by eq 5.

$$D\bullet + HOAr \longrightarrow DH + ArO\bullet \qquad (5)$$

The reactions of eqs 4 and 5 constitute a chain process which results in the conversion of HOAr to DOAr. This would presumably also occur in the thermolysis of **DPE-OH** under D_2 and, therefore, of itself, must not be sufficient to produce selective exchange in O-substituted rings. However, if, in the presence of silica, exchange of O-substituted rings with DOAr is catalyzed, selective D incorporation can be explained. To document the viability of eq 3, we heated **DPE** with phenol-O-$\underline{d}$ and showed deuterium to be present in the toluene produced.

Focussing on the non-oxygen-substituted rings reveals evidence that the free radical chain for H/D substitution is more efficient for gas-phase species than for surface immobilized molecules. Cleavage-produced free molecules, benzene, PhMe, PhEt as well as **DPE** (presumably formed by radical recombination) contain at least twice as much deuterium as the unoxygenated ring in recovered **DPE-OH** suggesting that the latter is a less active participant in the D-atom promoted exchange.[13] Particularly convincing is the lower D content of $PhCH_2'$ fragments from **DPE-OH** as compared with those from PhEt. As **DPE-OH** spends most of its time on the surface, this argues that D atoms react predominantly with gas-phase substrates.

SUMMARY

The important conclusions of this study are: 1. The presence of D_2 at 2000 psi does not alter the tendency of surface-attached radicals to rearrange. 2. Hydrocracking is observed for hydropyrolysis of surface-attached materials. 3. Radical D/H exchange is more efficient in the gas phase. 4. The reaction of benzylic radicals with phenols has been documented. 5. Phenoxyl radicals catalyze exchange between D_2 and SiOH groups on silica which in turn promotes exchange at ortho and para ring positions in phenolic compounds.

ACKNOWLEDGEMENTS

The authors gratefully acknowledge support from the Department of Energy, Office of Basic Energy Sciences, Division of Chemical Sciences, under Contract No. DE-AC05-840R21400 with Martin Marietta Energy Systems, Inc. (PFB and ACB) and from the United States Department of Energy, Pittsburgh, for a grant, DE-FG22-91-PC91291 (RDG, SR and BHD).

REFERENCES

1. (a) Guthrie, R. D.; Shi, B.; Sharipov, R.; Davis, B. ACS Div. Fuel Chem. Prepr., **1993**, 38, 526-533. (b) Guthrie, R. D.; Shi, B.; Rajagopal, V.; Ramakrishnan, S.; Davis, B. H., submitted to J. Am. Chem. Soc.

2. Rajagopal, V.; Guthrie, R. D.; Shi, B.; Davis, B. H. ACS Div. Fuel Chem. Prepr., **1993**, 38, 1114.

3. Ramakrishnan, S.; Guthrie, R. D.; Shi, B.; Davis, B. H. ACS Div. Fuel Chem. Prepr., **1993**, 38, 1122.

4. Sharipov, R.; Guthrie, R. D.; Shi, B.; Davis, B. H. ACS Div. Fuel Chem. Prepr., **1993**, 38, 1129.

5. Shi, B.; Ying, J.; Guthrie, R. D.; Davis, B. H., submitted to Energy and Fuels.

6. Vernon, L. W. FUEL **1980**, 59, 102-106.

7. Buchanan, A. C., III, Dunstan, T. D. J.; Douglas, E. C.; Poutsma, M. L. J. Am. Chem. Soc. **1986**, 108, 7703-7715.

8. (a) Buchanan, A. C., III; Britt, P. F.; Biggs, C. A. Energy and Fuels **1990**, 4, 415-417. (b) Buchanan, A. C., III.; Biggs, C. A. J. Org. Chem. **1989**, 54, 517-525. (c) Britt, P. F.; Buchanan, A. C., III J. Org. Chem. **1991**, 56, 6132-6140.

9. Mitchell, S.C.; Lafferty, C. J.; Garcia, R.; Snape, C. E.; Buchanan, A. C., III; Britt, P. F.; Klavetter, E. Energy and Fuels **1993**, 7, 331-333.

10. Data to be reported in future publications.

11. S. E. Stein in "Chemistry of Coal Conversion", Schlosberg, R., Ed.; Plenum Press, NY 1985, pp 13 - 44.

12. Bockrath, B. C.; Bittner, E. W.; McGrew, J. J. Am. Chem. Soc. **1984**, 106, 135-138.

13. It may be noticed that the D content of benzene, toluene and ethylbenzene from free DPE-OH is also high, but this is misleading because the DPE-OH reaction proceeded to higher conversion.

Table I. Product Distrihution in the Thermolysis of Surface-Attached 4'-Hydroxy-1,2-diphenylethane at 410 °C under N_2 and D_2. Coverage = 0.51 Mmoles/g.

Mole % of Total Products

Product[a]	10 min/N_2	10 min/D_2	30 min/N_2	30 min/D_2
Benzene	1.2	6.0	0.5	6.9
PhMe	28.6	25.9	31.5	22.8
PhEt	0.8	5.5	1.0	7.0
$PhCH_2CH_2Ph$	0.7	2.6	1.0	1.9
PhCH=CHPh	----	---	0.3	<0.02
TMSOPh[b]	2.8	6.8	1.3	8.7
TMSOPhMe[b]	27.4	23.3	28.6	27.5
TMSOPhEt[b]	0.8	4.8	1.2	6.2
$TMSOPhCH_2Ph$[c]	1.5	1.1	3.7	1.9
TMSOPhCHMePh[c]	11.3	11.5	9.2	11.3
$TMSOPhenH_2$[c,d]	<0.3	---	0.3	----
TMSOPhCH=CHPh[c]	23.2	10.7	18.6	2.6
TMSOPhen[c,d]	1.8	1.7	2.8	3.2

[a] Conversions were 33.5, 26.8, 53.0 and 58.1% for the 4 runs. Recoveries of listed products ranged from 75 to 85%. A few GC peaks for which tentative identification can be made are not listed. Majority appear to be siloxytriphenylpropane isomers. Some styrene may be present. A large numher of very small unidentified peaks were observed for which individual peaks represent less than 0.05 mole %. [b] Represents sum of volatile and hydrolysis-recovered products. [c] These were measured after hydrolysis of recovered silica and trimethylsilylation. [d] Phen = phenanthryl, $PhenH_2$ = dihydrophenanthryl.

Table II. Deuterium Content of Products from Thermolysis of **DPE-OSi** and **DPE-OH** for 10 Minutes at 410 °C Under D_2.

Average Number of D Atoms per Molecule

Product	**DPE-OSi** (0.32)[a]	**DPE-OSi** (0.51)[a]	**DPE-OH**[c]
Benzene	1.11	1.01	0.87
PhMe	0.66	0.95	0.80
PhEt	1.19	1.29	1.10
--> $PhCH_2^+$	0.74	0.69	0.43
PhOH	2.50 (2.55)[b]	1.55 (1.22)[b]	0.95 (0.91)[b]
MePhOH	2.20 (2.01)[b]	1.43 (1.09)[b]	0.79 (0.77)[b]
EtPhOH	2.37 (2.34)[b]	1.69 (1.23)[b]	1.23 (1.30)[b]
[d] --> $PhCH_2^+$	1.99	1.25	0.50
$PhCH_2CH_2Ph$	3.25	1.77	1.07
[d] --> $PhCH_2^+$	1.87	0.90	0.59
TMSOPhCHMePh	2.23	0.90	1.12
$TMSOPhCH_2CH_2Ph$	2.1	1.04	0.82
[d] --> $PhCH_2^+$	0.34	0.24	0.46
[d] --> $TMSOPhCH_2^+$	1.9	0.89	0.47

[a] Surface coverage in mmoles/g. [b] First value is for vacuum-transferred material. () represents trimethylsilylation products after hydrolysis of silica. The difference at high coverage appears to be real. Hydrolysis procedures do not change D content. [c] Conversion was higher for this material (60%) compared to 22% and 27% for first two columns. [d] Mass spectral fragment.

UNCATALYZED REACTION OF SELECTED UNSATURATED COMPOUNDS WITH D_2

Venkatasubramanian K. Rajagopal
Robert D. Guthrie
Department of Chemistry
University of Kentucky
Lexington, KY 40506

Buchang Shi
Burtron H. Davis
Kentucky Center for Applied Energy Research
3572 Iron Works Pike, Lexington, KY 40511

Keywords: hydroliquefaction, alkenes, polynuclear aromatic compounds

INTRODUCTION

In our previous study of the reaction of 1,2-diphenylethane (bibenzyl), **DPE**,[1] and other compounds[2] with D_2 at temperatures to 450 °C and pressures of 2000 psi in isolation from metal surfaces, we were able to provide strong evidence for a mechanistic scheme wherein radicals formed by the homolysis of weak bonds, react with D_2 to give D atoms. These participate in short radical-chain processes responsible for hydrocracking and exchange of H for D at unsubstituted aromatic positions. In contrast to the simple thermolysis of **DPE** wherein stilbene (PhCH=CHPh), **STB**, is formed as a major product, the reaction of **DPE** with D_2 produces relatively small amounts of this compound. Moreover, the mole % of **STB** among the products decreases as conversion increases, indicating that initially produced **STB** is consumed. It, therefore, seemed important to examine the reaction of **STB** with D_2. This study has subsequently been extended to other unsaturated compounds and the results are reported below.

EXPERIMENTAL

Reaction Procedure. Reactions were carried out as described earlier,[1] placing the reactants along with glass beads for agitation in a glass bulb (ca. 12 mL) with a long capillary neck. The vessel was then suspended in glass wool in the interior of a stainless steel reaction tube having a long neck to house the capillary section of the vessel. The entire apparatus was evacuated, pressured with D_2 gas, closed off and shaken at the desired temperature in a fluidized sand bath. Temperatures reported were corrected from bath calibrations using a thermocouple-containing reactor and were measured under H_2. Times reported are actual time-in-bath measurements and should be shortened by approximately 5 min to allow for a measured 8 min heat-up period. When the heating period was complete, carbon disulfide was added and products removed for analysis using a long syringe needle. In the absence of gas generation within the tube, our observation has been that at least for high concentration runs, an insignificant amount of material is lost from the interior of the bulb. Control experiments in which a hydrogenation catalyst was deliberately added showed complete saturation of aromatic compounds under the reaction conditions. Product mixtures were analyzed by gas chromatography (GC) and by gas chromatography/mass spectrometry (GC/MS). Products present in substantial quantities were separated by preparative gas chromatography and analyzed by ^1H and ^2H NMR at 400 MHz in carbon disulfide. cis-Stilbene did not separate from **DPE** by GC, but was determined from mass spectral analysis using calibrating mixtures of these compounds.

Reactants. Reactants were generally the best quality of commercially-available material. 1-methylstyrene was distilled to remove polymerization inhibitor. Several grades of trans-stilbene were tested and, as all contained small amounts of **DPE**, this compound was synthesized by a modified Wittig synthesis to produce **DPE**-free material.[3] The synthetic material was a mixture of cis- and trans-stilbene, but had no effect on reaction outcome because equilibrium between these two isomers was attained early in the reaction period.

RESULTS AND DISCUSSION

Table I presents data for reaction of several unsaturated compounds with D_2 at 2000 psi and 410 °C. It will be noted that for the four compounds studied to date, **STB**; α-methylstyrene ($Ph(CH_3)C=CH_2$), **MS**; anthracene, **AN**; and phenanthrene, **PN**; all except **PN** show substantial reaction with D_2 at 410 °C. The reactive compounds produce dihydro products which contain D atoms as well as incorporating deuterium themselves.

General Mechanistic Considerations. It was demonstrated in our earlier studies that D atoms add reversibly to phenyl rings in **DPE** and its hydrothermolysis products by eqs 1 and 2.

$$D\bullet \quad + \quad H\text{-}Ar \quad \text{-->} \quad H\bullet \quad + \quad D\text{-}Ar \tag{1}$$

$$H\bullet \quad + \quad D_2 \quad \text{-->} \quad H\text{-}D \quad + \quad D\bullet \tag{2}$$

As double bonds, lacking the resonance stability of benzene rings are certain to at least equally reactive toward D atoms, it seems clear that the general process of eq 3 will be important if D atoms are present.

$$D\bullet \quad + \quad C{=}C \quad \text{-->} \quad D\text{-}C\text{-}C\bullet \tag{3}$$

The radicals generated in eq 3 would then be expected to either undergo the reaction of eq 4, completing a kinetic-chain sequence, or undergo termination either by coupling or disproportionation. As coupling would be a reversible process under the conditions of this study, it is necessary only to consider disproportionation, eq 5.

$$D\text{-}C\text{-}C\bullet \quad + \quad D_2 \quad \text{-->} \quad D\text{-}C\text{-}C\text{-}D \quad + \quad D\bullet \tag{4}$$

$$2\ D\text{-}C\text{-}C\bullet \quad \text{-->} \quad D\text{-}C\text{-}C\text{-}(D \text{ or } H) \quad + \quad C{=}C(D \text{ or } H) \tag{5}$$

Several alternative mechanisms are possible. For the extreme case in which eqs 3 and 4 are fast and irreversible, dihydrocompounds containing exactly two D atoms would be obtained and there would be no D in recovered C=C. Clearly, this situation does not transpire for any of the reactions in Table I. In principle it should be possible to determine the extent to which products were formed via eq 5 from the amount of D introduced into recovered C=C. However, the analysis is confounded by the fact that aromatic exchange is expected via eqs 1 and 2. Of course, it is always possible that radical processes are not involved and that the reaction of C=C with D_2 would occur by a one-step cycloaddition process. In such a process one might expect to see simple second-order kinetics and no introduction of D atoms at sites other than those directly involved in the hydrogen transfer.

Stilbene, STB. The data presented in Table I show that **STB** is reduced to **DPE** and a total of approximately 2 atoms of D are introduced in the combined products. While it is difficult to distinguish aromatic and vinylic D in recovered stilbene, ^{2}H NMR shows 0.37 atoms of aromatic D in **DPE** produced in runs comparable to those in Table I. As aromatic sites in **STB** and **DPE** should have comparable reactivity with D atoms, most of the D in recovered stilbene seems likely to be at aromatic sites. Consistent with this, an ^{2}H NMR upper limit for vinyl D in stilbene at <0.05 atoms can be established. This suggests that products formed via eq 5 make a relatively minor contribution when low concentrations of **STB** are present.

A complication for **STB** is that as **DPE** is produced it undergoes thermolysis by processes detailed earlier.[1] In fact, under conditions only slightly more vigorous than those of Table I, stilbene can be completely converted to a mixture of **DPE** and its hydrothermolysis products with very high D content (average of 8.6 atoms of D in **DPE**). It seems likely that once **DPE** is produced in the reaction mixture, radicals produced in its thermolysis constitute the major initiating species via reaction with D_2 followed by the sequence of eqs 3 and 4. The question of how the process is initiated in the absence of all radical producing species is difficult to answer. The third entry of Table I shows that **DPE** is produced even when synthetic **STB** (free of **DPE** to detection limits) is employed.

Despite the complexities discussed, the strong concentration dependence of the reaction suggests that chains of moderate length are operative at low concentration. At low concentrations, we suggest that the predominant pathway for the reaction of **STB** with D_2 involves the sequence of eqs 3 and 4 plus some reaction with H atoms when these are generated by eq 1. When the initial concentration is increased, the efficiency of conversion to **DPE** is reduced by higher radical concentrations which increase competition by eq 5.

α-Methylstyrene, MS. On comparable treatment with D_2, **MS** produces cumene. However the D content is less than observed for **DPE** from **STB** and decreases with increasing concentration of **MS**. For the higher concentration runs of Table 1, the D atom content of cumene plus **MS** is close to 1 atom per equivalent of cumene formed. This is different from **STB** and **AN** for which two or more atoms of D are incorporated. This lower D incorporation suggests chain transfer involving **MS** as shown in eq 6 forming monodeuterated cumene and the 2-phenylallyl radical. It will be noted that for **STB** and **AN**, the substrate is unlikely to act as an H-atom donor.

$$\mathrm{Ph(CH_3)(CH_2D)C\bullet \;+\; Ph(CH_3)C{=}CH_2 \;\text{-->}\; Ph(CH_3)(CH_2D)C\text{-}H \;+\; Ph(H_2C{=})C\text{-}CH_2\bullet} \qquad (6)$$

It seems likely that the 2-phenylallyl radical thus formed reacts with **MS** to give higher molecular weight products as these are found in nearly equal amount to cumene and increase with increasing concentration of **MS** as might be expected. It will be noted that this substrate is the only one studied for which conversion increases with amount used.

Earlier study of the thermolysis of bicumyl ($Ph(CH_3)_2C\text{-}C(CH_3)_2Ph$) under D_2 has shown that cumyl radicals ($Ph(CH_3)_2C\bullet$) are relatively reluctant participants in the reaction of eq 4.[4] This being the case, it might be expected that eq 5 is the major route to product formation. However, such a scheme should lead to more D in recovered **MS** than observed. Perhaps because of the higher temperature and lower radical concentrations here, as contrasted with the bicumyl experiments, eq 4 becomes more competitive.

In contrast to the case of **SB**, the hydrogenation product from **MS** (cumene) would not seem to be capable of serving as an initiator, thus requiring some different type of initiation step. We suggest the reaction of eq 7 in which two molecules of **MS** undergo a "molecular disproportionation" reaction to give the 2-phenylallyl radical ($Ph(H_2C{=})C\text{-}CH_2\bullet$) and a cumyl radical.

$$\mathrm{2\ Ph(CH_3)C{=}CH_2 \;\text{-->}\; Ph(H_2C{=})C\text{-}CH_2\bullet \;+\; Ph(CH_3)_2C\bullet} \qquad (7)$$

The cumene formed via eq 6 would be monodeuterated but, to the extent that eq 6 was a viable path for the cumyl radical formed in eq 7, some of the cumene would be produced without deuterium. Significantly, the predominant cumene isotopomer is d_1 in the 50 mg run but d_0 in the 300 mg run.

Anthracene, AN. Under the same conditions, **AN** reacts with D_2 to give dihydroanthracene, **ANH$_2$** (taken to include ANHD, AND_2, etc.). This reaction has been reported earlier with H_2 at 430 °C in methylnaphthalene solvent.[5] The total amount of D incorporated in **AN** plus **ANH$_2$** was to 2.1 to 2.6 atoms of D per equivalent of **ANH$_2$** produced. This reaction shows no significant concentration dependence and, therefore seems unlikely to be a kinetic chain process. The mechanism probable for the preceding systems in which D atoms add to **AN** to form adduct radicals, **AND•**, and these disproportionate as shown in eq 8 is one possibility.

$$\mathbf{2\ AND\bullet \;\text{-->}\; AN \;+\; ANHD}\ \ (\text{or } \mathbf{AN\text{-}d_1 \;+\; ANH_2}) \qquad (8)$$

If this mechanism is correct, it is necessary to account for the initial production of D atoms. Coupling of two **AN** molecules as reported by Stein[6] is a possibility. The reaction of eq 8 is known to be reversible[7] so that once **ANH$_2$** and its isotopomers are formed, exchange of H and D atoms would be rapid and, moreover, this will occur via a radical mechanism. The question which remains is whether the adduct radicals (**ANH•** and **AND•**) are sufficiently reactive to remove D atoms from D_2. While further experiments will be required to answer this question definitively, it is significant that ^2H NMR studies show that there is very little aromatic D in **ANH$_2$**. Also the D atoms in recovered **AN** are located to > 80% (detection limit) in the 9,10-positions. A mechanism wherein half of the deuterium incorporated arrives as D atoms can be reconciled with these observations only if D atoms are highly selective for the 9,10-positions.

One possibility which cannot be discounted by any of the evidence presently at hand. is that the addition of D_2 to **AN** is a 2 + 4 cycloaddition. It is the only system in this study for which cycloaddition to give a stable product is symmetry allowed.

Phenanthrene, PN. **PN** does not react under these conditions. The fact that **AN** does react could be taken as evidence for 2 + 4 cycloaddition which is not symmetry allowed for **PN**. On the other hand, the 9,10-positions in **AN** are notoriously reactive[7d] and initiation processes with **AN** might be more effective than comparable reactions with **PN**. The striking difference in reactivity of these two compounds will require further study for complete analysis.

ACKNOWLEDGEMENTS

The authors gratefully acknowledge a grant from the United States Department of Energy, Pittsburgh, DE-FG22-91-PC91291, supporting this work.

SUMMARY

The reaction of D_2 with several unsaturated substrates has been documented. The reaction involved no intentionally added hydrogenation catalyst and, with the possible exception of **AN**, is believed to involve D atom addition to the unsaturated compound with the resultant adduct radical either reacting with D_2 or undergoing disproportionation. In the case of anthracene, the results are consistent with a direct 2 + 4 cycloaddition.

REFERENCES

1. (a) Guthrie, R. D.; Shi, B.; Sharipov, R.; Davis, B. ACS Div. Fuel Chem. Prepr., 1993, 38, 526-533. (b) Guthrie, R. D.; Shi, B.; Rajagopal, V.; Ramakrishnan, S.; Davis, B. H., submitted to J. Am. Chem. Soc.

2. (a) Rajagopal, V.; Guthrie, R. D.; Shi, B.; Davis, B. H. ACS Div. Fuel Chem. Prepr., 1993, 38, 1114. (b) Ramakrishnan, S.; Guthrie, R. D.; Shi, B.; Davis, B. H. ACS Div. Fuel Chem. Prepr., 1993, 38, 1122. (c) Sharipov, R.; Guthrie, R. D.; Shi, B.; Davis, B. H. ACS Div. Fuel Chem. Prepr., 1993, 38, 1129. (d) Shi, B.; Ying, J.; Guthrie, R. D.; Davis, B. H., submitted to Energy and Fuels.

3. Daniel, H.; LeCorre, M. Tetrahedron Letters 1987, 28, 1165-1168.

4. Bicumyl undergoes thermolysis at temperatures below 400 °C to give equal amounts of cumene and **MS** with only small D uptake, unpublished study by R. D. Guthrie, S. Ramakrishnan and B. Shi.

5. Chiba, K.; Tagaya, H.; Suzuki, T. Sato, S. Bull. Chem. Soc. Jpn. 1991, 64, 1034-1036.

6. Stein, S. E.; Griffith, L. L.; Billmers, R.; Chen, R. H. J. Org. Chem. 1987, 52, 1582-1591.

7. (a) Camioni, D. M.; Autrey, S. T.; Franz, J. A. J. Phys. Chem. 1993, 97, 5791-5792. (b) Billmers, R.; Griffith, L. L.; Stein, S. E. J. Phys. Chem., 1986, 90, 517-523. (c) Billmers, R.; Brown, R. L.; Stein, S. E. Int. J. Chem. Kin. 1989, 21, 375-386. (d) Stein, S. E. in "Chemistry of Coal Conversion", R. Schlosberg, Ed.; Plenum Press, NY 1985, pp 13-44.

Table I. Reaction of Unsaturated Compounds with D_2 (2000 psi) at 410 °C for 20 min.[a]

Compound	Amount[b] (mg)	% H-C-C-H[d]	D atoms in H-C-C-H[c]	D atoms in C=C[c]
STB	25[e]	22[g]	1.67	0.23
STB	50[f]	13[g]	1.47	0.10
STB	25[f]	22[g]	1.73	0.22
STB	50	5.4[k]	1.5[j]	<0.03
STB	100	1.8	1.5[j]	<0.01
MS	50	14[h]	1.34	0.13
MS	150	18[h]	0.80	0.09
MS	300	27[h]	0.65	0.16
AN	50	33[i]	1.55	0.37
AN	100	35[i]	1.20	0.48
AN	300	26[i]	1.10	0.57
PHN	50	<0.2	---	<0.05
PHN	100	<0.2	---	<0.05
PHN	300	<0.2	---	<0.05

[a] The 20 min time period refers to the time after temperature equilbrium is reached inside of the cell. There is an 8 min heat-up period. [b] This is the weight of material inside of an approximately 12 mL reaction vessel. [c] Average number of D atoms per molecule as determined by GC/MS analysis. [d] Balance of material is recovered C=C, except as otherwise noted. [e] Commercial material contains 0.7% of **DPE**. [f] Synthetic material contains < 0.01% **DPE**. [g] Product mixture also contains 5 - 10% of products of **DPE** reaction (benzene, toluene, ethylbenzene, styrene, 1,1-diphenylethane, diphenylmethane, etc. [h] Similar amounts (12, 17 and 21%) of other products, most of which appeared to be dimers and dehydrodimers of expected intermediate radicals. [i] Tetrahydroanthracenes were formed in amounts of up to 3% increasing with increasing concentration. [j] Corrected for **DPE** in starting **STB**. [k] This run should be the same as the previous 50 mg run, but gave lower conversion. It is believed that this is due to temperature variations. The first three **STB** runs were carried out on a different day from the last two.

THERMOLYSIS OF PHENETHYL PHENYL ETHER. A MODEL OF ETHER LINKAGES IN LOW RANK COAL.

Phillip F. Britt, A. C. Buchanan, III and E. A. Malcolm
Chemical and Analytical Sciences Division
Oak Ridge National Laboratory, P.O. Box 2008
Oak Ridge, TN 37831-6197

INTRODUCTION

Currently, an area of interest and frustration for coal chemists has been the direct liquefaction of low rank coal. Although low rank coals are more reactive than bituminous coals, they are more difficult to liquefy and offer lower liquefaction yields under conditions optimized for bituminous coals.[1] Solomon, Serio, and co-workers have shown that in the pyrolysis and liquefaction of low rank coals, a low temperature cross-linking reaction associated with oxygen functional groups occurs before tar evolution.[2,3] A variety of pretreatments (demineralization, alkylation, and ion-exchange) have been shown to reduce these retrogressive reactions and increase tar yields,[2,3] but the actual chemical reactions responsible for these processes have not been defined. In order to gain insight into the thermochemical reactions leading to cross-linking in low rank coal, we have undertaken a study of the pyrolysis of oxygen containing coal model compounds.[4] Solid state NMR studies suggest that the alkyl aryl ether linkage may be present in modest amounts in low rank coal.[5] Therefore, in this paper, we will investigate the thermolysis of phenethyl phenyl ether (PPE) as a model of β-aryl ether linkages found in low rank coal, lignites, and lignin, an evolutionary precursor of coal. Our results have uncovered a new reaction channel that can account for 25% of the products formed. The impact of reaction conditions, including restricted mass transport, on this new reaction pathway and the role of oxygen functional groups in cross-linking reactions will be investigated.

Background The thermolysis of PPE has been previously studied under a variety of conditions. Liquid-phase studies by Klein[9] and Gilbert[10] found phenol and styrene as the primary decomposition products, but different mechanisms were proposed to rationalize the data. Klein proposed a concerted retro-ene reaction based on the first-order reaction kinetics (1.16 ± 0.12 in PPE) which was unaffected by tetralin, and the Arrhenius parameters, log A = 11.1 ± 0.9 s^{-1} and $E_a = 45 \pm 2.7$ kcal mol^{-1}. It was proposed that secondary decomposition of styrene produced the minor amounts of toluene and ethylbenzene that were detected. Gilbert proposed a free radical chain mechanism for the decomposition of PPE based on the fractional reaction order (1.21 in PPE), the rate acceleration by added free radical initiator, and the Arrhenius parameters, log A = 12.3 s^{-1} and $E_a = 50.3$ kcal mol^{-1}. The chain propagation steps are shown below. PPE has also been studied under coal liquefaction conditions, i.e. in tetralin under high pressure of hydrogen,[11] and under catalytic hydropyrolysis conditions, with iron and zinc metal.[12] In both these studies, the dominant products were phenol and ethylbenzene, since under these reaction conditions, styrene would be hydrogenated to ethylbenzene.

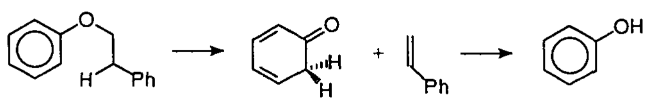

(1)

$$PhCH_2CH_2OPh + PhO\bullet \rightarrow PhCH(\bullet)CH_2OPh\ (1) + PhOH \qquad (2)$$

$$PhCH(\bullet)CH_2OPh \rightarrow PhCH{=}CH_2 + PhO\bullet \qquad (3)$$

EXPERIMENTAL

Phenethyl phenyl ether was synthesized by alkylation of phenol with phenethyl tosylate with K_2CO_3 in dimethylformamide. Vacuum fractional distillation afforded PPE in > 99.9% purity by GC. Biphenyl was purified by successive recrystallization from ethanol and benzene/hexanes while p-phenylphenol, 2-naphthol, and p-benzylphenol were recrystallized from benzene/hexanes until purity was > 99.9% by GC. Tetralin was purified by washing with conc H_2SO_4 until the layers were no longer colored, 10% Na_2CO_3, water, dried over Na_2SO_4, filtered, and fractionally distilled under vacuum from sodium two times taking the center cut. Purity was 99.4 % by GC. The synthesis of the surface-attached phenethyl phenyl ethers, $\approx PhCH_2CH_2OPh$ ($\approx$PPE-3) and $\approx PhOCH_2CH_2Ph$ ($\approx$PPE-1) has been previously reported.[6] Two-component surfaces were prepared by co-attachment of the phenols in a single step,[7] and had final purities of >99.7% (by GC). Surface coverages are listed in Table 2.

Thermolyses of PPE in the fluid and gas phase were performed in a fluidized sand bath (±1 °C) in Pyrex tubes, degassed by six freeze-pump-thaw cycles, and sealed under vacuum (ca. 10^{-5} Torr). Tubes were rinsed with acetone (high purity) containing standards, analyzed by GC and GC/MS, and quantitated by the use of internal standards with measured GC detector response factors. Thermolyses of surface-immobilized PPE were performed at 375 ± 1 °C in T-shaped tubes sealed under high vacuum (ca. 10^{-6} Torr). The volatile products were collected as they formed in a cold trap (77 K), analyzed by GC and GC/MS, as above. The surface-attached products were removed from the silica surface as the corresponding phenols by a base hydrolysis procedure,[8] silylated to the trimethylsilyl ethers, and analyzed as above. All products were identified by their mass spectra and whenever possible, by comparison to an authentic sample.

RESULTS AND DISCUSSION

Phenethyl Phenyl Ether Thermolysis of PPE in the liquid phase at 345 °C (1.2% conversion) produced styrene (36 mol%) and phenol (38 mol%), as the major products, and toluene (11 mol%) and benzaldehyde (12 mol%) as the minor products (eq 4). Small amounts

$$PhCH_2CH_2OPh \rightarrow PhCH{=}CH_2 + PhOH + PhCHO + PhCH_3 \tag{4}$$

of $Ph(CH_2)_2Ph$ (0.7 mol%), $Ph(CH_2)_3Ph$ (0.7 mol%), PhH (0.6 mol%) and $PhCH_2CH_3$ (0.3 mol%) were also formed. As the conversion increased, several secondary products, $Ph(CH_2)_3Ph$, $PhCH_2CH_3$, 1,3,5-triphenylpentane, and 1-phenoxy-2,4-diphenylbutane, grew in at the expense of the styrene. The material recovery decreased steadily with increasing conversion (based on recovered products), from 99.9% at 1.2% conversion, to 85% recovery at 17.9% conversion. The addition of 0.82 mol% and 7.0 mol%, 2,3-dimethyl-2,3-diphenylbutane, as a free radical initiator, increased the rate of reaction by 25% and 200%, respectively, while not altering the product distribution.

Thermolysis of PPE was also investigated at 375 °C with biphenyl (BP), as an inert diluent, (see Table 1) and in the gas phase from 28 - 260 kPa. Although the rate of decomposition is slower than in the liquid, the product composition is much simpler with $PhCH{=}CH_2$, PhOH, PhCHO, and $PhCH_3$ as the dominant products (>95%). The product selectivity, i.e. ($PhCH{=}CH_2$ + PhOH) / (PhCHO + $PhCH_3$), is independent of PPE concentration and conversion, if secondary products are taken into account. This indicates PhCHO and $PhCH_3$ are formed by a primary reaction pathway competitive with $PhCH{=}CH_2$ and PhOH. Additionally, a kinetic order of 1.30 ± 0.03 was determined from the slope of a log-log plot of initial rates vs. concentration.

A free radical chain pathway can be written for the thermal decomposition of PPE which can rationalize the primary and secondary products, acceleration by a free radical initiator, and the fractional kinetic order. Secondary products arise from the

$$PhCH_2CH_2OPh \rightarrow PhCH_2CH_2\bullet + PhO\bullet \tag{5}$$

$$PhO\bullet + PhCH_2CH_2OPh \rightarrow PhCH(\bullet)CH_2OPh\ (\mathbf{1}) + PhOH \tag{6}$$

$$\mathbf{1} \rightarrow PhCH{=}CH_2 + PhO\bullet \tag{7}$$

$$PhCH_2CH_2OPh + PhO\bullet \rightarrow PhCH_2CH(\bullet)OPh\ (\mathbf{2}) + PhOH \tag{8}$$

$$PhCH_2CH(\bullet)OPh \rightarrow PhCH_2CH(Ph)O\bullet \tag{9}$$

$$PhCH_2CH(Ph)O\bullet \rightarrow PhCH_2\bullet + PhCHO \tag{10}$$

$$PhCH_2\bullet + PhCH_2CH_2OPh \rightarrow \mathbf{1} + \mathbf{2} + PhCH_3 \tag{11}$$

reaction of $PhCH_2\bullet$, **1**, and **2** with $PhCH{=}CH_2$. Steps 8-11 have been added to the mechanism proposed by Gilbert[10] to explain the formation of PhCHO and $PhCH_3$ as primary products of a competitive reaction path. Although **1** is estimated to be ca. 7 kcal mol^{-1} more stable than **2**,[13] the unexpected competition between eq 8 with eq 6 can be rationalized by polar effects in the hydrogen transfer reaction between the electrophilic phenoxy radical and PPE (eq 8). Polar effects have been reported in the hydrogen abstraction reaction between the *t*-butoxy radical and substituted anisoles. A Hammet plot shows a good $\sigma\rho$ correlation with $\rho = -0.4$ indicating the development of cationic character in the transition state which can be stabilized by the adjacent oxygen.[14] Additionally, there is precedence for the competitive formation of products from the thermodynamically less stable radical of tetralin (2-tetralyl radical)[15] and 1,4-diphenylbutane (1,4-diphenyl-2-butyl radical)[8] at these temperatures. Since radical **2** does not have a facile β-scission route, it undergoes a 1,2-phenyl shift from oxygen to carbon (eq 9). β-Scission of the rearranged radical affords benzaldehyde and the chain carrying benzyl radical (eq 10). The chain length of the reaction, i.e. the number of chain turnovers per number of free radical formed, is ca. 10. Analogous intramolecular 1,2-phenyl shifts have been reported in the thermal decomposition of phenetole ($PhOCH_2CH_3$)[16] and anisole at 400 °C.[17] Also, spectroscopic and kinetic data have been obtained for the rearrangement of 1,1-diphenylethoxy radical (Ph2C(CH_3)O•) to 1-phenyl-1-phenoxyethyl radical (PhC(CH3)(•)OPh.[18]

The thermolysis of PPE was also studied in tetralin, a model liquefaction solvent, at various concentrations (Table 1). Dilution of PPE with tetralin or BP decreased the rate of decomposition in a similar fashion but the product selectivity increased from 3 to 9 as the tetralin concentration increased. This is a consequence of changing the chain carrying radical from phenoxy to the tetralyl radical. Hydrogen abstraction at the carbon adjacent to the oxygen to form **2** is enhanced for the electrophilic phenoxy radical as a consequence of favorable polar contributions. However, this polar effect is not present for hydrocarbon radicals such as tetralyl, and hydrogen abstraction to form **2** is less favorable resulting in an increase in product selectivity. Similar changes in the selectivity were obtained when diphenylmethane, $PhCH_2Ph$, was used as the hydrogen donating solvent.

Surface-Immobilized Phenethyl Phenyl Ether Thermolysis of surface-immobilized PPE, $\approx PhCH_2CH_2OPh$ ($\approx$PPE-3), at 375 °C at low conversions produces the products shown in eq 12. The selectivity

$$\approx PhCH_2CH_2OPh \rightarrow \approx PhCH{=}CH_2 + PhOH + \approx PhCH_3 + PhCHO \qquad (12)$$

of the reaction ($\approx PhCH{=}CH_2 + \approx PhCH_2CH_3 + PhOH$) / ($\approx PhCH_3 + PhCHO$) is slightly larger than that found for PPE as a consequence of the para-silyloxy substituent on the aromatic ring. This substituent enhances the hydrogen abstraction at the benzylic carbon and favors the production of $\approx PhCH{=}CH_2$ and PhOH. A similar increase in selectivity is observed for the thermolysis of *p*-$(CH_3)_3SiOPhCH_2CH_2OPh$, as a model of surface attached PPE, where in the gas phase at 375 °C, the selectivity is 4.4 ± 0.5. As for PPE, a free radical chain mechanism can be written for the decomposition of surface-immobilized PPE. Restricted mass transport does not affect the new reaction pathway, i.e. hydrogen abstraction at the β-carbon, rearrangement, and β-scission, to form $\approx PhCH_3$ and PhCHO.

The influence of co-attached aromatics on the rate and selectivity of the thermolysis of $\approx$PPE-3 are shown in Table 2. No new products were detected for the two component surfaces. Dilution of $\approx$PPE-3 with biphenyl ($\approx$BP) or naphthalene ($\approx$Naph) results in a decrease in the rate of decomposition compared to the high coverage $\approx$PPE-3. However, in the presence of $\approx$DPM, a rate acceleration was observed compared to $\approx$PPE-3 diluted with $\approx$BP or $\approx$Naph, which is in contrast to that observed in the fluid phase (Table 1). These results suggest that rapid hydrogen transfer reactions involving DPM are occurring on the surface that allows radical centers to migrate to the reactive substrate, i.e. $\approx$PPE. Evidently, the orientation of the molecules on the surface enhances the rate of hydrogen transfer, through the A-factor, relative to hydrogen transfer reactions in a nonconstrained environment, i.e. the fluid phase. A similar rate acceleration via radical relay processes has been reported in the thermolysis of surface-immobilized diphenylpropane and diphenylbutane in the presence of hydrogen donors.[7,8]

Interpretation of the selectivity data is more complicated. Surprisingly, the inert spacers increase the selectivity (Table 2). Since these spacers should not effect the thermodynamics of hydrogen abstraction, the packing of the molecules on the surface must be hindering the 1,2-phenyl shift such that a bimolecular hydrogen transfer reaction and β-scission (eq 13 and 14) can compete with rearrangement (eq 15). This hypothesis is currently

$$\approx PhCH_2CH_2OPh + \approx PhCH_2CH{\bullet}OPh \rightleftarrows \approx PhCH{\bullet}CH_2OPh + \approx PhCH_2CH_2OPh \tag{13}$$

$$\approx PhCH{\bullet}CH_2OPh \rightarrow \approx PhCH{=}CH_2 + PhO{\bullet} \tag{14}$$

$$\approx PhCH_2CH{\bullet}OPh \rightarrow \approx PhCH_2C(Ph)HO{\bullet} \rightarrow \approx PhCH_2{\bullet} + PhCHO \tag{15}$$

being investigated with the thermolysis of ≈PPE-3 and surface-attached benzene (≈PhH), which should not hinder the rearrangement but still dilute the molecules on the surface. Therefore, the change in the selectivity for ≈DPM/≈PPE-3 is likely a consequence of two factors. First, the methylene linkage in DPM allows the phenyl ring to rotate away from the adjacent ≈PPE such that the 1,2-phenyl shift should not be hindered, thus decreasing the selectivity (theoretically back to that observed for high coverage ≈PPE-3). Second, since ≈DPM can participate in a radical relay process, an increase in selectivity would be expected for this nonpolar radical, ≈PhCH•Ph, compared to the electrophilic phenoxy radical. It is interesting to note that in the fluid phase, dilution of PPE with an 8-fold excess of DPM increases the selectivity by a factor of 2.6, which is similar to the factor of 2.4 found for the surface-immobilized substrates.

The thermolysis of $\approx PhOCH_2CH_2Ph$, ≈PPE-1, at 375 °C produces the products shown in eq 16. The rate of decomposition is enhanced

$$\approx PhOCH_2CH_2Ph \rightarrow \approx PhOH + PhCH{=}CH_2 + \approx PhCHO + PhCH_3 \tag{16}$$

relative to ≈PPE-3 as a consequence of the para-silyloxy substituent. As for PPE and ≈PPE-3, a free radical chain mechanism can account for the products. Based on the selectivity, surface-immobilization does not appear to hinder the 1,2-phenyl shift to form ≈PhCHO and $PhCH_3$. However, ≈PhCHO undergoes free radical decomposition to form a surface-attached phenyl radical as shown in eq 17. The bond dissociation energy of benzaldehyde (87 kcal mol^{-1}) is similar to that of toluene ($PhCH_2$-H, 88 kcal mol^{-1}).[19].

$$\approx PhCHO + R{\bullet} \rightarrow \approx PhC{\bullet}O + RH \rightarrow \approx Ph{\bullet} + CO \tag{17}$$

At 13% conversion, over 41% of the ≈PhCHO has decomposed by decarbonylation to produce ≈PhH (73%) by hydrogen abstraction, ≈PhPh (14%) by aromatic substitution, and $\approx PhCH_2Ph$ (13%) by coupling with a gas phase benzyl radical. Stein has shown that the selectivity for hydrogen abstraction vs. arylation of toluene by the phenyl radical is 5.2 ± 0.5 at 400 °C in the gas phase.[20] Therefore, even in the presence of hydrogen donors, the phenyl radical could lead to arylation, which would form a more refractory linkage, i.e. a cross-link. These results show how decomposition of ether linkages may lead to cross-linking in low rank coal. Additionally, aromatic methoxy groups ($ArOCH_3$), which are present in high concentrations in low rank coals, could rearrange to aromatic aldehydes ($ArOCH_2{\bullet} \rightarrow ArCH_2O{\bullet} \rightarrow ArCHO$), under free radical reaction conditions. Subsquent decarbonylation could again lead to cross-linking.

SUMMARY

Investigations into the pyrolysis mechanisms of model β-aryl ether linkages have provided fundamental insights into the role of oxygen functional groups in retrogressive reactions. A previously undetected reaction pathway has been found for the free radical decomposition of PPE in the fluid phase and under conditions of restricted diffusion. Under conditions of restricted mass transport, the rates and product selectivities can be altered by the physical *and* chemical structure of the neighboring molecules. In the presence of a hydrogen donor, radical migration can occur on the the surface to transport radical sites to reactive molecules. Pyrolysis of the β-aryl ether linkage can lead to cross-linking reactions by the free radical decomposition of benzaldehyde to the highly reactive phenyl radical, which can undergo aromatic substitution reactions competitively with hydrogen abstraction.

ACKNOWLEDGEMENTS

Research was sponsored by the Division of Chemical Sciences, Office of Basic Energy Sciences, U. S. Department of Energy under contract DE-AC05-840R21400 with Martin Marietta Energy Systems, Inc.

REFERENCES

1. Derbyshire, F. J.; Whitehurst, D. D. *Fuel* **1981**, *60*, 655.
2. (a) Solomon, P. R.; Fletcher, T. H.; Purmire, R. J. *Fuel* **1993**, *72*, 587. (b) Solomon, P. R.; Serio, M. A.; Despande, G. V.; Kroo, E. *Energy Fuels* **1990**, *4*, 42.
3. Serio, M. A.; Kroo, E.; Charpenay, S.; Solomon, P.R. *Prep. Pap.-Am. Chem. Soc., Div. Fuel Chem.* **1993**, *38(3)*, 1021.
4. Britt, P. F.; Buchanan, III, A. C. *Proc., 7th Int. Conf. Coal Sci.*, Banff, Alberta, Canda, **1993**, *Vol 2*, 297.
5. Solum, M. S.; Pugmire, R. J.; Grant, D. M. *Energy Fuels* **1989**, *3*, 187.
6. Britt, P. F.; Buchanan, III, A. C.; Hitsman, V. H. *Proc., 6thInt. Conf. Coal. Sci.,* Newcastle-upon-Tyne, United Kingdom, **1991**, 207.
7. Buchanan, III, A. C.; Britt, P. F.; Biggs, C. A. *Energy Fuels* **1990**, *4*, 415.
8. Britt, P. F.; Buchanan, III, A. C. *J. Org. Chem.* **1991**, *56*, 6132.
9. Klein, M. T.; Virk, P. S. *Ind. Eng. Chem. Fundam.* **1983**, *22*, 35.
10. (a) Gilbert, K. E.; Gajewski, J. J. *J. Org. Chem.* **1982**, *47*, 4899. (b) Gilbert, K. E. *J. Org. Chem.* **1984**, *49*, 6.
11. Korobkov, V. Y.; Grigorieva, E. N.; Bykov, V. I.; Senko, O. V.; Kalechitz, I. V. *Fuel* **1988**, *67*, 657.
12. Cassidy, P. J.; Jackson, W. R.; Larkins, F. P. *Fuel* **1983**, *62*, 1404.
13. Benson, S. W. *Thermochemical Kinetics*, 2nd Ed.; Wiley-Interscience: New York, 1976.
14. Sakurai, H.; Hosomi, A.; Kumada, M. *J. Org. Chem.* **1970**, *35*, 993.
15. Franz, J. A.; Camaioni, D. M. *J. Org. Chem.* **1980**, *45*, 5247.
16. Collins, C. J.; Roark, W. H.; Raaen, V. F.; Benjamin, B. M. *J. Am. Chem. Soc.* **1979**, *101*, 1877.
17. Afifi, A. I.; Hindermann, J. P.; Chornet, E.; Overend, R. P. *Fuel* **1989**, *68*, 498.
18. Falvey, D. E.; Khambatta, B. S.; Schuster, G. B. *J. Phys. Chem* **1990**, *94*, 1056.
19. McMillen, D. F.; Golden, D. M. *Ann. Rev. Phys. Chem.* **1982**, *33*, 493.
20. Chen, R. H.; Kafafi, S. A.; Stein, S. E. *J. Am. Chem. Soc.* **1989**, *111*, 1414.

Table 1. Effect of Diluents on the Thermolysis of PPE at 375 °C

Diluent	Diluent[a]/PPE	Rate $*10^5$ Ms^{-1}	Selectivity[b]
None	--	32.8	2.8
BP	1.03	25.7	2.7
Tetralin	0.96	14	6.0
BP	4.54	5.1	2.9
Tetralin	3.87	6.5	9.3
BP	8.42	2.1	3.1
Tetralin	8.05	2.4	9.5
DPM	8.76	2.6	8.1
BP	19.1	0.67	3.7

[a] BP = biphenyl; DPM = diphenylmethane

[b] $PhCH{=}CH_2+PhOH/PhCH_3+PhCHO$

Table 2. Product Selectivity in the Thermolysis of Surface Attached PPE at 375 °C

Surface Comp.	Coverage (mmol g^{-1})	Rate (% h^{-1})	Selectivity[a]
≈PPE-3	0.54	8.3	5±1
≈PPE-3/≈BP	0.050/0.536	3.6	21±2
≈PPE-3/≈Naph	0.072/0.45	3.4	20±5
≈PPE-3/≈DPM	0.059/0.48	8.5	12±2
≈PPE-1	0.50	81	3.1±0.3[b]

[a] (≈$PhCH{=}CH_2$ +≈$PhCH_2CH_3$+PhOH)/(≈$PhCH_3$+PhCHO)

[b] $PhCH{=}CH_2/PhCH_3$

RESTRICTED MASS TRANSPORT EFFECTS ON FREE RADICAL REACTIONS

A. C. Buchanan, III, Phillip F. Britt, and Kimberly B. Thomas
Chemical and Analytical Sciences Division
Oak Ridge National Laboratory
P. O. Box 2008
Oak Ridge, Tennessee 37831-6197

Key words: Model compounds, free radicals, hydrogen transfer, mass transport

INTRODUCTION

Research aimed at the development of improved coal utilization technologies such as coal liquefaction and hydropyrolysis continue to benefit from the insights provided by well-designed model compound studies[1]. The importance of controlling hydrogen utilization in the development of economically competitive processes is well-recognized. The donation of hydrogen atoms to a reactive site in coal, such as a free radical, can occur from molecules native to the coal structure, hydrogen gas, or a liquefaction donor solvent. The hydrogen transfer can also be mediated by the presence of a catalyst. Model compound studies continue to probe the mechanisms of hydrogen transfer and utilization potentially involved in coal liquefaction.[1]

Coal possesses a complex chemical and physical structure. The cross-linked, network structure can lead to alterations in normal thermally-induced, free-radical decay pathways as a consequence of restrictions on mass transport. Moreover, in coal liquefaction, access of an external hydrogen donor to a reactive radical site can be hindered by the substantial domains of microporosity present in coals.[2,3] Larsen et al. have recently investigated the short contact time liquefaction of Illinois No. 6 coal in the presence of either tetralin or 2-*tert*-butyltetralin as the hydrogen donor solvent.[2] Remarkably, both the yields of pyridine extractables and the amount of hydrogen transferred from the donor solvent are the same despite the presence of the bulky *tert*-butyl group. Diffusion effects do not appear to be playing an important role in this coal conversion chemistry. Several possible explanations for this phenomenon were advanced including the potential involvement of a hydrogen hopping/radical relay mechanism recently discovered in model systems in our laboratories.[4,5]

We have employed silica-anchored compounds to explore the effects of restricted mass transport on the pyrolysis mechanisms of coal model compounds.[4-7] In studies of two-component systems, cases have been discovered where radical centers can be rapidly relocated in the diffusionally constrained environment as a consequence of rapid serial hydrogen atom transfers. This chemistry can have substantial effects on thermal decomposition rates[4] and on product selectivities.[5] In this study, we examine additional surfaces to systematically investigate the impact of molecular structure on the hydrogen atom transfer promoted radical relay mechanism. Silica-attached 1,3-diphenylpropane (≈Ph(CH$_2$)$_3$Ph, or ≈DPP) was chosen as the thermally reactive component, since it can be considered prototypical of linkages in coal that do not contain weak bonds easily cleaved at coal liquefaction temperatures (ca. 400°C), but which crack at reasonable rates if benzylic radicals can be generated by hydrogen abstraction. The rate of such hydrogen transfers under restricted diffusion will be highly dependent on the structure and proximity of neighboring molecules.[4,7]

EXPERIMENTAL

The two-component surfaces shown below were synthesized from the corresponding phenols by co-reaction with the surface hydroxyls of a nonporous, fumed silica (surface area of 200 ± 25 m^2/ g) as previously described.[4-7] The compounds are covalently anchored to the silica surface by a thermally robust Si-O-C$_{aryl}$ linkage. The resulting two-component surfaces had purities of ≥ 99.3%.

Pyrolyses were performed in sealed, evacuated (2 x 10^{-6} torr), T-shaped tubes at 375°C. During the reaction, any volatile materials formed migrated out of the heated zone and were collected in the sidearm cold trap (77K). After the reaction, the volatile products in the trap were dissolved in acetone and analyzed by GC and GC-MS with the use of internal calibration standards. Base hydrolysis (1N NaOH) of the silica residue liberated the surface-attached products and unreacted starting materials, which were isolated as the corresponding phenols following neutralization and extraction with CH_2Cl_2. These products were silylated with *N,O*-bis(trimethylsilyl)trifluoroacetamide in pyridine (2.5M), and the corresponding trimethylsilyl ethers were analyzed in the presence of internal standards by GC and GC-MS.

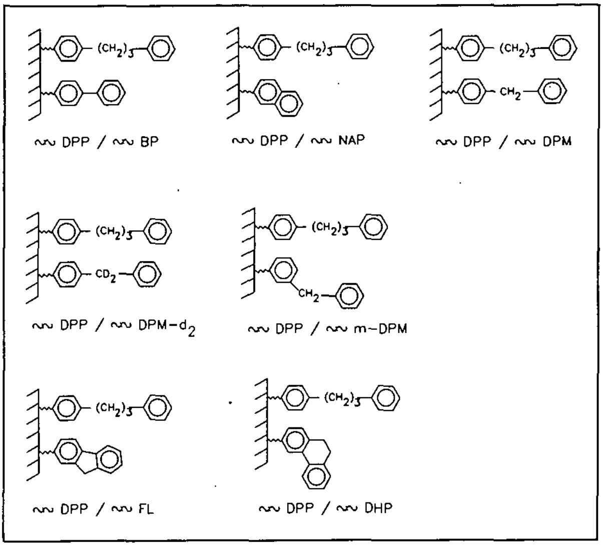

RESULTS AND DISCUSSION

If the rate of decomposition of 1,3-diphenylpropane were governed solely by homolysis of its weakest bond (about 74 kcal/mol) to form $PhCH_2\bullet$ and $\bullet CH_2CH_2Ph$, then DPP would be stable at 400°C with a half life on the order of 19 years.[8] The fact that DPP is thermally reactive even at 375°C derives from the incursion of a free-radical chain decomposition pathway that produces benzylic radicals capable of cracking by β-scission. For silica-immobilized DPP (≈DPP), this reaction produces the cracking products shown in Eq. 1 with the radical chain propagation steps shown in Eqs. 2-4.[7] As shown in Table 1, the rate of ≈DPP decomposition decreases substantially with decreasing surface coverage as the rate for the hydrogen atom transfer step 4 decreases. This should be particularly important

$$\approx Ph(CH_2)_3Ph \rightarrow PhCH_3 + \approx PhCH{=}CH_2 + \approx PhCH_3 + PhCH{=}CH_2 \qquad (1)$$

$$\approx PhCH\bullet CH_2CH_2Ph\ (\mathbf{1}) \rightarrow \approx PhCH{=}CH_2 + PhCH_2\bullet \qquad (2)$$

$$\approx PhCH_2CH_2CH\bullet Ph\ (\mathbf{2}) \rightarrow \approx PhCH_2\bullet + PhCH{=}CH_2 \qquad (3)$$

$$\approx PhCH_2\bullet\ (\text{and } PhCH_2\bullet) + \approx Ph(CH_2)_3Ph \rightarrow \approx PhCH_3\ (\text{and } PhCH_3) + \mathbf{1} + \mathbf{2} \qquad (4)$$

for hydrogen abstraction by the surface-attached benzyl radical, $\approx PhCH_2\bullet$, as the spatial separation between reactants increases with decreasing surface coverage. Similar rate decreases are observed in pyrolysis of liquid-phase DPP when the concentration is decreased by dilution with an inert solvent.

Discovery of the radical relay mechanism originated from studies of the pyrolysis of the surfaces, ≈DPP/≈BP, ≈DPP/≈NAP, and ≈DPP/≈DPM, where the biphenyl and naphthalene spacers were innocuous, but the diphenylmethane spacer molecules resulted in greatly enhanced decomposition rates (ca. 10-fold) for ≈DPP when compared at similar surface coverages of ≈DPP (see Table 1).[4] This is in contrast to liquid phase DPP pyrolyses where DPM behaves as other inert diluents.[4] In the surface-immobilized cases, no new products were formed, and the involvement of diphenylmethane moieties in the relay pathway was confirmed from the study of ≈DPP/≈DPM-d_2. In addition to an apparent deuterium isotope effect on the reaction rate, incorporation of substantial amounts of deuterium in the vapor-phase and surface-attached toluene products was detected. A pictorial representation of the radical relay process is shown below. The facility of this process, which leads to rates comparable to saturated coverages of ≈DPP without spacer molecules, is likely a consequence of enhanced A-factors for the bimolecular hydrogen transfer steps on the surface for these "pre-organized" reactants. Similar effects have been proposed to explain the enhanced rates often observed for organic reactions on clay surfaces, which are attributed to a "reduction in the dimensionality of the reaction space".[9]

Table 1. Effect of Spacer Structure on Pyrolysis of ≈DPP at 375°C

Surface Composition	*Coverage (mmol g^{-1})*	*Rate x 10^4 (% s^{-1})*
≈DPP	0.59	24.0
	0.14	1.1
	0.10	0.72
≈DPP / ≈BP	0.13 / 0.51	2.2
≈DPP / ≈NAP	0.12 / 0.44	1.9
≈DPP / ≈DPM	0.17 / 0.42	21.0
	0.13 / 0.37	17.0
≈DPP / ≈DPM-d_2	0.16 / 0.36	12.0
≈DPP / ≈*m*-DPM	0.17 / 0.31	27.0
≈DPP / ≈FL	0.17 / 0.42	86.0
≈DPP / ≈DHP	0.21 / 0.36	8.6
	0.065 / 0.47	13.0

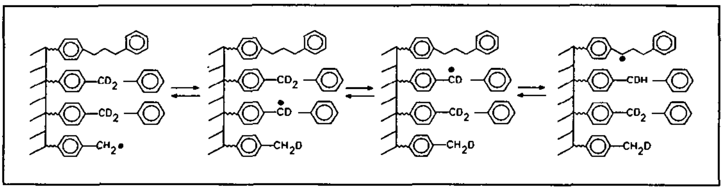

As shown in Table 1, the use of the isomeric *meta*-diphenylmethane spacer similarly produces enhanced rates, and appears even more effective than the *para*-analog at participating in the radical relay process. The fluorene spacer (≈FL) is a cyclic analog to ≈*m*-DPM, which is known to have faster kinetics for hydrogen donation to benzyl radicals because it does not require phenyl rotations to be frozen in the transition state.[8] However, in the surface-attached analog, the fact that the benzylic hydrogens are attached to a carbon locked in a ring could potentially lead to geometrical constraints in the hydrogen transfer steps on the surface. As shown in Table 1, the ≈DPP pyrolysis rate is substantially enhanced in the presence of ≈FL compared even with the DPM cases. However, for ≈DPP/≈FL, we have found that the majority of the ≈$PhCH{=}CH_2$ product has undergone reaction with fluorenyl radical in a chain transfer step (Eq. 5). The resulting radical does not terminate the chain, but abstracts hydrogen to provide an additional pathway for relaying radical centers on the surface (Eq. 6 and 7). This additional pathway apparently also contributes to the facile decomposition of ≈DPP.

$$\approx FL\bullet \;+\; \approx PhCH{=}CH_2 \;\rightarrow\; \approx PhCH\bullet CH_2\text{-}FL\approx \tag{5}$$

$$\approx PhCH\bullet CH_2\text{-}FL\approx \;+\; \approx Ph(CH_2)_3Ph \;\rightarrow\; \approx PhCH_2CH_2\text{-}FL\approx \;+\; 1 \;+\; \mathbf{2} \tag{6}$$

$$\text{or, } \approx PhCH\bullet CH_2\text{-}FL\approx \;+\; \approx FL\text{-}H \;\rightarrow\; \approx PhCH_2CH_2\text{-}FL\approx \;+\; \approx FL\bullet \tag{7}$$

The hydroaromatic, 9,10-dihydrophenanthrene (DHP), is often employed as a model hydrogen donor liquefaction solvent. It can be seen from Table 1 that ≈DPP reacts faster in the presence of co-attached DHP (≈DHP) than in the presence of the inert aromatics, biphenyl (≈BP) and naphthalene (≈NAP), although not as fast as in the presence of ≈DPM. The radical relay chemistry is more complicated with ≈DHP, however, because chain propagation can also occur via hydrogen atoms donated by the intermediate hydrophenanthryl radicals, ≈DHP•, which would not experience diffusional constraints (Eqs. 8 and 9). Consistent with this premise, we observe formation of modest amounts of surface-attached phenanthrene (≈PHEN), as well as new products resulting from hydrocracking of ≈DPP (accounting for ca. 2% of the reacted ≈DPP) to form ≈PhH + PhC_3H_7 and PhH + ≈PhC_3H_7. However, it is interesting that the ≈DPP decomposition rate is substantially greater for the diphenylmethane spacers which serve only as radical relay catalysts.

$$\approx\mathrm{DHP}\bullet \rightarrow \approx\mathrm{PHEN} + \mathrm{H}\bullet \qquad (8)$$

$$\mathrm{H}\bullet + \approx\mathrm{Ph(CH_2)_3Ph} \rightarrow \mathrm{H_2} + \mathbf{1} + \mathbf{2} \qquad (9)$$

CONCLUSIONS

This study shows that the rate at which surface-immobilized 1,3-diphenylpropane thermally decays at 375°C can span a substantial range that is dependent on the structure of neighboring molecules on the surface. It seems clear that it is possible for radical centers to relocate in diffusionally constrained environments at relevant coal liquefaction temperatures, without the need for physical movement, by means of rapid serial hydrogen atom transfers. There may exist an optimum set of chemical structures that possess the appropriate thermochemical and structural properties to promote the radical relay phenomenon under conditions of restricted diffusion, and we continue to explore additional spacer molecules.

The significance of these results for coal liquefaction encompasses two points. If the cleavage of a linkage embedded in a microporous domain in coal requires formation of a radical precursor (as typified by DPP in the current study), then a radical relay mechanism could transfer that needed "reactivity" to the linkage in question. Alternatively, if a radical is formed in an inaccessible region of the coal network and needs to be capped by a hydrogen source to prevent a retrogressive reaction, then a radical relay pathway could relocate the radical center to a region in the coal that is accessible to a hydrogen donor in the liquefaction medium. It remains to be determined whether such a phenomenon contributes to the coal liquefaction behavior recently reported by Larsen (*vide supra*).[2]

ACKNOWLEDGEMENT

This research was sponsored by the Division of Chemical Sciences, Office of Basic Energy Sciences, U.S. Department of Energy, under Contract No. DE-AC05-84OR21400 with Martin Marietta Energy Systems, Inc.

REFERENCES

1. Buchanan, III, A. C.; Britt, P. F. *Prepr. Pap.-Am. Chem. Soc., Div. Fuel Chem.* **1994**, *39(1)*, 22.
2. Larsen, J. W.; Amui, J. *Energy Fuels* **1994**, *8*, 513.
3. Walker, Jr., P. L.; Mahajan, O. P. *Energy Fuels* **1993**, 7, 559.
4. Buchanan, III, A. C.; Britt, P. F.; Biggs, C. A. *Energy Fuels* **1990**, *4*, 415.
5. Britt, P. F.; Buchanan, III, A. C. *J. Org. Chem.*, **1991**, *56*, 6132.
6. Buchanan, III, A. C.; Dunstan, T. D. J.; Douglas, E. C.; Poutsma, M. L. *J. Am. Chem. Soc.* **1986**, *108*, 7703.
7. Buchanan, III, A. C.; Biggs, C. A. *J. Org. Chem.* **1989**, *54*, 517.
8. Poutsma, M. L. *Energy Fuels* **1990**, *4*, 113.
9. Laszlo, P. *Acc. Chem. Res.* **1986**, *19*, 121.

THE EFFECT OF COAL ADDITION ON SOLVENT HYDROGENATION AND COAL CONVERSION IN A MODEL ALKYLNAPHTHALENE SOLVENT

Kurt S. Rothenberger, Anthony V. Cugini,
Karl T. Schroeder, Garret A. Veloski, and Michael V. Ciocco
U.S. Department of Energy, Pittsburgh Energy Technology Center,
P.O. Box 10940, Pittsburgh, PA 15236

INTRODUCTION

Model compounds are useful because they offer insight into the processes of more complex systems. They allow one to study a controlled system of known structure and relatively well mapped reaction pathways, in the hope that the information obtained therein is transferable to real systems. The problem with the study of model systems is that those very constraints which make the system easy to understand may in turn hinder the application of that understanding to real systems. This is particularly true in the study of coal liquefaction, where the complexity of the coal system often gives rise to unanticipated results.

The current paper discusses how the addition of even small amounts of coal (1:1 coal:catalyst) can dramatically affect the catalytic hydrogenation of model two-ring aromatic solvents. The catalyst, a novel, unsupported molybdenum catalyst preformed during a separate solvent hydrogenation step, appears to be selectively deactivated toward solvent hydrogenation, but not coal conversion. The effect is observed in two model solvent systems, 1-methylnaphthalene and Panasol. Adding coal-derived preasphaltene and asphaltene materials seems to have the same effect.

EXPERIMENTAL SECTION

Materials. Panasol®, a mixture containing mostly alkyl naphthalenes, was obtained from Crowley Chemical Company and used without further purification. Purified grade 1-methylnaphthalene from Fisher Scientific Company, found to be 99% pure by gas chromatography, was used without further purification. Blind Canyon coal, DECS-6, from the U.S. Dept. of Energy's Coal Sample Program, was used in these studies. A unique, high surface area, preformed molybdenum catalyst was prepared at the U.S. Dept. of Energy's Pittsburgh Energy Technology Center (PETC). The catalyst consisted of the recovered solid from a semi-batch 1-L stirred autoclave reaction of ammonium heptamolybdate, hydrogen sulfide, and Panasol under 17 MPa (2500 psi) hydrogen at 425°C [1]. The catalyst contained 50% C, 30% Mo, and 20% S, and possessed a BET surface area of approximately 250 m^2/g. The supported iron catalyst was prepared by precipitation of FeOOH from a solution of ferric nitrate onto Raven® carbon black. The supported molybdenum catalyst was prepared in a similar fashion from ammonium heptamolybdate.

Reactions. Reactions were completed in a stainless steel batch microautoclave reactor system constructed at PETC. The cylindrical reactor portion has a volume of 43 mL, and the total internal volume, including all tubing and connections, is 60 mL. The reactor was equipped with an internal thermocouple and a pressure transducer for continuous monitoring of pressure and temperature throughout the run. The reactor was mounted on a rocker arm, which extends into an electrically heated sand bath. In typical experiments, the reactor was charged with various combinations of solvent, coal, catalyst, a sulfur source, and then was pressurized with hydrogen. Unless otherwise stated, a full charge consisted of 6.6 g solvent, 3.3 g coal, 0.1 g catalyst, 0.1 g sulfur, and 7 MPa (1000 psi) ambient temperature hydrogen gas. The reactor was then attached to the rocker arm (180 cycles / minute) and plunged into a preheated sand bath, where it was heated up to 425°C in 2 to 4 minutes. It was held at temperature in the sand bath for 30 minutes, and then removed and allowed to air cool, typically in less than 5 minutes, to room temperature. The reactor was vented and the gas collected for analysis.

Sample Workup Procedure and Coal Conversion Calculation. During workup, the reactor (including tubing) was cleaned and rinsed with tetrahydrofuran (THF). The material collected was combined and filtered through a 0.45 micron filter under 40 psi nitrogen gas pressure, yielding the "THF solubles" and "THF insolubles." Coal conversion was calculated based on the mass of MAF coal from the measured mass of THF insolubles adjusted for catalyst and coal mineral matter. After the THF insolubles were weighed, the soluble material was stripped of solvent on a rotary evaporator until mass balance was obtained. Although this generally removed most of the THF solvent, some was occasionally observed by H-1 nuclear magnetic resonance (NMR) in the resulting THF soluble fraction. In runs where coal was used in the reactor, the THF solubles were extracted by heptane, and the procedure was repeated to obtain a heptane-soluble fraction. In each case, the soluble portion was derived essentially from the original Panasol or 1-methylnaphthalene solvent and its reaction products, and (when coal was present) a small amount of coal-derived material.

Gas and Pressure Analyses. At the completion of each run, product gases were collected and analyzed at PETC by a previously published method [2]. Total hydrogen consumption for the run was calculated based on the difference between initial and final (cold) gas pressure as adjusted for product gas slate. In some runs, gas composition data were not available, or had to be estimated from a similar experiment. Hydrogen consumption as a function of time was calculated from the total (hot) gas pressure, recorded at 10 s intervals during the run, total hydrogen consumption, and the assumption that product gases were produced in a linear fashion throughout the run. Assumptions were also made concerning the liquid-vapor equilibrium of the solvent, the solubility of hydrogen in the liquid phase, and the fact that part of the reactor tubing does not extend down into the hot sand bath. A more complete description of the hydrogen consumption measurements is found in reference 3.

Gas Chromatography. Gas chromatography was performed either with a Hewlett Packard HP5880A gas chromatograph (GC) equipped with flame ionization detector (FID) or a Hewlett Packard HP5890A GC equipped with an HP5970 mass selective detector (GC/MS).

Low-Voltage, High-Resolution Mass Spectrometry (LVHRMS). LVHRMS data were obtained on a Kratos MS-50 high-resolution mass spectrometer interfaced to a personal-computer-based data system developed at PETC. The sample was introduced into the ion source through the batch inlet system at a temperature of 200°C. The magnet was operated with a static resolving power exceeding one part in 30,000 with an average dynamic resolving power (while scanning) of one part in 26,000. Quantitative calibration of tetralins relative to naphthalenes was accomplished with known mixtures of tetralin and 1-methylnaphthalene. Further details on the LVHRMS technique and data reduction routines are provided in references 4 and 5.

Nuclear Magnetic Resonance. Both H-1 and C-13 NMR of the samples were recorded on CD_2Cl_2 solutions of the samples on a Varian VXR-300 NMR spectrometer equipped with a 5-mm broadband probe. C-13 NMR spectra were the result of 700 time-averaged scans recorded with 90° pulse widths and a recovery time of 60 s, requiring approximately 12 hours of spectrometer time per spectrum. Decoupling was applied only during acquisition.

RESULTS AND DISCUSSION

Verification of Analytical Results: 1-Methylnaphthalene and Panasol Solvents. In order to verify the accuracy and reproducibility of the analytical methods, microautoclave hydrogenations were made using 1-methylnaphthalene solvent, 7 MPa initial (cold) hydrogen pressure, and (if used) catalyst. The series consisted of a thermal (no catalyst) run, the preformed dispersed molybdenum catalyst (Mo), an iron (Fe/C) and a molybdenum (Mo/C) catalyst, the latter two supported on carbon black. 1-Methylnaphthalene, 5- and 1- methyltetralin, naphthalene, and tetralin constitute 97% of the products (by GC) from this simple solvent system. Independent determinations of 1-methylnaphthalene hydrogenation to tetralins were made by each of the analytical methods: gas analysis, GC, LVHRMS, and NMR. The results, their averages and standard deviations are listed in Table 1.

Panasol is a fairly complex hydrocarbon mixture, with some 130 GC peaks above the 0.01% threshold level. It contains about 80% alkylated naphthalenes (2-methylnaphthalene is the largest single constituent at 22%), and 5-10% each of alkylated benzenes, tetralins, and biphenyls. It has a proton aromaticity of 0.48, and a carbon aromaticity of 0.84, corresponding to an "average" structure of dimethylnaphthalene. Since the alkylnaphthalenes in Panasol were expected to hydrogenate similarly to 1-methylnaphthalene, a series of microautoclave reactions with Panasol was completed under the same conditions as those for the samples of Table 1.

The results are given in Table 2. For GC and LVHRMS, the hydrogenation determination was made from direct measurement of naphthalenes and tetralins in the products as compared to the starting Panasol. Hydrogenation was estimated from gas analysis by fitting the hydrogen consumption with that necessary to convert a given amount of dimethylnaphthalene to the corresponding tetralins. Hydrogenation was estimated from NMR data by fitting the aromaticity change to a given conversion of dimethylnaphthalene to the corresponding tetralins. Although the hydrogenation estimates for Panasol do not agree with each other as well as they do in Table 1, the average results are still within the standard deviation of the 1-methylnaphthalene hydrogenations.

Effect of Coal Addition on Solvent Hydrogenation Using Preformed, High Surface Area Mo Catalyst. A series of microautoclave experiments was completed using 6.6 g of either 1-methylnaphthalene or Panasol solvent, 7 MPa initial (cold) hydrogen pressure, and 0.1 g preformed high surface area molybdenum catalyst. The runs contained 0.0, 0.1, 0.2, and 3.3 g of coal, respectively. Figure 1 shows the hydrogen consumption plotted as a function of time over the course of each run. A substantial amount of hydrogen is consumed during the heat-up period (i.e., before time zero in Figure 1); in fact, the "liquefaction" of the 0.1 and 0.2 g coal samples is probably completed by the time the plot starts. The residual, or observed hydrogen consumption is most likely due to hydrogenation of the solvent. In the Figure, it can be seen that the rate of hydrogen consumption consistently follows the order 0.0 g > 0.1 g > 0.2 g. The rate for the 3.3 g coal sample is still trending downward at the end of the run, with hydrogen consumption probably attributable to coal conversion rather than solvent hydrogenation.

Total hydrogen consumption for these runs, including the heat-up periods, is listed in Table 3. Not surprisingly, the greatest hydrogen consumption, 55 mmol, was found with the highest loading of coal, 3.3 g. This can be attributed to the fact that two acceptors were available for the gaseous hydrogen - both the solvent and the coal. Consistent with Figure 1, the addition of small amounts of coal to the solvent does not produce an intermediate result. Rather, the total hydrogen consumption with both 0.1 g (26 mmol H_2) and 0.2 g (22 mmol H_2) of added coal is less than that for either no added coal (29 mmol H_2) or 3.3 g added coal. For comparison, the thermal hydrogenation of 1-methylnaphthalene and Panasol, listed in Tables 1 and 2, consumed only 2 and 3 mmoles hydrogen, respectively. The results are more striking when one examines hydrogenation of naphthalenes in the solvent as analyzed by LVHRMS. The percentage of naphthalenes converted to tetralins is highest in the no coal case, and decreases rapidly with increasing amounts of added coal, from 31% to 12%. Unfortunately, heptane contamination from the workup procedure makes it impossible to obtain a quantitative estimate of solvent hydrogenation from NMR aromaticity measurements. However, the results are qualitatively supported by examination of the NMR spectra.

These results demonstrate that the rate of hydrogenation of these solvents is diminished by the presence of small amounts of coal in the reactor. However, the total hydrogen consumption was still greatest for the maximum loading of coal. That is, hydrogen was still going to the coal though not to the solvent. One explanation for this phenomenon might be that the type of structures present in the coal and initial coal derived products hydrogenate more readily than the solvent. In a popular model of liquefaction, the first products of coal dissolution are the asphaltenes and preasphaltenes. These are generally thought of as large, aromatic systems consisting of three or more condensed rings. This argument is supported by work which has shown that three ring systems hydrogenate faster than two ring systems [6]. However, the argument is difficult to accept in circumstances where only a small amount of coal is present. The results of Figure 2 would seem to indicate that coal dissolution happens very quickly in these cases. Even if the coal-derived products hydrogenate more quickly, there would still be adequate time and hydrogen to hydrogenate the solvent.

Effect of Recycled Catalyst on Subsequent Reactions. The next sequence of experiments helps illustrate what happened to the catalyst on exposure to coal. These experiments begin with the THF insolubles from the reaction which had employed 0.2 g of coal with fresh catalyst, cited in the previous series ("A" in Figure 2). This material, presumably consisting of the recovered catalyst and a very small amount of unreacted coal, was used as the catalyst for a new experiment, hydrogenating 1-methylnaphthalene solvent with no fresh coal ("B" in Figure 2). The THF insolubles from the second run were used as the catalyst in a third run, this time containing 1-methylnaphthalene solvent and 3.3 g coal ("C" in Figure 2). The total hydrogen consumption, solvent hydrogenation as measured by LVHRMS, and coal conversion (in the cases where 3.3 g of coal was reacted) are summarized in Figure 2. The same data for experiments with 3.3 g coal with fresh catalyst ("D"), and 0.0 g of coal with fresh catalyst ("E"), are included for comparison.

Solvent hydrogenation, as seen in Figure 2, is highest for the case of fresh catalyst, and no added coal. Solvent hydrogenation drops by a factor of over two upon exposure of the catalyst to 0.2 g coal, and does not recover, maintaining its value when the recycled catalyst is used in a subsequent run. Solvent hydrogenation drops further when the catalyst is exposed to more coal. Coal conversion, on the other hand, is uninhibited by the use of recycled catalyst. Hydrogen consumption is highest for the experiments which employed a full charge (3.3 g) of coal, intermediate for the case of fresh catalyst and no coal, and lowest for cases in which the catalyst had been exposed to coal but there was not enough coal present to take up hydrogen itself.

In an effort to pinpoint the origin of the catalyst inhibitor, 0.4 g of the THF-solubles, heptane-insolubles fraction (i.e., asphaltenes and preasphaltenes) was taken from a reaction which had employed 3.3 g coal and fresh catalyst and added to a hydrogenation reaction containing 1-methylnaphthalene and fresh catalyst, but no coal. The result ("E") is displayed with the others in Figure 2. Solvent hydrogenation (at 4%) was almost completely suppressed to levels below those obtained with 3.3 g coal present. Hydrogen consumption was much the same as when fresh catalyst was used with small amounts of coal or recycled catalyst was employed.

Discussion and Conclusion. The results of Figure 2 are not consistent with a simple competition for catalyst sites. The fact that solvent hydrogenation with coal present did not recover to previous levels with the "recycled" catalyst indicates some persistent change in the catalyst, i.e., poisoning. The fact that there was no impairment of coal conversion when coal was added, together with a hydrogen consumption value similar to what it would have been for fresh catalyst, indicates that any deactivation of the catalyst did not affect coal conversion.

Plainly, some deactivation of the catalyst has taken place. Otherwise the diminution in solvent hydrogenation would not have occurred. However, a substantial amount of catalytic activity remains. There is no other explanation for the coal conversion or total hydrogen consumption data with 3.3 g coal.

Supported and unsupported catalysts have been used for first stage coal liquefaction. Exposure to coal has been known to affect the long-term activity of supported catalysts. Unsupported catalysts are normally once-through catalysts and are not exposed to coal for long times. Long term deactivation of unsupported catalysts would not be a problem. Rapid and selective deactivation of specific catalyst sites upon exposure to coal would be a greater concern.

Deactivation of supported catalysts has been the subject of a number of studies [7]. The poisoning effect of nitrogen bases on catalysts, especially for those catalysts which have acidic active sites, has been extensively studied in the areas of petroleum cracking [8], coal liquefaction [9], and coprocessing [10]. The formation of carbonaceous deposits on the catalyst surface has also been implicated in the loss of hydrogenation activity in coal liquefaction catalysts [11]. Studies have shown that carbon supports confer higher resistance to fouling by carbonaceous deposits than do alumina supports [12]. The preformed, high surface area molybdenum catalyst used in the coal addition studies reported here is an unsupported catalyst in the sense that it is being developed for once-through use. However, the catalyst still contains 50% carbon, and probably shares much in common with molybdenum catalysts on carbon supports. The observation of catalyst poisoning is therefore significant.

The fact that solvent hydrogenation (at least that of double-ring aromatic compounds) is inhibited while coal conversion, a process which also requires hydrogen, is not, would support the existence of different types of catalytically active sites. Suppose the catalyst contains different types of active sites, and some of these sites bind substrates more strongly than others. In this representation, the best, i.e., most strongly interacting sites are required for hydrogenation of Panasol. However, other weaker sites exist in greater numbers, and are adequate for providing hydrogen to the decomposing coal matrix. Most catalyst poisons act by adhering to an active site and preventing interaction with any other substrates. If the poisoning agent, whatever its identity, is not a particularly strong catalyst poison, it would only adsorb and adhere to the most strongly interacting sites. In this manner, the sites needed for solvent hydrogenation would no longer be available. On the other hand, the byproducts of coal conversion can use the less active sites, so conversion remains relatively unchanged. Such a system would exhibit the observed characteristics of both catalyst poisoning and competition for catalyst sites.

At this point, it is not known whether the hydrogen going to the coal is involved with hydrogenating aromatic rings, or simply capping fragments formed from bond scission. However, these preliminary results would appear to serve as a warning that the best catalysts for coal liquefaction may not necessarily be found by hydrogenating model compounds.

Further work is in progress to identify the poisoning agent or agents, and to determine if its effect on the catalyst is reversible.

ACKNOWLEDGEMENTS

The authors gratefully acknowledge Dr. Bradley D. Bockrath for suggestions and helpful conversations regarding this project.

DISCLAIMER

Reference in this report to any specific commercial product, process, or service is to facilitate understanding and does not necessarily imply its endorsement or favoring by the United States Department of Energy.

REFERENCES

1. Cugini, A.V.; Krastman, D.; Lett R.G.; Balsone, V.D. Catalysis Today, **1994**, 19(3) 395-408.

2. Hackett, J.P.; Gibbon, G.A. In Automated Stream Analysis for Process Control, Manka, D.P., Ed., Academic Press, 1982; pp 95-117.

3. Ciocco, M.V.; Cugini, A.V.; Rothenberger, K.S.; Veloski, G.A.; Schroeder, K.T. To be published in Proc. 11th Ann. Int. Pittsburgh Coal Conf.; September 12-16, 1994; Pittsburgh, PA.

4. Schmidt, C.E.; Sprecher, R.F.; Batts, B.D. Anal Chem., **1987**, 59, 2027-2033.

5. Schmidt, C.E.; Sprecher, R.F. In Novel Techniques in Fossil Fuel Mass Spectrometry, ASTM STP 1019, Ashe, T.R.; Wood, K.V., Eds., American Society for Testing and Materials: Philadelphia, 1989; pp 116-132.

6. Weisser, O.; Landa, S. In Sulphide Catalysts, Their Properties and Applications, Pergammon: London, 1973; pp 126-127.

7. Derbyshire, F.J. In Catalysis in Coal Liquefaction, IEA Coal Research: London, 1988; Chapter 8.

8. Mills, G.A.; Boedekker, E.R.; Oblad, A.G. J. Am. Chem. Soc., **1950**, 72, 1554-1560.

9. Adkins, B.D.; Milburn, D.R.; Davis, B.H. Prepr. Pap. - Am. Chem. Soc., Div. Fuel Chem., **1988**, 221-228.

10. Ting, P.S.; Curtis, C.W.; Cronauer, D.C. Energy and Fuels, **1992**, 6, 511-518.

11. (a) Kovach, S.M.; Bennett, J. Am. Chem. Soc. Div. Fuel Chem. Prepr., **1975**, 20(1), 143-160. (b) Ocampo, A.; Schrodt, J.T.; Kovach, S.M. Ind. Eng. Chem. Prod. Res. Dev., **1978**, 17, 56-61.

12. Scaroni, A.W.; Jenkins, R.G.; Walker, Jr., P.L. Appl. Catal., **1985**, 14, 173-183.

TABLE 1: Comparison of Analytical Results for 1-Methylnaphthalene Hydrogenation

Technique	Thermal	Mo	Mo/C	Fe/C
Gas Analysis	2%	37%	58%	33%*
GC	2%	31%	50%	25%
LVHRMS	0%	29%	50%	20%
C-13 NMR	2%	29%	45%	20%
AVERAGE±SD	2±1%	32±4%	51±5%	**25±6%**

* gas pressure data estimated due to leak

TABLE 2: Comparison of Analytical Results for Panasol Hydrogenation

Technique	Thermal	Mo	Mo/C	Fe/C
Gas Analysis	4%	34%	55%	27%
GC/MS	NA	NA	46%	17%
LVHRMS	1%	31%	56%	31%
C-13 NMR	5%	25%	36%	27%
AVERAGE	3%	**30%**	**48%**	**26%**

TABLE 3: Effect of Added Coal on Naphthalene Hydrogenation by Preformed Dispersed Molybdenum Catalyst

Solvent	Coal (g)	mmol H_2 Consumed	% Naph to Tet (LVHRMS)
Panasol	0.0	29	31
1-MeNp	0.1	26	22
Panasol	0.2	22	14
Panasol	3.3	55	12

Figure 1: Effect of Added Coal on the Rate of H2 Consumption.

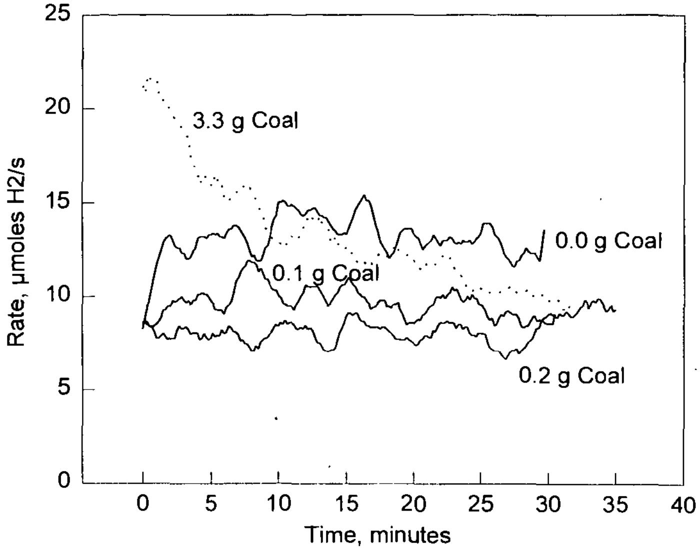

Figure 2: Summary of Coal Conversion, Solvent Hydrogenation and Hydrogen Consumption for Fresh and Recycled Catalyst

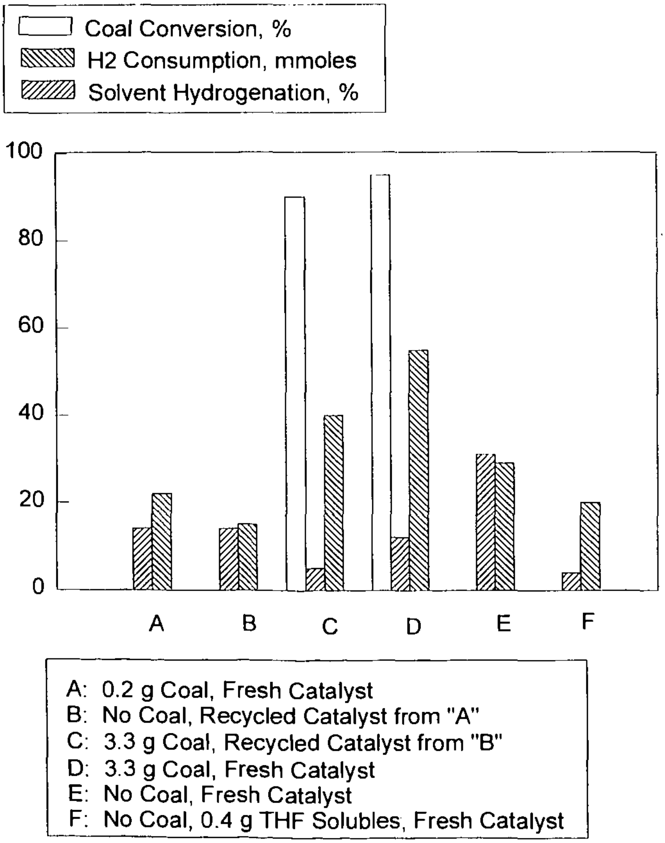

THE EFFECT OF PRESSURE AND SOLVENT QUALITY ON FIRST STAGE COAL LIQUEFACTION WITH DISPERSED CATALYSTS

A.V. Cugini, K.S. Rothenberger, M.V. Ciocco,
G.A. Veloski, and D.V. Martello,
U.S. Department of Energy, Pittsburgh Energy Technology Center,
P.O. Box 10940, Pittsburgh, PA 15236-0940.

Introduction

Dispersed catalysts, both molybdenum and iron based, have been shown to be effective for coal liquefaction.[1] Most studies have tested the effectiveness of these catalysts at moderate to high hydrogen pressures, on the order of 1500 to 2500 psig (10.3 to 17.2 MPa). Coal liquefaction at lower pressures is well known. Hydrogen donor solvents, such as tetralin and dihydrophenanthrene, are capable of transferring hydrogen to the coal at low pressures, less than 400 psig (2.8 MPa).[2]

This study is aimed at exploiting a combination of dispersed catalyst activity with donor solvent quality to reduce the overall pressure of first stage coal liquefaction. Two questions are being addressed in this study. The first is how effective are dispersed catalysts for hydrogenation at lower pressures and the second is to what extent are dispersed catalysts capable of catalyzing the transfer of hydrogen to the coal. This paper presents preliminary studies aimed at addressing these two questions with model coal liquefaction solvents PANASOL (non-hydrogen donor) and tetralin (hydrogen donor).

Experimental

Feed Coal. Experiments were conducted with Blind Canyon bituminous coal (DECS-6, from the DOE/Penn State Coal Sample Bank). This coal was selected because of its low pyritic sulfur content. An analysis of the coal was presented earlier.[1]

Catalyst. A high surface area MoS_2 catalyst was used. The catalyst preparation was discussed previously.[1] The MoS_2 was prepared by reduction of ammonium heptamolybdate under H_2/H_2S in the 1-L semi-batch autoclave at 2,500 psig (17.2 MPa), 4 SCFH (0.11 Nm^3/h) of $H_2/3\%H_2S$, 425°C, and 0.5 h.. The catalyst has a BET surface area of 261 m^2/g, and elemental composition of 30% Mo, 20 % S, and 50% C.

Liquefaction Studies. Experiments were conducted by adding 3.3 g coal to a 40-mL tubular microautoclave reactor with 6.6 g of a mixture of PANASOL (obtained from Crowley Chemical) and tetralin. In experiments in which catalysts were used, 1000 ppm of Mo was added as high surface area MoS_2. The reactor was charged with the desired pressure of hydrogen and sealed. The pressurized reactor was then rapidly (1-2 minutes) heated to the liquefaction temperature (425°C) in a fluidized sandbath. Following the liquefaction period (0.5 h), the reactor was cooled and depressurized. Coal conversion was calculated from the solubility of the coal-derived products in tetrahydrofuran (THF) and in heptane as determined by a pressure filtration technique.[3] One experiment was conducted in a 1-L flow-through reactor to hydrogenate PANASOL. The conditions used in this reactor were 400 g PANASOL, 1000 ppm Mo as MoS_2, 2,500 psig (17.2 MPa), 4 SCFH (0.11 Nm^3/h) of $H_2/3\%H_2S$, 425°C, and 0.5 h.

Solvent Hydrogenation Studies. Experiments were conducted by adding 6.6 g of PANASOL or tetralin to a 40-mL tubular microautoclave reactor. In experiments in which catalysts were used, 1000 ppm of Mo was added as high surface area MoS_2. The reactor was charged with the desired pressure of hydrogen and sealed. The pressurized reactor was then rapidly (1-2 minutes) heated to the liquefaction temperature (425°C) in a fluidized sandbath. Following the liquefaction period (0.5 h), the reactor was cooled and depressurized. The liquid products were recovered from a THF rinse of the reactor.

Analytical characterization of the products is discussed in a separate paper submitted to this symposium.[4]

Discussion of Results

Solvent-Only System

A series of tests was made to investigate the effect of pressure on solvent hydrogenation. Hydrogenation of PANASOL in the presence of a high surface area MoS_2 catalyst was studied in the microautoclave. The extent of hydrogenation was determined by hydrogen consumption from the gas phase, elemental analysis, combined gas chromatography-mass spectrometry (GC-MS), low voltage high resolution mass spectrometry (LVHRMS), and nuclear magnetic resonance (NMR). The % hydrogenation of the solvent is defined as the mol% naphthalenes converted to their corresponding tetralins. Figure 1 shows the levels of hydrogenation determined from the various techniques as a function of pressure. Also on Figure 1 are the equilibrium conversions calculated for the naphthalene/tetralin system at 425°C from the data reported by Frye and Weitkamp[5]. The hydrogenation of PANASOL at 1000 psig (6.9 MPa) with no catalyst and the hydrogenation of PANASOL in the 1-L semi-batch reactor are also shown. As shown in Figure 1, the levels of hydrogenation observed in the microautoclave are significantly lower than the equilibrium for the naphthalene/tetralin system. However, hydrogenation was observed at pressures as low as 400 psig cold (2.8 MPa), 780 psig (5.4 MPa) at temperature. The results in Figure 1 illustrate the range of values of % hydrogenation obtained by the different analytical techniques. Finally, Figure 1 indicates that higher levels of hydrogenation are obtainable in the stirred 1-L autoclave (with gas flow) than in the batch microautoclave.

The reverse of this reaction, dehydrogenation of tetralin, was also studied in the microautoclaves. The dehydrogenation was done at different hydrogen pressures, 400 psig (2.8 MPa) and 1000 psig(6.9 MPa), with and without a high surface area MoS_2 catalyst for 0.5 h at 425°C. The yields of dehydrogenated compounds (naphthalenes) determined by gas chromatography with flame ionization detection (GC-FID) were $<1.0\%$ for 1000 psig (6.9 MPa) and no catalyst, 8.0% for 1000 psig (6.9 MPa) with MoS_2, and $<1.0\%$ for 400 psig (2.8 MPa) and no catalyst. The equilibrium distribution of naphthalene and tetralin at the higher pressure condition is (from Frye and Weitkamp) between 7.5 and 8.0 mol% naphthalene. The results indicate that significant levels of dehydrogenation were only observed with the catalyst present. The MoS_2 is quite effective for tetralin dehydrogenation and, in this case, equilibrium was reached from the tetralin side within the 0.5 h reaction time.

Effect of Coal on Solvent Hydrogenation

The effect of coal addition on the hydrogenation of PANASOL was studied in another series of microautoclave tests. The effect of adding 0 g, 0.1 g, 0.2 g, and 3.3 g of DECS-6 Blind Canyon coal on the amount of hydrogen taken up by the solvent in the presence of MoS_2 was investigated. The total amount of hydrogen consumed in these tests were 0.029, 0.026, 0.022, and 0.055 (0.052 and 0.055 in replicate tests) for 0, 0.1, 0.2, and 3.3 g coal respectively. Note that with no catalyst and no coal present, 0.006 moles of hydrogen was consumed and when 3.3 g coal and no catalyst were present, 0.025 mol was consumed. Hydrogen consumption with 0.1 g (0.026) and 0.2 g (0.022) coal was lower than when no coal was added or with 3.3 g coal. The relative rates of hydrogen consumption are also informative. In the absence of coal, total pressure fell gradually over the entire span of reaction time. In the presence of 3.3 g coal, the pressure dropped rapidly, then approached a limiting value, asymptotically less than when no coal was added. The rate of hydrogen consumption is presented in a figure in a separate paper at this symposium.[4] Product inspection in the latter case indicated that 8 mol% of methyltetralins was formed, but 30 mol% was formed in the former case.

The effect of added coal (3.3 g) on the hydrogenation of PANASOL to tetralins at different pressures was determined by LVHRMS. The results are summarized in Figure 2. Also shown on Figure 2 is the effect of pressure on the hydrogenation of PANASOL with no added coal. Considerably less hydrogenation of PANASOL was observed when coal was added.

To distinguish whether the added coal was competing with the PANASOL for catalytic sites or if coal was suppressing catalytically active sites, THF washed catalyst (plus any residual insoluble coal) from the test using 0.2 g coal was added to a separate test with just PANASOL. The rate of hydrogen consumption was very similar to the original case in which 0.2 g coal was added. Since solvent hydrogenation was diminished in the absence of added coal, it appears suppression rather than competition for active sites takes place. In a third test the catalyst was washed with THF and again added with PANASOL and 3.3 g DECS-6 coal. The overall coal conversions and rate of hydrogen consumption was the same as with fresh catalyst. This indicates that even though the activity of the catalyst for solvent hydrogenation was suppressed by the presence of coal, the catalyst remained effective for coal liquefaction and conversion. A separate paper that discusses this effect in more detail has been submitted to this session.[4]

The effect of coal on MoS_2 catalyzed dehydrogenation of tetralin was also studied. The amount of hydrogen produced was determined by gas analysis. When no coal was present during the dehydrogenation of tetralin, under 1000 psig N_2 (6.9 MPa), 0.005 mol of hydrogen was evolved with no catalyst present and 0.050 mol of hydrogen was evolved with added MoS_2. Exposing the MoS_2 to 0.2 g of coal resulted in the evolution of 0.010 mol of hydrogen. It appears that the presence of coal also suppresses the dehydrogenation activity of the MoS_2 catalyst (though more hydrogen was evolved than with no catalyst added). Tetralin dehydrogenation was studied in the presence of 3.3 g of coal under 1000 psig (6.9 MPa) N_2. With coal and no catalyst present, 0.003 mol of hydrogen was produced. With added MoS_2 in the presence of coal, 0.013 mol of hydrogen was produced (about 4.3 times the amount produced with no catalyst). However, coal conversion to THF and heptane soluble products was similar for the two cases.

Effect of Pressure and Solvent Quality on Coal Conversion

The effect of varying the cold pressure from 200 to 1000 psig (1.4 to 6.9 MPa) on coal conversion with added MoS_2 catalyst was investigated. The conversion of coal to THF and heptane soluble product is shown in Figure 3. The results show that coal conversion is affected by pressure; however, higher conversions are observed at 400 psig cold (2.8 MPa) with catalyst than at 1000 psig cold (6.9 MPa) without catalyst. This indicates that the catalyst is effective even at pressures as low as 400 psig cold (2.8 MPa). Figure 4 presents the effect of pressure on C_1-C_4 gas produced. As shown in Figure 4, higher amounts of gas were produced with increasing pressure (also increasing conversion).

The effect of solvent quality on coal conversion with no added catalyst was investigated by varying the ratio of tetralin to PANASOL. These results are shown on Figure 5. Also shown in this Figure are the earlier results using added catalyst with 100% PANASOL at different pressures. In order to compare the magnitude of the catalytic (100% PANASOL) with the hydrogen donor (varying tetralin to PANASOL ratios) effect, a common basis was selected in the following way. The positioning of the catalytic data (obtained at different pressures with 100% PANASOL) with respect to the x-axis was determined based on the observed amounts of tetralins produced from PANASOL as a function of pressure in tests with no coal added (from Figure 1). Thus, these estimates represent the maximum expected concentration of tetralins in the PANASOL/coal/catalyst system that could be achieved by the end of the 0.5 h span of reaction. Using this as a basis, higher conversions of coal to soluble products are observed with added catalyst than with tetralin/PANASOL mixtures. The differences become smaller as maximum THF conversion is approached in both systems.

Effect of Catalyst Addition on Mixed Donor/Non-Donor Systems

In non-catalytic experiments at 400 psig H_2 (2.8 MPa), hydrogen was transferred to the coal from the dehydrogenation of tetralin. With a mixture of 25% tetralin with 75% PANASOL as the solvent for DECS-6 coal, the hydrogen transferred to the coal was calculated based on the amount of tetralin converted to naphthalene (by LVHRMS) and the detected hydrogen in the gas phase. The calculated amount of hydrogen transferred to the coal was 0.011 mol (the total hydrogen produced from the tetralin was 0.015 mol). This level of hydrogen transferred was equivalent to the hydrogen transferred from the gas phase in catalytic cases with a non-donor at 300-400 psig H_2 cold (2 to 2.8 MPa).

MoS_2 was added to a system containing a mixture of 20% tetralin and 80% PANASOL as the solvent for DECS-6 coal at 400 psig H_2 cold (2.8 MPa). Dehydrogenation of the tetralin produced 0.038 mol of hydrogen, and 0.024 mol of hydrogen were transferred to coal. Approximately 2.5 times the amount of hydrogen was produced from the tetralin than in the non-catalytic case, and 2.0 times the amount of hydrogen was transferred to the coal than in the non-catalytic case. It is not clear whether the additional hydrogen was transferred to the coal by direct catalytic hydrogen transfer or catalytic dehydrogenation to the gas phase followed by catalytic hydrogenation of the coal. Note that the addition of catalyst to the mixed hydrogen donor/non-donor system resulted in higher coal conversion to THF soluble product than in the non-catalytic system (80% with a catalyst compared to 68% without a catalyst).

Conclusions and Future Efforts

The major results from this effort can be summarized as:

1) Catalyst activity for coal conversion is observed at pressures as low as 400 psig (2.8 MPa).

2) MoS_2 catalysts can act as effective dehydrogenation catalysts even under hydrogen pressures, therefore these catalysts may be effective for transferring hydrogen from solvents to coal.

3) Production of C_1-C_4 gases increases with increasing hydrogen pressure.

4) While coal can inhibit the activity of MoS_2 catalysts for solvent hydrogenation, the activity of these catalysts for coal conversion remains high after several passes in a coal liquefaction environment.

Future tests are planned to investigate the interrelationship of solvent quality, pressure, and catalyst activity in an effort to reduce the overall pressure used in coal liquefaction. Based on the results obtained thus far, an appropriate combination of solvent quality and catalyst activity may allow significant reductions in the overall pressure of first stage coal liquefaction.

Disclaimer

Reference in this report to any specific commercial product, process, or service is to facilitate understanding and does not necessarily imply its endorsement or favoring by the United States Department of Energy.

References

1) Cugini, A.V., Krastman, D., Martello, D.V., Frommell, E.F., Wells, A.W., and Holder, G.D., Energy & Fuels, **8**(1), 83-87(1994).

2) Schindler, H., "Coal Liquefaction: A Research Needs Assessment," DOE/ER-0400, UC-108 (available from NTIS, Springfield, VA), 1989.

3) Utz, B.R., Narain, N.K., Appell, H.R., and Blaustein, B.D., "Coal and Coal Products: Analytical Characterization Techniques" (Ed. E.L. Fuller, Jr.), ACS Symposium Series No. 205, 1982, 225-237.

4) Rothenberger, K.S., Cugini, A.V., Schroeder, K.T., Veloski. G.A., and Ciocco, M.V., Am. Chem. Soc., Div. of Fuel Chem., Preprints, submitted.

5) Frye, C.G. and Weitkamp, A.W., Journal of Chemical and Engineering Data, **14**(3), 372-375(1969).

Figure 1. Effect of Reactor Pressure on PANASOL Hydrogenation in a Microautoclave at 425 °C with 1000 ppm Mo

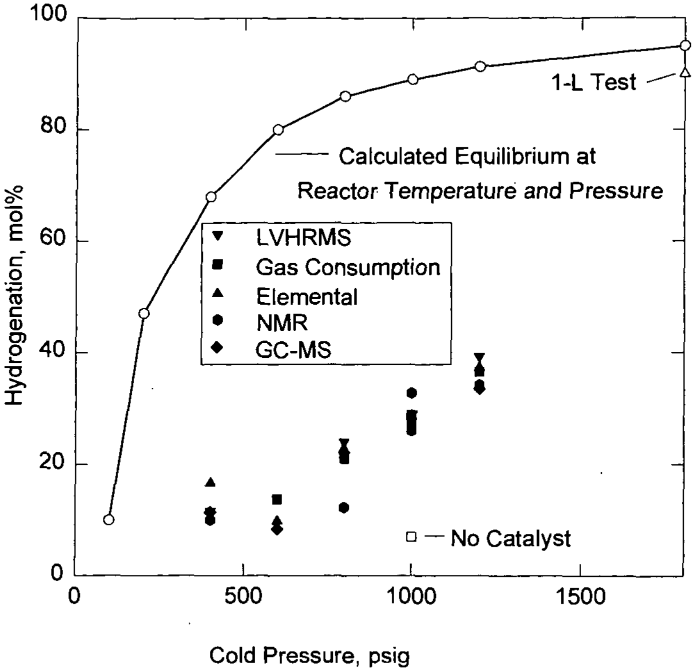

Figure 2. Effect of Pressure on %Tetralins in Total Product from a Microautoclave at 425 °C with 1000 ppm Mo

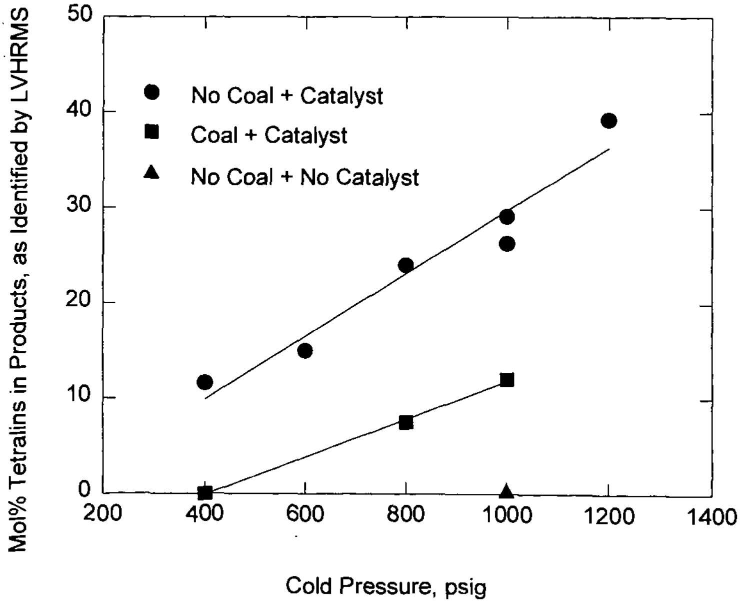

Figure 3. Effect of Pressure on DECS-6 Coal Conversion with PANASOL in a Microautoclave at 425 °C with 1000 ppm Mo

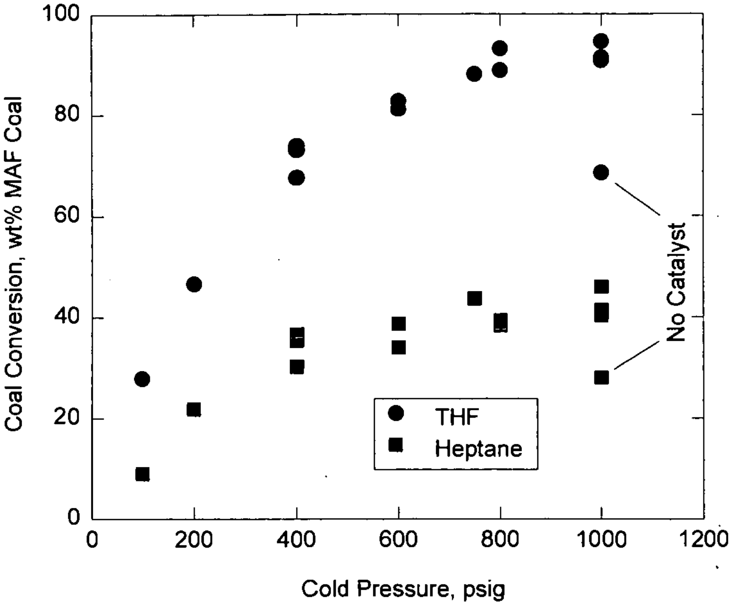

Figure 4. Effect of Pressure on C_1-C_4 Produced in Microautoclave at 425 °C with 1000 ppm Mo using DECS-6 and PANASOL

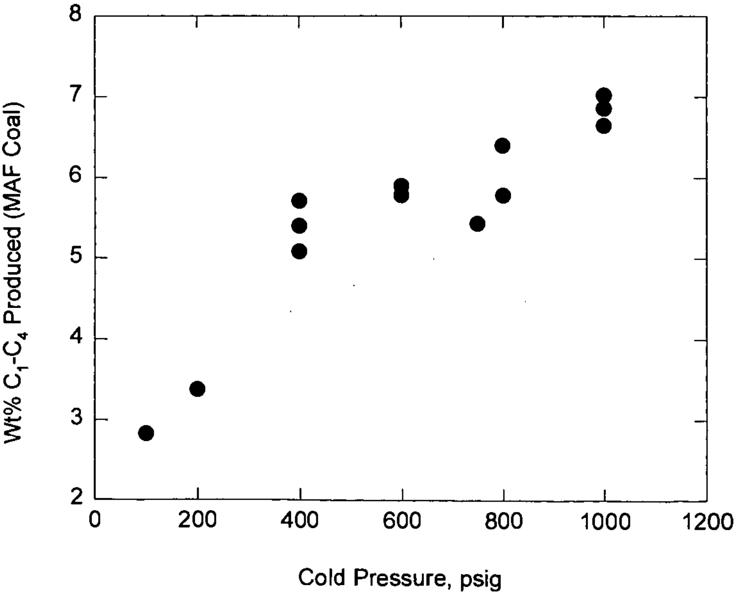

Figure 5. Comparison of coal conversions in mixtures of tetralin/PANASOL with no catalyst to 100% PANASOL (at different pressures) with a catalyst.

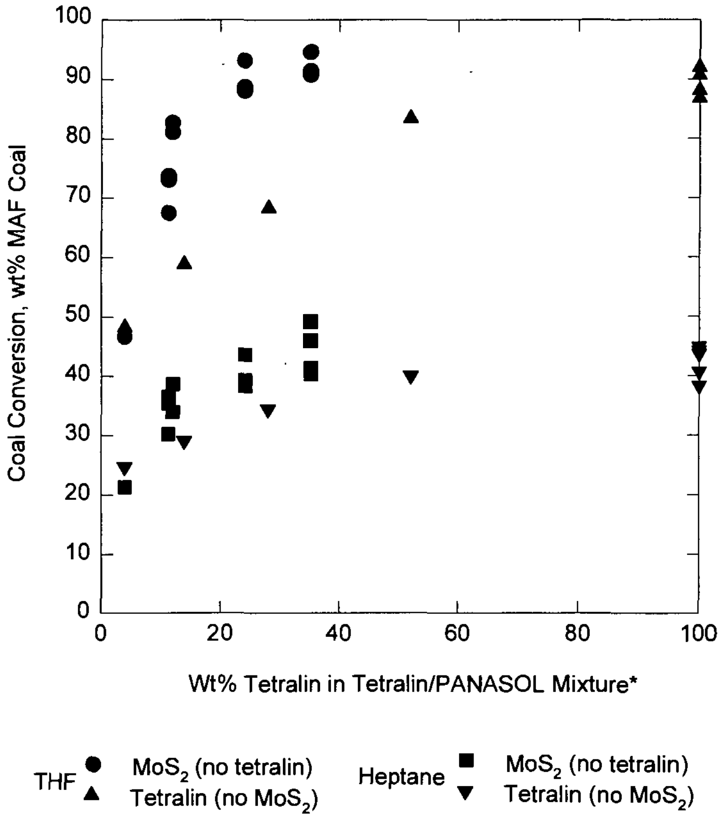

* Calculated for Catalytic System

PILLARED MONTMORILLONITE CATALYSTS FOR COAL LIQUEFACTION

R.K. Sharma and E.S. Olson
University of North Dakota
Energy & Environmental Research Center
Grand Forks, ND 58202

Keywords: coal liquefaction, catalysts, clays

ABSTRACT

Pillared clays contain large micropores and have considerable potential for catalytic hydrogenation and cleavage of coal macromolecules. Pillared montmorillonite-supported catalysts were prepared by the intercalation of polynuclear hydroxychromium cations and subsequent impregnation of nickel and molybdenum. Infrared and thermogravimetric studies of pyridine-adsorbed catalysts indicated the presence of both Lewis and Brönsted acid sites. Thus, the catalysts have both acidic properties that can aid in hydrocracking and cleavage of carbon–heteroatom bonds as well as hydrogen-activating bimetallic sites. These catalysts were applied to the hydrodesulfurization and liquefaction of coal-derived intermediates. The reactions of model organosulfur compounds and coal liquids were carried out at 300°-400°C for 3 hours in the presence of 1000 psi of molecular hydrogen. Reaction products were analyzed by GC/FT-IR/MS/AED. The catalysts have been found to be very effective in removing sulfur from model compounds as well as liquefaction products.

INTRODUCTION

Catalytic functions required for coal liquefaction are hydrogenation of aromatics and hydrocracking of C–C bonds as well as C–S, C–O, and C–N bonds. Thus, metal or metal sulfide sites activate hydrogen for addition to aromatic rings or for hydrogen transfer reactions, and acidic sites are important for bond cleavage activity in coal liquefaction catalysts. High surface areas for the metal sulfide sites are desired for high activity; this can be achieved by dispersion of the metals on a supporting material with some acidic properties.

Because of their acidic properties, smectite clays have been used as catalysts in petroleum cracking and various other reactions. Unfortunately, they dehydrate and collapse at temperatures above 200°C. New coal liquefaction catalysts being investigated at EERC utilize pillared clays as supports for the metal sulfide sites (1–3). Artok and others used a copper-pillared clay for coal liquefaction (4). In pillared clays, large polyoxymetal cluster cations are exchanged (intercalated) between the negatively charged clay layers in place of the hydrated metal ions. When calcined to drive off the water, the polyoxymetal cations form pillars that maintain the clay layer structure, thus creating large spacings between the layers. These structures are stable to 450° and 500°C. Hypothetically, the micropore volumes will be large enough to accommodate macromolecules of the feedstock to be hydrocracked. Chromia-pillared clays, which have interlayer spacings somewhat larger than those present in alumina-pillared clays used in petroleum refining, have considerable potential for coal liquefaction.

RESULTS AND DISCUSSION

A survey of the catalytic hydrocracking activities of various derivatives of natural montmorillonite clay was conducted. These derivatives included both pillared and unpillared forms of the clay as well as the catalysts obtained by impregnating nickel–molybdenum sulfide on the pillared clay as a support. These tests were carried out in a rocking microreactor (tubing bomb) under 1000 psi of hydrogen at temperatures of 300° to 400°C. Bibenzyl (1,2-diphenylethane), diphenyl sulfide, diphenyl ether, and other hydrocarbon compounds were utilized as substrates to model the structural moieties of the coal, especially the bridging groups believed to link the aromatic clusters. Some of the catalysts were then tested with first-stage coal liquids (low-severity Wyodak liquefaction product), and conversions to distillate materials were determined.

To study the effects of acidic sites present on a clay, the concentration of acidic sites on montmorillonite was maximized by converting the clay to an acid-exchanged form. This form of montmorillonite was prepared by washing the cleaned sodium form of the clay with hydrochloric acid. The reaction of the acid-washed clay (AM) with bibenzyl at 350°C gave a 75% conversion of bibenzyl, whereas a blank hydrogenation reaction of bibenzyl with no clay or catalyst gave only 1% conversion to toluene. The yield of benzene resulting from the clay-catalyzed hydrocracking test was only 34 wt%. The yields of ethylbenzene and toluene were very small (1.9% for each). A two-step reaction of the bibenzyl is believed to occur, producing benzene and ethylbenzene in the first step, and ethylbenzene is further cleaved to benzene and ethane in the second step. Yields of the gas products such as ethane were not measured. Toluene is produced in a different type of reaction. The higher yield of benzene compared to toluene in the montmorillonite reaction indicates that Brönsted acid catalysis (ipso protonation mechanism) is more important in the reaction than Lewis acid catalysis (5, 6). Much of the bibenzyl was converted to condensation products such as phenylethylbibenzyl. These products are formed from addition reactions (Friedel-Crafts reactions) of the carbonium ion intermediates with bibenzyl or products. The large amounts of condensation products observed in the reaction of bibenzyl with the clay indicate that the selectivity of the acid-washed clay for condensation versus cracking is poor.

Chromia-pillared montmorillonite was prepared with two different concentrations of chromia pillars. The low-concentration chromia-pillared clay (LCPC) gave an 80% conversion of bibenzyl, but as with the acid-washed clay, low yields of benzene (27 wt%), toluene (1 wt%), and ethylbenzene (3 wt%) were obtained from hydrocracking. Condensation products were abundant in the reaction products, indicating poor selectivity for hydrocracking. Results with the clay having a high concentration of chromia pillars (HCPC) gave somewhat higher conversion (93%) and more benzene (47 wt%). Formation of cyclohexanes by single-ring hydrogenation reactions was not observed with either of the chromia-pillared clays or with the unpillared acid-washed clay.

Nickel and molybdenum were impregnated in the high chromia-pillared clay and sulfided to give the active clay-supported catalyst (NMHCPC), and the hydrotreatment reaction with bibenzyl was conducted to determine its effectiveness. A conversion of 91% was achieved at 350°C. This conversion is significantly better than the 64% conversion obtained with the high-chromia-pillared clay support, which did not contain the nickel and molybdenum catalyst. The conversion increased to 99% when the reaction was carried out at 400°C.

The products from the reactions of bibenzyl catalyzed by the NMHCPC were found to be a mixture of aromatics and cycloalkanes. The major products were benzene and ethylbenzene, and the minor products were cyclohexane, methylcyclohexane, and alkylbenzenes. These products resulted from hydrocracking as well as from hydrogenation of the aromatic compounds. In contrast to the reactions carried out with HCPC, the amounts of oligomeric condensation products formed during the reaction with NMHCPC were negligible. From these data, we conclude that the introduction of nickel and molybdenum has moderated the activity of the support so that selectivity for hydrocracking relative to condensation is obtained. The high conversion may be attributed to bimetallic sulfide activation of hydrogen to effect at least partial hydrogenation of the aromatic rings. Activation energies for bond cleavage reactions may be lower in the reduced intermediates. Carbonium ion intermediates are more easily reduced by hydride transfer reactions from the hydrogenated intermediates or dissociated hydrogen on the metal sulfide. Thus, the carbonium ions are rapidly reduced and do not survive long enough to undergo addition reactions to aromatic rings that result in condensation and coking.

Reactions of the LCPC with other alkylbenzenes were investigated to determine if the reactions were consistent with the proposed carbonium ion mechanism. Isopropylbenzene (cumene) reacted very rapidly, giving 100% conversion. Benzene was the major product. The more rapid reaction is expected for a reaction involving cleavage of the aryl–alkyl bond of the *ipso*-protonated ring intermediate to give the secondary isopropyl carbonium ion plus benzene. The reaction with phenyldecane occurred with 81% conversion to give benzene as the major product. A large number of various alkylbenzene and indan products were formed in the reaction as a result of carbonium ion rearrangements and cleavage reactions. Cyclohexanes were not observed in the reaction products.

Although single aromatic rings were not hydrogenated by the clay supports, it was interesting to find out whether multiring aromatic systems could be hydrogenated as they are with other acid catalysts such as zinc chloride. Thus, pyrene was reacted with the chromia-pillared montmorillonite to determine if acid-catalyzed hydrogenation of the multiring systems could be effected. The conversion of pyrene to a hydrogenated pyrene mixture was found to be 15%, which is considerably less than that observed for zinc chloride catalysts. For catalysts containing molybdenum and other transition metals, hydrogenation of multiring systems occurs readily. The reaction with pyrene at 350°C did not result in hydrocracking or rearrangements of the pyrene or hydropyrene rings to phenanthrene or other ring systems.

Reactions of diphenyl sulfide were extensively investigated in order to determine the effects of pillaring and nickel molybdenum sulfide loading on hydrodesulfurization activities. The acid-exchanged form of montmorillonite gave a 99+% conversion at 300°C. The products were benzene and thiophenol in a molar ratio of 9.3:1. The relatively high benzene-to-thiophenol ratio shows that the catalyst is effective in cleaving both carbon–sulfur bonds of the diphenyl sulfide; that is, the thiophenol intermediate is further converted to benzene and hydrogen sulfide. The blank hydrogenation reactions of diphenyl sulfide carried out with no clay or catalyst present resulted in conversions of 1 % at 300°C and 10% at 400°C. The excellent conversion obtained with the acid-exchanged clay may be attributed to the high acidity of the catalyst. The anionic aluminosilicate layers of the clay may also have some ability to stabilize cationic intermediates prior to a reduction step in the hydrodesulfurization mechanism.

The catalytic activity of sodium-exchanged montmorillonite was also tested at 300°C with diphenyl sulfide, and a conversion of only 11 % was obtained. Both benzene and thiophenol were formed (molar ratio of 6.9:1). The sodium-exchanged clay has some residual Brönsted acidity from the polarization of the water of hydration of the sodium cations and the hydroxyl groups of the clay layers.

Our hydrodesulfurization studies were then extended to the chromia-pillared montmorillonites. Hydrogenation of diphenyl sulfide with the LCPC resulted in a conversion of 95% to benzene and thiophenol in equimolar amounts. The high conversion can again be attributed to the high Brönsted acidity of the pillared clay. Catalytic acidic sites may be present on the polyoxychromium cation pillars, since they retain some hydroxyl functionality (7).

Formation of equal moles of benzene and thiophenol in the pillared clay-catalyzed reaction suggests that cleavage of only one carbon–sulfur bond of the diphenyl sulfide occurred. In order to determine if the second carbon–sulfur bond can actually be cleaved in this catalytic system, a reaction of thiophenol was carried out with LCPC under the same conditions used for diphenyl sulfide. Analysis of the reaction products showed 95% conversion of the thiophenol to benzene. These results suggest that during the hydrogenation of diphenyl sulfide, the acidic sites in the clay may be poisoned by the hydrogen sulfide product. Further studies at higher temperatures are in progress to determine whether the deactivation can be reversed.

The HCPC was also tested in the reaction with diphenyl sulfide. This catalyst gave a conversion similar to that obtained with the LCPC, but a much higher molar ratio of benzene to thiophenol (12:1) was found in this test. Thus, the final step of the reaction, which involves hydrogenolysis of the thiophenol, proceeded much more completely with the HCPC catalyst.

Hydrotreating diphenyl sulfide with the NMHCPC catalyst resulted in a 98% conversion. A nearly quantitative amount of benzene was formed with only a trace of thiophenol and a small amount of cylcohexane from reduction of the benzene.

Coal liquefaction tests were carried out with the low-severity product from Wyodak subbituminous coal (LSW) and 1000 psi hydrogen at 400°C in rocking microreactors without added solvent, and the product was distilled to determine the conversion of the nonvolatile portion of the LSW to distillate. Acid-washed clay, pillared clay supports, and NMHCPC catalyst, as well as a commercial silica–alumina-supported Ni-Mo catalyst, gave results paralleling the reactions with the test substrates described above. With a commercial nickel–molybdenum (HDN) catalyst, the conversion to distillate was only 20% under the conditions used. The LSW in the presence of acid-washed montmorillonite gave a conversion of 10%. The LCPC and HCPC with LSW gave very poor conversions (2% and 8% respectively) to distillate. Thus, the supports by themselves are evidently too acidic or too nonselective to be useful for coal liquefaction. But addition of metal sulfides to the support modifies this behavior substantially. A conversion of 29% to distillate was obtained for the NMHCPC catalyst. This is a significant improvement over the conversion obtained with the commercial catalyst. Further testing is required to determine whether the catalysis is actually occurring in the interlayer micropores or simply on the outer surface of the clay. Higher conversions of the LSW to distillate were reported earlier for montmorillonite-supported zinc chloride catalyst (1). Zinc chloride complex catalysts are exceptionally active and efficient in cracking coal, but suffer some disadvantages such as deactivation and emission of hydrogen chloride in the presence of sulfur.

CONCLUSION

Hydrotreatment of first-stage coal liquids and model compounds with a selection of acidic and pillared clays with and without incorporated bimetallic hydrogenation catalysts showed that the combination of support acidity and hydrogen activation catalysis was effective in cleaving C–S and aryl–alkyl bonds and hydrocracking coal materials. Some differences in the activities of the support were noted that depended on the nature and concentration of oxymetal ion used in pillaring the clay. Further efforts are needed to clearly understand these differences.

REFERENCES

1. Olson, E.S.; Diehl, J.W.; Sharma, R.K. *Prepr. Pap. Am. Chem. Soc., Div. Fuel Chem.* **1990**, *35*, 563.
2. Olson, E.S.; Yagelowich, M.L.; Sharma, R.K. *Prepr. Pap. Am. Chem. Soc., Div. Fuel Chem.* **1992**, *37*, 262.
3. Sharma, R.K.; Olson, E.S. *Prepr. Pap. Am. Chem. Soc., Div. Fuel Chem.* **1993**, *38*, 1008.

4. Artok, L.; Malla, P.B.; Komarneni, S.; Schobert, H.H. *Energy & Fuels* **1993**, *7*, 430–431.
5. Sharma, R.K.; Olson, E.S.; Diehl, J.W. *ACS Div. of Fuel Chem. Preprints* **1990**, *35*, (2), 463.
6. Olson, E.S.; Diehl, J.W.; Sharma, R.K. *ACS Div. Fuel Chem. Preprints* **1991**, *36*, (2), 578.
7. Pinnavaia, T.J.; Tzou, M.S.; Landau, S.D. *J. Amer. Chem. Soc.* **1985**, *107*, 4783–4785.

ACKNOWLEDGMENT
The support of the U.S. Department of Energy (Contract No. DOE-FC21-86MC10637) is gratefully acknowledged.

TABLE 1

Catalytic Hydrocracking of Bibenzyl
(1000 psig hydrogen pressure, 350°C, 3 hr, catalyst wt/substrate wt = 0.5)

Catalyst	Conv. %	Yield of Products, wt%
None	1	Toluene (trace)
AM	75	Benzene (34.1) Toluene (1.9) Ethylbenzene (1.9)
LCPC	80	Benzene (27.3) Toluene (1.0) Ethylbenzene (3.4)
HCPC	93	Benzene (47.1) Ethylbenzene (3.6)
NMHCPC	91	1-ring (49.1) 2- and 3-ring (46.8)
NMHCPC*	99	1-ring (76.2) 2- and 3-ring (23.1)

* At 400°C.

TABLE 2

Catalytic Hydrotreating of LSW

	Product (%)			
Catalyst	THF-I	THF-S	Distillate	Actual Distillate
AM	20.0	46.0	28.0	10.0
HDN*	14.3	49.6	35.0	20.0
HCPC	29.4	27.6	26.3	8.0
NMHCPC	6.0	46.0	43.0	28.8

THF-I = Tetrohydrofuran - insoluble
THF-S = Tetrohydrofuran - soluble
HDN* = Commercial Nickel-Molybdenum catalyst

SYNTHETIC CLAY-SUPPORTED CATALYSTS FOR COAL LIQUEFACTION

E.S. Olson and R.K. Sharma
University of North Dakota
Energy & Environmental Research Center
Grand Forks, ND 58202

Keywords: coal liquefaction, catalysts, clays

ABSTRACT

Synthetic clays with nickel substitution in the lattice structure are highly active catalysts for hydrogenation and hydroisomerization and, consequently, have considerable promise for the catalytic upgrading of coal liquids. Nickel-substituted synthetic mica montmorillonite (NiSMM) was prepared and subsequently impregnated with molybdenum and sulfided. The reaction of model compounds with these catalysts in the presence of hydrogen has been investigated to provide mechanistic models for coal liquefaction. The results indicate that NiSMM has active Brönsted acid sites for hydrocracking and hydroisomerization. The hydrogen-activating ability of the molybdenum and nickel sulfide sites proximate to the acid sites results in effective depolymerization catalysis.

INTRODUCTION

Acid smectite clays have been used as catalysts in petroleum-cracking and various other reactions. Unfortunately, they dehydrate and collapse at temperatures above 200°C. In pillared clays, intercalation of hydroxylated or complexed metal cations maintains the clay layer structure after loss of water and generates large micropore volumes. These structures are stable to 450° and 500°C. The alumina cluster-pillared clays are effective supports for use in hydrogenation and hydrocracking catalysis as well as in coal liquefaction (1–3). Chromia-pillared clays with even larger pore spacings have considerable potential for upgrading large coal macromolecules (4). Schobert and others reported copper-impregnated montmorillonite was effective for catalysis of coal liquefaction (5).

Synthetic clays were reported to be more active catalysts than natural clays (6–8). Synthetic mica montmorillonite (SMM) containing cobalt or nickel or another hydrogen-activating component dramatically improves the hydrocracking and hydroisomerization activity (9-12). Exactly how the activity is enhanced is not known (13). In the EERC catalyst program, a selection of synthetic clays with and without incorporated hydrogen-activating components were tested for coal liquefaction as well as with model compounds. The catalysis of C-S and alkyl-aryl bond breakage as well as arene hydrogenation and hydroisomerization of n-alkanes was investigated.

EXPERIMENTAL

Catalyst Preparation. NiSMM was prepared by the procedure of Heinerman and others (14). SMM was prepared by the procedure from the French patent (15).

Preparation of Clay-Supported Molybdenum Catalysts. The synthetic clays were loaded with 5 wt% molybdenum using the incipient wetness method. Ammonium molybdate tetrahydrate (0.046 g) was dissolved in 50 mL of deionized water. To this solution 0.5 g of desired clay was added and stirred overnight. The solvent was removed by evaporation, and the resulting product was calcined in air at 350°C for 6 hours.

Sulfidation. The catalyst was placed in a 12-mL microreactor. The reactor was evacuated and pressurized with 200 psi of hydrogen sulfide. The reactor was placed in a rocking heater preheated to 350°C. The heating was continued for 3 hours. The reactor was cooled to room temperature, degassed, and opened. The catalyst was recovered and stored in airtight bottles.

Reduction. Nickel-substituted synthetic mica montmorillonite was reduced in hydrogen (1000 psi) at 450°C for 16 hours. The reduction was carried out in a microreactor heated in a rocking heater as described above.

Catalytic Reactions. In a typical run, 0.5 g of model compound and 0.25 g of the catalyst were placed in a tubing bomb (12-mL microreactor). The microreactor was evacuated, pressurized with 1000 psig of hydrogen, and placed in a rocking autoclave heated to desired temperature. The heating was continued for 3 hours. At the end of the reaction period, the microreactor was cooled in a dry ice–acetone slurry, degassed, and opened. The desired amount of the internal standard was added to the product slurry, and the product slurry was transferred into a centrifugation tube by washing with methylene chloride and the solid catalyst removed by centrifugation. The liquid sample was analyzed by gas chromatography(GC)/flame ionization detection(FID) and GC/Fourier transformation infrared (FT-IR)/mass spectroscopy (MS). The solid was dried in vacuum at 110°C for 3 hours.

RESULTS AND DISCUSSION

Synthetic mica montmorillonite (SMM) and nickel-substituted synthetic mica montmorillonite (NiSMM) were prepared and used as supports for molybdenum sulfide. Both the synthetic clays and the molybdenum-loaded catalysts were tested for hydrocracking, hydrodesulfurization, hydroisomerization, and hydrogenation activities using bibenzyl, pyrene, dibenzothiophene, and *p*-cresol as test substrates.

Bibenzyl Cracking. The synthetic clay support materials were tested to determine their reactivities prior to molybdenum incorporation. The reaction of bibenzyl with synthetic mica montmorillonite (SMM) gave a very small conversion of bibenzyl into products. However, in the nickel-substituted SMM, where octahedrally coordinated aluminum ions were replaced by nickel ions, the hydrocracking activity increased considerably. The reaction of bibenzyl with NiSMM catalyst converted 67% of bibenzyl into lighter products. Major products were benzene and ethylbenzene. Formation of these products is indicative of a carbonium ion mechanism catalyzed by Brönsted acid sites (16). This mechanism proceeds via ipso protonation followed by cleavage of the aryl–alkyl bond to form the phenylethyl carbonium ion intermediate. The carbonium ion is then reduced to the alkyl group. Ethylbenzene is further cracked to benzene via the same steps, the extent depending on the activity of the catalyst. The formation of toluene may have been Lewis-acid catalyzed. In addition to these products, a very large number of other products in much smaller concentrations were also observed. Detailed characterization of these products is under investigation. These products may have been formed from the hydrogenation, hydroisomerization, or ring-opening reactions. No oligomeric material was observed.

NiSMM was reported to have activity comparable to that of zeolites. It was suggested that nickel-substituted clays crystallize in smaller platelets, resulting in more exposed edges and, consequently, higher surface area and increased activity (13). Based on the FT-IR measurements of adsorbed ammonia on NiSMM, it has been shown that the number of Brönsted acid sites increases following Ni reduction (14, 17). These newly created acidic sites are responsible for the increased activity of NiSMM compared with SMM in which no nickel is substituted for Al^{3+} in the octahedral sites. Robschlager and others (17) reported that for this catalyst to be active for the isomerization of pentane, lattice Ni^{2+} has to be reduced to zero-valent nickel, and the activity of the catalyst decreased when metallic nickel was removed by treatment with carbon monoxide. In contrast, the bibenzyl hydrocracking data for the reduced NiSMM indicates that the activity of the catalyst did not change significantly with reduction of Ni^{2+} to metallic nickel. In fact, a slight decrease in the catalytic activity was seen for the reduced catalyst. However, reduction of the Ni^{2+} during hydrotreating cannot be ruled out.

Sulfidation of the NiSMM gave a substantial increase in catalytic activity for hydrocracking. The reaction of bibenzyl with presulfided NiSMM gave significantly higher conversion (82%) than NiSMM. The product distribution was similar to that of NiSMM reaction. Small amounts of benzene and alkylbenzenes were converted into cyclohexane and cycloalkanes probably by NiS-catalyzed hydrogenation of the single aromatic rings. The increase in hydrocracking activity on sulfidation might be attributed to a facilitation of the addition of hydrogen to some intermediate involved in hydrogen (hydride) transfer, but further work is required to fully understand the nature of the catalytic activity in the NiSMM catalysts.

The reaction of bibenzyl with SMM- and NiSMM-supported MoS_2 gave significantly higher conversions (34% and 92%, respectively) of bibenzyl into products. Major products were found to be benzene, toluene, and ethylbenzene. Small amounts of cyclohexane, methyl cyclohexane, and ethyl cyclohexane were also formed. A significant portion of the bibenzyl was reduced to benzylcyclohexane and other hydrogenated products, but no oligomeric products were formed. Extensive conversion to isomeric aliphatic compounds also occurred. The conclusion from the hydrocracking experiments is that the NiSMM is a very active support for the molybdenum sulfide and the combination has high activity as a hydrogenation, hydrocracking, and hydroisomerization catalyst.

Almost quantitative amounts of catalyst were recovered at the end of each reaction. Unlike highly acidic zeolite catalysts, these catalysts do not catalyze retrogressive reactions or coke formation (18).

Hydrogenation of Pyrene. Pyrene was used as a test compound to investigate hydrogenation activity of NiSMM catalysts. The reactions were carried out by heating pyrene and the desired catalyst at 350°C for 3 hours in the presence of 1000 psi of molecular hydrogen. The effects of sulfiding the NiSMM and supporting the (MoS_2) hydrogenation catalyst on NiSMM were also investigated.

The reaction of pyrene with NiSMM gave a high conversion (90%) of pyrene into hydrogenated products. The majority of the products were di-, hexa-, and decahydropyrenes. Small amounts of hexadecahydro- and tetrahydropyrenes were also formed. Numerous other components were formed by hydrocracking and rearrangement reactions.

The synthetic clay-supported MoS_2 catalyst gave similar high conversions of pyrene, and the product distribution was changed. Much more of the decahydropyrene (three isomers) and hexadecahydropyrene (three isomers) were formed, owing to the increased activity for hydrogenation of the di- and monoaromatic intermediates. The products also included those formed by rearrangement and hydrocracking reactions.

The commercial nickel-molybdenum catalyst (HDN-30) gave a lower conversion of pyrene (69%). Yields of the hexadecahydropyrene and decahydropyrene products were considerably lower than those obtained with either the NiSMM or MoS_2-NiSMM catalysts, but the dihydropyrene component was greater.

A reaction of pyrene with NiSMM was also carried out at 400°C. As expected, the conversion was lower because of the lower equilibrium constant at the higher temperature. The yields of the hexadecahydropyrene and decahydropyrene were low, but somewhat more cracking occurred.

Heteroatom Removal from Model Compounds. The hydrodeoxygenation, hydrodesulfurization, and hydrodenitrification activities of NiSMM were investigated by using *p*-cresol, dibenzothiophene, and quinoline as test substrates. The reactions were carried out at 400°C for 3 hours in the presence of 1000 psi of molecular hydrogen. Relevant analytical data are given in Table 1.

The reaction of *p*-cresol with NiSMM gave a high conversion (83%) of the substrate into many hundreds of products. Some of the major components are reported in Table 1. The reaction of *p*-cresol gave considerable amounts of o- and *m*-cresols, which could have been formed by acid-catalyzed rearrangement reactions. Toluene and methylcyclohexane were also major products. The reaction of dibenzothiophene also gave hundreds of products, including methylcyclopentane, benzene, toluene, ethylbenzene, and biphenyl as the major products. Quinoline gave tetrahydroquinoline, alkylbenzenes, aniline, and methylpyridine as the major products.

REFERENCES

1. Olson, E.S.; Diehl, J.W.; Sharma, R.K. *Prepr. Pap.—Am. Chem. Soc., Div. Fuel Chem.* **1990**, *35*, 563.
2. Olson, E.S.; Yagelowich, M.L.; Sharma, R.K. *Prepr. Pap.—Am. Chem. Soc., Div. Fuel Chem.* **1992**, *37*, 262.
3. Sharma, R.K.; Olson, E.S. *Prepr. Pap.—Am. Chem. Soc., Div. Fuel Chem.* **1993**, *38*, 1008.
4. Sharma, RK.; Olson, E.S. *Prepr. Pap.—Am. Chem. Soc., Div. Fuel Chem.* **1994**, *39*.
5. Artok, L.; Malla, P.B.; Komarneni, S.; Schobert, H.H. *Energy & Fuels* **1993**, *7*, 430–431.
6. Granquist, W.T. U.S. Patent 3 252 757, 1966.
7. Capell, R.G.; Granquist, W.T. U.S. Patent 3 252 889, 1966.
8. Granquist, W.T. *BRD Offenlegungsschrift* 1973, *231*, 2743.
9. Jaffe, J.; Kittrell, J.R. U.S. Patent 3 535 229, 1970.
10. Kittrell, J.R. U.S. Patent 3 632 501, 1970.
11. Swift, H.E.; Black, E.R. *Ind. Eng. Chem. Prod. Res. Dev.* **1974**, *13*, 106.
12. Swift, H.E.; Black, E.R. *ACS Div. of Petr. Chem. Preprints* **1974**, *19* (1), 7.
13. Bercek, P.G.; Metzger, K.J.; Swift, H.E. *Ind. Eng. Chem. Prod. Res. Dev.* **1978**, *17*, 214.
14. Heinerman, J.J.L.; Freriks, I.L.C.; Gaaf, J.; Pott, G.T.; Coqlegem, J.G.F. *Journal of Catalysis* **1983**, 80, 145.
15. Plee, D.; Schutz, A.; Borg, F.; Poncelet, G.; Jacobs, P.; Gatineau; Fripiat, J. French patent 2, 563, 446, 1984.
16. Olson, E.S.; Diehl, J.W.; Sharma, R.K. *Prepr. Pap.—Am. Chem. Soc., Div. Fuel Chem.* **1991**, *36* (2), 578.
17. Robschlager, K.H.W.; Emms, C.A.; Van Santen, R.A. *Journal of Catalysis* **1984**, *86*, 1.
18. Sharma, R.K.; Olson, E.S.; Diehl, J.W. *Prepr. Pap.—Am. Chem. Soc., Div. Fuel Chem.* **1990**, *35* (2), 463.

ACKNOWLEDGEMENT

The support of the U.S. Department of Energy (Contract No. DOE-FC21-86MC10637) is gratefully acknowledged.

TABLE I

Hydrocracking and Hydrogenation Activity of Synthetic Clays
Reaction Time = 3 h, H_2 = 1000 psi
Catalyst wt/Substrate wt = 0.5

Catalyst	Temperature, °C	Substrate, mmol	Conv., %	*Major Products,* mmol
SMM	350	BB (2.71)	2	Benzene (0.03) Toluene (0.03) Ethylbenzene (0.01)
NiSMM	350	BB (2.72)	67	Benzene (1.46) Toluene (0.11) Ethylbenzene (0.41)
Reduced NiSMM	350	BB (2.79)	65	Benzene (1.29) Toluene (0.13) Ethylbenzene (0.45)
Sulfided-NiSMM	350	BB (2.75)	82	Benzene (1.84) Toluene (0.02) Ethylbenzene (0.65)
Sulfided-MoSMM	350	BB (2.89)	34	Benzene (0.05) Toluene (0.05) Ethylbenzene (0.05) Cyclohexane (0.08)
Sulfided-MoNiSMM	350	BB (2.80)	92	Benzene (1.18) Toluene (0.10) Ethylbenzene (0.40) 4,5-Dihydropyrene (0.21) Methylcyclohexane (0.14) Ethylcyclohexane (0.10) Tetralin (0.15)
Sulfided-NiSMM	350	Pyrene (2.43)	90	Hexadecahydropyrene (0.07) (3 isomers) Decahydropyrene (0.36) (3 isomers) 1,2,3,3_a,4,5-Hexahydropyrene (0.26) 1,2,3,6,7,8-Hexahydropyrene (0.38) 4,5,9,10-Tetrahydropyrene (0.06)
Sulfided-HDN-30 Ni-Moly	350	Pyrene (2.47)	69	Hexadecahydropyrene (0.03) (3 isomers) Decahydropyrene (0.12) (3 isomers) 1,2,3,3_a,4,5-Hexahydropyrene (0.21) 1,2,3,6,7,8-Hexahydropyrene (0.45) 4,5,9,10-Tetrahydropyrene (0.24) 4,5-Dihydropyrene (0.64)
Sulfided-NiSMM	400	Pyrene (2.66)	65	Hexadecahydropyrene (trace) Decahydropyrene (0.05) (3 isomers) 1,2,3,3_a,4,5-Hexahydropyrene (0.13) 1,2,3,6,7,8-Hexahydropyrene (0.17) 4,5,9,10-Tetrahydropyrene (0.06) 4,5-Dihydropyrene (0.41)
Sulfided-NiSMM	350	Naph. (3.98)	62	Tetralin (2.18) Benzene (0.04) Toluene (0.02) Indan (0.02)
Sulfided-NiSMM	400	*p*-Cresol (4.66)	83	Toluene (0.17) Methylcyclohexane (0.16) *m*-Cresol (0.74) *o*-Cresol (1.90)
Sulfided-NiSMM	400	DBT (2.78)	84	Methylcyclopentane (0.26) Benzene (0.28) Toluene (0.10) Ethylbenzene (0.14) Biphenyl (0.13)
Sulfided-NiSMM	400	Quinoline(4.11)	87	C_3-benzene (0.25) Tetrahydroquinoline (0.10) Aniline (0.20) Methylpyridine (0.10)

DBT = Dibenzothiophene.
BB = Bibenzyl.

MODEL REACTIONS AS A MEASURE OF MoS_2 ACTIVITY

Karl T. Schroeder, Bradley C. Bockrath, Ronald D. Miller
U.S. Department of Energy, Pittsburgh Energy Technology Center, P.O. Box 10940,
Pittsburgh, PA 15236

ABSTRACT The activity of dispersed molybdenum sulfide liquefaction catalysts was studied using a high-temperature (≤400°C), low-pressure (≤400 kPa) micro-flow reactor. Model compounds were introduced by one of three methods: injection, continuous flow, or injection into a continuous flow. The dehydrogenation of tetralin, the hydrodesulfurization of benzothiophene, and the hydrodeoxygenation of benzofuran were used as examples of reaction types thought to be important for coal conversion. Transient effects, such as the adsorption of the model compound, could be seen in the injection mode of operation. Under steady-state flow conditions, the catalytic conversion of the reactant could be measured. Injection into the continuous flow demonstrated transient and longer lasting effects of quinoline on the catalytic activity. Two dispersed MoS_2 catalysts were compared in terms of their activity, selectivity, and sensitivity to temperature change.

INTRODUCTION This work employed the known catalytic reactions of model compounds to compare the effectiveness of two dispersed MoS_2 liquefaction catalysts. The HDS of benzothiophene, the dehydrogenation of tetralin, the reaction of benzofuran, and the effect of quinoline on activity were used as the basis of the comparison. The reaction mechanisms of these and other model compounds under hydroprocessing conditions have been critically reviewed recently.[1] One of the catalysts studied was a MoS_2 sample recovered as part of the residue from a liquefaction experiment; the other was a MoS_2 formed under dispersing conditions in the absence of coal. This work used a packed column heated in the oven of a GC as a reactor. Although only low hydrogen pressures could be employed, the GC was used to differentiate transient from steady-state behavior and allowed for the rapid adjustment of reaction temperature. This provided an experimental technique which allowed kinetic data to be obtained within a reasonable time period.

EXPERIMENTAL A Hewlett-Packard 5890 gas chromatograph was used as the basis for a high-temperature, low-pressure reactor. A packed column injection port was used to provide a large volume for the expansion of the vaporizing model compound solution. The catalyst was packed into a stainless steel tube and connected to the injector. The amount of catalyst or catalyst-containing residue was adjusted to give 90 mg of molybdenum in the reactor. Reactor pressures up to about 400 kPa of hydrogen were obtained by adding lengths of metal-clad capillary tubing to the end of the reactor. The total effluent flow was monitored using the Hewlett-Packard TCD detector. Model compound solutions were injected into the hydrogen carrier gas in the usual manner except that a slow injection speed was used. Reactants and products were recovered by condensation upon exiting the reactor. The eluant was analyzed by GC-FID and/or GC-MS to determine the identity and quantity of the products. An alternative method of introducing the model compound solution used a Hewlett-Packard Series 1050 pump to provide a continuous stream of solution. In a third type of experiment, a pulse of material was injected into the continuous stream. Regardless of the technique used to introduce the sample, all of the material was vaporized in the injection port of the GC before entering the reactor. Three types of catalytic materials have been studied. The first was a coal liquefaction residue recovered from a batch reaction which had been prepared using a Blind Canyon coal (DECS-17). The residue (IK87-5) contained 50% by weight MoS_2. The remaining 50% was coal ash and organic matter insoluble in THF. Recycling IK87-5 in a second liquefaction experiment with fresh coal showed it was still active for coal conversion and hydrogen up-take. Only a preliminary report has appeared on this material,[2] but its preparation and recycle activity are similar to those found for an Illinois No. 6 coal.[3] IK87-5 was used as an example of a used dispersed catalyst. The second material was an MoS_2 formed by heating ammonium molybdate and tetralin under liquefaction conditions but in the absence of coal or other added solid support (BCP-287). It was used as an example of a fresh, dispersed catalyst. Third, a commercial (Harshaw 0402T) alumina-supported CoMo catalyst was sulfided *in situ* using injections of dimethyldisulfide into the flowing hydrogen. To date, the majority of the work has been done using the first catalyst.

RESULTS AND DISCUSSION The three methods of sample introduction provide different types of information. The injection technique provides a limited amount of material which passes through the reactor as a nearly Gaussian-shaped peak. Strong adsorption on the catalyst and/or support may appear as a peak tail if desorption is fast relative to the time the material is in contact with the catalyst, or as a loss of peak intensity due to material losses if the desorption is relatively slow. Although significant peak tailing was not seen in our experiments, the preferential loss of material from some samples was seen. Material balances were determined by quantitative GC analysis of the condensed eluant. The preferential adsorption of diphenylether from injections of a 10% solution in n-undecane is shown in Figure 1. The recovered material contained n-undecane, diphenylether and a small amount of benzene amounting to about 3% of the diphenylether injected. No phenol was detected. The recovery of undecane in these experiments averaged 90% and was fairly constant from injection to injection. In contrast, the diphenylether recovery ranged from 65% to 80% and appeared to increase with injection number. A similar though less severe loss of a different oxygenate was seen when aliquots of a 10% solution of benzofuran were injected under the same conditions. In this case, the undecane recovery was 97% while the benzofuran recovery was only 91%. Although the loss of oxygenate in the presence of catalysts dispersed in coal solids has been fairly small, the extent of adsorption can become large in some cases. This can be seen in Figure 2 where the loss of benzofuran is shown for a commercial supported catalyst. In these experiments, benzofuran was introduced as 10 μL injections of a 10% solution, 5 μL injections of the neat material, or 10 μL injections of the neat material. The three sets of data form a single curve showing increased recovery as a function of the total amount of benzofuran injected. Thus, the catalyst appears to adsorb only a certain amount of model compound. Once its capacity has been reached, no further adsorption occurs. Such phenomenon may be important for the proper interpretation of batch data, especially when the amount of model compound is comparable to the amount the catalyst can adsorb. However, they would be expected to disappear in flow experiments where steady-state can be attained. This is the second type of experiment conducted with this reactor.

Steady-state flow conditions were attained by continuously introducing the model compound solution into the injection port of the GC using an HPLC pump. Flows of less than 20 μL/min were necessary to prevent overloading the packed-column injection port. Injector overload caused a decrease in recovery. A similar effect is seen when too much material is injected into an analytical gas chromatograph.[4] In addition to alleviating the problems associated with model compound adsorption, steady-state operation allows for kinetic measurements. For example, the conversion of tetralin to naphthalene at 400°C in the presence of residue IK87-5 is shown in Figure 3. At the lowest flow rate of 2 μL/min, a naphthalene yield of nearly 15% was obtained, well above the amount attributable to a thermal reaction. Increasing the flow rate produced less conversion and the rate appears to be first order in tetralin. Similar measurements at 375°C and 350°C were used to determine the temperature coefficient for the reaction. A value of 300 kj/mol was obtained. Thermolysis reactions typically have values of this magnitude.

Benzothiophene was also used as a model compound to investigate the effectiveness of the residue for HDS reactions. A solution containing 1% benzothiophene yielded recovered starting material along with ethylbenzene as its only product. No styrene was detected in any of the product solutions. When the initial concentration of benzothiophene was raised to 10%, an additional product was also found. The material produced a mass spectrum consistent with dihydrobenzothiophene, C_8H_8S. The recoveries of the benzothiophene and its two products are shown in Figure 4. The amount of C_8H_8S obtained in these experiments decreased with increasing residence time. The presence of dihydrobenzothiophene has been observed in some[5,6], but not all[7] reports on the MoS_2 catalyzed HDS of benzothiophene. Benzothiophene desulfurization by a molybdenum naphthenate derived material has been proposed to follow a pathway dominated by the initial hydrogenation to form dihydrobenzothiophene.[5]

In the third type of experiment, an injection of a second material is made into a steady flow of model compound in solution. An example of this type of experiment is shown in Figure 5 where the TCD trace resulting from injections into a flowing solution is simulated. The recovery data from experiments in which a 10% solution of quinoline was injected into a continuous flow of 1% benzothiophene in tetralin are displayed in Figure 6. The first three determinations in Figure 6 correspond to samples taken on the plateau prior to the first injection of quinoline, roughly between 50 and 100 time units in Figure 5. These determinations consistently gave the conversion of benzothiophene to ethylbenzene to be 50% and the overall material balance to be 91%. The fourth determination results from the collection of the material that elutes with the quinoline pulse from about 110 to 130 time units. The quinoline recovered from the pulse amounted to 80% of that injected. No tetrahydroquinoline or further reduction products were detected. The major effect of the pulse was to inhibit the production of ethylbenzene. The total recovery of benzothiophene remained constant but the proportion of HDS product decreased to less than 43%. Determination 5 represents a sample taken on the plateau after the quinoline pulse had passed, roughly in the area of 150 to 175 time units. This sample contained neither quinoline nor its reduction products. Figure 6 shows that the conversion of benzothiophene to ethylbenzene had regained about half of the activity lost during the pulse but had not yet fully recovered. Sample 6 contained the material eluting with the second pulse of quinoline and sample 7 contained the material eluting on the plateau after the quinoline pulse. The same results as were obtained with the first pulse are repeated in the second pulse. This indicates that at least two mechanisms of nitrogen base inhibition are operative in this residue. Competitive inhibition in which the quinoline competes with the benzothiophene for adsorption at catalyst active sites may account for a portion of the lost activity seen during the pulse. However, the loss in activity that persists after the quinoline pulse has passed more likely arises from a poisoning of catalyst HDS sites by the base. This poisoning is thought to result from an adsorption mechanism similar to that seen for the diphenylether.

In summary, the liquefaction residue IK87-5 has shown only moderate catalytic activity in the model compound studies. Dehydrogenation and HDS reactions occurred but were significant only when the reaction temperature approached 400°C. Adsorption of heteroatom species occurred and, in the case of quinoline, appeared to be associated with a loss in catalytic activity. The temperature coefficient for the dehydrogenation was quite large and may reflect a thermal rate limiting step.

Work using the fresh, dispersed catalyst BCP-287 is just beginning. Preliminary results indicate much higher rates of tetralin dehydrogenation and benzothiophene HDS than were seen with the liquefaction residue.

CONCLUSIONS Model compound reactions have been used to investigate the catalytic activity of a coal liquefaction residue. The poor dehydrogenation effectiveness of the residue makes it a poor candidate for a hydrogenation catalyst at higher hydrogen pressures. However, in liquefaction experiments at 375°C, this material has been shown to be effective at inducing the uptake of hydrogen gas by coal and the conversion of coal.[2] On the basis of the above results, this ability must be related to some activity other than aromatic hydrogenation.

ACKNOWLEDGEMENT The authors gratefully acknowledge Anthony Cugini for the donation of a sample of the BCP-287 catalyst.

DISCLAIMER Reference to a brand or company name is made to facilitate understanding and does not imply endorsement by the U.S. Department of Energy.

REFERENCES

[1] Girgis, M.J.; Gates, B.C. *Ind. Eng. Chem. Res.* **1991**, *30*, 2021-2058.
[2] Bockrath, B.; Illig, E,; Keller, III, M.; Schroeder, K.; Bittner, E.; Solar, J. *Proceedings, Coal Liquefaction and Gas Conversion Contractors' Review Meeting, September 27-29, 1993* **1993**, 71-83.
[3] Bockrath, B.C.; Illig, E,G.; Keller, III, M.J. *Prepr. Pap.-Am. Chem. Soc., Div. Fuel Chem.* **1992**, *37*(1), 133-140.
[4] Schomburg, G.; Behlau, H.; Dielmann, R.; Weeke, F.; Husmann, H. *J. Chromatogr.* **1977**, *142*, 87-102. Wylie, P.L.; Philips, R.J.; Klein, K.J.; Thompson, M.Q.; Hermann, B.W. *J. High Res. Chromatog.* **1991**, *14*, 649-655.
[5] Ng, F.T.T.; Walker, G.R. *Can. J. Chem. Eng.* **1991**, *69*, 844-851.
[6] Van Parijs, I.A.; Hosten, L.H., Froment, G.F. *Ind. Eng. Chem. Prod. Res. Dev.* **1986**, *25*, 437-443.
[7] Kilanowski, D.R.; Gates, B.C. *J. Catal.* **1980**, *62*, 70-78.

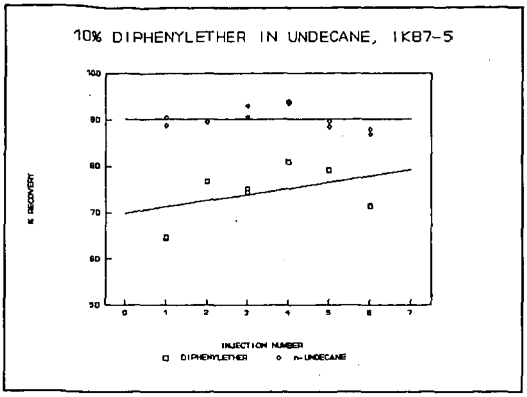

Figure 1. Coal Residue Containing MoS_2 Exhibiting Preferential Adsorption of Diphenylether at 300°C, 100 kPa Hydrogen.

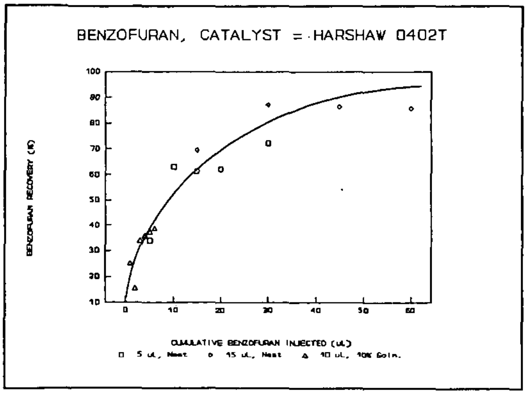

Figure 2. Data Illustrating the Adsorption of Oxygenate by a Supported Catalyst at 300°C, 100 kPa Hydrogen.

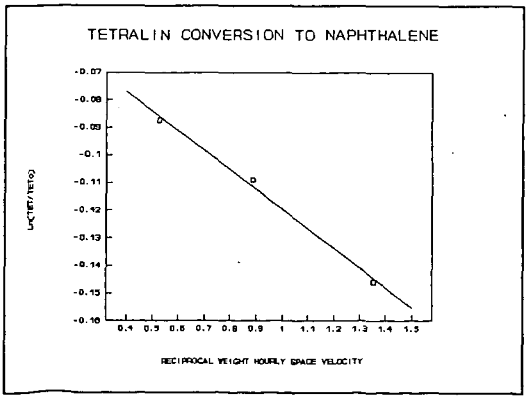

Figure 3. First Order Rate Constant Determination, 400°C, 340 kPa Hydrogen.

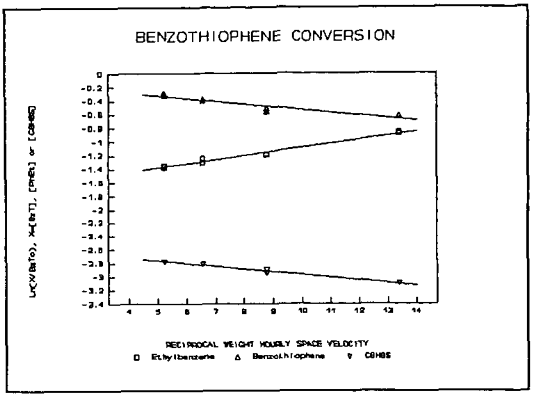

Figure 4. First Order Rate Constant Determination Showing Dihydrobenzothiophene Intermediate Formed at 400°C, 340 kPa Hydrogen.

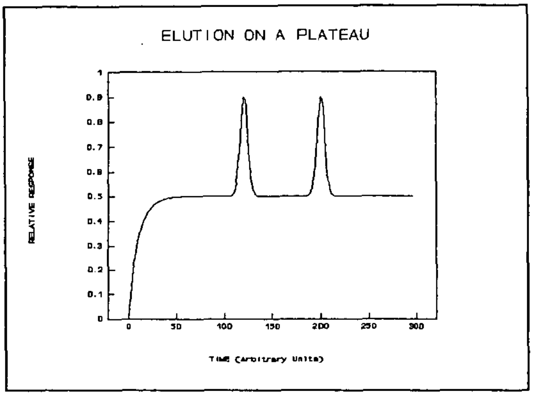

Figure 5. Typical TCD Signal from an Elution on a Plateau Type of Experiment. Units Are Arbitrary.

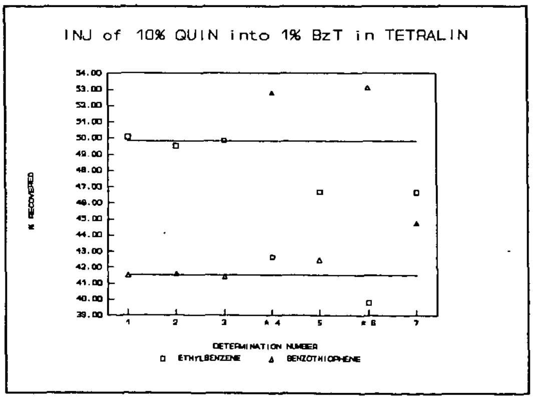

Figure 6. Quinoline Inhibition of the HDS of Benzothiophene, 400°C, 340 kPa. Injection on a Plateau Type Experiment.

ROLES OF MOLECULAR HYDROGEN AND A HYDROGEN DONOR SOLVENT IN THE CRACKING OF COAL MODEL COMPOUNDS WITH DISPERSED CATALYST

Toshimitsu SUZUKI, Na-oki IKENAGA, Takahiro SAKOTA, Takao MATSUI

Department of Chemical Engineering, Faculty of Engineering, Kansai University
Suita, Osaka, JAPAN 564

Keywords: benzyl phenyl ether, dibenzyl ether, metal carbonyl catalyst

Introduction

Roles of a catalyst and a hydrogen-donor solvent in the direct coal liquefaction involves still controversial arguments, because complex reactions such as thermal decomposition or hydrocracking of C-O and C-C bonds and hydrogenation of polycyclic aromatic compounds are involved in coal liquefaction reaction. Therefore, it is of great importance to evaluate quantitative hydrogen transfer process by using coal model compounds with a hydrogen-donor solvent.

Cronauer *et al.* showed that in the cracking of benzyl phenyl ether the hydrogen required to stabilize free radicals comes from a donor solvent or intramolecular rearrangement and not from gaseous hydrogen in the absence of a catalyst .[1] Korobkov *et al.*[2] and Schlosberg *et al.*[3,4] showed that the thermolysis of benzyl phenyl ether and dibenzyl ether were accomplished by intramolecular rearragements. Yokokawa *et al.* reported that tetralin retarded the catalyzed hydrocracking of coal model compounds containing C-C and C-O bonds.[5] However, few studies dealt with quantitative discussion in the hydrogen transfer process from a hydrogen-donor solvent or molecular hydrogen to free radicals derived from a model compound except a series of studies by Nicole and co-workers.[6,7]

On the other hand, it is well known that the amount of naphthalene produced from tetralin decreases after the liquefaction of coal in tetralin with catalyst as compared to the liquefaction in the absence of catalyst.[8-10] To account for this, two mechanisms are proposed. One is that the catalyst hydrogenates naphthalene produced from tetralin,[8] and the other is that the catalyst promotes the direct hydrogen transfer from molecular hydrogen to free radicals.[10,11]

The purpose of this work is to elucidate the role of catalyst and tetralin by means of the quantitative treatment of the hydrogen transfer reaction stabilizing thermally decomposed free radicals. Cracking of benzyl phenyl ether (BPE), dibenzyl ether (DBE), 1,2-diphenylethane, and 1,3-diphenylpropane was studied in tetralin in the presence of highly dispersed catalyst.

Experimental

Cracking of coal model compounds was carried out in a batch 50 mL autoclave made of Hastelloy C. Prescribed amounts of a model compound (3.6 - 3.9 g, 19.5 mmol), a catalyst (0.01 - 0.08 g, 0.025 - 0.4 mmol), tetralin (4.0 g, 30.0 mmol) or tetralin/naphthalene (4.0 g / 0.5 g, 30.0 mmol / 4.0 mmol), and an activated carbon (0.5 g) as a dispersing agent for the catalyst were put into the autoclave. Activated carbon was added in uncatalyzed runs, in order to elucidate catalytic effect of activated carbon. In catalyzed runs with $Fe(CO)_5$ and $Mo(CO)_6$, a molecular sulfur was added.

The reactor was pressurized with a hydrogen to 5.0 MPa at a room temperature. The autoclave was heated to the desired temperature (648 or 698 K) with a preheated stainless-steel heat block equipped with a shaker. After a given reaction time (20 - 240 min.), the autoclave was cooled to room temperature by air blowing. The gas was collected into a gas buret. The liquid products were recovered from the autoclave by filtering off the activated carbon with a sintered glass filter, followed by repeated washing with tetrahydrofuran.

The amount of hydrogen transferred from gas phase was determined with the difference between the amount of hydrogen charged and recovered.

Results and Discussion

Cracking of Benzyl Phenyl Ether. Table I summarizes results of the reactions carried out under different reaction conditions by using several catalysts. Conversion of BPE was 100 % in all cases at 648 K for the reaction time of 30 min.

As shown in Scheme I, the identified products from cracking of BPE were benzene (PhH), toluene (PhMe), phenol (PhOH), diphenylmethane (DPM), 1,2-diphenylethane (DPE), isomeric (hydroxyphenyl)phenylmethanes (HPPM), benzyltetralins[7] (BT, m/z=222 in GC-MS), and benzylnaphthalenes[7] (BN, m/z=218 in GC-MS). The major products were PhMe and PhOH, and the other products such as DPM and DPE were minor. BPE was thermally decomposed at a relatively low temperature and seemed to produce quantitatively benzyl radical and phenoxy radical, and these radicals abstract hydrogen from tetralin or benzyl radical may combine with tetralyl radical. The material balances between charged BPE and recovered products in these reactions were good to very good and in the range of 87 mol% to 98 mol%. The products formed from tetralin were naphthalene, decalin and 1-methylindan.

H_2-R in Table I indicates the amounts of hydrogen required for stabilizing thermally produced organic free radicals from BPE. They were calculated from the amounts of cracked products assuming the following over all stoichiometric reactions (not showing exact chemical path).

$$\text{Ph-CH}_2\text{O-Ph} \rightarrow \text{Ph-CH}_2 + \text{Ph-O}\cdot \qquad (1)$$

$$\text{Ph-CH}_2\cdot + 3\text{H} \rightarrow \text{Ph-H} + \text{CH}_4 \qquad (2)$$

$$\text{Ph-CH}_2\cdot + \text{H} \rightarrow \text{Ph-CH}_3 \qquad (3)$$

$$\text{Ph-O}\cdot + \text{H} \rightarrow \text{Ph-OH} \qquad (4)$$

$$\text{Ph-CH}_2\text{-(C}_6\text{H}_4\text{)-OH} + 2\text{H} \rightarrow \text{Ph-CH}_2\text{-Ph} + \text{H}_2\text{O} \qquad (5)$$

The rest of the products such as DPE and HPPM can be produced by the recombination of radicals or rearrangements of BPE, and no hydrogen were required.[7] H_2-TL in Table I exhibits the amount of hydrogen transferred from tetralin. It was calculated from the amount of naphthalene and decalin formed by the dehydrogenation and the hydrogenation of tetralin, assuming that all four hydrogens in tetralin are utilized. H_2-G shows the amount of hydrogen transferred from gas phase. Considering the experimental error, fair agreement between the amount of hydrogen required (H_2-R) and that of hydrogen transferred (H_2-G plus H_2-TL) was obtained.

In the reaction without catalyst (Run 1) the amounts of PhMe and PhOH were 11.3 mmol and 13.7 mmol respectively, these amounts were smaller than those in the reactions with $Mo(CO)_6$-S and $Ru(acac)_3$. The reaction in a smaller amount of tetralin (Run 2 BPE/TL= 2), the amounts of PhMe and PhOH further decreased and those of DPM and DPE slightly increased.

The amount of hydrogen required for stabilizing free radicals (H_2-R) were 13.9 mmol (Run 1) and 12.4 mmol (Run 3) in the reactions under a hydrogen or a nitrogen atmosphere. They were predominantly supplied from tetralin (12.0 mmol and 10.4 mmol respectively). These results clearly show that all four hydrogen atoms in tetralin are utilized to transfer to fragment radicals. With a decrease in the tetralin concentration contribution of hydrogen in gas phase increased even in the absence of catalyst (Run 2 probably catalyzed by wall).

$$R\cdot + TL \rightarrow RH + TL\cdot \tag{6}$$
$$2TL\cdot \rightarrow TL + DHN\ (\text{dihydronaphthalene}) \tag{7}$$
$$R\cdot + DHN \rightarrow RH + DHN\cdot \tag{8}$$
$$DHN\cdot + TL\cdot\ (\text{or } DHN\cdot) \rightarrow Naph + TL\ (\text{or } DHN) \tag{9}$$
$$R\cdot + TL\cdot \rightarrow R\text{-}TL \tag{10}$$
$$R\cdot \xrightarrow{H_2/\text{catalyst}} RH \tag{11}$$
$$TL\cdot \xrightarrow{H_2/\text{catalyst}} TL \tag{12}$$

The amount of hydrogen absorbed slightly increased with $Fe(CO)_5$-S, although ten times larger amount of Fe was used in these runs as compared to Mo and Ru. The ability of $Fe(CO)_5$-S catalyst to activate molecular hydrogen seems not to be high.

In the reactions with $Mo(CO)_6$-S (Runs 6 - 8), or $Ru(acac)_3$ (Runs 9-11) the amounts of toluene and phenol increased, and the amount of HPPM decreased correspondingly. These results indicate that the hydrogen transfer from gas phase to benzyl radical and phenoxy radical proceeded more smoothly than in the uncatalyzed reactions. Decreases in H_2-TL and increases in H_2-G in the catalyzed runs with $Mo(CO)_6$-S and $Ru(acac)_3$ suggest the possibility of direct hydrogen transfer from gaseous hydrogen to benzyl and phenoxy radicals more efficiently (equation 11).

Cracking of Dibenzyl Ether. Cracking of DBE was carried out under the same condition as the cracking of BPE except that the reaction time was shortened to 20 min. The results are summarized in Table II. The identified products from cracking of DBE were benzene, toluene, benzaldehyde (PhCHO), benzyl alcohol (BA), 1,2-diphenylethane, benzyltetralins, and benzylnaphthalenes. H_2-R was calculated according to the following over all stoichiometric equations (not showing exact chemical paths).

$$Ph\text{-}CH_2OCH_2\text{-}Ph \rightarrow Ph\text{-}CH_2\cdot + Ph\text{-}CH_2O\cdot \tag{13}$$
$$Ph\text{-}CH_2\cdot + 3H \rightarrow Ph\text{-}H + CH_4 \tag{14}$$
$$Ph\text{-}CH_2\cdot + H \rightarrow Ph\text{-}CH_3 \tag{15}$$
$$Ph\text{-}CH_2\cdot + Ph\text{-}CH_2O\cdot \rightarrow Ph\text{-}CH_3 + Ph\text{-}CHO \tag{16}$$
$$Ph\text{-}CH_2O\cdot + H \rightarrow Ph\text{-}CH_2OH \tag{17}$$
$$Ph\text{-}CH_2O\cdot + 3H \rightarrow Ph\text{-}CH_3 + H_2O \tag{18}$$

It is noteworthy in these reactions that PhMe was produced more than the amount that was evaluated from equations 15 and 16. An excess amount of PhMe could be originated from the hydrogenation of oxygen containing compound as shown in equation 18. Amount of H_2O was about 14.2 mmol, corresponding to the occurrence of reaction 18. Estimated H_2-R was smaller than H_2-G plus H_2-TL due to unidentified minor products in most catalyzed runs.

As shown in Table II, in the uncatalyzed reactions at 648 K (Runs 12 in H_2 and Run 13 in N_2) the amounts of PhMe were 23.2 and 23.1 mmol and those of PhCHO were 6.1 and 7.5 mmol respectively indicating the lowest yields of PhMe and the highest yields of PhCHO. In addition under a nitrogen atmosphere DPE increased to 3.2 mmol, suggesting that the recombination of benzyl radicals most likely proceeded. On the other hand, H_2-R (15.1 mmol) is in fair agreement with H_2-TL (14.7 mmol), indicating that most of hydrogen required to stabilize fragment radicals transferred from tetralin.

When $Fe(CO)_5$-S was employed for the cracking of DBE (Runs 14 and 15), the amounts of H_2-TL and H_2-G (15.4 mmol and 1.9 mmol in Run 14) were approximately same as those in the uncatalyzed run (14.7 mmol and 0.5 mmol in Run 12). However, H_2-TL decreased to 9.0 mmol and H_2-G increased to 9.8 mmol when smaller amount of tetralin was used (8.0 mmol, Run 15). The amount of PhCHO (2.1 mmol in Run 14) was less than that in Run 12 (6.1 mmol). These results suggest that the possibility of direct hydrogen transfer from gaseous hydrogen to benzyl and $Ph\text{-}CH_2O\cdot$ radicals to form toluene is enhanced.

In the catalyzed runs with $Mo(CO)_6$-S and $Ru(acac)_3$ (Runs 16 and 19), PhCHO and BA were scarcely detected and PhMe was increased to 27.5 mmol and 29.6 mmol suggesting considerable possibility of reaction 18. Although H_2-R was estimated to be smaller than H_2-G plus H_2-TL due to unidentified minor products, correspondingly increases in H_2-R could be expected. Furthermore, with these catalysts, decreases in H_2-TL to 1/3 of the H_2-R (11.7 and 9.2 mmol) and increases in H_2-G to about 80 % of H_2-R (22.5 and 22.7 mmol) were observed similar to the reaction with BPE. However, in the reaction with $Mo(CO)_6$-S the amount of H_2-TL was larger than that in the cracking of BPE with the same catalyst. The contribution of tetralin for the hydrogen transfer process to stabilize the thermally decomposed free radicals increased in the cracking of DBE. Whereas, if we decreased the amount of tetralin to 8 mmol (Run 17 and 20), H_2-TL decreased to 5.5 and 4.6 mmol and H_2-G increased to 25.7 and 27.3 mmol as seen in the reaction with $Fe(CO)_5$-S, suggesting that the possibility of direct hydrogen transfer from gaseous hydrogen to radicals increased.

Cracking of benzyl phenyl ether and dibenzyl ether in tetralin-naphthalene mixed solvent. In the cracking of BPE and DBE in tetralin using finely dispersed catalyst, two possibilities were proposed for the decrease in the amount of naphthalene after the reactions. One is the direct hydrogen transfer process from molecular hydrogen activated on the catalyst to free radicals, consequently contribution of the hydrogen transfer from tetralin to free radicals decreased. The other is the hydrogenation of naphthalene formed after hydrogen transfer to radicals with catalyst. In order to confirm the possibility of hydrogenation of naphthalene, the cracking of BPE or DBE was carried out in tetralin/naphthalene mixed solvents, and the results are summarized in Runs 8, 11, 18 and 21 in Tables I and II.

In the reactions in tetralin with the catalyst (Runs 4, 6 and 9), 3.3 - 4.9 mmol of decreases in naphthalene were observed as compared to the uncatalyzed run (Run 1 in Table I). If these decreases are ascribed to the hydrogenation of naphthalene, a certain amount of added naphthalene would be hydrogenated to give tetralin in the reaction with mixed solvents. As seen in Runs 8 and 11, 4.1 and 5.7 mmol of naphthalene was recovered respectively. If we assume that the same amount of naphthalene was formed from tetralin (Runs 6 and 9) in the presence of tetralin-naphthalene mixed solvents and no hydrogenation of added naphthalene did occur, hypothetical amount of naphthalene after the reaction would be estimated to be 4.7 (0.7 + 4.0) and 4.2 (0.2 + 4.0) mmol for Runs 8 and 11, respectively. In Run 8 , 4.1 mmol of naphthalene was observed, indicating that only 0.6 mmol of naphthalene was hydrogenated in the course of the reaction. In Run 11, 5.7 mmol of naphthalene was detected. This is rather increase in 1.5 mmol of naphthalene, as compared to the hypothetical amount of naphthalene. These results suggest that hydrogenation of naphthalene did not or slightly occurred during the cracking of BPE. As shown in Runs 18 and 21 in Table II, hydrogenation of naphthalene during the reaction was also examined in the cracking of DBE. It was found that 0 - 1.3 mmol of naphthalene was hydrogenated in the course of cracking of DBE.

In separate experiments, hydrogenation of naphthalene or naphthalene in tetralin did proceed considerable extent with all the catalysts employed here. Thus in the presence of polar substances or free radicals, the activity toward the hydrogenation of aromatic nuclei would be reduced considerably due to the stronger interaction of the catalyst with them.

On the other hand, 0.3 mmol to 2.1 mmol of BT were produced in the cracking of BPE and DBE even with the active catalyst such as $Mo(CO)_6$-S and $Ru(acac)_3$, and BT increased in the cracking of DBE at 698 K. This seems to provide possibility of formation of tetralyl radical which in turn combined with benzyl radical or were hydrogenated to tetralin on the catalyst surface as proposed in the previous study.[12] Cochran *et al.* have suggested that the direct hydrogen transfer is the predominant route in tin-catalyzed coal liquefaction.[10] Importance of molecular hydrogen in the catalyzed coal liquefaction with highly dispersed catalysts has been pointed out by Charcosset et al.[13] The direct hydrogen transfer from gas phase hydrogen activated on the catalyst not only to free radicals derived from BPE or DBE but also tetralyl radical.

Cracking of 1,2-diphenyl ethane and 1,3-diphenylpropane Cleavage of C-C bonds in coal is much more important reactions in the hydroliquefaction of subbituminous or bituminous coal. In order to examine catalytic effects of dispersed catalyst on the dissociation of C-C bond, 1,2-DPE and 1,3-diphenylpropane (1,3-DPP) in tetralin was carried out without or with dispersed catalysts. Results are summarized in Table III. Cracked products are benzene, toluene, and ethylbenzen, in addition to small amounts of BT and BN.

Much lower conversions were obtained in both model compounds even at higher reaction temperature of 425 °C and longer reaction period of 60 min. In the absence of catalyst, the amount of hydrogen required to stabilize thermally cracked free radical is in good agreement with the amount of hydrogen produced from tetralin calculated from the amount of naphthalene formed (see Runs 22 and 23).

With the addition of dispersed catalysts not significant differences in the amounts of cracked products were observed, indicating poor capability of metal sulfides or metal species on the hydrocracking of C-C bond. Due to the lower conversion of model compounds, the amounts of hydrogen absorbed from gas phase could not be measured accurately. However, the amount of naphthalene formed after the reaction decreased as compared to the run without catalyst, when a smaller amount of tetralin was employed. Such phenomena were pronouncedly observed, when $Mo(CO)_6$-S and $Ru(acac)_3$ catalysts were used. In these cases (Runs 27 and 30), the amount of hydrogen required to stabilize free radicals from DPE exeeded the amount of hydrogen dehydrogenated from tetralin. This indicates that hydrogen transfer from molecular hydrogen to organic radicals on the catalyst occurred. However, in the abundant hydrogen donor solvent, hydrogen transfer from tetralin to benzy radical did proceed more effectively to give toluene.

Such tendencies are seen in the cracking of DPP. Only Ru based catalyst effectively promoted hydrogen transfer from gas phase hydrogen to organic free radicals.

These results indicate that C-C bonds in the coal model structure were thermally dissociate to give free radicals and they abstract hydrogen to give stable organic compounds either from a hydrogen donor solvent or molecular hydrogen activated on the catalsyst. However, even in the presence of an active catalsyst, hydrogen was pronouncedly supplied to such hydrocarbon radicals from a hydrogen donor solvent like tetralin.

Two reasons for this can be proposed. One is that due to a higher bond dissociation energy of C-C bonds in the model compounds, the rate of benzyl radical formation is small, and consequently abundant hydrogen donor solvent could provide hydrogen to organic free radicals. The other is that benzyl radical could be less strongly adsorbed on the active catalyst as compared to the oxygen containing free radicals derived from BPE and DBE. Therefore, hydrogen transfer from gas phase to benzyl radical only slightly occurred.

Conclusion

Quantitative hydrogen transfer process from tetralin to organic free radicals was clarified. Direct hydrogen transfer from molecular hydrogen on the dispersed catalyst was proposed for the cracking of oxygen containing coal model compounds, in the presence of hydrogen donor such as tetralin.

References

1) Cronauer, D.C.; Jewell, D.M.; Shah, Y.T.; Modi, R.J. *Ind. Eng. Chem. Fundam.* **1979**, *18*, 153-162.
2) Korobkov, V.Y.; Grigorieva, E.N.; Bykov, V.I.; Senko, O.V.; Kalechitz, I.V. *Fuel* **1987**, *67*, 657-662.
3) Schlosberg, R.H.; Ashe, T.A.; Pancirov, R.J.; Donaldson, M. *Fuel* **1981**, *60*, 155-157.
4) Schlosberg, R.H.; Davis, W.H.; Ashe, T.A. *Fuel* **1981**, *60*, 201-204.
5) Yokokawa, C.; Ikenaga, N.; Fukumi, J.; Oda, H. *Proceedings of International Conference on Coal Science* ; pp. 911-914, 1989, Tokyo.
6) Meyer, D.; Nicole, D.; Delpuech, J.J. *Fuel Process. Technol.* **1986**, *12*, 255-268.
7) Meyer, D.; Oviawe, P.; Nicole, D.; Lauer, C.; Clement, J. *Fuel* **1990**, *69*, 1309-1316.
8) Guin, J.A.; Tarrer, A.R., Lee, J.M.; Lo, L.; Curtis, C.W. *Ind. Eng. Chem. Process Des. Dev.* **1979**, *18*, 371-376.
9) Moritomi, H.; Nagaishi, H.; Naruse, M.; Sanada, Y.; Chiba, T. *J. Fuel Soc. Jpn.* **1983**, *62*, 254-262.
10) Cochran, S.J.; Hatswell, M.; Jackson, W.R.; Larkins, F.P. *Fuel* **1982**, *61*, 831-833.
11) Suzuki, T.; Yamada, O.; Takahashi, Y.; Watanabe, Y. *Fuel Process. Technol.* **1985**, *10*, 33-43.
12) Suzuki, T.; Yamada, H.; Sears, P.L.; Watanabe, Y. *Energy Fuels* **1989**, *3*, 707-713
13) Charcosset, H.; Bacaud, R.; Besson, M.; Jeunet, A.; Nickel, B; Oberson, M. *Fuel Process. Technol.* **1986**, *12*, 189-201.

Table 1 Cracking of Benzyl Phenyl Ether and the Amount of Hydrogen Transferred to Radicals[a]

Run	Catalyst	Solv.	PhMe	PhOH	DPM	DPE	HM	BT[b]	BN[b]	Naph	TL	H_2-R[c]	H_2-T[d]	H_2-G[e]
		mmol					mmol							
1	none	28.9	11.2	13.7	1.5	0.7	4.0	0.7	0.5	5.1	19.9	13.9	12.0.	0.6
2	none	8.8	8.7	11.8	1.8	1.0	3.9	0.3	0.6	2.9	3.1	12.0	7.5	4.4
3	none(N_2)	30.6	10.9	12.3	1.4	0.2	3.7	0.7	0.5	4.5	23.0	12.4	10.4	—
4	$Fe(CO)_5$-S[f]	29.1	6.0	12.8	0.3	0.9	5.3	2.5	0.6	1.8	24.6	9.6	6.3	2.6
5	$Fe(CO)_5$-S[f]	8.1	8.8	12.2	0.4	1.2	4.3	0.4	0.5	2.4	4.4	9.8	4.2	6.6
6	$Mo(CO)_6$-S[i]	29.5	14.2	15.7	0.4	0.4	2.3	0.9	0.3	0.7	28.0	15.4	2.6	17.0
7	$Mo(CO)_6$-S[g]	8.3	12.4	14.5	0.8	0.5	2.5	0.6	0.4	0.9	6.2	14.3	3.0	15.5
8	$Mo(CO)_6$-S[g]	T/N[h]	14.6	15.6	0.3	0.2	2.0	0.4	0.4	4.1	29.2	16.0	1.5	15.4
9	$Ru(acac)_3$	30.3	14.2	15.5	0.7	0.2	1.8	0.5	0.2	2.0	26.2	15.6	5.7	9.1
10	$Ru(acac)_3$	8.2	13.3	16.1	0.7	0.7	2.0	0.6	0.4	0.9	6.1	15.4	3.0	19.3
11	$Ru(acac)_3$	T/N[h]	13.5	14.9	0.8	0.1	2.3	0.5	0.6	5.7	26.8	15.5	4.9	11.3

a) BPE 19.5mmol, active carbon 0.5g, P(H_2) = 5.0MPa, reaction time 30min, conversion = 100%.

b) m/z=222 (BT, benzyltetralins) and 218 (BN, benzylnaphthalenes).

c) Calculated amount of hydrogen to stabilize radicals.

d) Amount of hydrogen transferred from tetralin. e) Amount of hydrogen transferred from gas.

f) Sulfur 0.8mmol. g) Sulfur 0.22mmol. h) Solvent : TL, 30.0mmol; Naph, 4.0mmol.

Abbreviations : DPM, diphenylmethane; DPE, 1,2-diphenylethane;
HM, (hydroxyphenyl)phenylmethanes; Naph, naphthalene; TL, tetralin.

Table II Cracking of Dibenzyl Ether and the Amount of Hydrogen Transferred to Radicals [a]

Run	Catalyst	Solv.	PhMe	PhCHO	BA	DPE	BT[b]	BN[b]	Naph	TL	H_2-R[c]	H_2-T[d]	H_2-G[e]
			mmol								mmol		
12	none	29.8	23.2	6.1	trace	1.2	0.6	1.0	6.4	21.1	15.1	14.7	0.5
13	none(N_2)	30.1	23.1	7.5	1.6	3.2	0.4	0.8	5.6	21.7	19.8	13.6	—
14	$Fe(CO)_5$-S [g]	29.3	24.3	2.1	—	1.0	1.6	2.4	4.4	16.3	21.9	15.4	1.9
15	$Fe(CO)_5$-S [g]	8.3	22.8	3.8	—	1.7	0.3	1.3	2.8	3.1	18.1	9.0	9.8
16	$Mo(CO)_6$-S [i]	30.0	27.5	—	trace	1.4	1.8	1.7	3.3	21.4	27.9	11.7	22.5
17	$Mo(CO)_6$-S [i]	8.1	25.7	—	—	2.0	0.9	1.1	2.0	4.0	29.8	5.5	25.7
18	$Mo(CO)_6$-S [i]	T/N [h]	25.2	trace	—	1.2	1.7	1.9	6.0	23.3	24.8	8.7	21.0
19	$Ru(acac)_3$	30.2	29.6	0.7	trace	0.8	1.2	0.7	3.4	22.8	27.9	9.2	22.7
20	$Ru(acac)_3$	8.0	29.0	trace	—	1.4	0.8	0.7	1.3	5.0	28.9	4.6	27.3
21	$Ru(acac)_3$	T/N [h]	29.6	trace	—	0.7	1.1	0.8	6.7	25.2	29.4	7.5	25.0

a) DBE 19.5mmol, active carbon 0.5g, $P(H_2) = 5.0$ MPa, reaction time 20min,

b) m/z=222 (BT, benzyltetralins) and 218 (BN, benzylnaphthalenes).

c) Amount of hydrogen transferred to radicals.

d) Amount of hydrogen from tetralin. e) Amount of hydrogen from gas.

f) Mol percent against DBE charged. g) Sulfur 0.8mmol.

h) Solvent : TL, 30.0mmol; Naph, 4.0mmol. i) Sulfur 0.22mmol.

Abbreviations : BA, benzyl alcohol; DPE, 1,2-diphenylethane; Naph, naphthalene; TL : tetralin.

Table III Cracking of 1,2-diphenylethane and 1,3-diphenylpropane in tetralin[a]

Run	Catalyst	metal mmol	Time min	Solv	PhH	PhMe	PhEt	Naph	TL	H_2-R	H_2-TL
						mmol					
		Diphenylethane									
22	None		60	8.3	0.86	5.20	0.83	1.4	5.7	3.3	2.9
23	None		60	30.1	0.53	5.30	0.46	2.1	25.4	3.1	4.2
24	None		240	29.9	1.47	15.74	1.67	5.3	17.6	9.4	10.6
25	$Fe(CO)_5$-S	0.40	60	8.3	0.92	5.81	1.06	1.2	5.5	3.9	2.3
26	$Fe(CO)_5$-S	0.40	60	29.5	0.52	5.31	0.55	2.8	24.2	3.2	5.5
27	$Mo(CO)_6$-S	0.05	60	8.2	0.93	4.96	0.97	0.8	6.5	3.2	1.6
28	$Mo(CO)_6$-S	0.05	60	28.8	0.69	6.03	0.99	5.6	19.1	4.0	11.1
29	$Mo(CO)_6$-S	0.05	240	30.9	1.43	17.20	2.03	5.9	16.8	10.6	11.9
30	$Ru(acac)_3$	0.025	60	8.1	0.88	4.92	0.86	0.9	5.8	3.3	1.8
31	$Ru(acac)_3$	0.025	60	30.0	0.49	5.72	0.53	2.3	24.8	3.4	4.6
		Diphenylpropane									
32	None		60	4.1	0.13	1.36	1.14	0.54	2.1	1.3	1.1
33	$Fe(CO)_5$-S	0.06	60	4.12	0.11	1.99	2.07	0.82	2.6	2.1	1.6
34	$Mo(CO)_6$-S	0.08	60	4.11	0.22	1.99	1.95	1.05	2.3	2.1	2.1
35	$Ru(acac)_3$	0.04	60	4.11	0.18	2.01	2.12	0.42	3.27	2.16	0.9

a) Diphenylethane: 19.5 mmol, Diphenyl propane: 2.5 mmol active carbon 0.50 g, 425 °C, $PH_2 = 5.0$ MPa,

Other abbreviations are the same as Table I.

MECHANISMS OF IRON-BASED CATALYSIS INVESTIGATED USING MODEL COMPOUNDS

John C. Linehan, Dean W. Matson, John G. Darab, S. Thomas Autrey,
James A.. Franz, and Don M. Camaioni.
Pacific Northwest Laboratory[1]
P.O. Box 999, Richland, WA

Key words: Model compounds, catalysis, iron oxides.

Abstract. The catalytic mechanism of highly active, nanophase iron-based coal liquefaction catalysts was investigated using a series of model compounds. The iron-oxide phases ferric oxyhydroxysulfate (OHS), 6-line ferrihydrite, hematite, and goethite, were evaluated as catalyst precursors with systematically substituted diphenylmethanes in the presence of a hydrogen donating solvent. The activity of the catalysts was observed to be dependent upon the functionality on the model compounds. The results of these model compound studies and their relationship to possible reaction mechanisms are presented.

Introduction. There has been recent interest in the development of inexpensive, new, and potentially disposable, catalysts for the first stage direct liquefaction of coal.[2] A major emphasis has been placed on developing highly active iron-based liquefaction catalysts as substitutes for the current molybdenum-based catalysts which are more expensive. The new iron-containing catalysts for this purpose have been screened using either model compounds or select coals. While numerous studies have been undertaken to synthesize and test iron-based catalysts with enhanced catalytic activity for hydrogenolysis,[2] few studies have systematically focused on the bond cleavage or hydrogenation mechanism(s) involved when these catalysts are employed.[3]

In previous papers we have focused on either developing techniques for the production of nanoscale iron-oxides or the identification of active iron oxide catalyst precursor phases.[4-6] In this paper we concentrate on the organic structures which are attacked by the iron-based catalysts. We describe our preliminary results using systematically altered model compounds with a variety of iron oxide catalyst precursors to elucidate carbon-carbon bond scission pathways supported by iron-based catalysts.

Experimental. The model compounds diphenylmethane (DPM) (Aldrich) and 4,4'-dimethyl diphenylmethane (4,4'DPM) (TCI) were used as received. The model compounds methyl diphenylmethane (MeDPM), 2,5 -dimethyl diphenylmethane (Me2DPM), and 2,4,6-trimethyl diphenylmethane (Me3DPM) were synthesized from neat mixtures of the appropriate methylated aromatic (toluene, p-xylene, and mesitylene respectively) and benzyl alcohol with the addition of concentrated sulfuric acid. The reaction products were distilled under reduced pressure and the products were shown to be 99% pure by GC and proton NMR. The only exception was MeDPM which was found to be an inseparable 50:50 isomeric mixture of 2-methyldiphenylmethane and 4-methyl diphenylmethane by NMR.

The catalyst precursors were made according to literature procedures and milled to -325 mesh, except for the 6-line ferrihydrite[4] which was produced by the RTDS method[5,7] at low reaction temperatures and was also sieved to -325 mesh. The catalyst testing procedure, which has been detailed previously, consisted of loading 15 µl of the model compound with 3 mg of the catalyst precursor, 3 mg of elemental sulfur and 100 mg of pure (>99%) 9,10-dihydro-phenanthrene into a Pyrex tube. The tube was sealed under vacuum and heated at 400±3 °C for 1 hour in a fluidized sand bath. The products were identified by GC and the residual model compounds were quantified with an internal standard.

Results and Discussion. Table I shows the percent consumption of the five model compounds using four iron oxide catalyst precursors. As can be seen from the Table, the relative order of model compound consumption increases with increasing methyl substitution. Figure 1 shows these results as a function of the number of methyl groups on substituted diphenylmethanes. Both Table I and Figure 1 show the dramatic increase in consumption of the model compound in going from Me2DPM to Me3DPM. The yields more than double for most of the catalysts. All of the iron oxide precursors used promoted over 75% consumption of Me3DPM. These results support the findings that many different forms of iron-containing powders have been found to be active bond scission catalysts under the appropriate reaction conditions.

The increase in the percent consumption of model compound correlates with the decrease in the oxidation potential of benzene upon increasing methyl substitution. The oxidation potential drops approximately 0.6 V in going from toluene to 1,2,3,5-trimethylbenzene.[8,9] We estimate that the oxidation potentials of the model compounds used here would decrease in a corresponding manner with increasing methyl substitution. The observed relationship between oxidation potential and bond scission enhancement does not necessarily prove a REDOX mechanism. The cyclohexyldienyl radical intermediate generated by a free radical pathway would also be stabilized with an increase in methyl substitution and would increase the rate of bond cleavage.

The products of the model compound consumption reactions were mixtures of products resulting from cleavage of bonds A , B, and C (see Figure 2). For DPM and 4,4'DPM, the products of bond A and bond B cleavage were indistinguishable, the products from bond A being toluene and the methylated aromatic. For MeDPM, Me2DPM, and Me3DPM, the bond A methylated aromatic products were toluene, p-xylene, and mesitylene respectively. Bond B cleavage yielded benzene and the methylated aromatic with one additional methyl group. For MeDPM, Me2DPM, and Me3DPM, bond B cleavage yielded xylene, 1,2,5-trimethyl benzene, and 1,2,3,5-tetramethyl benzene respectively. Bond C cleavage involved the loss of a methyl group from the model compound and yielded the parent compound minus one methyl group.

For the uncatalyzed reactions, products from bonds B and C cleavage predominated. The bond B:C cleavage product ratios were less than one and the bond B:A cleavage ratios were greater than one. The small thermal conversions with some of the uncatalyzed model compound reactions precluded accurate or statistically significant reporting of product distributions.

The products of the catalyzed reactions of the methylated diphenylmethane compounds were almost exclusively derived from bond A cleavage. The major products were toluene and the methylated aromatic (toluene, p-xylene, mesitylene) derived from the substituted ring. Very little benzene, from bond B cleavage, was detected. There was little evidence for methyl cleavage from the methylated diphenylmethanes in the iron catalyzed reactions. This has also been seen for other methylated systems when using other iron and molybdenum-based catalysts.[10] The B:A bond cleavage ratio for the ferric oxyhydroxysulfate catalyzed reaction was over 50 and the B:C ratio over 100 for Me3DPM model compound. The ratios of B:A products and B:C products increased with increasing number of methyl substitution for a given catalyst. There was little difference in these ratios between the products of reactions involving different catalyst precursors when similar conversions were obtained.

The total amount of the model compound hydrogenation was less than 2% of the total products for any of the model compounds or catalyst precursors. This is consistent with other results with iron-based catalysts in the presence of sulfur for both diphenylmethane and naphthyl bibenzylmethane, even under high hydrogen pressures.[3,4] Other iron-based catalysts have previously been shown to be active for hydrogenation of polycyclic aromatics in the absence of good leaving groups.[10]

Summary Iron-based materials catalyze the consumption of more substituted diphenylmethanes faster than less substituted diphenylmethanes. The catalyzed reactions were very selective for cleavage between the aromatic carbon of the most substituted ring and the methylene carbon. Little evidence for catalyzed cleavage of methyl groups was detected. The relative reactivity of the iron oxide precursors was similar to that previously found for NBBM.

Acknowledgements We gratefully thank Dr. Glen Fryxell (PNL) for developing the methodology for the model compound synthesis. The model compound work was supported by the Director, Office of Energy Research, Office of Basic Energy Sciences, Chemical Sciences Division of the Department of Energy and the catalyst development work was supported by the U. S. Department of Energy, Office of Fossil Energy under contract DE-AC06-76RLO 1830.

REFERENCES

1. Pacific Northwest Laboratory is operated for the U.S. Department of Energy by Battelle Memorial Institute under contract DE-ACO6-76RLO 1830.
2. See the first 21 papers in *Energy & Fuels*, **1994**, 1, and references therein.
3. Wei, X. Y.; and Zong, Z-M. *Energy & Fuels,* **1992**, 6, 236. Wei, X. Y.; Ogata, E.; Zong, Z.-M.; and Niki, E. *Energy & Fuels*, **1992**, 6, 868.
4. Linehan, J. C.; Matson, D. W.; and Darab, J. G. *Energy & Fuels* **1994**, 8, 56.
5. Matson, D. W.; Linehan, J. C.; Darab, J. G.; and Buehler, M. F. *Energy & Fuels* **1994**, 8, 10.
6. Darab, J. G.; Linehan, J. C.; Matson, D. W.; and Campbell, J. A. In Proceedings of the 7th International Conference on Coal Science Vol I, pg 24, 1993.
7. Matson, D. W.; Linehan, J. C.; and Bean, R. M. *Materials Lett.*, **1992**, 14, 222.
8. Gould, I.R; Ege, D.; Moser, J.E.; and Farid, S. *J. Am. Chem. Soc.* **1990**, 112, 4290.
9. Howell, J.O.; Goncalves, J.M.; Amatore, C.; Klasine, L.; Wightman, R.M.; and Kochi, J.K. *J. Am. Chem. Soc.*, **1984**, 106, 3968.
10. Tang, Y. and Curtis, C.W. *Energy & Fuels*, **1994**, 8, 63.

Table I
Percent Consumption of Model Compounds with
Iron-Based Catalysts at 400°C in the Presence of 9,10-Dihydrophenanthrene

	Catalyst Precursor				
Model Compound	Hematite	Goethite	6-Line Ferrihydrite	Ferric Oxyhydroxy-Sulfate	None
DPM[a]	nm	4 ± 3	6 ± 3	9 ± 3	0
MeDPM	13 ± 2	3 ± 2	8 ± 3	29 ± 2	1 ± 1
Me2DPM	36 ± 3	9 ± 3	19 ± 2	58 ± 2	6 ± 3
Me3DPM	86 ± 5	95 ± 5	75 ± 5	98 ± 2	5 ± 3
4,4'DPM	43 ± 4	7 ± 3	6 ± 2	60 ± 5	3 ± 2

a) See reference 6.

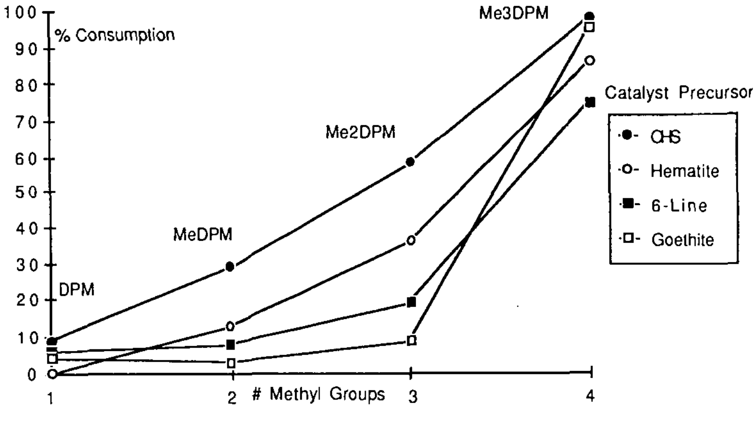

Figure 1. A plot of model compound consumed (at 400°C, 60 minutes, with catalyst and dihydrophenanthrene) vs methyl substitution for diphenylmethane.

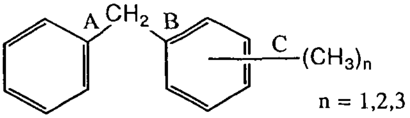

Figure 2. Schematic of the substituted diphenylmethanes and the bond designation.

HETEROGENOUS CATALYSIS:
Mechanisms of Selective Cleavage of Strong Carbon-Carbon Bonds.

Malvina Farcasiu and Steven C. Petrosius
U.S. Department of Energy
Pittsburgh Energy Technology Center
P.O. Box 10940, Pittsburgh, PA 15236

Key Words: heterogenous catalysis, carbon-carbon bond cleavage, mechanism

INTRODUCTION

This paper discusses the catalytic cleavage of strong carbon-carbon bonds in compounds which also contain relatively weaker carbon-carbon bonds which can be cleaved thermally by a homolytic, free radical process. The majority of the reactions described here are performed under condition where the thermal background is very small or nonexistent.

We will discuss the reactivity of two model compounds (Figure 1) relevant to fossil fuels (oil and coal) in the presence of several heterogenous catalysts: carbon black, graphite and solid acids. Previously, we have reported a very selective carbon black C-C cleavage of bonds between a polycondensed aromatic moiety and an adjacent aliphatic carbon[1-4] and on carbon black catalyzed dehydroxylation and dehalogenation of polycondensed aromatic phenols and halogenated polycondensed compounds[5]. We attributed the observed catalytic activity and selectivity in hydrocracking reactions to the formation of radical cations on the surface of carbon-based catalysts at temperatures over 320 °C[2] and the dehydroxylation and dehalogenation reactions to a free radical mechanism identical with that of the thermal reaction[5]. We concluded that two types of catalytic active centers are present on carbon black. In this presentation we will elaborate on the nature of carbon black catalytic activity and contrast it to that of graphite.

The ion radical mechanism for the C-C cleavage mechanism which we observe in the case of carbon black catalysts is disputed by Penn and Wang based on an extensive presentation of literature data and on their own experimental results for radical-cation generated in solution in the presence of polar solvents[6]. Under their reported conditions, no cleavage of any C-C bond is observed unless a tetraaryl-substituted ethane was used as a substrate. They conclude that the ion-radical mechanism we proposed for the carbon black catalyzed reactions is incorrect and that the solvent-assisted ipso addition of a hydrogen atom[7] is the most likely explanation for both thermal and catalytic carbon-carbon cleavage of the type we observed. The role of the catalyst is considered to be to accelerate either the formation of the hydrogen atom or the addition of the hydrogen atom to the substrate, or both. The source of the H-atom is the solvent.

We will discuss in this paper the data that rise doubts about extending the free radicals (including ipso addition of hydrogen atoms from solvents) as the initial step in the cleavage of specific strong C-C bonds under the conditions of heterogenous catalysis on carbon catalysts.

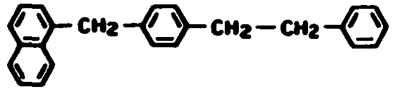

4-(1-naphtylmethyl) bibenzyl (I)

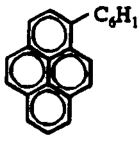

n-hexyl-pyrene (II)

Fig. 1 Model compounds used in this study

EXPERIMENTAL

The experimental conditions for testing the model compounds described in Fig.1 and the methods used for products identification and conversion calculations have been already published[2,3]. In this study, the catalytic reactions of I and II have been studied both in tetralin and perdeuterated tetralin, both from Aldrich Co.

RESULTS AND DISCUSSION

Carbon-catalyzed C-C cleavage reactions were performed for I and II, compounds having the general formula Aryl-CH^2-R, where aryl is naphthalene (I) or pyrene (II). The selective cleavage is catalyzed by carbon black at temperatures of 320 to 420^{0}C. The graphite does not catalyze the cleavage. Unlike the dehydroxylation and dehalogenation reactions which require the presence of a H-donor, the carbon black catalyzes the C-C cleavage both in the presence and absence of the H-donor. Another reaction observed in the presence of deuterotetralin is H-D exchange. This reaction is catalyzed both by carbon black and graphite. At 350^{0}C and reaction time of one hour the degree of H-D exchange is 58% in the presence of BP2000 and 12% in the presence of graphite. At 400^{0}C and one hour reaction time the H-D exchange is 93% in the presence of BP2000 and 74.6% in the presence of graphite. However, the yield of selective cracking of the bond adjacent to the naphthalene ring is 20.4% in the case of BP2000 and zero for graphite. In the presence of graphite, the cracking is less than 1% and the selectivity is typical of the thermal reaction[2]. We conclude that it is no connection between the mechanism of H-D exchange and the selective cleavage of C-C bond described above. We believe that this result, together with the calculations of Ades et.al.[8,9] and the results of Charge Distribution Analysis reported previously[2] make the ipso addition unlikely as the mechanism of the carbon black catalyzed C-C cleavage.

The mechanism we propose can be described as follows: the condensed polyaromatic moiety of the compounds studied is adsorbed preferentially on the surface of the carbon black concurrent with the carbon surface becoming positively charged (at temperatures over 320 °C). Subsequently an electron is transferred from the condensed aromatic ring to the carbon catalyst. In the ion radical formed, the weakest bond becomes the C_{ar} - C_{aliph} adjacent to the polyaromatic system[8,9]. If the temperature is high enough for cleavage of this bond, the reaction will take place and the free radical formed from the substituent group will abstract a hydrogen atom from another molecule (for example the hydrogen donor present in excess). The naphthalene fragment resulting from cleavage has a higher oxidation potential than I (1.54 eV for naphthalene[10] vs 1.257 eV for I[11] and will not transfer an electron to the carbon black. Consequently, a free naphthalene radical will desorb and abstract a hydrogen from another molecule. This initial cleavage of the ion radical could explain why cleavage reactions are obtained only at temperatures where the surface becomes positively charged and why the cleavage is observed at temperatures much below the thermal background.

The high energy, very likely more delocalized radical ions typically formed in mass spectrometers could also exhibit very different reactivity from the radical ions formed on a surface. The extrapolation, therefore, of gas-phase ion-radical reactivity to surface reactions is tenuous at best and can be misleading when interpreting results from heterogeneous catalytic reactions.

The data presented above may be useful for understanding some of the observed differences in the chemistry of radical ions in the gas phase or solution as compared with reactions on a surface. They could also be helpful for understanding why many of the heterogeneously catalyzed reactions require higher temperature than those under homogenous catalysis conditions.

CONCLUSIONS

Our data indicate that the mechanism of selective C-C cleavage in the presence of carbon black involves in the first step an electron transfer from a condensed aromatic ring to the carbon black surface when this surface become positively charged (i.e. at temperatures higher than 320^0 C). The result is a very different reactivity and selectivity of the ion-radicals toward C-C bond cleavage than that taking place in solution or in a mass spectrometer.

ACKNOWLEDGEMENTS

The contribution of Dr. R.R. Anderson, Dr. P.B. Kaufman and of E.P. Ladner, to the study of the deuterium isotopic effect is gratefully acknowledged. A full manuscript with their participation is in preparation. Helpful discussions and exchange of experimental information with Dr. J.H. Penn are acknowledged. This research was supported in part by an appointment (SCP) to the U.S. Department of Energy Fossil Energy Postgraduate Research Training Program administered by Oak Ridge Institute for Science and Education.

Present address for S.C. Petrosius: Mines Safety Appliances Co. P.O. Box 439, Pittsburgh, PA 15230.

REFERENCES

1. Farcasiu, M.; Smith, C.M. *Prepr. Pap.- Am. Chem. Soc. Div. Fuel Chem.* **1990**, *35*, 404.
2. Farcasiu, M.; Smith, C.M. *Energy & Fuels*, **1991**, *5*, 83.
3. Farcasiu, M.; Smith, C.M.; Hunter, E.A. 1991 Conference on Coal Science Proceedings, ed. IEA Coal Research Ltd., Butterworth, Heinemann Ltd., **1991**, p.166.
4. Farcasiu, M.; Smith, C.M.; Ladner, E.P.; Sylwester A.P. *Prepr. Pap.- Am. Chem. Soc. Div. Fuel Chem.* **1991**, *36*, 1869.
5. Farcasiu,M.; Petrosius, S.C.: Ladner, E.P. *J. Catal.* **1994**,*146*, 313.
6. Penn, J.H.; Wang, J *Energy & Fuels*, **1994**, *8*, 421 and the references therein.
7. (a) Mc.Millen, D.F.; Malhotra, R.; Chang, S.J.; Ogler, S.; Nigenda, S.E.;Fleming, R.H. *Fuel* **1987**,*66*, 1611. (b) Malhotra, R.; McMillen D.F. 1991 Conference on Coal Science Proceedings, ed. IEA Coal Research Butterworth, Heinemann Ltd., **1991**, p.174.
8. Ades, H.F., Companion A.L., Subbaswamy K.R. *J. Phys. Chem. Soc.*, **1991**, *95*, 2226.
9. Ades, H.F., Companion A.L., Subbaswamy K.R. *J. Phys. Chem. Soc.*, **1991**, *95*, 6502.
10. Pysh, E.S.; Yang, E.C. *J.Am. Chem. Soc.*, **1963**, *85*, 2124.
11. Alnajjar, M., Franz, J., personal communication.

These pages intentionally left blank.

The Effect of Promoter Metals on the Catalytic Activity of Sulfated Hematite for Model Compound Reactions

G. T. Hager, R. Ochoa, E. N. Givens, P. C. Eklund, F. J. Derbyshire
Center for Applied Energy Research
University of Kentucky
3572 Iron Works Pike
Lexington, KY 40511-8433

Abstract

Iron based catalysts have long been known to enhance the conversion in a direct coal liquefaction process. Attempts to increase the moderate activity of these catalysts have focussed on reducing particle size, enhancing and maintaining dispersion, and modifying the structure by addition of promoters. The use of sulfated hematite has been shown to yield enhanced conversion for the liquefaction of a subbituminous coal as compared to hematite. Further, the use of promoter metals such as molybdenum and tungsten on the sulfated hematite was shown to further improve the activity of these particles. More recently it has been shown that the addition of combinations of promoters, such as nickel and molybdenum, may increase the activity of the particles at lower promoter loading. The role of the promoter metals on sulfated hematite will be compared to other unsupported catalysts using model compound reactions.

Introduction

The utility of iron based dispersed catalysts in direct coal liquefaction has been well established since the early 1900's, particularly for the liquefaction of low rank coals. Since that time considerable effort has been directed at improving the activity of these catalysts. This effort has focussed on reducing the particle size, enhancing and maintaining the dispersion, and modifying the structure by addition of promoters. Reducing the particle size will increase the surface area to volume ratio and result in higher activity at similar weight loadings. Further, sufficiently small particles may have properties different from those of the bulk, particularly with regard to surface energetics.

The use of oil soluble organometallic precursors offer the highest possible initial dispersion. However, one study found that these precursors tend to agglomerate and form larger particles at a faster rate than a particulate precursor.[1] This agglomeration quickly reduces the high dispersion and associated surface area for the oil soluble precursors. This would seem to indicate that particulate catalysts can maintain high dispersion for longer times and may therefore have higher activities than the organometallic precursors.

Efforts to improve the activity of iron oxide particulate catalysts by reducing the particle size may have reached a limit in the form of Nanocat produced by Mach I. These particles are reported to have an average diameter of 30 Å. The small size of the particles makes identification of the phase difficult by traditional techniques. The Nanocat particles have been identified as α-Fe_2O_3, γ-Fe_2O_3, and FeOOH by the manufacturer and various researchers, respectively.[2] [3] These particles have shown improved activity for the liquefaction of a low rank coal.[4]

Several studies have shown the high activity of sulfated hematite for both liquefaction and coprocessing of coal with a petroleum resid.[5] [6] [7] The use of molybdenum or tungsten as a promoter metal further improved the activity of these particles.[8] [9] The use of nickel, cobalt, tungsten, and molybdenum have been examined as promoter metals, both individually and in combination.[10] Molybdenum showed the largest increase in activity when used as a promoter on the sulfated hematite. While the activity of tungsten and cobalt, when used in combination with molybdenum, appeared nearly additive, the combination of nickel and molybdenum exhibited a synergistic effect, resulting in higher conversions and lower promoter loading.

Unsupported molybdenum carbides and nitrides have been prepared and tested for their activity using model compound reactions.[11] [12] The results indicate the significant activity of these particles for hydrodesulfurization (HDS) and hydrodenitrogenation (HDN). The molybdenum carbide was found to be resistant to bulk sulfidation during the reaction, although it was reported that a surface layer of MoS_2 may have been formed. The sulfided Mo_2N was reported to have higher activity for HDS than either MoS_2 or molybdate indicating that the surface was not MoS_2, although the exact surface composition was not determined.

The role of catalysts in coal liquefaction is obscured by the complexity of the coal molecule itself. The exact nature of the structure of coal has been the object of considerable study. While the structure is not known, it is generally accepted that coal is composed of highly aromatic clusters connected by crosslinking bonds. These crosslinks may consist of aliphatic (methyl or ethyl) bridges or heteroatom (O,S,N) bridges. The role of catalyst in selective cleavage of these bonds may be elucidated by the use of model compound reactions. The activity for cleavage of the sulfur bridges may be studied by the HDS of benzothiophene. Similarly, the activity for cleavage of the etheric bond may be inferred from the HDO of diphenyl ether and the activity for nitrogen removal by the HDN of quinoline.

Experimental

The reactions were carried out using 25 ml stainless steel microautoclave reactors. The reactors were loaded with a 5 wt% solution of reactant in hexadecane. The catalysts were loaded at 5 wt% on reactant basis and 0.017 g dimethyldisulfide (DMDS) was added in most runs. Experiments were carried out using DMDS alone in order to determine its influence on activity and selectivity. The reactors were purged and pressurized to 800 psig (cold) with hydrogen. The loaded reactors were placed in a heated fluidized sand bath at 385°C and agitated vertically at 400 cycles/minute to minimized any mass transfer constraints. The reactions were carried out for times of 15 to 60 minutes after which the reactor was quenched in a cool sand bath.

The reaction products were removed from the reactor by washing with THF. A gas chromatograph (Hewlett Packard 5890 Series 2) using both a 30 m DB-5 and a 30m carbowax column was utilized to analyze the products of the reaction. The activity was determined by the rate of model compound disappearance.

The spent catalyst was collected and stored with the product to reduce oxidation from exposure to air. The major phase of the particles was determined by XRD and the average particle diameter was estimated from the peak broadening using the Debye-Scherrer relationship. This allowed the comparison of catalyst conversion to reaction conversion.

Catalyst Synthesis and Characterization

The iron based catalysts used in this study were prepared using an aqueous precipitation technique. This method involves the coprecipitation of iron and a promoter metal in the presence of sulfate ions. In this study, urea was used to effect the precipitation of ferric ammonium sulfate (iron alum), following the method of Kotanigawa et al.[5] The promoter metal molybdenum was incorporated by addition of ammonium molybdate to the iron alum solution, as described previously.[10] Ammonium nickel sulfate hydrate and cobalt sulfate hydrate were used to add nickel and cobalt, respectively. The precipitated catalysts were filtered and dried in an air flow oven overnight and then calcined in air at 475 °C for 30 minutes.

The promoted sulfated hematite catalysts were analyzed by XRD, XPS, TEM, SEM, and nitrogen BET adsorption. The results of the electron microscopy have shown that the catalysts consist of a loose agglomeration of particles with an acicular shape with average dimensions of ~10x50 nm, shown in Figure 1. Surface areas were measured by the nitrogen BET adsorption and were found to be in the range of 100-200 m^2/g. The addition of up to 10 wt% of molybdenum had little effect on the particle size and no apparent effect on the major phase identified by XRD, shown in Figure 2. The XRD spectra of the as-formed catalyst indicate the major phase is α-FeOOH in addition to a trace of α-Fe also present. After calcination the major phase was α-Fe_2O_3 with α-Fe still present. The relative amount of α-Fe does not appear to be affected by the calcination.

Elemental analysis of the sulfated hematites indicated sulfur contents of 2-6 wt%. It has been reported that the sulfur is present on the surface of the hematite as chemisorbed SO_3. XPS confirmed this showing that the surface sulfur concentration was significantly higher than the bulk concentration. It was found that the sulfur content decreased with increasing molybdenum concentration. This may indicate that molybdenum is chemisorbed as MoO_3 displacing the sulfur on the surface. The XPS studies confirm this, showing that the surface concentrations of molybdenum, sulfur, and tungsten are substantially higher than the bulk concentrations. Nickel and cobalt, on the other hand, have similar bulk and surface concentrations indicating that they are substituted into the iron oxide matrix. It follows from Goldschmidt's rules of substitution that the hexavalent ions, Mo, W, and S cannot substitute for iron while the nickel and cobalt can substitute.[13]

The molybdenum nitride (Mo_2N), molybdenum carbide (Mo_2C), and molybdenum sulfide (MoS_2) catalysts were produced by a laser pyrolysis technique. This method utilizes the intersection of a tunable CO_2 laser with a gas stream to create a small (~1mm^3) pyrolysis zone. The flow rate of the gases determines the residence time in the reaction zone and, consequently, the particle size and phase. This method has been shown to produce monophasic particles with a narrow size distribution. The particles have an average diameter of ~5 nm and a surface area of 65 m^2/g.

Results

The use of the unsulfided molybdenum promoted sulfated hematite showed little impact on the hydrogenation of naphthalene varying only slightly from the thermal conversion of 7% at 60 minutes. The addition of sulfur alone impacted more favorably on the reaction increasing the conversion at 60 minutes to 19%. The synergism between the sulfur and the promoted sulfated hematites is clear in the experiments using added sulfur with the catalyst. In these runs the conversion increased to 82% at 60 minutes. This corresponds well with other work which has shown that the activity of iron based catalysts is dependent on the partial pressure of H_2S present.[14]

The unsulfided molybdenum nitride, with a conversion of 59% at 60 minutes, showed higher activity for naphthalene hydrogenation than the unsulfided molybdenum promoted sulfated hematite. The addition of sulfur to the molybdenum nitride had only a minor effect on conversion. However, the use of a molybdenum sulfide resulted in a significant increase in conversion to 46% at 30 minutes compared to 29% for the sulfided molybdenum nitride. This indicates that the nitride is stable at these conditions and resists surface sulfidation, agreeing well with previous findings.[12]

The activity of the promoted sulfated hematite for the HDO of diphenyl ether followed a similar trend. The unsulfided molybdenum promoted sulfated hematite showed a slight increase in conversion to 26% at 60 minutes, compared to 21% for the thermal run. The addition of sulfur alone caused a significant decrease in conversion at 60 minutes to 12%. The combination of sulfur and molybdenum promoted sulfated hematite resulted in an increase in conversion to 39% at 60 minutes again due to the attainment of the active phase.

The molybdenum nitride showed a higher activity for HDO than molybdenum promoted sulfated hematite both with and without sulfur. The conversion at 60 minutes was 53%, significantly higher than the 39% achieved with the promoted hematite with sulfur. The addition of sulfur to the molybdenum nitride resulted in a substantial loss of activity yielding a conversion of only 20% at 60 minutes. This indicates that the addition of sulfur severely inhibits the catalytic activity of the molybdenum nitride.

Conclusions

The activity of promoted sulfated hematite has been compared to the activity of other unsupported catalysts using model compound reactions. Preliminary results indicate that the molybdenum promoted sulfated hematite shows significantly higher activity for the hydrogenation of naphthalene to tetralin when sufficient sulfur is added to the reaction. In the absence of added sulfur the activity of the promoted sulfated hematite was negligible.

The molybdenum nitride exhibits the highest activity for HDO of diphenyl ether. The addition of sulfur increased the activity of the promoted sulfated hematite but severely inhibited the activity of the molybdenum nitride.

In both reactions the catalyst loading was 1 wt% on reactant solution. Since the cost of the promoted sulfated hematite is substantially lower that the molybdenum nitride, due to a lower molybdenum content, the results of this study indicate that significant improvements in process economics may be achieved through the use of these catalysts.

Acknowledgements

The authors would like to gratefully acknowledge support for this project recieved from the United States Department of Energy under contracts DE-AC22-91PC91040 and DE-FC22-93PC93053.

References

1. Djega-Mariadassou, G., *et al. Fuel Processing Technology* **12**, 143-153 (1986).
2. Srinivasan, R., Keogh, R.A. & Davis, B.H. *ASC-Division of Fuel Chemistry Preprints* **38**, 203-210 (1993).
3. Zhou, J., Feng, Z., Huggins, F.E., Shah, N. & Huffman, G.P. *ACS-Division of Fuel Chemistry Preprints* **38**, 196-202 (1993).
4. Anderson, R., Givens, E.N. & Derbyshire, F. *ACS-Division of Fuel Chemistry Preprints* **38**, 495-502 (1993).
5. Kotanigawa, T., Yokoyama, S., Yamamoto, M. & Maekawa, Y. *Fuel* **68**, 618-621 (1989).
6. Pradhan, V.R., Tierney, J.W., Wender, I. & Huffman, G.P. *Energy & Fuels* **5**, 497-507 (1991).
7. Pradhan, V., Tiemey, J.W. & Wender, I. *ACS Preprint - Fuel* **36**, 597-604 (1991).
8. Pradhan, V.R., Herrick, D.E., Tiemey, J.W. & Wender, I. *Energy & Fuels* **5**, 712-720 (1991).
9. Pradhan, V.R., Hu, J., Tierney, J.W. & Wender, I. *Energy & Fuels* **7**, 446-454 (1993).
10. Hager, G.T., Givens, E.N. & Derbyshire, F.J. *ACS-Division of Fuel Chemistry Preprints* **38**, 1087-1092 (1993).
11. Schlatter, J.C., Oyama, S.T., Metcalfe, J.E., III & Lambert, J.M., Jr. *Ind. Eng. Chem. Res.* **27**, 1648-1653 (1988).
12. Markel, E.J. & Zee, J.W.V. *Journal of Catalysis* **126**, 643-657 (1990).
13. Faure, G. *Principles and Applications of Inorganic Geochemistry* 1-626 (Macmillan Publishing Company, New York, 1991).
14. Sweeny, P.G., Stenberg, V.I., Hei, R.D. & Montano, P.A. *Fuel* **66**, 532-541 (1987).

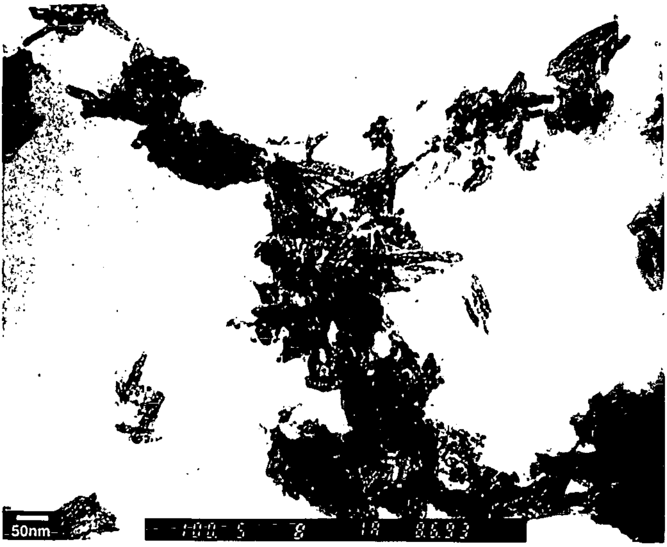

Figure 1. TEM micrograph of molybdenum promoted sulfated hematite

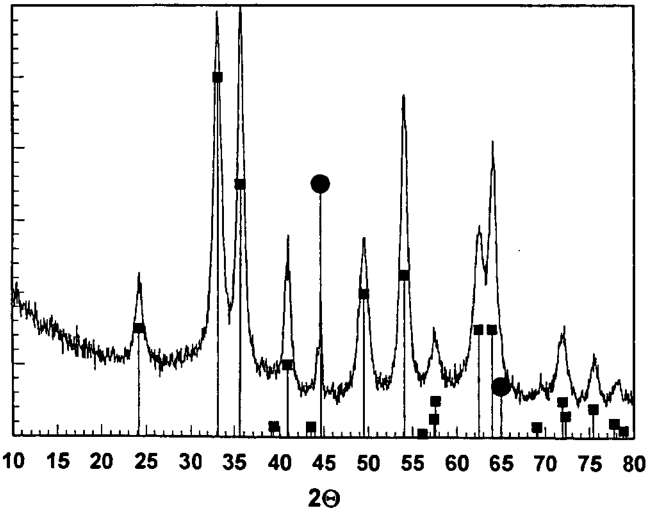

Figure2. XRD spectrum of molybdenum promoted sulfated hematite indicating peaks identified as hematite and α–Fe

MODEL HYDROCRACKING REACTIONS OVER MONOMETALLIC AND BIMETALLIC DISPERSED CATALYSTS.

Eckhardt Schmidt and Chunshan Song*

Fuel Science Program, Department of Materials Science and Engineering, 209 Academic Projects Building, The Pennsylvania State University, University Park, PA 16802

Coal liquefaction involves cleavage of methylene and dimethylene bridges connecting polycyclic aromatic units. The selected compound for model coal liquefaction reactions is 4-(1-naphthylmethyl)bibenzyl (NMBB). This work describes the synthesis and screening of several hetero- and homometallic complexes as precursors of dispersed catalysts for hydrocracking of NMBB. Experiments were carried out at 400 °C for 30 min under 6.9 MPa H_2 pressure. $(NH_4)_2MoS_4$ and $MoCl_3$ converted NMBB predominately into naphthalene and 4-methylbibenzyl. Small amounts of secondary products were formed by hydrogenation and fragmentation of the primary products. Lewis acid-type $MoCl_3$ catalyst gave lower selectivity to the primary products, with relatively larger amounts of methyltetrahydronaphthalene- and methylnaphthalene-derivatives. In contrast, the organometallic catalyst precursors $Cp_2Co_2Mo_2(CO)_2S_4$, $Cp_4Fe_4S_4$ and $(Ph_4P)_2(Ni(MoS_4))$ inflict less fragmentation and less hydrogenation of primary cleavage products. $Cp_2Co_2Mo_2(CO)_2S_4$ converted a substantial amount of starting material even at 350 °C; whereas, a noncatalytic run under the same conditions showed only small conversion. Greater product selectivity can be achieved by means of organometallic precursur and low severity reaction conditions. Inorganic and bimetallic catalyst precursors gave similar conversions. The synergistic effect of heterometallic over homometallic catalyst precursors was demonstrated by Co-Mo and Ni-Mo, which gave far higher conversion than the thiocubane-type catalyst containing four iron atoms. The addition of sulfur to $Mo(CO)_6$ and $Co_2(CO)_8/Mo(CO)_6$ gave higher conversion but reduced the yield of hydrogenation products.

Keywords: Model reactions, hydrocracking, dispersed catalysts, monometallic and bimetallic catalysts.

Introduction

First attempts to liquefy coal were carried out in the beginning of the 20th century by Bergius (1). The process is intricit and involves hundreds of different coal components with various functional groups in interconnected aromatic systems. The complexity of coal liquefaction reactions makes it very difficult to study the reaction mechanisms. Therefore, it is extremely difficult to find optimum reaction conditions for selective bond cleavage. Furthermore, coals from different sources may react differently with different catalysts. We selected therefore the model compound 4-(1-naphthylmethyl)bibenzyl (NMBB), which consists of functionalities that are related to coal structures (2-6). Among these are alkyl groups which interconnect aromatic moieties and different ring systems. Of particular interest to our group was the fact that its reaction can give us information about the features of different catalysts. In a typical hydroliquefaction reaction, coal reacts at temperatures above 400 °C with 7 MPa H_2 pressure for a period of ca. 30 min to primary liquefaction products. Efficient conversion can only be achieved by transition metal containing catalysts and metal concentrations of 1 wt % or lower. Suitable catalytic systems contain Co, Ni, Mo or its combinations, either as inorganic complexes, or organometallic species. Good solubility of catalyst precursors generally leads to better catalyst dispersion and greater effectiveness for liquefaction reactions (7,8). One way to achieve better dispersion is the use of soluble organometallic precursors which produce in situ finely dispersed active catalyst particles at elevated tempertures. Greater catalyst surface area increases the yield of products dramatically, due to greater hydrogen acitivation by augmented reactive catalyst sites. Hirschon and Wilson (9,10) demonstrated that highly dispersed catalysts from organometallic precursors can be effective for hydrogenating the coal with molecular hydrogen without relying upon a donor solvent .

This paper reports our work on hydrocracking experiments of NMBB over different transition metal catalyst precursors. .The effects of inorganic and organometallic (monometallic and bimetallic) catalyst precursors on conversion and product selectivity will be discussed. Also, the influence of the reaction temperature on the product distribution will be investigated.

Experimental Section

Preparation of Catalyst Precursors. The complexes $(Ph_4P)_2(Ni(MoS_4))$ (11) (Ni-Mo) and $Cp_4Fe_4S_4$ (12) (Fe4) were prepared according to the methods described in the literature, based on the procedures of Brunner and Wachter (11) and Schunn, Fritchie and Prewitt (12). The thiocubane cluster $Cp_2Co_2Mo_2(CO)_2S_4$ (CoMo-TC2) was synthesized earlier (13) in our laboratory. Samples were stored at - 25 °C prior to use. All recrystallizations of the homo- and heterometallic cluster compounds were carried out quickly. The crystalline products are stable on exposure to air but decompose slowely in solution. Sulfur and $(NH_4)_2MoS_4$ (ATTM) were purchased from Aldrich, $Mo(CO)_6$, $Co_2(CO)_8$ from Alfa and the model compound MNBB from TCI America. GC-MS confirmed sufficient purity of NMBB (> 99 %) and it was used without further purification.

Model compound reactions. A stainless steel reactor (tubing bomb) with a capacity of 33 ml was loaded with ca. 0.25 g NMBB, 2.11 wt % catalyst precursor and 0.125 g solvent (tridecane). The reactor was purged three times with H_2 and then pressurized with 6.9 MPa H_2 at room temperature for all experiments. A preheated fluidized sand bath was used as heating source and the reactor agitated via an oscillator by vertical shaking of the horizontal micro reactor (about 240 strokes/min.) After the reaction the hot tubing bomb was quenched in cold water and the gaseous products collected in a gas bag for further analysis. The liquid contents were washed with 15 ml CH_2Cl_2 through a low speed filter paper and stored in small glass bottles for qualitative and quantitative GC analysis. All runs were carried out at least twice to confirm reproducibility.

The compounds were identified by capillary gas chromatography-mass spectrometry (GC-MS) using a Hewlett-Packard 5890 II GC coupled with a HP 5971A mass-selective detector operating at electron impact mode (EI, 70 eV). The column used for GC-MS was a J&W DB-17 column; 30-m X 0.25-mm, coated with 100 % phenylmethylpolysiloxane with a coating film thickness of 0.25 μm. For quantification a HP 5890 II capillary GC with a flame ionization detector and the same type of column (DB-17) was used. Both Hewlett-Packard GC and GC-MS were programmed from 40 to 280 °C at a heating rate of 4 °C/min and a final time of 30 min. The response factors of 10 pure compounds were determined. More experimental and analytical details may be found elsewhere (14-17).

Results and Discussion

Hydrocracking of NMBB. Tables 1 and 2 show the results of hydrocracking of the model compound NMBB over different catalyst precursors. In the absence of a catalyst, the conversion at 300 °C is only 1 % and increases to about 4 % at 400 °C. The inorganic catalyst precursor ATTM increased the conversion at 350 °C relative to the thermal run by 54 %. A run at 400 °C shows the effect of elevating reaction temperatures. The conversion increased by additional 30 %. Molybdenum trichloride proved to be less effective and gave about 70 % conversion.

Of the catalysts tested, $(Ph_4P)_2(Ni(MoS_4))$ and $Co_2(CO)_8$+S showed the highest conversion (95 %). Ni-Mo consists of a chain like structure with tetrahedral enviroment around nickel and molybdenum (Scheme 1).

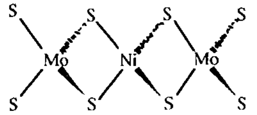

Scheme1: Structure of the bimetallic sulfide $[Ph_4P]_2[Ni(MoS_4)_2]$

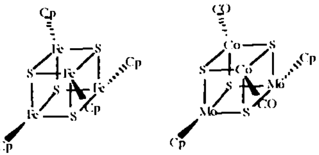

$Cp_4Fe_4S_4$ $Cp_2Co_2Mo_2(CO)_2S_4$

Scheme 2: Structure of the thiocubane-type catalyst precursors $Cp_4Fe_4S_4$, and $Cp_2Co_2Mo_2(CO)_2S_4$.

From the data in Tables 1 and 2 Ni-Mo is apparentely the best precursor and $Cp_4Fe_4S_4$ is the worst among the catalyst precursors tested. A general observation is that the activity of the in situ generated catalysts is smaller at lower temperatures and increases at elevated temperatures. In an attempt to examine the role of bonding between transition metals, we tested the bimetallic thiocubane-type catalyst $Cp_2Co_2Mo_2(CO)_2S_4$ (Scheme 2), the homometallic cluster $Cp_4Fe_4S_4$ (Scheme 2), and different metal carbonyl combinations which may give (after thermal decomposition) similar catalyst composition as Co-Mo-TC2.

There are direct metal-metal bonds between Co-Mo, Co-Co and Mo-Mo, besides the sulfur bridges in CoMo-TC2. The question is, do in situ generated catalysts from catalyst precursors which have metal-metal bonds, show different catalytic behaviour. Table 1 shows the superior performance of catalysts containing either Mo, or Co+Mo. Using $Mo(CO)_6$ alone gave similar results as runs with the mixture of two corresponding metal compounds that can also be found in $Cp_2Co_2Mo_2(CO)_2S_4$. Among the testet metal carbonyls, $Co_2(CO)_8$ is less active compared to the thiocubane type catalyst Co-Mo-TC2 and mixed metal carbonyls. A beneficial effect could be observed, when sulfur was added to $Co_2(CO)_8$. NMBB conversion increased dramatically. Addition of sulfur to $Mo(CO)_6$ did not improve the convertibility of NMBB, but added sulfur to $Mo(CO)_6/Co_2(CO)_8$ gave 10 % higher conversion. Work on the advantage of using different metals in a single catalyst reports the synergistic effect of heterogeneous catalysis. The addition of Co or Ni to MoS_2-containing precursors increased their catalytic activity considerably. However, little work has been done on comparison of catalytic effects between mixed metal carbonyls, inorganic- and organometallic heteroatomic precursors. Previous work (18-22) reports mainly the mixture of different transition metal salts.It is known (24-27) that catalyst precursors like metal carbonyls require the addition of sulfur for sufficient activity. The beneficial effect of sulfur addition to hydrogenation reactions was studied on the system molybdenum sulfide and oxide (21). There seems (23) to be consensus that the sulfides of the transition metals are more active in catalytic hydroliquefaction than their oxides. The reason for this remains unclear. Montano and co-workers (28,29) have emphasized the importance of correct stoichiometry between molybdenum oxides and sulfur in high temperature conversion reactions in order to generate catalytically active MoS_2 particles. Temperatures as high as 350 °C are required for this activation process. The analogue transformation of $Fe(CO)_5$ into pyrrhotite ($Fe_{1-x}S$, where $0 \leq x \leq 0.125$) is difficult to perform and iron carbonyls tend to form less reactive iron carbides and oxides (25) during the activation process. This might explain the low activity of our catalyst precursor $Cp_4Fe_4S_4$. The iron catalyst from $Cp_4Fe_4S_4$.would not be active due to the difficulty of forming pyrrhotite. Another reason for the low effectiveness of the iron-cluster in hydrocracking reactions may be that iron appears to function by removing oxygen functionalities whereas Mo catalysts are good hydrogenation catalysts (9). In our previous work, it has been demosntrated that the thiocubane CoMo-TC2 is superior to the mixtures of $Mo(CO)_6$, $Co_2(CO)_8$, and sulfur for liquefaction of a subbituminous coal (13). Comparison of the results in tables 1 and 2 indicates that the thiocubane bimetallic catalysts are not superior to the corresponding mixtures of Co, Mo and sulfur. The rather expensive preparation of the bimetallic catalyst precursors leads to the conclusion that cheaper metal combinations can achieve comparable results. We focused therefore our attention to product selectivity under low severity reaction conditions to study product distribution of NMBB hydrocracking reactions under the influence of homo- and bimetallic catalyst precursors.

Product Distribution

Hydrocracking of NMBB yields three product categories that can be explained by the cleavage of the bonds between the aromatic moieties. The identified products can be classified into hydrocracking, hydrogenation and isomerization products. Those coming from hydrocracking reactions form the major pool of reaction products, followed by hydrogenation and isomerization products. Figure 1 shows the product distribution from catalyst-free reactions. The thermal reaction of NMBB at 300 °C yields only two products, 4-methylbibenzyl (4-MBB) and napththalene (N). Higher temperature (400 °C) gave enhanced conversion and twice as much products. Besides 4-MBB and N, 1-(naphthyl)-4-tolyl methane (NTM) and tetralin can be found as high temperature products. Generally, increased temperature results in lower selectivity. The ratio of major products in our model reactions over thiocubane catalysts (Figure 2) remains similar over a wide temperature range. We can see in Figure 2 more 4-MBB than BB and more naphthalene (N) than tetralin. Several studies, including the present work have shown that NMBB tends to undergo cleavage of bond a connecting the naphthyl group to the remainder of the molecule when subjected to a variety of catalysts under a variety of conditions. Farcasiu et al. suggested a reaction mechanism in which the first stage consists of the formation of a radical cation. The loss of electron density leads to a weakened a-bond which can then be broken relatively easily. This is in contrast to model studies in which phenyl-containing compounds undergo preferably b-cleavage (6).

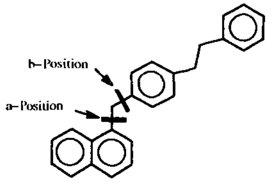

Scheme 3: Potential Cleavage sites in 4-(1-naphthylmethyl)bibenzyl.

In the work of Penn and Wang (6) radical cations were generated in the mass spectrometer under a variety of conditions which had little impact on the bond clevage pathway. Preference for b-cleavage was observed. It was explained by resonance stablization of the intermediates formed via bond b cleavage. Both intermediates are resonance stabilized. Thermochemical calculations (30) show that reaction pathway b is 30 kcal/mol lower for both neutral and radical cationic species than pathway a. In contrast, neither of the intermediates resulting from bond a cleavage is stabilized. However, in the presence of a catalyst, the major reaction pathway mainly involves the cleavage of bond a (Scheme 3). These studies indicate that a new decomposition pathway mechanism must be

developed to explain the results of bond cleavage involving model reactions on NMBB. The product distribution is different over metal carbonyls (Figure 3). The main reaction product is 4-MBB, but the ratio of tetralin/naphthalene depends on the addition of sulfur. Sulfur-free metal carbonyl precursors are relatively better hydrogenating catalysts than sulfur containing metal carbonyls and their combinations. This becomes more apparent in the case of Co+Mo and Co+Mo+S. Sulfur enhances the formation of naphthalene and surpresses the generation of tetralin. In order to get more information about the influence of sulfur on hydrogenation reaction, we carried out experiments with tetralin in tridecane as solvent, with and without added sulfur. A sulfur-free run showed only a negligible amount of naphthalene (naphthalene/tetralin ration ≈ 0), but the addition of sulfur lead to a substantially higher naphthalene-to-tetralin ratio (0.08).
Products found in hydrocracking of NMBB over the inorganic catalyst precursor (Figure 4) at 400 °C are similar to those found in runs with organometallic precursors. Unlike all other catalysts, the lewis-acid-type complex $MoCl_3$ gave a different product distribution. $MoCl_3$ is the only catalyst that cleaved both bond a and b in NMBB with about equal probability. The aggressiveness of $MoCl_3$ as catalyst precursor is also demonstrated by a relatively larger percentage of isomerization products. The general observation is that low serverity reaction conditions benefit higher selectivity. At 350 °C ATTM gives a considerable amount of hydrogenation and isomerization products, whereas the organometallic complex CoMo-TC2 yields only products, coming from hydrocracking and hydrogenation reactions. The latter category of compounds can not be found in a reaction involving $Cp_2Co_2Mo_2(CO)_2S_4$ at 300 °C. Higher product selectivity can also be found in experiments with Fe4. This relatively inreactive precursor yields at 400 °C mainly hydrocracking products.

Acknowledgment. This project was supported by the U.S. Department of Energy, Pittsburgh Energy Technology Center under contract DE-AC22-92PC92122. We are grateful to Professor Harold Schobert for his encouragement and to Dr. Udaya Rao of PETC for his support. We also thank Mr. R. Copenhaver for the fabrication of micro-tubing bomb reactors.

References cited

1. Stranges, A. N. *Fuel Proc. Technol.*, **1987**, **16**, 205-225 .
2. Farcasiu, M.; Smith, C. *Prepr. Pap. - Am. Chem. Soc., Div. Fuel Chem.* , **1990**, **35**, 404-13.
3. Farcasiu, M.; Smith, C. *Fuel Processing Technology* , **1991**, **29**, 199-208.
4. Farciasiu, M.; Smith, C. and Ladner, E. P. *Prepr. Pap. - Am. Chem. Soc., Div. Fuel Chem.*, **1991**, **36**, 1869-77 .
5. Tang, Y.; Curtis, C. W. *Energy Fuels*, **1994**, **8**, 63-70.
6. Penn, J. H.; Wang, J.-H. *Energy Fuels*, **1994**, **8**, 421-425 .
7. Weller, S.; Pelipetz, M. G. *Ind. Eng. Chem.*, **1951**,**43**, 1243.
8. Weller, S. W. *Coal Liquefaction with Molybdenum Catalysts. In Chemistry and Uses of Molybdenum; Climax Molybdenum Co.*, **1982**, 179-186.
9. Hirschon, A. S.; Wilson Jr, R. B. *Coal Science II* , ***ACS Sym. Ser.***, **1991**, 273-83.
10. Hirschon, A. S.; Wilson Jr, R. B. *Fuel*, **1992**, **71**, 1025-31.
11. Mueller, A.; Ahlborn, E.; Heinsen, H.-H. *Z. anorg. allg. Chem.*, **1991**, **386**, 102-106.
12. Schunn, R. A.; Fritchie, C. J.; Prewitt, C. T. *Inorganic Chemistry*, **1966**, 892-899.
13. Song, C.; Parfitt, D. S.; Schobert, H. H. *Energy Fuels*, **1994**, **4**, 313-219.
14. Song, C.; Hanaoka, K.; Nomura, M.: *Energy Fuels*, **1988**, **2**, 639.
15. Song, C.; Schobert, H. H. *Prep. Pap.- Am. Chem. Soc., Div. Fuel Chem.*, **1992**, **37**, 976.
16. Song, C.; Lai, W.-C.; Schobert, H. H. *Ind. Eng. Chem. Res.*, **1994**, **33**, 534-547.
17. Song, C.; Saini, A. K.; Schobert, H. H. *Proc. 1993 Int. Conf. Coal Sci., Banff, Canada, Sept. 12-17, 1993*, **1993**, **1**, 291.
18. Nomura, M.; Miyake, M.; Sakashita, H.; Kikkawa, S. *Fuel* , **1982**, **61**, 18-20.
19. Garg, D.; Givens, E. N. *Fuel Process. Technol.*, **1984**, **8**, 123-143.
20. Song, C.; Nomura, M.; Miyake, M. *Fuel*, **1986**, **65**, 922-926.
21. Song, C.; Nomura, M.; Ono, T. *Prepr. Pap. - Am. Chem. Soc., Div. Fuel Chem.*,**1991**, **36**, 586-596.
22. Sommerfeld, D. A.; Jaturapitpornsakul, J.; Anderson, L.; Eyring, E. M. *Prepr. Pap. - Am. Chem. Soc., Div. Fuel Chem.*, **1992**, **37**, 749-755.
23. Weller, S. *Energy Fuels*, **1994**, **8**, 415-420.
24. Yamada, O.; Suzuki, T.; Then, J.; Ando, T.; Watanabe, Y. *Fuel Process. Technol.*, **1985**, **11**, 297-311.
25. Herrick, D.; Tierney, J.; Wender, I.; Huffamn, G. P.; Huggins, F. E. *Energy and Fuels* , **1990**, **4**, 231.
26. Suzuki, T.; Ando, T. ; Watanabe, Y. *Energy Fuels* , **1987**, **1**, 299-300.
27. Artok, L.; Davis, A.; Mitchell, G. D.; Schobert, H. H. and Schobert, H. H. *Energy Fuels* , **1993**, **7**, 67-77.
28. Montano, P.; Bommannavar, A. J. *J. Mol. Catal.*, **1983**, **20**, 393.
29. Montano, P. *ACS Fuel Prepr.*, **1986**, **31**, 226.
30. Ades, H. F.; Companion, A. L.; Subbaswamy, K. R. *Prepr. Pap. - Am. Chem. Soc., Div. Fuel Chem.*,**1991**, **36**, 420-4.

Table 1. Hydrocracking of NMBB over dispersed metal carbonyls and mixed metal carbonyl with and without added sulfur at 400 °C

Reaction temperature (°C)	300	400	400	400	400	400	400	400
Catalyst Precursor	None	None	$Mo(CO)_6$	$Mo(CO)_6$+ S	$Mo(CO)_6$+ $Co_2(CO)_8$	$Mo(CO)_6$+ $Co_2(CO)_8$ +S	$Co_2(CO)_8$	$Co_2(CO)_8$ +S
Products [wt %]								
Cyclohexane							1.1	2.1
Bezene		0.6	0.2	0.7	0.7	0.7		
Toluene		0.3	1.4	0.5	0.4	0.1	0.7	0.8
p-Xylene			0.7	0.2	0.1		0.3	
Tetralin		0.2	17.3	15.1	21.0	11.7	6.8	5.3
Naphthalene	0.4	0.6	13.8	15.3	5.1	19.2	5.4	28.0
2-MTHN			0.8	0.9	0.6	0.8		0.2
1-MTHN			1.8	1.2	2.4	0.9	1.0	0.5
2-MN			0.5	0.4	0.4	0.5		1.2
1-MN			1.7	1.6	0.5	2.0	0.4	3.0
Bibenzyl			7.7	10.5	6.3	10.3	1.0	9.9
2-MBB			0.4					
4-MBB	0.6	1.3	39.8	38.6	38.3	40.7	14.0	44.8
1-NB							0.4	
NTM		0.9						
THNMBB							6.6	
Other-THNMBB							7.9	
Conversion [wt %]	1.0	3.9	86.1	85	75.8	86.9	45.6	95.8

[a] Reactor residence time in preheated sand bath 30 min. [b] wt % based on the initial weight of NMBB feed.

Table 2: Effect of inorganic and thiocubane-type precursors on hydrocracking reactions[a] of NMBB at 300-400 °C

Reaction temperature (°C)	350[a]	400[a]	400[a]	400[a]	400[a]	300[a]	350[a]	400[a]	400[b]
Catalyst Precursor	ATTM	ATTM	$MoCl_3$	Ni-Mo	Fe4	Co-Mo	Co-Mo	Co-Mo	Co-Mo
Products [wt %]									
Benzene		0.7	0.6	4.9	0.6			0.5	0.6
Toluene		0.1	1.3	1.0				0.6	0.9
p-Xylene			0.3	0.5			0.3		0.4
Tetralin	6.5	14.2	4.5	8.5		0.5	1.6	6.7	9.4
Naphthalene	14.3	16.9	20.9	23.6	4.3	4.0	11.0	24.4	23.2
2-MTHN	0.2			0.4					
1-MTHN	0.8	1.2	0.4	0.8			0.1	0.5	0.6
2-MN	0.1			0.7					
1-MN	1.5	1.7	2.7	2.7			0.6	2.0	2.2
Bibenzyl	3.4	6.3	19.2	6.9	0.3	0.5	1.7	4.7	6.0
2-MBB			3.7	0.2					
4-MBB	28.9	45.1	16.4	44.5	6.5	6.8	18.2	40.9	44.5
Conversion [wt %]	55.7	86.2	70.0	94.7	11.7	11.8	33.5	80.3	87.8

[a] Reactor residence time in preheated sand bath: 30 min. [b] 60 min.

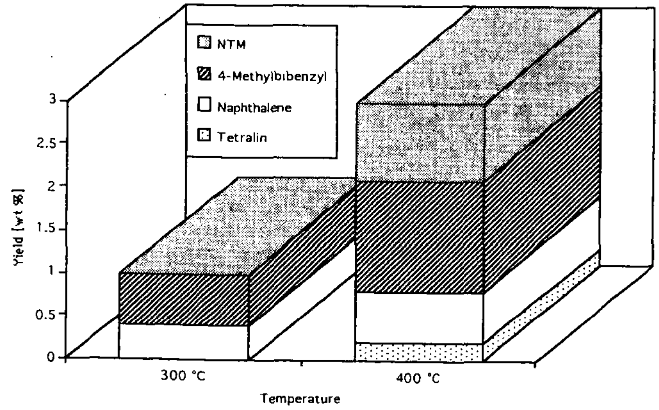

Figure 1: Yields of products excluding gases for non-catalytic thermal hydrocracking of NMBB at 300-400 °C.

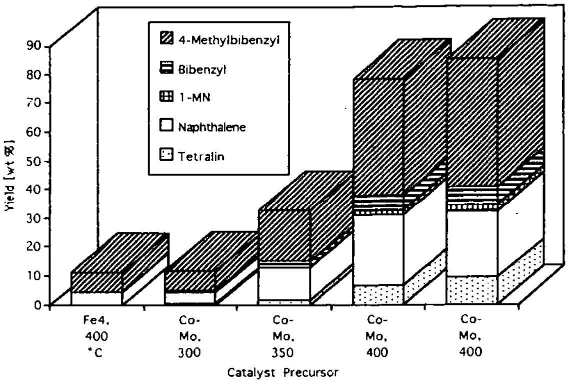

Figure 2: Catalytic activity of thiocubane-type catalysts in the temperature range of 300-400 °C for 30-60 min.

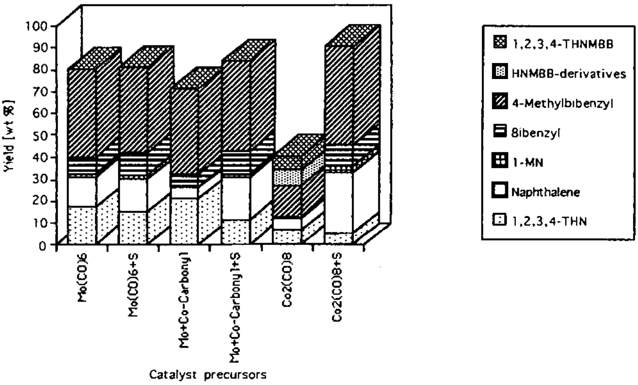

Figure 3. Catalytic activity of mixed metal carbonyls and the mixture plus added sulfur on hydrocracking of NMBB.

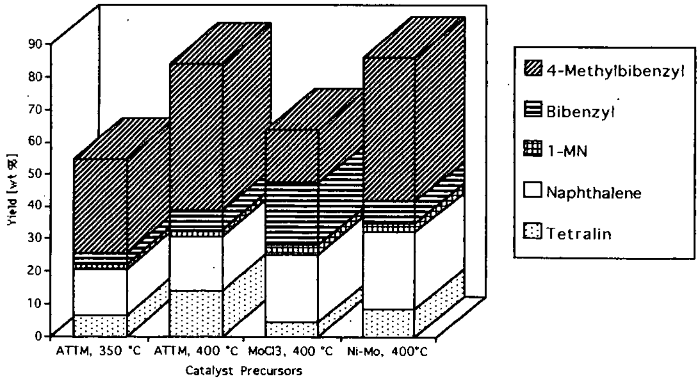

Figure 4: Effect of temperature on hydrocracking of NMBB using inorganic catalyst precursors at 350-400 °C for 30 min.

MICROBIAL DESULFURIZATION MECHANISMS

Edwin S. Olson, Daniel C. Stanley, Ramesh K. Sharma, and John R. Gallagher
Energy & Environmental Research Center
University of North Dakota
Grand Forks, ND 58202

Key Words: Bacterial desulfurization, sulfur-specific degradation

ABSTRACT

Sulfur-specific desulfurization with *Rhodococcus rhodochrous* IGTS8 and related microorganisms may be a useful technology for upgrading high-sulfur carbonaceous materials to more environmentally acceptable fuels. Model compound studies with the organism showed that dibenzothiophene was converted to 2-hydroxybiphenyl or 2,2-dihydroxybiphenyl, depending on whether growth or nongrowth conditions were used in the desulfurization experiments. The pathways that lead to the two key intermediates in the degradation (2'-hydroxybiphenyl-2-sulfinic acid and 2'-hydroxybiphenyl-2-sulfonic acid) and the subsequent conversion of these intermediates to the phenol products required further understanding. The synthesis of an ^{18}O-enriched sulfone substrate has been accomplished, and experiments were performed to elucidate the mechanism of the conversion to the sultine intermediate.

INTRODUCTION

Microbial systems that desulfurize organosulfur compounds have potential use in removing sulfur from fossil fuels. Some organisms utilize a catabolic pathway that results in excision of the sulfur without converting organic carbon to carbon dioxide. Dibenzothiophene (DBT) has been useful as a model compound to investigate the sulfur-specific behavior in bacterial systems. Intermediates corresponding to this thiophenic-ring scission (4S) pathway have been isolated and characterized (1).

The desulfurization of DBT by *Rhodococcus rhodochrous* IGTS8 was recently demonstrated to proceed via two pathways that result in formation of either 2-hydroxybiphenyl or of 2,2'-dihydroxybiphenyl, depending on whether growth or nongrowth conditions are used in the desulfurization experiments (2). Under nongrowth conditions, the DBT was converted to 2'-hydroxybiphenyl via the 2'-hydroxybiphenyl-2-sulfinate (analyzed as the cyclic sultine ester form). Under growth conditions, very little of the 2'-hydroxybiphenyl-2-sulfinate was converted to 2-hydroxybiphenyl; instead, most was oxidized to 2'-hydroxybiphenyl-2-sulfonate (analyzed as the sultone form), and 2,2'-dihydroxybiphenyl was the major product. The oxidation of the sulfinate to the sulfonate occurs spontaneously (nonenzymatically) in aqueous buffer exposed to air, but the sulfinate may also be oxidized in an enzyme-catalyzed reaction. These pathways are summarized in Figure 1. Further understanding of the details of the pathways and mechanisms of the various steps in the pathways is needed.

The initial reaction in the 4S pathway is the oxidation of DBT to the sulfoxide (DBT-5-oxide) (Reaction A). Further oxidation to the sulfone (DBT-5,5-dioxide) also occurs. What is not known is whether the sulfoxide (Reaction B) or the sulfone (Reaction G) is the immediate precursor for the 2'-hydroxybiphenyl-2-sulfinate under nongrowth conditions and whether the sulfone can be converted directly to 2'-hydroxybiphenyl-2-sulfonate (Reaction E) under growth conditions. Is the sulfone an intermediate in the 4S pathway or a by-product?

When sulfone was fed to the bacterium under nongrowth conditions, 2'-hydroxybiphenyl-2-sulfinate and 2'-hydroxybiphenyl were produced (2). Since the sulfone is reduced back to the sulfoxide, whether the sulfoxide or the sulfone is the precursor of 2'-hydroxybiphenyl-2-sulfinate could not be distinguished in the earlier experiments.

This paper describes the use of ^{18}O-enriched sulfone (DBT-5,5-dioxide-^{18}O$_2$) to elucidate the pathway involving the sulfone. If prior reduction of the sulfone to sulfoxide occurred in the pathway (reverse of Reaction D), then loss of one labeled oxygen would be observed in the sultine and sultone intermediates.

RESULTS AND DISCUSSION

The ^{18}O-labeled DBT sulfone substrate (98% isotopic purity) was utilized in the desulfurization experiment with the bacterium *Rhodococcus rhodochrous* (ATCC #53968) under nongrowth conditions. The supernatant from centrifugation of the culture medium was extracted with ethyl acetate, and gas chromatography (GC) analysis showed only starting sulfone and final product, 2-hydroxybiphenyl, and no sultine (cyclic form of the sulfinate) was present. From experiments with unlabelled sulfone, we know that all the sulfinic acid intermediate present in the culture medium is present in the open sulfinate form, but cyclizes to the sultine when the pH is lowered. The sultine can then be easily extracted with ethyl acetate and analyzed by GC. Therefore, the aqueous layer obtained after the initial extraction (from the experiment with ^{18}O-enriched substrate) was acidified and again extracted. GC/mass spectrometry (MS) was performed to obtain the isotopic abundances for the peaks corresponding to the sultine and sultone.

It must be pointed out that the cyclization to the sultine or sultone form displaces one oxygen from the sulfur, thus half of the label will be eliminated from each molecule of sultine. Hence, the sultine molecules will contain a single labeled oxygen if Reaction G is followed. If the pathway involving Reaction B is followed, half of the sultine molecules will be single labeled and half unlabeled, as a result of the oxygen displacement. These projections assume no occurrence of exchange or disproportionation, which would decrease or increase the numbers of labeled oxygens on sulfur.

The mass spectrum of the sultine product showed molecular ions at m/e 218 and 216 (corresponding to single-labeled and unlabeled species, respectively) in the ratio 2.7. Since this greatly exceeds the ratio of 1 predicted for Pathway B, the ratio is consistent with Reaction G, and the much smaller number of unlabeled molecules must have been formed by exchange with water or disproportionation. The sultine mass spectrum shows a large fragment ion at m/e 190, resulting from loss of $C^{16}O$, and no peak at m/e 188, corresponding to loss of $C^{18}O$. Therefore, all the ^{18}O must be attached to the sulfur, and none is on the phenolic carbon.

Thus, the pathway must proceed directly from the sulfone to the sulfinate (**Reaction G**) rather than reducing sulfone back to the sulfoxide intermediate. The reaction that forms the sulfinate from the sulfone is actually a reduction with respect to the sulfur. When the carbon–sulfur bond is cleaved, the electrons flow to the sulfur to form the sulfinate anion.

The cleavage reaction that involves formation of the sulfinate is similar to that in the electrochemical (3) and metal reduction of sulfones (4), except that hydroxyl is introduced at one aryl site in bacterial reaction, whereas hydrogen is added in the electrochemical and metal reduction reactions. The reactions of DBTs with basic reagents, such as KOH, have been investigated. Attack of nucleophilic oxygen was reported to occur at the ring carbon at high temperatures in the presence of crown ether, resulting in the formation of 2'-hydroxybiphenyl-2-sulfinate (5). In the absence of crown ether, very small amounts of the sulfinate were formed, and attack at the sulfur occurred (5, 6).

In the bacterial system, the initial stage of the mechanism is more likely to involve addition of oxygen to the benzene ring via a hydroperoxyflavin cofactor. This type of mechanism has been described for oxygenase reactions, such as the salicylic acid and *p*-hydroxybenzoic acid oxygenase reactions that occur in other bacteria.

Formation of the sulfonate anion by simple addition of oxygen to the sulfinate anion would not be expected to change the number of labeled oxygens on the sulfur, and the sulfonate would be expected to be double-labeled. Cyclization of the sulfonate to the sultone involves loss of one of the oxygens on the sulfur. Thus one-third of the sultone would be double-labeled and two-thirds would be single-labeled. But the sulfinate oxidation reaction might be more complex, and the labeling will provide some information on this oxidation.

The mass spectrum of the sultone exhibited the molecular ion peaks at 236, 234, and 232 in the ratio 5.6:3.2:1. Thus the sulfonic acid corresponding to the sultone must have been primarily triple-labeled. The obvious explanation for this fact is that the sulfinate undergoes a dimerization reaction and subsequently transfers labeled oxygen between sulfur atoms as the sulfonic acid is formed (7). The sulfur that lost oxygen in the reaction of the dimer may end up, after subsequent oxidation, as part of the unlabeled sultine that was observed.

The results not only prove that the sulfone is directly converted to the sulfinate, but also that the oxidation of the sulfinate to sulfonate follows accepted chemical mechanisms. A pathway involving Reaction E is therefore very unlikely to occur, since it would not produce triple-labeled sultone product.

The results would be more straightforward if the sulfinate were analyzed by conversion to a derivative that preserves both labeled oxygens attached to sulfur. The methylsulfone derivative was prepared by treating the sulfinate with methyliodide, and analysis of this derivative will be used to confirm the findings from the sultine derivative.

REFERENCES

1. Olson, E.S.; Stanley, D.C.; Gallagher, J.R. *Energy Fuels* **1993**, *7*, 159–164.
2. Gallagher, J.R.; Olson, E.S.; Stanley, D.C. *FEMS Microbiol. Lett.* **1993**, *107*, 31–36.
3. Simonet, J. In *The Chemistry of Sulfones and Sulphoxides*; Patai, S.; Rappoport, Z.; Stirling, C.J.M., Eds; John Wiley and Sons: New York, 1988; Chapter 22.
4. Rossi, R.A.; Bunnett, J.F. *J. Amer. Chem. Soc.* **1974**, *96*, 112.

5. Squires, T.G.; Venier, C.G.; Hodgson, B.A.; Chang, L.W. *J. Org. Chem.* 1981, *46*, 2373–2376.
6. LaCount, R.B.; Friedman, S. *J. Org. Chem.* 1977, *42*, 2751.
7. Kice, J.L.; Pawlowski, N.E. *J. Amer. Chem. Soc.* 1963, *28*, 1162.

ACKNOWLEDGMENTS
This work was supported in part by the U.S. Department of Energy (Contract No. DE-FC21-93MC30097). The assistance of David J. Miller is gratefully acknowledged.

FIGURE 1

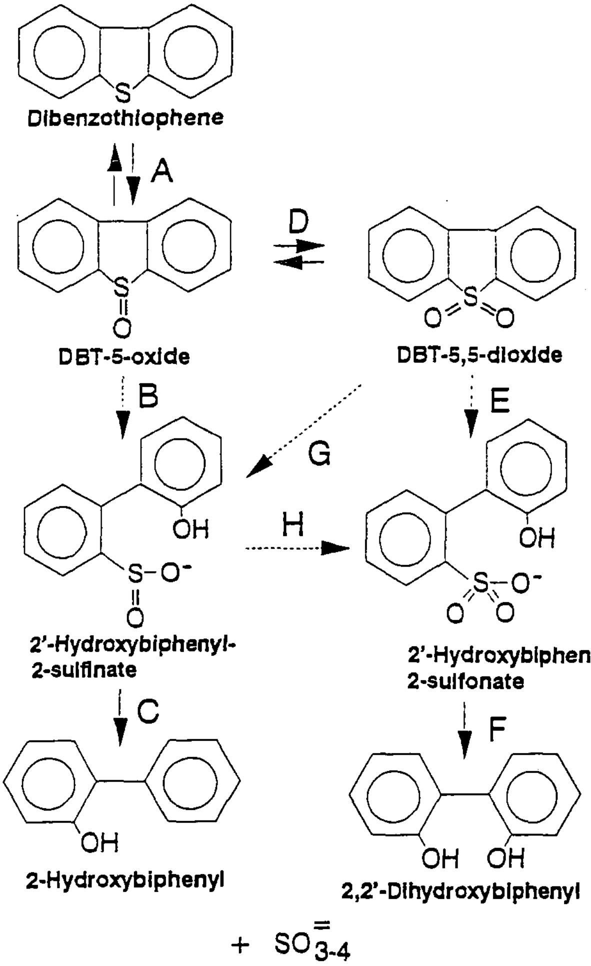
Dibenzothiophene
A
D
DBT-5-oxide
DBT-5,5-dioxide
B
E
G
H
2'-Hydroxybiphenyl-2-sulfinate
2'-Hydroxybiphenyl-2-sulfonate
C
F
2-Hydroxybiphenyl
2,2'-Dihydroxybiphenyl
+ $SO_{3-4}^{=}$